

**SÃO PAULO STATE UNIVERSITY
SCHOOL OF AGRICULTURAL AND VETERINARIAN SCIENCES
CAMPUS OF JABOTICABAL**

**GENOMIC STUDY FOR FEMALE SEXUAL PRECOCITY,
CARCASS, AND MEAT QUALITY TRAITS IN NELLORE
CATTLE**

Leonardo Machestropa Arikawa

Animal Scientist

2022

**SÃO PAULO STATE UNIVERSITY
SCHOOL OF AGRICULTURAL AND VETERINARIAN SCIENCES
CAMPUS OF JABOTICABAL**

**GENOMIC STUDY FOR FEMALE SEXUAL PRECOCITY,
CARCASS, AND MEAT QUALITY TRAITS IN NELLORE
CATTLE**

Leonardo Machestropa Arikawa

Advisor: Prof.^a Dra. Lucia Galvão de Albuquerque

Co-Advisor: Prof.^a Dra. Ana Fabrícia Braga Magalhães

Dissertation presented to the School of Agricultural and Veterinarian Sciences – São Paulo State University, Campus of Jaboticabal in partial fulfillment of requirements for the degree of master in Genetics and Animal Breeding.

A699g

Arikawa, Leonardo Machestopa

Genomic study for female sexual precocity, carcass, and meat quality traits in Nellore cattle / Leonardo Machestopa Arikawa. -- Jaboticabal, 2022

151 p. : il., tabs.

Dissertação (mestrado) - Universidade Estadual Paulista (Unesp), Faculdade de Ciências Agrárias e Veterinárias, Jaboticabal

Orientadora: Lucia Galvão de Albuquerque

Coorientadora: Ana Fabrícia Braga Magalhães

1. Beef cattle. 2. Carcass. 3. Genetic parameters. 4. GWAS. 5. Meat quality. I. Título.

Sistema de geração automática de fichas catalográficas da Unesp. Biblioteca da Faculdade de Ciências Agrárias e Veterinárias, Jaboticabal. Dados fornecidos pelo autor(a).

Essa ficha não pode ser modificada.

CERTIFICADO DE APROVAÇÃO

TÍTULO DA DISSERTAÇÃO: GENOMIC STUDY FOR FEMALE SEXUAL PRECOCITY, CARCASS, AND MEAT QUALITY TRAITS IN NELLORE CATTLE

AUTOR: LEONARDO MACHESTROPA ARIKAWA

ORIENTADORA: LUCIA GALVÃO DE ALBUQUERQUE

COORIENTADORA: ANA FABRÍCIA BRAGA MAGALHÃES

Aprovado como parte das exigências para obtenção do Título de Mestre em GENÉTICA E MELHORAMENTO ANIMAL, pela Comissão Examinadora:



Prof.ª. Dra. LUCIA GALVÃO DE ALBUQUERQUE (Participação Virtual)
Departamento de Zootecnia / FCAV Unesp Jaboticabal



Prof. Dr. FERNANDO SEBASTIAN BALDI REY (Participação Virtual)
Departamento de Zootecnia / FCAV / UNESP - Jaboticabal



Ph.D. LUCIO FLAVIO MACÊDO MOTA (Participação Virtual)
Department of Agronomy Food Natural Resources Animals and Environment - DAFNAE / University of Padova - Campus Agripolis

Jaboticabal, 24 de fevereiro de 2022

ABOUT THE AUTHOR

Leonardo Machestropa Arikawa – born on May 8, 1995, in Taquaritinga, São Paulo, Brazil, son of Hisanori Arikawa and Sueli Machestropa. He started his undergraduate in Animal Science in March 2013 at School of Agricultural and Veterinarian Sciences, UNESP, campus of Jaboticabal. He performed an extracurricular internship at the Department of Animal Science in the area of Genetics and Animal Breeding, from August 2018 to August 2019, under the supervision of Prof. Dr. Ana Fabrícia Braga Magalhães. From September to November 2019, he completed the mandatory curricular internship at the “Instituto de Zootecnia – Centro Avançado de Pesquisa Tecnológica dos Agronegócios de Bovinos de Corte (APTA)”, in the area of Animal Breeding with Prof. Dr. Lucia Galvão de Albuquerque and Prof. Dr. Maria Eugenia Zerlotti Mercadante as advisors. He obtained his bachelor's degree in Animal Science in February 2020. In March 2020, he started his Master of Science (MSc.) studies in the Graduate Program in Genetics and Animal Breeding at School of Agricultural and Veterinarian Sciences, UNESP, campus of Jaboticabal, under the supervision of Prof. Dr. Lucia Galvão de Albuquerque and co-supervision of Prof. Dr. Ana Fabrícia Braga Magalhães. His M.Sc studies have been granted with a scholarship from “Coordenação de Aperfeiçoamento de Pessoal de Nível Superior (CAPES)”, from March 2020 to February 2022.

“Who among you can at the same time laugh and be exalted? He who climbeth on the highest mountains, laugheth at all tragic plays and tragic realities. Courageous, unconcerned, scornful, coercive - so wisdom wisheth us; she is a woman, and ever loveth only a warrior.”

Friedrich Nietzsche (Thus Spake Zarathustra)

I dedicate this work to all Brazilian researchers who remain resilient, fighting for value and working to promote advances in knowledge, critical thinking, and development, even in the midst of a country that devalues and contests scientific thinking.

ACKNOWLEDGMENTS

Firstly, I thank my family, especially my parents Hisanori and Sueli, for their support at all times, for the education they provided me, and for never measuring efforts to help me, whatever the circumstances. I can only thank you, saying that this achievement belongs to you. To my sister, Amanda, and my nephews, Davi, Henrique, and Nicolas, for their love and affection, and for being an inspiration to me.

To my advisor Prof. Dr. Lucia Galvão de Albuquerque, first of all for having received me and for the opportunity to work in her research group. For all the availability, support, patience, and help offered for the development of this project. Thank you for your extensive professional and personal advice, for believing in my potential and my work. You are a great inspiration to me.

To my co-advisor Dr. Ana Fabricia Braga Magalhães and also Dr. Larissa Fernanda Simielli Fonseca, for all the attention, support, and help they've been offering since undergraduate. I am extremely grateful for being excellent professors and for awakening in me an interest in the area of Genetics and Animal Breeding.

I would like to express my gratitude to Prof. Dr. Roberto Carneiro and Dr. Delvan Alves da Silva, for their support, attention, suggestions to improve this work and for dedicating their time to transmit valuable knowledge to me.

To the members of my Master's dissertation and general qualification exam committee, Prof. Dr. Fernando Sebastian Baldi Rey, Dr. Lucio Flavio Macedo Mota, and Dr. Gerardo Alves Fernandes Júnior, for the valuable suggestions that contributed to the improvement of the work.

To the "Albuquerque" team, to the friends and co-workers from graduate program in Genetics and Animal Breeding, who welcomed me, helped, and taught me from the first day I came to the research group.

I thank everyone who gave me strength and encouragement in difficult times and also celebrated the happy times, especially my great friend Daiane. I was very lucky to be around amazing people who were fundamental to my personal growth.

To my brothers from the eternal "Casa Verde", André (Reditube), Felipe (Falo), Jorge (Pran-xana), Lindomar (Libumba), and Matheus (Télson), for the

companionship, the coexistence, and all the good times we had living together in Jaboticabal.

To the School of Agricultural and Veterinarian Sciences – UNESP, for the support and structure provided to us, and all the professors from graduate program in Genetics and Animal Breeding, for all the help, classes, and knowledge offered.

To Coordenação de Aperfeiçoamento de Pessoal de Nível Superior - Brasil (CAPES) for granting the scholarship.

I am very grateful to everyone who contributed directly or indirectly, either with knowledge or support, so that I could succeed during this stage.

This study was financially supported by FAPESP #2009/16118-5; #2017/10630-2; and #2018/20026-8, and in part by the Coordenação de Aperfeiçoamento de Pessoal de Nível Superior - Brasil (CAPES) - Finance Code 001.

This study was financed in part by the Coordenação de Aperfeiçoamento de Pessoal de Nível Superior - Brasil (CAPES) - Finance Code 001.

SUMMARY

	pages
RESUMO.....	i
ABSTRACT.....	iii
Chapter 1 – General Considerations	1
1. INTRODUCTION.....	1
2. LITERATURE REVIEW	3
2.1. Reproductive traits.....	3
2.2. Carcass traits.....	5
2.3. Meat quality traits.....	7
2.4. Genetic correlations.....	9
2.5. Genome-wide association studies	12
3. OBJECTIVES	18
3.1. General objective.....	18
3.2. Specific objectives	18
4. REFERENCES.....	19
Chapter 2 – Genetic parameters estimates using genomic information for female sexual precocity, carcass and meat quality traits in Nellore cattle	33
1. INTRODUCTION.....	34
2. MATERIAL AND METHODS.....	36
2.1. Database	36
2.1.1. Phenotypic data.....	36
2.1.2. Genotypic data	39
2.2. Estimates of (co)variance components and genetic parameters	39
3. RESULTS AND DISCUSSION	41
3.1. Genetic parameters for carcass and meat quality traits.....	41

3.2. Heritability estimates for female sexual precocity and their genetic correlations with carcass and meat quality traits	43
4. CONCLUSIONS.....	45
5. REFERENCES.....	46
Chapter 3 – Genome-wide scans for carcass and meat quality traits in Nellore cattle	53
1. INTRODUCTION.....	54
2. MATERIAL AND METHODS	56
2.1. Phenotypic data	56
2.2. Genotypic data.....	58
2.3. Genome-wide association analysis.....	58
2.4. Functional analysis	60
3. RESULTS AND DISCUSSION	60
3.1. GWAS for carcass traits.....	60
3.2. GWAS for meat quality traits.....	70
4. CONCLUSIONS.....	80
5. REFERENCES.....	81
6. SUPPLEMENTARY INFORMATION	100

ESTUDO GENÔMICO PARA CARACTERÍSTICAS DE PRECOCIDADE SEXUAL DE FÊMEAS, CARÇAÇA E QUALIDADE DA CARNE EM BOVINOS DA RAÇA NELORE

RESUMO – O Brasil é o maior exportador de carne bovina do mundo e o país com o maior rebanho bovino comercial. O Nelore é a principal raça de gado de corte do país; entretanto, os animais desta raça tendem a produzir carcaças e carne de qualidade inferior às raças *Bos taurus*. Além disso, as características de carcaça obtidas no *post-mortem* e a qualidade da carne são atributos de expressão tardia e de difícil mensuração e, conseqüentemente, são difíceis de selecionar pelos métodos convencionais. Em termos reprodutivos, os zebuínos atingem a puberdade tardiamente e essas características, principalmente as observadas nas fêmeas, são altamente influenciadas por fatores ambientais. Assim, o uso de abordagens genômicas torna-se uma alternativa para contornar esses desafios. Nesse contexto, os objetivos deste estudo foram: i) estimar parâmetros genéticos para características de precocidade sexual de fêmeas, carcaça e qualidade da carne, utilizando informação genômica; ii) conduzir um estudo de associação genômica ampla (GWAS) para características de carcaça e qualidade da carne em bovinos Nelore. A base de dados utilizada é composta por informações de características de carcaça obtidas no *post-mortem* (AOL: área de olho de lombo, EGS: espessura de gordura subcutânea e PCQ: peso da carcaça quente); qualidade da carne (MAC: maciez, MARM: marmoreio e LIP: teor de lipídios); e precocidade sexual (IPP: idade ao primeiro parto e PE: perímetro escrotal). No Capítulo 2, o conjunto de dados utilizado para estimação de parâmetros genéticos foi de 602.122 registros para características de precocidade sexual e 6.910 para características de carcaça/carne, e registros genotípicos de 15.000 animais Nelore genotipados ou imputados com o Illumina Bovine HD Beadchip. Os componentes de (co)variância e os parâmetros genéticos foram obtidos considerando a abordagem single-step (ssGBLUP) por dois métodos: 1) para características de carcaça e qualidade de carne, um modelo multi-característica e inferência bayesiana foram aplicados usando o software GIBBS2F90, e o peso ao sobreano (PS) foi incluído na análise como característica âncora; 2) modelos bi-característica e inferência frequentista foram adotados utilizando o software AIREMLF90 para estimar as correlações genéticas entre as características de precocidade sexual com as de carcaça e qualidade da carne. As estimativas de herdabilidade variaram de 0,13 a 0,34 para as características de carcaça e qualidade de carne, e foram de 0,06 e 0,45 para IPP e PE, respectivamente. Correlações genéticas favoráveis foram estimadas entre PS–PCQ (0,79±0,03), PS–AOL (0,28±0,05), PCQ–AOL (0,44±0,05), MARM–LIP (0,90±0,07), MAC–LIP (-0,20±0,11), EGS–MARM (0,29±0,08), EGS–LIP (0,22±0,09), PCQ–MAC (-0,22±0,09) e EGS–IPP (-0,26±0,11). No Capítulo 3, um total de 6.910 animais Nelore fenotipados e 25.000 genotipados foram utilizados para o estudo de GWAS. Os efeitos dos SNP foram estimados com base na abordagem weighted single-step GBLUP (WssGBLUP). As 10 principais regiões genômicas explicaram 8,79%, 12,06% e 9,01% da variância genética aditiva e abrigaram um total de 134, 158 e 93 genes candidatos posicionais para AOL, EGS e PCQ, respectivamente. Para as características de qualidade da carne, as janelas de maior efeito foram responsáveis por 14,72%, 14,79% e 14,13% da variância aditiva, e 137, 163 e 89 genes candidatos foram encontrados para MAC, MARM e LIP, respectivamente. Entre os genes candidatos encontrados, estão

PPARGC1A, AQP3, AQP7, MYLK2, PLAGL2, PLAG1, XKR4, MYOD1, KCNJ11, WWOX, CARTPT, RAC1, PSAP, PLA2G16 e PLCB3, genes que foram anteriormente associados a diversas características produtivas, como de crescimento, carcaça, qualidade da carne, ingestão alimentar e reprodutivas em Nelore e outras raças de bovinos.

Palavras-chave: bovinos de corte, carcaça, GWAS, parâmetros genéticos, precocidade sexual, qualidade da carne

GENOMIC STUDY FOR FEMALE SEXUAL PRECOCITY, CARCASS, AND MEAT QUALITY TRAITS IN NELLORE CATTLE

ABSTRACT – Brazil is the largest beef exporter in the world and the country with the largest commercial bovine herd. Nellore is the main beef cattle breed in Brazil; however, animals of this breed tend to produce carcasses and beef of lower quality than *Bos taurus*. In addition, carcass traits obtained in *post-mortem* and meat quality are attributes that are late expressed and difficult to measure, consequently, they are difficult to select by conventional methods. In reproductive terms, Zebu cattle reach puberty late and these traits, especially those observed in females, are highly influenced by environmental factors. Thus, the use of a genomic approach becomes an alternative to overcome these challenges. In this context, the aims of this study were: i) to estimate genetic parameters for female sexual precocity, carcass, and meat quality traits, using genomic information; ii) to perform a genome-wide association study (GWAS) for carcass and meat quality traits in Nellore cattle. The database used is composed of information for carcass traits obtained in the *post-mortem* (LMA: longissimus muscle area, BF: backfat thickness, and HCW: hot carcass weight); meat quality (SF: shear-force tenderness, MARB: marbling, and IMF: intramuscular fat content); and sexual precocity traits (AFC: age at first calving and SC: scrotal circumference). In Chapter 2, the dataset used to estimate genetic parameters consisted of 602,122 records for sexual precocity traits and 6,910 for carcass/meat traits, and genotypic records of 15,000 Nellore animals genotyped or imputed to the Illumina Bovine HD Beadchip. The (co)variance components and genetic parameters were obtained considering a Single-step approach (ssGBLUP) in two methods: 1) for carcass and meat quality traits, a multi-trait model and Bayesian inference were applied using the GIBBS2F90 software, and yearling weight (PW) was included in the analysis as an anchor trait; 2) bi-trait models and frequentist inference were adopted using the AIREMLF90 software to estimate the genetic correlations of sexual precocity traits with carcass and meat quality traits. Heritability estimates ranged from 0.13 to 0.34 for carcass and meat quality traits, and were 0.06 and 0.45 for AFC and SC, respectively. Favorable genetic correlations were estimated between YW–HCW (0.79 ± 0.03), YW–LMA (0.28 ± 0.05), HCW–LMA (0.44 ± 0.05), MARB–IMF (0.90 ± 0.07), SF–IMF (-0.20 ± 0.11), BF–MARB (0.29 ± 0.08), BF–IMF (0.22 ± 0.09), HCW–SF (-0.22 ± 0.09), and BF–AFC (-0.26 ± 0.11). In Chapter 3, a total of 6,910 phenotyped and 25,000 genotyped Nellore animals were used for GWAS. The effects of SNPs were estimated based on the weighted single-step GBLUP (WssGBLUP) approach. The top 10 genomic regions explained 8.79, 12.06, and 9.01% of the additive genetic variance and harbored a total of 134, 158, and 93 positional candidate genes for LMA, BF, and HCW, respectively. For meat quality traits, the windows of greatest effect accounted for 14.72, 14.79, and 14.13% of the additive variance, and 137, 163, and 89 candidate genes were found for SF, MARB, and IMF, respectively. Among the candidate genes found, there are *PPARGC1A*, *AQP3*, *AQP7*, *MYLK2*, *PLAGL2*, *PLAG1*, *XKR4*, *MYOD1*, *KCNJ11*, *WVOX*, *CARTPT*, *RAC1*, *PSAP*, *PLA2G16*, and *PLCB3*, genes that were previously associated with several production traits, such as growth, carcass, quality of meat, feed intake and reproductive traits in Nellore and other cattle breeds.

Keywords: beef cattle, carcass, genetic parameters, GWAS, meat quality, sexual precocity

Chapter 1 – General Considerations

1. INTRODUCTION

With the globalization process combined with the growing demand for safe food, Brazil has become one of the largest producers and exporters of beef, due to its high technological potential, high level of production and, mainly, the quality of its production (Almeida and Michels, 2012; Gomes et al., 2017). Currently, the country stands out on the world stage as the largest exporter of meat, in addition to having the largest cattle herd. In 2018, the Brazilian cattle herd reached about 214.7 million heads. In total, 44.2 million heads were slaughtered, producing, approximately, 10.9 million tons of carcass weight equivalent (CWE). From the total meat produced, 20.2% was exported and the rest supplied the domestic market, guaranteeing average consumption per capita of 49.12 kg/year. Beef exports totaled 1,600 tons, with a value of US\$ 6,572.30 million, representing 3.5% of agribusiness exports (ABIEC, 2019).

The Brazilian bovine population consists of a variety of Taurine (*Bos taurus taurus*) and Zebu (*Bos taurus indicus*) breeds. Approximately 80% of the national herd is made up of zebu animals of different breeds, with Nellore being the most expressive with an aptitude for beef (Costa et al., 2015; Lopes et al., 2016; Magalhães et al., 2016). Thus, Brazilian beef cattle are kept, predominantly, with the genetics of zebu cattle.

Brazilian Nellore has undergone an intense process of genetic improvement over time, becoming the most important national beef cattle breed. Animals of this breed have productive and reproductive attributes that best adapt to tropical climatic conditions. Its rusticity, natural resistance to ecto and endoparasites and to heat, are examples of favorable traits of Nellore in Brazil. Moreover, cows have outstanding reproductive longevity and excellent maternal ability (Santos, 2000; Albuquerque et al., 2006; Lopes et al., 2016; Feitosa et al., 2017). However, *Bos indicus* animals tend to show moderate growth rate and adult weight, late testicular development, and reach puberty at older ages (Cundiff et al., 2004). Compared to Taurine breeds, Nellore animals produce leaner meat, with less marbling index and less tenderness, besides finishing late, partially due to the extensive production system adopted in Brazil (Cundiff et al., 2004; Albuquerque et al., 2006). Albuquerque et al. (2006), in a review

paper, concluded that in order to increase animal productivity and, consequently, the production of quality food, besides of selecting Zebu cattle raised extensively, it is important to be concerned with animal welfare and food safety conditions.

In order to reach production levels that meet consumer demand, it is essential to deepen the understanding of the genetic mechanisms involved in the expression of carcass and meat traits in Nelore cattle. So that, it will be possible to identify genetic variants that control these traits, and to assist ranchers in planning breeding programs and achieving their goals related to the final product (Xia et al., 2016; Bhuiyan et al., 2017). However, information for these characteristics obtained *post-mortem* are still insufficient, due to the fact that they are late expressed and difficult to measure, requiring progeny tests since the candidate animals cannot be directly evaluated, which increases the costs and the length of generation intervals (Fernandes Júnior et al., 2016a; Fonseca et al., 2017; Leal-Gutiérrez et al., 2019; Magalhães et al., 2019).

The reproductive traits also are important for the production system, as they have a great economic impact on the production of beef cattle. In this context, sexual precocity has been increasingly explored by breeding programs with the objective of reducing production costs and generation intervals, as well as increasing genetic gain rates (Moorey and Biase, 2020). Furthermore, these traits guarantee a greater number of born calves throughout the productive life of precocious heifers (Eler et al., 2014). Thus, as it is a decisive factor in the total production efficiency, traits associated with female sexual precocity must be included in the indexes as a selection criterion. However, reproductive problems in Brazilian beef cattle are the main limiting on the productive efficiency of a herd, due to the sexual precocity traits, especially those observed in females, are highly influenced by environmental factors and, thus, are little inheritable (Cardoso et al., 2015). Furthermore, considering that Brazilian cattle are predominantly composed of Zebu breeds, heifers tend to reach puberty later than *Bos taurus* animals (Albuquerque et al., 2006; Nascimento et al., 2016).

Thus, in the face of such difficulties in the breeding of Zebu breeds, it is necessary to search for alternative methods, such as those that use genomic approaches, which allow for accurate genetic evaluations, which can be used to improve female sexual precocity, carcass and meat quality traits (Fernandes Júnior et al., 2016a; Magalhães et al., 2019). In this sense, the inclusion of molecular tools in

genetic analysis can improve the scanning of the genetic architecture of these traits, which in turn are of complex inheritance since their variation is determined by many genes with small effects.

Genome-wide association studies (GWAS) aim to associate genomic regions with the phenotypes of interest through statistical analysis, to identify variations in the genome (mainly single nucleotide polymorphisms - SNP) linked to regions of great effect on a given characteristic, providing a better understanding of biological functions and genetic influence on phenotypic expression (Zhang et al., 2012; Yang et al., 2013; Magalhães et al., 2016; Magalhães et al., 2019; Pegolo et al., 2020). The basic principle of GWAS is that a set of phenotypes of a target trait in a sample of animals, is tested for a panel of SNP markers across the genome, in order to identify statistical associations between the trait and all markers, simultaneously, and quantify the size of the effect that each marker contributes to the expression of the characteristic (Goddard and Hayes, 2009).

Therefore, whether in the application of estimates of genetic parameters and/or GWAS, the trend is that, increasingly, the use of molecular tools in genetic analyzes will become effective and routine in animal breeding programs. Thus, due to the small number of studies and the difficulty in improving sexual precocity rates and selecting carcass and meat quality traits using the traditional method, it is essential to develop genomic studies aiming to better understand the expression of these traits in Nellore cattle.

2. LITERATURE REVIEW

2.1. Reproductive traits

Reproductive efficiency plays a key role in the economic sustainability of the livestock production system, especially traits related to sexual precocity in heifers (Brumatti et al., 2011). These traits are directly related to the availability of animals in the herd, influencing, consequently, the intensity of the selection, in order to guarantee greater genetic gains, shorter generation intervals, and the economic success of production (Kluska et al., 2018; Ramos et al., 2020).

In reproductive terms, compared to the Taurine breeds, Zebu cattle reach puberty at a later age (Albuquerque et al., 2006; Nascimento et al., 2016), probably due to low human interference in the selection process of Zebu herds, and may delay the beginning of a cow's reproductive life, impairing the production chain and the profitability of the system. In addition, the sexual precocity traits are generally highly influenced by environmental factors, such as nutrition and heat stress (Samadi et al., 2014; Nepomuceno et al., 2017; Ferraz et al., 2018), which affect the genetic gain per generation (Cardoso et al., 2015; Mota et al., 2020).

The age at first calving (AFC) is one of the main traits used to assess female fertility and sexual maturity. AFC is an economically important trait in beef cattle, as it is directly linked to the reproductive longevity of the cow and the interval between generations, and, in this context, the longevity of beef cows ensures a lower replacement rate and greater utilization of the herd (Perotto et al., 2006). The inclusion of heifers at young ages in reproduction is strongly important so that genetic differences in reproductive capacity are detected early (Boligon et al., 2015), providing a reduction in production costs and increasing rates of genetic gain. However, producing breeding stock that has these attributes is one of the biggest challenges for beef cattle breeders, since reproductive traits, especially those evaluated in females, generally have low heritability, implying the difficulty of direct selection for younger ages at first calving (Boligon et al., 2010).

Several studies conducted on the Nelore breed in recent years have reported heritability for AFC ranging from 0.08 to 0.24 (Boligon et al., 2015; Terakado et al., 2015; Buzanskas et al., 2017; Kluska et al., 2018; Lacerda et al., 2018; Schmidt et al., 2018; Brunet et al., 2020; Costa et al., 2020). According to Buzanskas et al. (2017), the increase in heritability estimates for AFC could be due to the increase in genetic variability that has been introduced through the selection of sexually precocious heifers and through greater control of environmental factors.

Due to the problems associated with female sexual performance, for many years, the inclusion of easy-to-measure traits, genetically correlated to female reproductive events as selection criteria, was an excellent alternative to decrease the generation interval and increase the genetic gain for sexual precocity in females (Boldt et al., 2016; Kluska et al., 2018). The scrotal circumference (SC), although it has no

economic value, has been widely used to improve sexual precocity and the reproductive performance of cattle herds, since males and females share genes that are involved in physiological mechanisms linked to reproductive events (Toelle and Robinson, 1985). This trait is easy to measure with relatively low cost and it is favorably correlated with young female reproductive traits (Terakado et al., 2015; Buzanskas et al., 2017; Soares et al., 2017). Lacerda et al. (2018) report that SC has been widely used also to improve sexual precocity and reproductive performance in males, such as early onset of spermatogenesis, in addition to being a good indirect indicator of puberty in females, provided it is measured at a young age.

Heritability estimates for SC are generally of moderate to high magnitudes. When measured at yearling, heritability estimates found in the literature for the Nellore breed range from 0.33 to 0.52 (Bolognon et al., 2015; Terakado et al., 2015; Buzanskas et al., 2017; Kluska et al., 2018; Lacerda et al., 2018; Brunet et al., 2020). Based on the results of a meta-analysis study, which grouped several other studies with Nellore cattle, Oliveira et al. (2017) reported a heritability estimate of 0.56 for SC measured at yearling, indicating that the trait must respond quickly to selection events.

2.2. Carcass traits

Attributes such as carcass are economically important traits, since the beef industry pays producers based on some conditions of the carcass, such as weight and finish (Vaz et al., 2013; Fernandes Júnior et al., 2016a; McPhee et al., 2020). Measuring carcass traits is necessary to analyze qualitative and quantitative parameters related to the composition of the final product (Tonussi et al., 2015). Besides, selection for these characteristics can lead to improvements in carcass composition, increasing the proportion of edible body parts (Tonussi et al., 2015; Kluska et al., 2018), ensuring a higher percentage of yield from commercial cuts.

The longissimus muscle area (LMA) is a carcass trait expressed in square centimeters (cm²) and measured in the *Longissimus thoracis* dorsal muscle, between the 12th and 13th ribs. LMA is an efficient indicator of muscle mass, carcass composition and edible portion (Caetano et al., 2013; Gordo et al., 2018), and this trait is positively associated with the amount of muscle, growth rates, carcass yield and, mainly, with the proportion of cuts that add commercial value for meat products (Bertrand et al.,

2001; Caetano et al., 2013; Tonussi et al., 2015; Gordo et al., 2018). The heritability coefficients observed in the literature for LMA in Nellore cattle are of moderate to high magnitude, ranging from 0.10 to 0.28 for LMA measured *post-mortem* (Tonussi et al., 2015; Fernandes Júnior et al., 2016a; Gordo et al., 2018;), and from 0.29 to 0.44 when was obtained by ultrasonography (Ceacero et al., 2016; Buzanskas et al., 2017; Kluska et al., 2018; Silva Neto et al., 2020) indicating that selection for LMA can promote a rapid genetic progress.

The backfat thickness (BF) is directly related to the quality of the final product. BF indicates the degree of finishing of the carcass (Tonussi et al., 2015; Gordo et al., 2018). It influences the cooling speed after slaughtering, acting as a thermal insulator, protecting the carcass against the stiffness and darkening of muscles, in addition to avoiding the reduction of weight and tenderness caused by dehydration during the cooling process (Caetano et al., 2013; Baldassini et al., 2017; Silva-Vignato et al., 2017). Scarce fat covering causes problems in the carcass, devaluing its quality but, when in excess, it is undesirable, as it provides a negative look to the consumer, in addition to reducing the edible portion. The heritability estimates for BF in the Nellore breed assume values with wide variation in the literature, between 0.08 and 0.21 for BF obtained *post-mortem* (Fernandes Júnior et al., 2016a; Feitosa et al., 2017; Gordo et al., 2018), and 0.17 to 0.59 for BF measured by ultrasound (Yokoo et al., 2015; Ceacero et al., 2016; Silva Neto et al., 2020).

The hot carcass weight (HCW) is a phenotypic measure expressed in kilograms (kg) and is related to the weight of the newly slaughtered animal, which is obtained from the weighing of the carcass after skinning, evisceration, and carcass toilet processes. This is a classificatory trait used by slaughterhouses and is directly related to the commercial value of the animal, since the amount paid to cattle breeders is, mainly, based on the carcass weight (Fernandes Júnior et al., 2016a; Gordo et al., 2018). Studies with Nellore animals showing HCW genetic parameter estimates are still scarce. The heritability estimates found in the literature for the breed range from 0.11 to 0.39 (Tonussi et al., 2015; Fernandes Júnior et al., 2016a; Gordo et al., 2018; Carvalho et al., 2019). In a review work, Utrera and Van Vleck (2004) reported a mean value of 0.40 for heritability estimates for HCW for several bovine breeds, ranging from 0.09 to 0.92. The authors reported that the wide variation may be associated with

differences in racial groups, estimation methods, model effects, number of observations, measurement errors, animal sex, and farm management.

2.3. Meat quality traits

Meat quality traits are fundamental to guarantee consumers satisfaction (Gordo et al., 2018). The concept of "quality meat" most demanded by buyers includes a series of sensory factors, such as tenderness, juiciness, and flavor, which together contribute to a better palatability of the meat, in addition to a more attractive visual appearance that includes attributes such as color and distribution of the fat (Magnabosco et al., 2016; Xia et al., 2016; Gordo et al., 2018; Leal-Gutiérrez et al., 2019).

Among the meat attributes, tenderness is considered the most important sensory parameter for consumers. This trait is usually determined by shear force (SF) and is influenced by genetic and environmental factors, such as genotype, age, sex, management, *post-mortem* pH drop, and carcass composition (Zhao et al., 2012; Fonseca et al., 2017; Mwangi et al., 2019). Considering the high percentage of Zebu animals in the Brazilian bovine population, the improvement of meat tenderness is essential to meet the quality demanded by buyers, since animals belonging to this genetic group present unfavorable genes for tenderness (Ferraz and Felício, 2010; Magnabosco et al., 2016; Fonseca et al., 2017). Heritability estimates for SF range from low to moderate (0.09 to 0.21) in studies carried out for the Nellore breed (Castro et al., 2014; Tonussi et al., 2015; Gordo et al., 2018; Magalhães et al., 2018; Bonin et al., 2021), suggesting the possibility of obtaining relatively slow genetic progress through selection.

Marbling fat contributes to the juiciness of the meat, providing the necessary lubrication between the muscle fibers, increasing the perception of juiciness, in addition to preventing the loss of water by cooking (Mwangi et al., 2019). Another factor influenced by this trait is the flavor through a complex interaction between precursors of fatty and lean meat components (Arshad et al., 2018; Mwangi et al., 2019). Studies with Nellore animals have reported heritability estimates ranging from 0.11 to 0.32 (Neves et al., 2014; Tonussi et al., 2015; Gordo et al., 2018; Magalhães et al., 2018). In a search to estimate genetic parameters for quality meat traits of Nellore evaluated at different anatomical points of the *Longissimus thoracis* muscle, Bonim et al. (2021)

found heritability estimates of 0.15 and 0.16 for MARB, obtained from samples taken from longissimus in the 5th and 12th ribs, respectively. In addition, the authors found a high genetic association (0.89 ± 0.33) between the different MARB measures used in the study, suggesting that the collection region does not influence the estimates, and any of the measures can be used for selection purposes, with similar direct and correlated responses.

The percentage of lipids can also be associated with the same attributes as the marbling score and it is also used to assess meat quality. The intramuscular fat content (IMF) represents the content of accumulated lipids between fibers or inside muscle cells (Cesar et al., 2015). It is a polygenic trait influenced by several factors (such as sex, age, race, nutrition, and genetics) and is directly associated with the texture and quality of meat, and its quantity in the meat tends to influence acceptability by consumers (Jiang et al., 2017). Intramuscular fat content consists of a variety of fats, including omega-3 long-chain polyunsaturated fatty acids, which are beneficial to the brain and retinal development, in maternal and fetal health during pregnancy, cognitive system, and psychological state in humans (Williams, 2007; Mwangi et al., 2019). In addition, IMF also contains fatty acids resulting from the ruminal biohydrogenation of lipids, such as conjugated linoleic acid (CLA), which is an isomer of linoleic acid from food and has anticarcinogenic properties (Ferraz and Felício, 2010). The lipid content of meat is also rich in monounsaturated fatty acids (MUFA) which influence the melting point of fat, thus reducing the levels of bad cholesterol (LDL) in the bloodstream in humans (Jakobsen et al., 2008; Cesar et al., 2014). Although the many benefits to human health, animal fat consumption levels should be moderated, as beef also has saturated fatty acids (SFA), which, in excess, significantly increase the plasma concentration of low-density lipoprotein cholesterol (LDL), potentially increasing the risk of cardiovascular problems (Feitosa et al., 2017; Nettleton et al., 2017).

For the Nellore breed, there are few studies that estimate genetic parameters for IMF. Feitosa et al. (2017) and Magalhães et al. (2018) observed relatively low values of heritability, 0.07 and 0.13, respectively. In a review, Utrera and Van Vleck (2004) summarized heritability estimates for IMF from works published up to 2004 and the mean estimate was 0.51, ranging from moderate (0.35) to high (0.65) in different taurine breeds.

2.4. Genetic correlations

Researches that seek to investigate genetic associations between sexual precocity and meat quality traits are scarce in the literature. Studying animals Red Angus, McAllister et al. (2011) described estimates of genetic correlation between SC with marbling (MARB) and intramuscular fat content (IMF) of 0.01 and 0.05, respectively, suggesting that selection for SC will not promote a genetic gain in intramuscular fat deposition in the studied breed. In a work carried out in Japan with Wagyu cattle, Oyama et al. (1996) reported a negative and moderate genetic relationship between AFC and MARB (-0.39), higher than that found by Oyama et al. (2004) for the same breed (-0.24). Despite the difference in magnitude, these results indicate the existence of genes acting together in early sexual maturation and intramuscular adipogenesis.

Scrotal circumference was moderately correlated with LMA and BF (0.31 and 0.25, respectively) in the study by Buzanskas et al. (2017), while Kluska et al. (2018) found lower genetic association values for SC–LMA and SC–BF (both 0.17). Despite the differences in magnitude in the works, the results suggest that selection for greater SC, in the long or medium time, should genetically increase LMA and BF.

Some studies with Nellore animals showed negative and desirable genetic correlation estimates of moderate magnitude between BF and AFC (Caetano et al., 2013; Buzanskas et al., 2017; Kluska et al., 2018). Pires et al. (2016) reported an association of -0.69 ± 0.35 between the same traits in Canchim animals, indicating that greater fat deposition can result in benefits in sexual precocity. These findings are biologically expected since lipid production or fat deposition is directly associated with the metabolism of certain hormones (such as steroids and eicosanoids) that modulate reproductive events, in addition to having a direct effect on the transcription of encoding genes of proteins essential for reproduction (Mattos et al., 2000). Also in Nellore, low and close to zero genetic correlations were estimated between LMA and AFC (Buzanskas et al., 2017; Kluska et al., 2018; Caetano et al., 2013) indicating that the progress of one trait doesn't tend to interfere with the other.

Genetic correlations between carcass traits vary greatly in studies found in the literature. Between LMA and BF, some authors found genetic associations low or close to nullity in the Nellore breed (Ceacero et al., 2016; Buzanskas et al., 2017; Kluska et

al., 2018) indicating that selection for one of these traits will not imply in correlated response in the other. On the other hand, other studies have found positive correlations of moderate magnitude in the same breed (Gordo et al., 2012; Caetano et al., 2013). In a meta-analysis study in Nellore, Oliveira et al. (2017) reported a genetic association of 0.1694 between these traits, a result similar to the estimates of the aforementioned authors.

Genetic correlation estimates of HCW with LMA and BF show a wide range from practically null to 0.62. Elzo et al. (2017), studying a multibreed Angus-Brahman population, observed genetic correlations of 0.57 ± 0.08 and 0.12 ± 0.13 of HCW with LMA and BF, respectively. Working with Hanwoo cattle, Do et al. (2016) obtained an association similar to that of Elzo et al. (2017) between HCW and LMA (0.62 ± 0.003), however, they found a higher estimate between HCW and BF (0.31 ± 0.005). Savoia et al. (2019) reported absence of genetic correlation between HCW and LMA (0.003 ± 0.116) in young Piemontese bulls.

In general, the marbling index can be considered a determining factor in the tenderness of beef (Warner et al., 2021). This relationship is supported by the strong and favorable genetic correlation estimates reported by Wheeler et al. (2010) and Mateescu et al. (2014), which were -0.52 and -0.50, respectively, suggesting that a lower shear force is genetically associated with higher marbling scores. Similar, genetic correlations between IMF and SF were estimated by the same authors to be -0.52 (Wheeler et al., 2010) and -0.47 (Mateescu et al., 2014). However, the role of intramuscular fat content on beef tenderness is still quite controversial. Reverter et al. (2003), studying bovine breeds of temperate climate (TEMP) and breeds adapted to tropical climate (TROP), observed genetic associations between IMF and SF of -0.38 and -0.09, for TEMP and TROP, respectively, concluding that the inconsistencies between the estimates are likely due to differences in genetic architecture between breeds, or to other factors such as age differences and environmental influence on traits.

In the literature, genetic associations between intramuscular fat content and marbling scores are high and positive. Several studies using pure or composite Taurine breeds have obtained estimates ranging from 0.56 to 1.00 (MacNeil et al., 2010; Wheeler et al., 2010; McAllister et al., 2011; Mateescu et al., 2014), which is expected

since these two traits are different ways of measuring the amount of fat in the meat. Working with Nellore animals, Bonin et al. (2021) reported estimates of the genetic correlation between MARB and IMF measured in meat samples taken from the Longissimus muscle in the 5th and 12th ribs, of 0.74 and 0.78, respectively, results consistent with the findings for the *Bos taurus* breeds and their crosses.

Estimates of genetic correlations found in the literature between carcass and meat quality traits vary between studies, from different magnitudes to opposite signs of association. Gordo et al. (2018) reported a correlation of -0.47 between SF and LMA for Nellore cattle, indicating that selection for a higher yield of meat cuts should lead to favorable correlated responses in meat tenderness. In contrast, Wheeler et al. (2010) reported a correlation of 0.28 between SF and LMA, similar to that estimated by Reverter et al. (2003), that obtained a value of 0.27 for the group of Taurine animals (TEMP), and a low relationship between the traits (-0.14) for the group of animals of tropical climate (TROP). Between SF and HCW, Gordo et al. (2018) estimated a genetic correlation of -0.27, in agreement with the findings by Reverter et al. (2003), who reported similar estimates between the two groups of animals studied, of -0.20 (TEMP) and -0.21 (TROP). In turn, Wheeler et al. (2010) reported an association of 0.46, contrary to the results found by the authors previously mentioned. Between SF and BF, the traits were not genetically correlated in the study carried out by Gordo et al. (2018), suggesting that selection for one trait should not imply genetic gains in the other. However, Smith et al. (2007) reported correlation estimates between BF and tenderness at 7- and 14-day of maturation of -0.82 and -0.36, respectively. These divergences may be due to differences between the studied populations, adopted managements, and applied methodologies.

Among the associations between marbling index and carcass composition traits, Gordo et al. (2018) obtained positive correlations of low and moderate magnitude, between MARB–BF (0.14) and MARB–LMA (0.38), respectively, and close to zero between MARB–HCW (-0.04), suggesting that in the long and medium term, the production of carcasses with greater finish or ribeye area should promote genetic progress towards marbling. Smith et al. (2007) estimated a genetic correlation of 0.17 between MARB and LMA, supporting, partially, the one reported by Gordo et al. (2018), however, obtained discordant estimates for MARB–BF (0.04) and MARB–HCW (0.51),

indicating that part of genes expressing HCW have an influence on MARB. Wheeler et al. (2010), contrary to the studies cited, reported estimates of -0.13 ± 0.18 and -0.28 ± 0.26 between MARB–LMA, and MARB–HCW, respectively. However, the genetic correlation estimates in the study by Wheeler et al. (2010) showed high standard errors, indicating low predictive reliability, requiring caution in interpreting the results.

The associations of intramuscular fat content and ribeye area indicate an antagonism in the action of shared genes between traits, with correlation estimates ranging from -0.15 to -0.22 (Reverter et al., 2003; Wheeler et al., 2010). For HCW, the genetic associations with IMF were -0.03 and -0.30, according to the studies carried out by Reverter et al. (2003) and Wheeler et al. (2010), suggesting nullity or an antagonism in the expression of characteristics. Torres-Vazquez et al. (2018), working with an Australian Angus herd, found divergent estimates from the aforementioned authors, of 0.06 for IMF–LMA and 0.21 for IMF–HCW. The authors also reported a low, negative genetic correlation of -0.11 between IMF and BF. Differently, in a recent study with Nellore cattle, Bonin et al. (2021) obtained genetic correlations between IMF and BF of 0.17 and 0.41, when IMF was measured in muscle samples taken from the 5th and 12th rib, respectively, indicating that both IMF and BF must have genes in common acting in the same direction on fat metabolism.

Considering the scarcity of information in the literature, it is necessary to design studies, as well as to develop methodologies and tools that seek to improve the accuracy of genetic evaluations. Moreover, it will be useful to better elucidate the relationship between female sexual precocity, carcass composition and meat quality traits, in order to find economically viable alternatives to improve them and thus achieve sustainable and high-quality production of Nellore meat.

2.5. Genome-wide association studies

Genome-wide association studies (GWAS) aim to associate genomic regions with the phenotypes of interest through statistical analysis. Identification of variations in the genome (mainly single nucleotide polymorphisms - SNP) linked to or in regions (QTL - Quantitative Trait Loci) with great effect on a given characteristic, can provide a better understanding of biological functions and genetic influence on phenotypic

expression (Zhang et al., 2012; Yang et al., 2013; Magalhães et al., 2016; Magalhães et al., 2019; Pegolo et al., 2020).

GWAS studies explore the existence of linkage disequilibrium (LD), which is an existing correlation structure between SNP and variants in the genome, resulting from evolutionary events, such as mutation, drift, and selection (Visscher et al., 2012; Visscher et al., 2017). Thus, LD structures arise because, when molecular markers are passed from one generation to another, in the absence of recombination, markers close to each other tend to be inherited together, causing alleles or SNP to correlate with each other in close regions in the DNA sequence (Lee et al., 2017).

SNP are sequence polymorphisms, caused by the mutation of a single nucleotide at a specific locus in the DNA sequence. For a variation to be considered a molecular marker of the SNP type, the least frequent allele (MAF) must be present in at least 1% in the population (Brookes, 1999; Vignal et al., 2002). Currently, SNP are the most used markers in association studies, as they are widely distributed across the genome, with the necessary density for fine mapping (Vignal et al., 2002), in addition to the possibility of being in LD with the regions responsible for the expression of economically important traits (Zhang et al., 2012). With the emergence and availability of high-density SNP panels, it became possible to measure the variability found within the bovine genome in studies of genomic similarity, in order to characterize genomic regions and genetic profiles associated with several phenotypes (Mudado et al., 2016).

One of the methods widely used in genomic evaluations is the single-step GBLUP (ssGBLUP), which was initially proposed by Misztal et al. (2009) and adapted for association analysis (ssGWAS) by Wang et al. (2012). This procedure, simultaneously, combines pedigree information, phenotypes and genotypes in a single step analysis, through the construction of relationship matrix H which encompass genomic (G) and pedigree-based (A) relationship matrices (Wang et al., 2012). The advantages of ssGWAS are that the method allows obtaining more accurate genomic evaluations in a simple way and fast computation, it can incorporate data from non-genotyped animals without the need to use pseudophenotypes, besides calculating the effects of each SNP and to estimate variations of these effects in the genome (Aguilar et al., 2010; Wang et al., 2012).

In beef cattle, few studies have identified genetic variants associated with carcass traits and meat quality in Nellore breed (Tizioto et al., 2013; Espigolan et al., 2015; Fernandes Júnior et al., 2016b; Lemos et al., 2016; Magalhães et al., 2016; Castro et al., 2017; Oliveira Silva et al., 2017). Using high-density (~770k) SNP genotyping data in Nellore cattle, Fernandes Júnior et al. (2016b) confirmed the polygenic nature of carcass traits, reporting important genomic regions distributed in 16 of 29 autosome chromosomes. In the study, the authors highlighted regions on chromosomes 5, 7, 8, 10, 12, 20, and 29 explaining 8.72% of the additive genetic variance for the eye area of the Longissimus muscle (LMA). Among the genes found, *TSHR*, *CDKN2A/CDKN2B*, *SLC38A1/SLC38A2* and *WWC1* stand out (Fernandes Júnior et al.; 2016b). These genes are involved in thyroid cell metabolism, cell cycle regulation, amino acid transport, and cell proliferation, respectively (van den Heuvel, 2005; Klimienė et al., 2008; Schiöth et al., 2013; Wennmann et al., 2014; Fernandes Júnior et al., 2016b), functions that can influence muscle growth.

Oliveira Silva et al. (2017), identified genomic regions located on chromosomes 1, 6, 7, 8, 14, 15, 21, 24, and 28 associated with LMA in Nellore cattle and highlighted the genes *ALKBH3* and *HSD17B12* both playing a role in DNA repair, being related to fibroblast death (Nay et al., 2012) and steroid metabolism (Visus et al., 2011), respectively. Saatchi et al. (2014) conducted a series of genomic association studies using 50k panel genotyped data for different *Bos taurus* breeds. The authors identified QTL in the genomic regions in BTA6 and BTA14, regions later identified in the study by Oliveira Silva et al. (2017) and in BTA5, later identified by Fernandes Júnior et al. (2016b). These QTL, also harbor genes that have been associated with birth weight, weaning weight, yearling weight, mature weight, carcass weight, carcass yield, lipid content, and calving ease, indicating that QTL have pleiotropic properties (Saatchi et al., 2014).

Liu et al. (2019) performed a GWAS to systematically detect additive and dominance variants for different traits in Chinese Simmental cattle. The authors detected *FGF5* gene, in additive association with carcass weight (HCW), which is a gene of the Fibroblast Growth Factor (FGF) family, a group that is involved in embryonic development, cell growth, morphogenesis, tissue repair, tumor growth, and invasion (Ornitz and Itoh, 2015; Liu et al.; 2019). Working with a Nellore cattle

population, Espigolan et al. (2015) identified the *EFCAB8* and *VSTM2L* genes, both related to skeletal muscle formation and development (Maki et al., 2002; Rossini et al., 2011; Espigolan et al., 2015), and might be excellent candidates for HCW. Furthermore, *EFCAB8* belongs to the EF-hand calcium binding family, a set of genes that act directly on calpain and sorcin, proteins related to muscle synthesis and modulation of cellular Ca^{2+} channels, respectively (Espigolan et al., 2015).

Through haplotype block analysis, Utsunomiya et al. (2017) reported that a mutation in the *PLAG1* gene was associated with body size, weight, and reproduction in cattle. Functional evidences report that *PLAG1* expresses a transcription factor that regulates IGF-2, insulin-like growth factor 2 (Van Dyck et al., 2007; Fortes et al., 2013; Utsunomiya et al., 2017). Fernandes Júnior et al. (2016b) identified and highlighted *PLAG1* (BTA14) as the most promising gene associated with carcass weight, as it has a pleiotropic effect on several traits of economic interest in livestock (Fortes et al., 2013). Oliveira Silva et al. (2017) reported the same genomic region in BTA14, explaining 1.89% of the additive variance, linked to the expression of subcutaneous fat thickness (BF) in Nellore cattle. Comparing different approaches for GWAS studies (ssGWAS, Bayes A and Bayes B), Hay and Roberts (2018) identified *LYN* and *RPS20* in BTA14 associated with BF in the three methods used, consistent with the reports by Oliveira Silva et al. (2017), showing the high influence of the 24Mb region on chromosome 14 for carcass traits.

In the study by Oliveira Silva et al. (2017), 16 windows were associated with BF explaining more than 14% of the total genetic variance. The authors found the *XKR4* gene, located on chromosome 14, previously identified as a candidate for rump fat thickness (Porto Neto et al., 2012). The gene *XKR4* has been linked to the regulation of prolactin secretion in cattle (Bastin et al., 2014). In research conducted in hamsters, Cincotta and Meier (1987) observed a reduction in abdominal fat stores due to inhibition of prolactin secretion, concluding that the hormone plays an important role in the regulation of fat metabolism.

In the search for candidates related to variation in meat and carcass traits in Nellore cattle, Tizioto et al. (2013) found a cluster of 20 genes associated with BF, acting in neuroactive ligand-receptor interaction pathway, indicating that the genes connected to this pathway play a role in the deposition of fat in beef cattle. Investigating

the regulation of adipogenesis in a transcriptome study, Khan et al. (2020) confirmed the evidence of Tizioto et al. (2013) by identifying differentially expressed genes involved in the fat deposition process in cattle, acting in neuroactive ligand-receptor interaction pathway.

Also, in the study by Tizioto et al. (2013), genes for calpain and calpastatin associated with measures of meat tenderness at different stages of maturation were identified. The proteolytic system of calpain (CAPN1) is the main factor responsible for myofibrillar proteolysis during the *post-mortem* period, providing tenderness to meat. Calpastatin (CAST) is a regulator of *post-mortem* proteolysis, acting in the inhibition of CAPN1 and its increased activity leads to reduced tenderization of the meat (Koochmaraie, 1996). In this sense, it can be said that calpain and calpastatin genes are excellent candidates based on their biological functions and associations with beef tenderness. Several studies have reported *CAPN1* and *CAST* associated with the tenderness of *Bos taurus* meat (Smith et al., 2000; Gill et al., 2009; Bolormaa et al., 2011; McClure et al., 2012; Ramayo-Caldas et al., 2016). However, few studies have observed the same genes related to meat quality traits in *Bos indicus* populations and their crosses (Tizioto et al., 2013; Magalhães et al., 2016; Leal-Gutiérrez et al., 2018). In a study associating μ -Calpain and Calpastatin polymorphisms with meat tenderness in a multibreed Angus–Brahman herd, Leal-Gutiérrez et al. (2018) found a significant effect on meat tenderness ($p < 0.0001$) in animals with more than 80% Angus composition, thus it is expected that crossbreds tend to segregate a higher percentage of tenderness related alleles than pure Zebu breeds. These references show that genetic polymorphisms discovered in *Bos taurus* animals cannot be predictive in *Bos indicus* populations (Leal-Gutiérrez et al., 2019).

Given the genetic differences between zebu and taurine animals, different regions of QTL have been reported in the literature associated with the marbling index (MARB). For example, Bedhane et al. (2019), when performing a genome-wide scanning study for meat quality traits in Hanwoo cattle, identified the *GALR1* gene close to the most significant SNP in BTA24 for MARB. *GALR1* is responsible for binding neuropeptides and peptide hormones (Jurkowski et al., 2013), in addition to being associated with the synthesis of bioactive lipids, lipids that affect cell functions due to changes in their concentration (Contos et al., 2002; Bedhane et al., 2019).

Several bioactive lipids were associated with the marbling index in Wagyu–dairy cross beef cattle (Bermingham et al., 2018) and, considering that all Wagyu's fame is attributed to the high degree of marbling of its meat, *GALR1* becomes a candidate gene option for MARB.

In the Nellore breed, Magalhães et al. (2016) located genomic regions associated with marbling, on chromosomes 5, 15, 16, and 25, explaining 3.89% of the total additive genetic variance. The authors observed that marbling and tenderness of the meat shared the same QTL in the BTA5, an interesting result since there is evidence that the marbling score gives the meat a feeling of tenderness (Wheeler et al., 2010; Mateescu et al., 2017; Luo et al., 2018). In the same study, the *TNFRSF12A* (BTA25) gene was identified, a TNF receptor superfamily member, associated with MARB. There are no reports in the literature on the role of this family of genes in regulating pathways associated with intramuscular fat deposition. However, Fonseca et al. (2020) through transcriptomics analysis, identified the *TNFRSF12A* gene differentially expressed in muscle tissue of Nellore cattle, associated with a low marbling score, corroborating with the finding by Magalhães et al. (2016).

Another way to assess the intramuscular fat content of beef is by determining the percentage of lipids (IMF) through chemical analysis. However, studies investigating genomic regions associated with this measure are scarce in the literature, especially for Zebu breeds. In a survey conducted in Taurine animals, Hay and Roberts (2018) identified *LYN* and *LYPLA1* associated with intramuscular fat content and subcutaneous fat thickness, genes that were previously related to feeding intake and growth in cattle (Lindholm-Perry et al., 2011). In addition, the region of chromosome 14 that harbors these genes has been associated with several other phenotypes of economic interest in livestock (Lindholm-Perry et al., 2011; Fortes et al., 2013; Fernandes Júnior et al., 2016b; Oliveira Silva et al., 2017; Magalhães et al., 2016; Hay and Roberts, 2018). In the same study, Hay and Roberts (2018) identified the *SCD5* gene in a QTL on BTA6 that explained 1.47% of the additive genetic variance for IMF. *SCD5* is a member of the family of genes that encode stearoyl-coenzyme A desaturase (SCD), an integral membrane protein of the endoplasmic reticulum, associated with increased fat accumulation, which catalyzes the conversion of saturated to monounsaturated fatty acids in several body tissues (Zheng et al., 2001; Lengi and

Corl, 2008). Considering the important role that these genes play in lipid biosynthesis, *SCD5* may be of interest to improve the quality and accumulation of fat in beef.

In general, traits of economic importance in beef cattle are polygenic in nature and are under the control of genetic and environmental factors. Therefore, detecting variations within the genome associated with carcass composition and meat quality traits can be a great challenge, mainly because these traits are controlled by numerous genes with small effects. Thus, conducting genome-wide association studies, aiming to investigate regions of great effect on carcass and meat quality traits, is of importance to identifying new genes, as well as validating those already found in the literature, in order to better understand the biological processes involved in the expression and, consequently, the phenotypic variability of these traits.

3. OBJECTIVES

3.1. General objective

To estimate genetic parameters for female sexual precocity, carcass and meat quality traits and carry out a genomic-wide association study (GWAS) for carcass and meat quality traits in Nellore cattle, aiming to better understand the genetic inheritance of these traits in order to contribute for the genetic evaluation including genomic information in beef cattle in Brazil.

3.2. Specific objectives

- Estimate (co)variance components and genetic parameters for female sexual precocity (age at first calving and scrotal circumference), carcass (longissimus muscle area, backfat thickness, and hot carcass weight), and meat quality traits (tenderness, marbling, and intramuscular fat content) in Nellore cattle, using genomic information;
- Conduct GWAS in order to identify genomic regions and potential candidate genes acting in biological processes and metabolic pathways of meat and carcass traits.

4. REFERENCES

- Aguilar, I.; Misztal, I.; Johnson, D. L.; Legarra, A.; Tsuruta, S.; Lawlor, T. J. Hot topic: A unified approach to utilize phenotypic, full pedigree, and genomic information for genetic evaluation of Holstein final score. **Journal of Dairy Science**, v. 93, n. 2, p. 743-752, 2010.
- Albuquerque, L. G. Mercadante, M. E. Z.; Eler, J. P. Recent studies on the genetic basis for the selection of *Bos indicus* for beef production. In: **Proceedings of the 8th World Congress on Genetics Applied to Livestock Production, Belo Horizonte, Minas Gerais, Brazil, 13-18 August, 2006**. Instituto Prociência, 2006. p. 03-22.
- Almeida, A. K.; Michels, I. L. O Brasil e a economia-mundo: o caso da carne bovina. **Ensaio FEE**, v. 33, n. 1, 2012.
- Arshad, M. S.; Sohaib, M.; Ahmad, R. S.; Nadeem, M. T.; Imran, A.; Arshad, M. U.; Kwon, J. H.; Amjad, Z. Ruminant meat flavor influenced by different factors with special reference to fatty acids. **Lipids in health and disease**, v. 17, n. 1, p. 223, 2018.
- Associação Brasileira Das Indústrias Exportadoras De Carne (ABIEC). **Beef Report: Perfil da Pecuária no Brasil**. 2019. Disponível em: <http://abiec.com.br/publicacoes/beef-report-2019/.aspx>. Acesso em: 07 de abr. 2020.
- Baldassini, W. A.; Chardulo, L. A. L. et al. Meat quality traits of Nellore bulls according to different degrees of backfat thickness: a multivariate approach. **Animal Production Science**, v. 57, n. 2, p. 363-370, 2017.
- Bastin, B. C., Houser, A. et al. A polymorphism in XKR 4 is significantly associated with serum prolactin concentrations in beef cows grazing tall fescue. **Animal genetics**, v. 45, n. 3, p. 439-441, 2014.
- Bedhane, M.; van der Werf, J.; Gondro, C.; Duijvesteijn, N.; Lim, D.; Park, B.; Park, M. N.; Hee, R. S.; Clark, S. Genome-Wide Association Study of Meat Quality Traits in Hanwoo Beef Cattle Using Imputed Whole-Genome Sequence Data. **Frontiers in genetics**, v. 10, p. 1235, 2019.
- Bermingham, E. N.; Reis, M. G.; Subbaraj, A. K.; Cameron-Smith, D.; Fraser, K.; Jonker, A.; Craigie, C. R. Distribution of fatty acids and phospholipids in different

- table cuts and co-products from New Zealand pasture-fed Wagyu-dairy cross beef cattle. **Meat science**, v. 140, p. 26-37, 2018.
- Bertrand, J. K.; Green, R. D.; Herring, W. O.; Moser, D. W. et al. Genetic evaluation for beef carcass traits. **Journal of animal science**, v. 79, n. suppl_E, p. E190-E200, 2001.
- Bhuiyan, M. S. A.; Kim, H. J.; Lee, D. H.; Lee, S. H.; Cho, S. H.; Yang, B. S.; Kim, S. D.; Lee, S. H. Genetic parameters of carcass and meat quality traits in different muscles (longissimus dorsi and semimembranosus) of Hanwoo (Korean cattle). **Journal of animal science**, v. 95, n. 8, p. 3359-3369, 2017.
- Boldt, R. J.; Speidel, S. E.; Thomas, M. G.; Keenan, L.; Enns, R. M. Genetic parameters for production traits and heifer pregnancy in Red Angus cattle. **Journal of Animal Science**, v. 94, p. 187-187, 2016.
- Boligon, A. A.; Albuquerque, L. G.; Mercadante, M. E. Z.; Lôbo, R. B. Study of relations among age at first calving, average weight gains and weights from weaning to maturity in Nelore cattle. **Revista Brasileira de Zootecnia**, v. 39, p. 746-751, 2010.
- Boligon, A. A.; Silveira, F. A.; Silveira, D. D.; Dionello, N. J. L.; Santana Junior, M. L.; Bignardi, A. B.; Souza, F. R. P. Reduced-rank models of growth and reproductive traits in Nelore cattle. **Theriogenology**, v. 83, n. 8, p. 1338-1343, 2015.
- Bolormaa, S.; Porto Neto, L. R.; Zhang, Y. D.; Bunch, R. J.; Harrison, B. E.; Goddard, M. E.; Barendse, W. A genome-wide association study of meat and carcass traits in Australian cattle. **Journal of animal science**, v. 89, n. 8, p. 2297-2309, 2011.
- Bonin, M. N.; Pedrosa, V. B. et al. Genetic parameters associated with meat quality of Nelore cattle at different anatomical points of longissimus: Brazilian standards. **Meat Science**, v. 171, p. 108281, 2021.
- Brookes, A. J. The essence of SNPs. **Gene**, v. 234, n. 2, p. 177-186, 1999.
- Brumatti, R. C.; Ferraz, J. B. S.; Eler, J. P.; Formigoni, I. B. Desenvolvimento de índice de seleção em gado corte sob o enfoque de um modelo bioeconômico. **Archivos de zootecnia**, v. 60, n. 230, p. 205-213, 2011.
- Brunes, L. C.; Baldi, F.; e Costa, M. F. O.; Lobo, R. B.; Lopes, F. B.; Magnabosco, C. U. Genetic-quantitative analysis for reproductive traits in Nellore cattle selected for sexual precocity. **Animal Production Science**, v. 60, n. 7, p. 896-902, 2020.

- Buzanskas, M. E.; Pires, P. S.; Chud, T. C. S.; Bernardes, P. A.; Rola, L. D.; Savegnago, R. P.; Lôbo, R. B.; Munari, D. P. Parameter estimates for reproductive and carcass traits in Nelore beef cattle. **Theriogenology**, v. 92, p. 204-209, 2017.
- Caetano, S. L.; Savegnago, R. P.; Boligon, A. A.; Ramos, S. B.; Chud, T. C. S.; Lôbo, R. B.; Munari, D. P. Estimates of genetic parameters for carcass, growth and reproductive traits in Nelore cattle. **Livestock Science**, v. 155, n. 1, p. 1-7, 2013.
- Cardoso, R. C.; Alves, B. R. C.; Sharpton, S. M.; Williams, G. L.; Amstalden, M. Nutritional programming of accelerated puberty in heifers: involvement of pro-opiomelanocortin neurones in the arcuate nucleus. **Journal of neuroendocrinology**, v. 27, n. 8, p. 647-657, 2015.
- Carvalho, M. E.; Baldi, F. S. et al. Genomic regions and genes associated with carcass quality in Nelore cattle. **Genetics and Molecular Research**, v. 18, n. 1, p. 1-15, 2019.
- Carvalho, T. H.; Fernandes, E. A. Demandas de importação e exportação: uma análise para o setor agropecuários brasileiro. **Revista de Desenvolvimento e Políticas Públicas**, v. 1, n. 1, p. 55-69, 2017.
- Castro, L. M.; Rosa, G. J. M.; Lopes, F. B.; Regitano, L. C. A.; Rosa, A. J. M.; Magnabosco, C. U. Genomewide association mapping and pathway analysis of meat tenderness in Polled Nelore cattle. **Journal of animal science**, v. 95, n. 5, p. 1945-1956, 2017.
- Ceacero, T. M.; Mercadante, M. E. Z.; Cyrillo, J. N. S. G.; Canesin, R. C.; Bonilha, S. F. C.; Albuquerque, L. G. Phenotypic and genetic correlations of feed efficiency traits with growth and carcass traits in Nelore cattle selected for postweaning weight. **PLoS One**, v. 11, n. 8, p. e0161366, 2016.
- Cesar, A. S. M.; Regitano, L. C. A. et al. Genome-wide association study for intramuscular fat deposition and composition in Nelore cattle. **BMC genetics**, v. 15, n. 1, p. 1-15, 2014.
- Cesar, A. S. M.; Regitano, L. C. A. et al. Putative regulatory factors associated with intramuscular fat content. **PloS one**, v. 10, n. 6, p. e0128350, 2015.
- Cincotta, A. H.; Meier, A. H. Reduction of body fat stores by inhibition of prolactin secretion. **Experientia**, v. 43, n. 4, p. 416-417, 1987.
- Contos, J. J. A.; Ishii, I.; Fukushima, N.; Kingsbury, M. A.; Ye, X.; Kawamura, S.;

- Beown, H.; Chun, J. Characterization of Ipa2 (Edg4) and Ipa1/Ipa2 (Edg2/Edg4) lysophosphatidic acid receptor knockout mice: signaling deficits without obvious phenotypic abnormality attributable to Ipa2. **Molecular and cellular biology**, v. 22, n. 19, p. 6921-6929, 2002.
- Costa, E. V.; Ventura, H. T.; Veroneze, R.; Silva, F. F.; Pereira, M. A.; Lopes, P. S. Estimated genetic associations among reproductive traits in Nellore cattle using Bayesian analysis. **Animal reproduction science**, v. 214, p. 106305, 2020.
- Costa, N. V.; Aboujaoude C.; Vieira, G. S.; Paiva, V. V.; Moraes Neto, R. A.; Gondim, V. S.; Alves, L. R.; Torres, M. C. L.; Antunes, R. C. Carcass and meat quality traits in Nellore and F1 Nellore-Araguaia crosses. **Genetics and Molecular Research**, v. 14, n. 2, p. 5379-5389, 2015.
- Crouse, J. D.; Cundiff, L. V.; Koch, R. M.; Koohmaraie, M.; Seideman, S. C. Comparisons of *Bos indicus* and *Bos taurus* inheritance for carcass beef characteristics and meat palatability. **Journal of Animal Science**, v. 67, n. 10, p. 2661-2668, 1989.
- Cundiff, L. V. Genetic selection to improve the quality and composition of beef carcasses. In: **Proc. Rec. Meat Conference, Colorado State University**. 1992. p. 123-31.
- Cundiff, L. V.; Pond, W. G.; Bell, A. W. Beef cattle: Breeds and genetics. **Encyclopedia of Animal Science**. Ithaca: **Cornell University**, p. 74-76, 2004.
- Do, C.; Park, B.; Kim, S.; Choi, T.; Yang, B.; Park, S.; Song, H. Genetic parameter estimates of carcass traits under national scale breeding scheme for beef cattle. **Asian-Australasian journal of animal sciences**, v. 29, n. 8, p. 1083, 2016.
- Eler, J. P.; Bignardi, A. B.; Ferraz, J. B. S.; Santana Junior, M. L. Genetic relationships among traits related to reproduction and growth of Nelore females. **Theriogenology**, v. 82, n. 5, p. 708-714, 2014.
- Elzo, M. A.; Mateescu, R. G. et al. Genomic-polygenic and polygenic predictions for nine ultrasound and carcass traits in Angus-Brahman multibreed cattle using three sets of genotypes. **Livestock Science**, v. 202, p. 58-66, 2017.
- Espigolan, R.; Baldi, F. et al. Associations between single nucleotide polymorphisms and carcass traits in Nellore cattle using high-density panels. **Genetics and Molecular Research**, v. 22, p. 11133-11144, 2015.

- Feitosa, F. L. B.; Olivieri, B. F. et al. Genetic correlation estimates between beef fatty acid profile with meat and carcass traits in Nelore cattle finished in feedlot. **Journal of applied genetics**, v. 58, n. 1, p. 123-132, 2017.
- Fernandes Júnior, G. A. F.; Rosa, G. J. M. et al. Genomic prediction of breeding values for carcass traits in Nelore cattle. **Genetics Selection Evolution**, v. 48, n. 1, p. 7, 2016a.
- Fernandes Júnior, G. A.; Costa, R. B. et al. Genome scan for postmortem carcass traits in Nelore cattle. **Journal of animal science**, v. 94, n. 10, p. 4087-4095, 2016b.
- Ferraz, J. B. S.; Felício, P. E. Production systems—An example from Brazil. **Meat science**, v. 84, n. 2, p. 238-243, 2010.
- Ferraz, M. V. C.; Pires, A. V.; Santos, M. H.; Silva, R. G.; Oliveira, G. B.; Polizel, D. M.; Biehl, M. V.; Sartori, R.; Nogueira, G. P. A combination of nutrition and genetics is able to reduce age at puberty in Nelore heifers to below 18 months. **animal**, v. 12, n. 3, p. 569-574, 2018.
- Fonseca, L. F. S.; Gimenez, D. F. J.; Santos Silva, D. B.; Barthelson, R.; Baldi, F.; Ferro, J. A.; Albuquerque, L. G. Differences in global gene expression in muscle tissue of Nelore cattle with divergent meat tenderness. **BMC genomics**, v. 18, n. 1, p. 945, 2017.
- Fonseca, L. F. S.; Santos Silva, D. B.; Gimenez, D. F. J.; Baldi, F.; Ferro, J. A.; Chardulo, L. A. L.; Albuquerque, L. G. Gene expression profiling and identification of hub genes in Nelore cattle with different marbling score levels. **Genomics**, v. 112, n. 1, p. 873-879, 2020.
- Fortes, M. R. S.; Kemper, K. et al. Evidence for pleiotropism and recent selection in the PLAG1 region in Australian Beef cattle. **Animal genetics**, v. 44, n. 6, p. 636-647, 2013.
- Gill, J. L.; Bishop, S. C.; McCorquodale, C.; Williams, J. L.; Wiener, P. Association of selected SNP with carcass and taste panel assessed meat quality traits in a commercial population of Aberdeen Angus-sired beef cattle. **Genetics Selection Evolution**, v. 41, n. 1, p. 1-12, 2009.
- Goddard, M. E.; Hayes, B. J. Mapping genes for complex traits in domestic animals and their use in breeding programmes. **Nature Reviews Genetics**, v. 10, n. 6, p.

- 381-391, 2009.
- Gomes, R. C.; Feijó, G. L. D.; Chiari, L. Evolução e Qualidade da Pecuária Brasileira. **EMBRAPA**, 2017.
- Gordo, D. G. M.; Baldi, F.; Lôbo, R. B.; Koury Filho, W.; Sainz, R. D.; Albuquerque, L. G. Genetic association between body composition measured by ultrasound and visual scores in Brazilian Nelore cattle. **Journal of Animal Science**, v. 90, n. 12, p. 4223-4229, 2012.
- Gordo, D. G. M.; Espigolan, R.; Bresolin, T.; Fernandes Júnior, G. A.; Magalhães, A. F. B.; Braz, C. U.; Fernandes, W. B.; Baldi, F.; Albuquerque, L. G. Genetic analysis of carcass and meat quality traits in Nelore cattle. **Journal of animal science**, v. 96, n. 9, p. 3558-3564, 2018.
- Hay; E. H.; Roberts, A. Genome-wide association study for carcass traits in a composite beef cattle breed. **Livestock Science**, v. 213, p. 35-43, 2018.
- Jakobsen, M. U.; Overvad, K.; Dyerberg, J.; Heitmann, B. L. Intake of ruminant trans fatty acids and risk of coronary heart disease. **International journal of epidemiology**, v. 37, n. 1, p. 173-182, 2008.
- Jiang, M.; Fan, W. L. et al. Effects of balanced selection for intramuscular fat and abdominal fat percentage and estimates of genetic parameters. **Poultry science**, v. 96, n. 2, p. 282-287, 2017.
- Jurkowski, W.; Yazdi, S.; Elofsson, A. Ligand binding properties of human galanin receptors. **Molecular membrane biology**, v. 30, n. 2, p. 206-216, 2013.
- Khan, R.; Raza, S. H. A. et al. RNA-seq reveal role of bovine TORC2 in the regulation of adipogenesis. **Archives of biochemistry and biophysics**, v. 680, p. 108236, 2020.
- Klimienė, I.; Mockeliūnas, R.; Spakauskas, V.; Černauskas, A.; Sakalauskienė, R. Review Metabolic changes of thyroid hormones in cattle. **Vet. Zootech.** v. 42, n. 64, 2008.
- Kluska, S.; Olivieri, B. F. et al. Estimates of genetic parameters for growth, reproductive, and carcass traits in Nelore cattle using the single step genomic BLUP procedure. **Livestock science**, v. 216, p. 203-209, 2018.
- Koohmaraie, M. Biochemical factors regulating the toughening and tenderization processes of meat. **Meat science**, v. 43, p. 193-201, 1996.

- Lacerda, V. V.; Campos, G. S.; Roso, V. M.; Souza, F. R. P.; Brauner, C. C.; Boligon, A. A. Effect of mature size and body condition of Nelore females on the reproductive performance. **Theriogenology**, v. 118, p. 27-33, 2018.
- Leal-Gutiérrez, J. D.; Elzo, M. A.; Johnson, D. D.; Hamblen, H.; Mateescu, R. G. Genome wide association and gene enrichment analysis reveal membrane anchoring and structural proteins associated with meat quality in beef. **BMC genomics**, v. 20, n. 1, p. 151, 2019.
- Leal-Gutiérrez, J. D.; Elzo, M. A.; Johnson, D. D.; Scheffler, T. L.; Scheffler, J. M.; Mateescu, R. G. Association of μ -calpain and calpastatin polymorphisms with meat tenderness in a brahman–angus population. **Frontiers in genetics**, v. 9, p. 56, 2018.
- Lee, S.; Yang, J.; Huang, J.; Chen, H.; Hou, W.; Wu, S. Multi-marker linkage disequilibrium mapping of quantitative trait loci. **Briefings in bioinformatics**, v. 18, n. 2, p. 195-204, 2017.
- Lengi, A. J.; Corl, B. A. Comparison of pig, sheep and chicken SCD5 homologs: Evidence for an early gene duplication event. *Comparative Biochemistry and Physiology Part B: Biochemistry and Molecular Biology*, v. 150, n. 4, p. 440-446, 2008.
- Lindholm-Perry, A. K. Kuehn, L. A.; Smith, T. P. L.; Ferrell, C. L.; Jenkins, T. G.; Freetly, H. C.; Snelling, W. M. A region on BTA14 that includes the positional candidate genes LYPLA1, XKR4 and TMEM68 is associated with feed intake and growth phenotypes in cattle 1. **Animal genetics**, v. 43, n. 2, p. 216-219, 2011.
- Liu, Y.; Xu, L. et al. Genomic Prediction and Association Analysis with Models Including Dominance Effects for Important Traits in Chinese Simmental Beef Cattle. **Animals**, v. 9, n. 12, p. 1055, 2019.
- Lopes, F. B.; Magnabosco, C. U. et al. Improving genomic prediction accuracy for meat tenderness in Nelore cattle using artificial neural networks. **Journal of Animal Breeding and Genetics**, v. 137, n. 5, p. 438-448, 2020.
- Luchiari Filho, A. **Pecuária da carne bovina**. 1. ed. São Paulo: Edição do autor, 2000. 134p.
- Luo, L.; Guo, D.; Zhou, G.; Chen, K. An investigation on the relationship among marbling features, physiological age and Warner–Bratzler Shear force of steer

- longissimus dorsi muscle. **Journal of food science and technology**, v. 55, n. 4, p. 1569-1574, 2018.
- MacNeil, M. D.; Nkrumah, J. D.; Woodward, B. W.; Northcutt, S. L. Genetic evaluation of Angus cattle for carcass marbling using ultrasound and genomic indicators. **Journal of animal science**, v. 88, n. 2, p. 517-522, 2010.
- Magalhães, A. F. B.; Camargo, G. M. F. et al. Genome-wide association study of meat quality traits in Nelore cattle. **PloS one**, v. 11, n. 6, p. e0157845, 2016.
- Magalhães, A. F. B.; Schenkel, F. S. et al. Genomic selection for meat quality traits in Nelore cattle. **Meat science**, v. 148, p. 32-37, 2019.
- Magalhães, A. F. B.; Teixeira, G. H. A. et al. Prediction of meat quality traits in Nelore cattle by near-infrared reflectance spectroscopy. **Journal of animal science**, v. 96, n. 10, p. 4229-4237, 2018.
- Magnabosco, C. U.; Lopes, F. B.; Fragoso, R. R.; Eifert, E. C.; Valente, B. D.; Rosa, G. J. M.; Sainz, R. D. Accuracy of genomic breeding values for meat tenderness in Polled Nelore cattle. **Journal of animal science**, v. 94, n. 7, p. 2752-2760, 2016.
- Maki, M.; Kitaura, Y.; Satoh, H.; Ohkouchi, S.; Shibata, H. Structures, functions and molecular evolution of the penta-EF-hand Ca²⁺-binding proteins. **Biochimica et Biophysica Acta (BBA)-Proteins and Proteomics**, v. 1600, n. 1-2, p. 51-60, 2002.
- Martins, T. S.; Sanglard, L. M. P. et al. Molecular factors underlying the deposition of intramuscular fat and collagen in skeletal muscle of Nelore and Angus cattle. **PLoS One**, v. 10, n. 10, p. e0139943, 2015.
- Mateescu, R. G.; Garrick, D. J.; Garmyn, A. J.; VanOverbeke, D. L.; Mafi, G. G.; Reecy, J. M. Genetic parameters for sensory traits in longissimus muscle and their associations with tenderness, marbling score, and intramuscular fat in Angus cattle. **Journal of animal science**, v. 93, n. 1, p. 21-27, 2014.
- Mateescu, R. G.; Garrick, D. J.; Reecy, J. M. Network analysis reveals putative genes affecting meat quality in Angus cattle. **Frontiers in genetics**, v. 8, p. 171, 2017.
- Mattos, R.; Staples, C. R.; Thatcher, W. W. Effects of dietary fatty acids on reproduction in ruminants. **Reviews of reproduction**, v. 5, n. 1, p. 38-45, 2000.
- McAllister, C. M.; Speidel, S. E.; Crews Jr., D. H.; Enns, R. M. Genetic parameters for

- intramuscular fat percentage, marbling score, scrotal circumference, and heifer pregnancy in Red Angus cattle. **Journal of animal science**, v. 89, n. 7, p. 2068-2072, 2011.
- McClure, M. C.; Ramey, H. R. et al. Genome-wide association analysis for quantitative trait loci influencing Warner-Brazler shear force in five taurine cattle breeds. **Animal genetics**, v. 43, n. 6, p. 662-673, 2012.
- McPhee, M. J.; Walmsley, B. J.; Dougherty, H. C.; McKiernan, W. A.; Oddy, V. H. Live animal predictions of carcass components and marbling score in beef cattle: model development and evaluation. **Animal**, p. 1-10, 2020.
- Misztal, I.; Legarra, A.; Aguilar, I. Computing procedures for genetic evaluation including phenotypic, full pedigree, and genomic information. **Journal of Dairy Science**, v. 92, n. 9, p. 4648-4655, 2009.
- Moorey, S. E.; Biase, F. H. Beef heifer fertility: importance of management practices and technological advancements. **Journal of Animal Science and Biotechnology**, v. 11, n. 1, p. 1-12, 2020.
- Mota, L. F. M.; Fernandes Jr, G. A.; Herrera, A. C.; Scaletz, D. C. B.; Espigolan, R.; Magalhães, A. F. B.; Carvalheiro, R.; Baldi, F.; Albuquerque, L. G. Genomic reaction norm models exploiting genotype x environment interaction on sexual precocity indicator traits in Nelore cattle. **Animal Genetics**, v. 51, n. 2, p. 210-223, 2020.
- Mudadu, M. A.; Porto-Neto, L. R. et al. Genomic structure and marker-derived gene networks for growth and meat quality traits of Brazilian Nelore beef cattle. **Bmc Genomics**, v. 17, n. 1, p. 235, 2016.
- Mwangi, F. W.; Charmley, E.; Gardiner, C. P.; Malau-Aduli, B. S.; Kinobe, R. T.; Malau-Aduli, A. E. O. Diet and Genetics Influence Beef Cattle Performance and Meat Quality Characteristics. **Foods**, v. 8, n. 12, p. 648, 2019.
- Nascimento, A. V.; Matos, M. C.; Seno, L. O.; Romero, A. R. S.; Garcia, J. F.; Grisolia, A. B. Genome wide association study on early puberty in *Bos indicus*. **Genet Mol Res**, v. 15, n. 1, p. 1-6, 2016.
- Nay, S. L.; Lee, D. H.; Bates, S. E.; O'Connor, T. R. Alkbh2 protects against lethality and mutation in primary mouse embryonic fibroblasts. **DNA repair**, v. 11, n. 5, p. 502-510, 2012.

- Nepomuceno, D. D.; Pires, A. V.; Junior, M. V. F.; Biehl, M. V.; Gonçalves, J. R.; Moreira, E. M.; Day, M. L. Effect of pre-partum dam supplementation, creep-feeding and post-weaning feedlot on age at puberty in Nelore heifers. **Livestock Science**, v. 195, p. 58-62, 2017.
- Oliveira Silva, R. M.; Stafuzza, N. B. et al. Genome-wide association study for carcass traits in an experimental Nelore cattle population. **PloS one**, v. 12, n. 1, 2017.
- Oliveira, H. R.; Ventura, H. T.; Costa, E. V.; Pereira, M. A.; Veroneze, R.; Duarte, M. S.; Siqueira, O. H. G. B. D.; Fonseca e Silva, F. Meta-analysis of genetic-parameter estimates for reproduction, growth and carcass traits in Nelore cattle by using a random-effects model. **Animal Production Science**, v. 58, n. 9, p. 1575-1583, 2017.
- Ornitz, D. M.; Itoh, N. The fibroblast growth factor signaling pathway. **Wiley Interdisciplinary Reviews: Developmental Biology**, v. 4, n. 3, p. 215-266, 2015.
- Oyama, K.; Katsuta, T.; Anada, K.; Mukai, F. Genetic parameters for reproductive performance of breeding cows and carcass traits of fattening animals in Japanese Black (Wagyu) cattle. **Animal Science**, v. 78, n. 2, p. 195-201, 2004.
- Oyama, K.; Mukai, F.; Yoshimura, T. Genetic relationships among traits recorded at registry judgment, reproductive traits of breeding females and carcass traits of fattening animals in Japanese Black cattle. **Animal Science and Technology (Japan)**, 1996.
- Pegolo, S.; Cecchinato, A.; Savoia, S.; Di Stasio, L.; Pauciullo, A.; Brugiapaglia, A.; Bittante, G.; Albera, A. Genome-wide association and pathway analysis of carcass and meat quality traits in Piemontese young bulls. **Animal**, v. 14, n. 2, p. 243-252, 2019.
- Pires, B. C.; Tholon, P. et al. Genetic analyses on bodyweight, reproductive, and carcass traits in composite beef cattle. **Animal Production Science**, v. 57, n. 3, p. 415-421, 2016.
- Porto Neto, L. R.; Bunch, R. J.; Harrison, B. E.; Barendse, W. Variation in the XKR4 gene was significantly associated with subcutaneous rump fat thickness in indicine and composite cattle. **Animal genetics**, v. 43, n. 6, p. 785-789, 2012.
- Ramayo-Caldas, Y.; Renand, G.; Ballester, M.; Saintilan, R.; Rocha, D. Multi-breed and multi-trait co-association analysis of meat tenderness and other meat quality

- traits in three French beef cattle breeds. **Genetics Selection Evolution**, v. 48, n. 1, p. 1-9, 2016.
- Ramos, P. V. B.; Fonseca e Silva, F. et al. Genomic evaluation for novel stayability traits in Nelore cattle. **Reproduction in Domestic Animals**, v. 55, n. 3, p. 266-273, 2020.
- Reverter, A.; Johnston, D. J. et al. Genetic and phenotypic characterisation of animal, carcass, and meat quality traits from temperate and tropically adapted beef breeds. 4. Correlations among animal, carcass, and meat quality traits. **Australian Journal of Agricultural Research**, v. 54, n. 2, p. 149-158, 2003.
- Rodrigues, R. T. S.; Chizzotti, M. L.; Vital, C. E.; Baracat-Pereira, M. C.; Barros, E.; Busato, K. C.; Gomes, R. A.; Ladeira, M. M.; Martins, T. S. Differences in beef quality between Angus (*Bos taurus taurus*) and Nelore (*Bos taurus indicus*) cattle through a proteomic and phosphoproteomic approach. **PloS one**, v. 12, n. 1, 2017.
- Rossini, L.; Hashimoto, Y. et al. VSTM2L is a novel secreted antagonist of the neuroprotective peptide Humanin. **The FASEB Journal**, v. 25, n. 6, p. 1983-2000, 2011.
- Saatchi, M.; Schnabel, R. D.; Taylor, J. F.; Garrick, D. J. Large-effect pleiotropic or closely linked QTL segregate within and across ten US cattle breeds. **BMC genomics**, v. 15, n. 1, p. 1-17, 2014.
- Samadi, F.; Blache, D.; Martin, G. B.; D'Occhio, M. J. Nutrition, metabolic profiles and puberty in Brahman (*Bos indicus*) beef heifers. **Animal reproduction science**, v. 146, n. 3-4, p. 134-142, 2014.
- Santos, R. **Nelore: A vitória Brasileira**. Uberaba: Agropecuária Tropical, 2000, v. 4, 260 p.
- Savoia, S.; Albera, A.; Brugiapaglia, A.; Di Stasio, L.; Cecchinato, A.; Bittante, G. Heritability and genetic correlations of carcass and meat quality traits in Piemontese young bulls. **Meat science**, v. 156, p. 111-117, 2019.
- Sbardella, A. P.; Watanabe, R. N.; Costa, R. M.; Bernardes, P. A.; Braga, L. G.; Baldi Rey, F. S.; Lôbo, R. B.; Munari, D. P. Genome-Wide Association Study Provides Insights into Important Genes for Reproductive Traits in Nelore Cattle. **Animals**, v. 11, n. 5, p. 1386, 2021.

- Schiöth, H. B.; Roshanbin, S.; Hägglund, M. G.; Fredriksson, R. Evolutionary origin of amino acid transporter families SLC32, SLC36 and SLC38 and physiological, pathological and therapeutic aspects. **Molecular aspects of medicine**, v. 34, n. 2-3, p. 571-585, 2013.
- Schmidt, P. I.; Campos, G. S.; Lôbo, R. B.; Souza, F. R. P.; Brauner, C. C.; Boligon, A. A. Genetic analysis of age at first calving, accumulated productivity, stayability and mature weight of Nelore females. **Theriogenology**, v. 108, p. 81-87, 2018.
- Silva Neto, J. B.; Peripolli, E. et al. Genetic correlation estimates between age at puberty and growth, reproductive, and carcass traits in young Nelore bulls. **Livestock Science**, v. 241, p. 104266, 2020.
- Silva-Vignato, B.; Coutinho, L. L.; Cesar, A. S. M.; Poleti, M. D.; Regitano, L. C. A.; Balieiro, J. C. C. Comparative muscle transcriptome associated with carcass traits of Nelore cattle. **BMC genomics**, v. 18, n. 1, p. 506, 2017.
- Smith, T. P. L.; Casas, E.; Rexroad, C. E.; Kappes, S. M.; Keele, J. W. Bovine CAPN1 maps to a region of BTA29 containing a quantitative trait locus for meat tenderness. **Journal of animal science**, v. 78, n. 10, p. 2589-2594, 2000.
- Smith, T.; Domingue, J. D.; Paschal, J. C.; Franke, D. E.; Bidner, T. D.; Whipple, G. Genetic parameters for growth and carcass traits of Brahman steers. **Journal of Animal Science**, v. 85, n. 6, p. 1377-1384, 2007.
- Soares, A. C. C.; Guimarães, S. E. F.; Kelly, M. J.; Fortes, M. R. S.; Silva, F. F.; Verardo, L. L.; Mota, R.; Moore, S. Multiple-trait genomewide mapping and gene network analysis for scrotal circumference growth curves in Brahman cattle. **Journal of animal science**, v. 95, n. 8, p. 3331-3345, 2017.
- Terakado, A. P. N.; Boligon, A. A.; Baldi, F.; Silva, J. A. II V.; Albuquerque, L. G. Genetic associations between scrotal circumference and female reproductive traits in Nelore cattle. **Journal of Animal Science**, v. 93, n. 6, p. 2706-2713, 2015.
- Tizioto, P. C.; Decker, J. E. et al. Genome scan for meat quality traits in Nelore beef cattle. **Physiological genomics**, v. 45, n. 21, p. 1012-1020, 2013.
- Toelle, V. D.; Robison, O. W. Estimates of genetic correlations between testicular measurements and female reproductive traits in cattle. **Journal of animal science**, v. 60, n. 1, p. 89-100, 1985.
- Tonussi, R. L.; Espigolan, R. et al. Genetic association of growth traits with carcass

- and meat traits in Nellore cattle. **Genetics and Molecular Research**, v. 14, n. 4, p. 18713- 18719, 2015.
- Torres-Vázquez, J. A.; Van Der Werf, J. H. J.; Clark, S. A. Genetic and phenotypic associations of feed efficiency with growth and carcass traits in Australian Angus cattle. **Journal of animal science**, v. 96, n. 11, p. 4521-4531, 2018.
- Utrera, A. R.; Van Vleck, L. D. Heritability estimates for carcass traits of cattle: a review. 2004.
- Utsunomiya, Y. T.; Milanesi, M. et al. A PLAG1 mutation contributed to stature recovery in modern cattle. **Scientific reports**, v. 7, n. 1, p. 1-15, 2017.
- van den Heuvel, S. Cell-cycle regulation. **WormBook: The Online Review of C. elegans Biology [Internet]**, 2005.
- Van Dyck, F.; Declercq, J.; Braem, C. V.; Van de Ven, W. J. M. PLAG1, the prototype of the PLAG gene family: versatility in tumour development. **International journal of oncology**, v. 30, n. 4, p. 765-774, 2007.
- Vaz, F. N.; Restle, J.; Pádua, J. T.; Fonseca, C. A.; Pacheco, P. S. Características de carcaça e receita industrial com cortes primários da carcaça de machos nelore abatidos com diferentes pesos. **Ciência Animal Brasileira**, v. 14, n. 2, p. 199-207, 2013.
- Vignal, A.; Milan, D.; SanCristobal, M; Eggen, A. A review on SNP and other types of molecular markers and their use in animal genetics. **Genetics Selection Evolution**, v. 34, n. 3, p. 275, 2002.
- Visscher, P. M.; Brown, M. A.; McCarthy, M. I.; Yang, J. Five years of GWAS discovery. **The American Journal of Human Genetics**, v. 90, n. 1, p. 7-24, 2012.
- Visscher, P. M.; Wray, N. R.; Zhang, Q.; Sklar, P.; McCarthy, M. I.; Brown, M. A.; Yang, J. 10 years of GWAS discovery: biology, function, and translation. **The American Journal of Human Genetics**, v. 101, n. 1, p. 5-22, 2017.
- Visus, C.; Ito, D.; Dhir, R.; Szczepanski, M. J.; Chang, Y. J.; Latimer, J. J.; Grant, S. G.; DeLeo, A. B. Identification of Hydroxysteroid (17 β) dehydrogenase type 12 (HSD17B12) as a CD8+ T-cell-defined human tumor antigen of human carcinomas. **Cancer immunology, immunotherapy**, v. 60, n. 7, p. 919-929, 2011.
- Wang, H.; Misztal, I.; Aguilar, I.; Legarra, A.; Muir, W. M. Genome-wide association

- mapping including phenotypes from relatives without genotypes. **Genetics Research**, v.94, n.2, p.73-83, 2012.
- Warner, R.; Wheeler, T. L. et al. Meat tenderness: advances in biology, biochemistry, molecular mechanisms and new technologies. **Meat Science**, p. 108657, 2021.
- Wennmann, D. O.; Schmitz, J. et al. Evolutionary and molecular facts link the WWC protein family to Hippo signaling. **Molecular biology and evolution**, v. 31, n. 7, p. 1710-1723, 2014.
- Wheeler, T. L.; Cundiff, L. V.; Shackelford, S. D.; Koohmaraie, M. Characterization of biological types of cattle (Cycle VIII): Carcass, yield, and longissimus palatability traits. **Journal of animal science**, v. 88, n. 9, p. 3070-3083, 2010.
- Williams, P. Nutritional composition of red meat. **Nutrition & Dietetics**, v. 64, p. S113-S119, 2007.
- Xia, J.; Qi, X. et al. Genome-wide association study identifies loci and candidate genes for meat quality traits in Simmental beef cattle. **Mammalian Genome**, v. 27, n. 5-6, p. 246-255, 2016.
- Yang, J.; Lee, S. H.; Goddard, M. E.; Visscher, P. M. Genome-wide complex trait analysis (GCTA): methods, data analyses, and interpretations. In: **Genome-wide association studies and genomic prediction**. Humana Press, Totowa, NJ, 2013. p. 215-236.
- Yokoo, M. J.; Lôbo, R. B.; Magnabosco, C. U.; Rosa, G. J. M.; Forni, S.; Sainz, R. D.; Albuquerque, L. G. Genetic correlation of traits measured by ultrasound at yearling and 18 months of age in Nellore beef cattle. **Livestock Science**, v. 180, p. 34-40, 2015.
- Zhang, H.; Wang, Z.; Wang, S.; Li, H. Progress of genome wide association study in domestic animals. **Journal of animal science and biotechnology**, v. 3, n. 1, p. 26, 2012.
- Zhao, C.; Tian, F. et al. Muscle transcriptomic analyses in Angus cattle with divergent tenderness. **Molecular biology reports**, v. 39, n. 4, p. 4185-4193, 2012.
- Zheng, Y.; Prouty, S. M.; Harmon, A.; Sundberg, J. P.; Stenn, K. S.; Parimoo, S. Scd3—a novel gene of the stearyl-CoA desaturase family with restricted expression in skin. **Genomics**, v. 71, n. 2, p. 182-191, 2001.

Chapter 2 – Genetic parameters estimates using genomic information for female sexual precocity, carcass and meat quality traits in Nellore cattle

ABSTRACT – The objective of the present study was to estimate genetic parameters for longissimus muscle area (LMA), backfat thickness (BF), hot carcass weight (HCW), shear-force tenderness (SF), marbling score (MARB), intramuscular fat content (IMF), age at first calving (AFC), and scrotal circumference (SC) in Nellore cattle. The dataset available for this study were from 602,122 animals phenotyped for sexual precocity traits and 6,910 for carcass/meat traits and a total of 15,000 genotyped Nellore animals. The animals were genotyped using the Illumina Bovine HD Beadchip and the GeneSeek® Genomic Profilers HDi 75K and Low-Density 35K. The animals genotyped with GGP panels were imputed to the HD panel by the FImpute v3 software, using the ARS-UCD1.2 reference map. The (co)variance components and genetic parameters were estimated in two different ways, considering the Single-step (ssGBLUP) approach: 1) in a multi-trait analysis, performed for carcass and meat quality traits, by Bayesian inference using the GIBBS2F90 software; 2) and bi-trait analyzes, performed for sexual precocity traits with carcass and meat quality traits, by frequentist inference using the AIREMLF90 software. The animal model included additive and residual genetic effects as random; the fixed effects of GC (for all traits) and date of analysis as classes (for BF, SF, and MARB); and the linear effects of age at slaughter (all carcass and meat traits) and age at yearling (YW and SC) as covariates. Heritability estimates ranged from 0.13 to 0.34 for carcass and meat quality traits, and were 0.06 and 0.45 for AFC and SC, respectively. Favorable genetic correlations were estimated between YW–HCW (0.79 ± 0.03), YW–LMA (0.28 ± 0.05), HCW–LMA (0.44 ± 0.05), MARB–IMF (0.90 ± 0.07), SF–IMF (-0.20 ± 0.11), BF–MARB (0.29 ± 0.08), BF–IMF (0.22 ± 0.09), HCW–SF (-0.22 ± 0.09), and BF–AFC (-0.26 ± 0.11); and an undesirable correlation between AFC–HCW (0.24 ± 0.10). The results indicate that carcass traits and SC should respond quickly to selection; meat quality traits, with lower heritability estimates, will show a slower response, while AFC should not respond to selection efficiently. In general, the correlations between carcass traits and those of meat quality were low to moderate, thus, in the short or medium term, selection will imply small gains in correlated responses. Thus, to achieve significant genetic advances in carcass composition and meat quality traits, both groups of traits must compose selection indices. Overall, carcass and meat quality traits were not genetically correlated with the indicative traits of female precocity. Despite the report of the existence of genetic correlations between AFC with HWC and BF in this study, the selection to obtain correlated responses in the other trait should not be efficient, since AFC showed practically null heritability, and HCW and BF are traits evaluated in the *post-mortem*, so the candidates for selection are slaughtered and cannot be subjected to reproduction.

Keywords: beef cattle, carcass, genetic parameters, meat quality, Nellore, sexual precocity

1. INTRODUCTION

Widespread throughout the national territory, Brazilian beef cattle industry is one of the main economic activities in the country. With the globalization process, combined with the growing demand for safe food, Brazil has become one of the largest meat producers and exporters in the world. Currently, the country has the largest cattle herd, is the largest exporter, and second-largest consumer of beef, standing out on the world stage (ABIEC, 2019). Associated with the growing demand for food, there is a great demand for products of animal origin with superior quality. Therefore, new technologies that aim to increase production and the quality of the final product must be developed and validated, in order to meet this growing global demand for safe food.

For development of breeding programs, it is essential to fully understand the characteristics with economic relevance in beef cattle, in order to define the objectives and selection criteria, which will guide the improvement of animals (Rosa et al., 2013; El-Hack et al., 2018) based on animals' genetic evaluation. In this context, attributes such as carcass traits are economically important, since they are related to meat production and carcass yield and finishing. Furthermore, the beef industry pays producers based on some conditions of the carcass, such as weight and finish (Vaz et al., 2013; Fernandes Júnior et al., 2016a; Mcphee et al., 2020). In addition, the final product quality influences consumer acceptance and purchase intention (Pegolo et al., 2019), through the combination of a series of sensory factors, such as tenderness, juiciness, and flavor, which together contribute to a better meat palatability, besides to a more attractive visual appearance that includes attributes such as color and distribution of the fat (Magnabosco et al., 2016; Xia et al., 2016; Gordo et al., 2018; Leal-Gutiérrez et al., 2019). Thus, improving meat quality traits should lead to an increase in demand for beef (Mateescu et al., 2015).

Despite the importance of these characteristics in beef cattle, their evaluation is not part of the routine in breeding programs in Brazil and, therefore, they are not included in most of the selection indexes. To indirectly select for carcass composition, visual scores such as carcass conformation, finishing precocity and muscling, have been considered in some Nellore indexes (Shiotsuki et al. 2009). These traits are moderately correlated with carcass traits in Nellore (Bonin et al., 2015; Gordo et al., 2016; Silveira et al., 2018). Limitations to directly select for carcass and meat quality

traits, obtained *post-mortem*, include their late expression and the costs and difficulty of measuring. Moreover, it is necessary to carry out progeny tests, as potential candidates to selection are slaughtered, increasing costs and the generations interval (Fernandes Júnior et al., 2016a; Leal-Gutiérrez et al., 2019; Magalhães et al., 2019). Because of this, most of genetic parameter estimates for these traits in Brazilian Zebu cattle have been obtained using small data sets, which reduces the accuracy of the estimates. Consequently, heritability estimates for carcass and meat quality traits obtained after slaughtering in the Nelore breed assume values in a wide range, varying from 0.09 to 0.59 and from 0.07 to 0.28, respectively (Castro et al., 2014; Neves et al., 2014; Tonussi et al., 2015; Fernandes Júnior et al., 2016a; Feitosa et al., 2017; Gordo et al., 2018; Silva et al., 2018; Magalhães et al., 2018; Carvalho et al., 2019; Bonin et al., 2021).

For using these traits as selection criteria, is fundamental to know how they relate with others of economic importance, as those indicators of sexual precocity. Compared to European breeds, Nelore females present late sexual precocity (Cundiff et al., 2004). The reduction in age at puberty together with the increase in the conception rate of young heifers results in the dilution of herd replacement costs, greater heifers' longevity, greater availability of animals for sale or reproduction, better-accumulated productivity per animal, and, consequently, greater profitability for the producer (Eler et al., 2014; Guarini et al., 2014, Terakado et al., 2015). However, direct selection for sexual precocity is generally difficult to apply. Age at first calving, the most common trait used as an indicator of sexual precocity, is strongly influenced by environmental factors (Mota et al., 2020). In general, females are exposed to reproduction on a certain age or weight and in a short breeding season, affecting heritability estimates (Dias et al., 2004). Studies conducted on the Nelore breed in recent years have reported heritability estimates for age at first calving ranging from 0.08 to 0.24 (Boligon et al., 2015; Buzanskas et al., 2017; Kluska et al., 2018; Schmidt et al., 2018; Brunet et al., 2020; Costa et al., 2020). Another sexual precocity indicator trait, scrotal circumference, is included in almost all Nelore breeding program selection indexes, as it is ease and relatively of low-cost to measure. Moreover, it presents moderate to high heritability estimates (0.33 to 0.52) and is favorably genetic correlated with AFC, with estimates ranging from -0.22 to -0.60 (Boligon et al., 2015; Terakado et

al., 2015; Buzanskas et al., 2017; Kluska et al., 2018; Brunet et al., 2020; Costa et al., 2020). In this sense, bulls with higher SC values tend to reach puberty earlier, and transmit precocity to their progeny (Regatieri et al., 2017; Schmidt et al., 2019).

One could hypothesize that selecting for early finishing would increase female sexual precocity, since fat deposition is directly associated with the metabolism of steroids and eicosanoids, hormones that modulate reproductive events (Mattos et al., 2000). In this sense, in some studies using ultrasonography in Nelore animals, moderate and negative genetic correlation estimates between backfat thickness and age at first calving were found, indicating that long term selection for greater fat deposition can result in benefits in sexual precocity (Caetano et al., 2013; Buzanskas et al., 2017; Kluska et al., 2018).

Genetic correlation estimates between carcass and meat quality traits, obtained after slaughtering, and sexual precocity indicator traits in Nelore, are rare. Thus, the aim of this study was to estimate the (co)variance components and genetic parameters for carcass and meat quality traits and their genetic correlations with sexual precocity indicator traits in Nelore cattle, in order to providing subsidies for improving the genetic evaluation of these traits.

2. MATERIAL AND METHODS

2.1. Database

2.1.1. Phenotypic data

The dataset available for this study were from 755,798 Nelore animals, born between 1984 and 2018, belonging to commercial herds, located in different regions of the country, which are part of the breeding programs of DeltaGen, Cia do Melhoramento, Paint (CRV Lagoa) and Nelore Qualitas. The animals were raised in grazing systems, with mineral supplementation during the dry season and water for consumption *ad libitum*, and were confined only in the finishing stage, for a period of around 90 days, with a diet based on roughage.

The database is composed of information for:

- carcass traits obtained in the *post-mortem*: longissimus muscle area (LMA), backfat thickness (BF), and hot carcass weight (HCW);

- meat quality traits: shear force tenderness (SF), marbling (MARB), and intramuscular fat content (IMF);
- reproductive traits: age at first calving (AFC) and scrotal circumference (SC);
- and yearling weight (YW).

As for reproductive management, producers adopt two breeding seasons, in the first, lasting 60 days, the heifers are exposed to the first mating at around 16 months of age. Heifers that don't conceive have a second chance in the last breeding season, which occurs over a period of approximately 70 days, where all females participate, both heifers and multiparous. This process, which began in the 1990s, is carried out to identify precocious heifers in an out-of-season breeding season and generate data to be used in genetic evaluations. Recently, some of the breeders started to expose females to reproduction around 14 months of age, in a 90 days breeding season, seeking to intensify selection for sexual precocity. Reproduction is carried out through artificial insemination of females or through natural mating, where they are exposed to the bull. The diagnosis of pregnancy in heifers is performed by rectal palpation, approximately 60 days after the end of the breeding season, and females that conceived neither in the first nor second breeding season were discarded. Thus, AFC was defined by the difference in days between the date of first calving and the date of birth of the heifer. SC was measured in centimeters at yearling, with the aid of a tape measure.

The animals were slaughtered in commercial plants located in several states of the country, with an average age of 706.5 ± 79.6 days. In Brazil, it is common for cattle to be slaughtered intact, since this category has a better performance in terms of weight gain, feed conversion, better muscle:bone ratio with a lower proportion of fat (Arthaud, 1977).

In the process of slaughtering, after the skinning and evisceration steps, the carcasses were divided in half and the two halves were weighed, obtaining the HCW, in kilograms. Then, the half carcasses were stored in the cooling chamber for a period of 24 to 48 hours (*post-mortem*). After that, boning was performed and samples of the *Longissimus thoracis* muscle were collected between the 12th and 13th ribs of the left half carcass to measure LMA (in square centimeters) using the points quadrants method; BF (in millimeters) with the assistance of a caliper and for additional meat

analysis. It is important to note that the carcasses didn't undergo to a maturation process, since this is the routine procedure in Brazil.

For the analysis of tenderness, 2.54 cm thick samples of the *Longissimus thoracis* muscle were prepared according to the standardized procedure proposed by Wheeler et al. (1995). The meat tenderness was determined using the Salter Warner-Bratzler Shear Force equipment. For the intramuscular fat content, the methodology described by Bligh and Dyer (1959) was adopted to determine the percentage of lipids in the samples. The marbling index was defined using a visual grading scale based on the USDA – Quality and Yield Grade (2000), receiving scores from 1 to 10 according to the marbling score.

For carcass and meat traits the contemporary groups (CG) included the variables: year and season of birth, farm (at birth, weaning, and yearling stages), and slaughter date. For reproductive traits and YW, CG was composed by: year and season of birth, farm and management group (at weaning and yearling stages), and yearling valuation date. The season of birth was divided into Spring (for animals born from August to January) and Autumn (from February to July).

For data consistency, the assumptions of normality and homogeneity were tested by Shapiro-Wilk test using the software R (R Core Team 2020). For a better data uniformity, backfat thickness (BF) was submitted to transformation by the root cubic. Also, observations with measurements of 3.5 standard deviations above or below the CG mean and CG with less than 5 animals were excluded from the analysis. The number of animals and descriptive statistics for each trait after the data consistency are shown in Table 1.

Yearling weight was included only in the multi-trait analysis, along with carcass and meat quality traits. All animals in the database had phenotypes for YW. However, only those animals that had information for meat and carcass traits, their paternal siblings and all other animals sharing the same contemporary group as the previous ones were included in the analyzes, reaching a total of ~27,000 animals with YW records.

Table 1. Descriptive statistics of phenotypic information for scrotal circumference (SC), age at first calving (AFC), yearling weight (YW), hot carcass weight (HCW), longissimus muscle area (LMA), subcutaneous fat thickness (BF), marbling score (MARB), shear force tenderness (BF), and intramuscular fat content (IMF).

Trait	N	Mean	SD	*CV	Min	Max	NCG
AFC (days)	174,236	1,008.53	134.19	13.31	701	1,220	8,416
SC (cm)	427,886	27.03	3.77	13.93	15.40	38.80	12,522
YW (kg)	27,129	310.85	41.01	13.19	200	524	737
HCW (kg)	6,611	290.24	34.02	11.72	166	424.60	108
LMA (cm ²)	6,190	70.56	9.63	13.64	40	112	103
BF (mm)	6,128	5.32	2.62	49.28	1	23	101
MARB	6,276	2.76	0.58	21.18	1.10	6	102
SF (kgf)	6,295	6.22	1.93	30.95	1.60	12.84	102
IMF (%)	3,812	0.78	0.37	48.20	0.12	3.61	75

*Percentage representation

N: number of observations; SD: standard deviation; CV: coefficient of variation; Min and Max: minimum and maximum values; NCG: number of contemporary groups.

2.1.2. Genotypic data

The genotypic dataset contained 15,000 Nellore animals that were genotyped using the Illumina Bovine HD Beadchip (770K, Illumina Inc., San Diego, CA, USA), the GeneSeek® Genomic Profiler HDi 75K (GeneSeek In / c., Lincoln, NE) and the GeneSeek® Genomic Profile Low-Density 35K (GeneSeek In / c., Lincoln, NE). The animals genotyped with GGP panels (75K and 35K) were imputed to the HD panel using the FImpute v3 software (Sargolzaei et al., 2014), using the ARS-UCD1.2 reference map. All animals with records for carcass and meat quality traits were genotyped.

2.2. Estimates of (co)variance components and genetic parameters

The (co)variance components and genetic parameters were obtained considering the Single-step approach (ssGBLUP) proposed by Misztal et al. (2009). For carcass and meat quality traits, it was applied a multi-trait model via Bayesian inference using the GIBBS2F90 software (Misztal et al., 2002). Yearling weight (YW) was included in the multi-trait analysis as an anchor trait, in order to minimize the

influence of sequential selection (Fernandes Júnior et al., 2016a). The average heritabilities for AFC and SC, and their genetic correlations with carcass and meat quality traits, were estimated with bi-trait models and frequentist inference using the AIREMLF90 software (Misztal et al., 2002).

The animal model included additive and residual genetic effects as random, and the fixed effects of GC (for all traits) and date of analysis as classes (for BF, SF, and MARB) and the linear effects of age at slaughter (all carcass and meat traits) and age at yearling (YW and SC) as covariates.

The matrix representation of the model is:

$$\mathbf{y} = \mathbf{X}\boldsymbol{\beta} + \mathbf{Z}\mathbf{a} + \mathbf{e}$$

where, \mathbf{y} is a vector of observations; $\boldsymbol{\beta}$ is the vector of fixed effects; \mathbf{a} is the vector of direct additive genetic effects; \mathbf{e} is the vector of residual effects; \mathbf{X} is the fixed effects incidence matrix relating $\boldsymbol{\beta}$ to \mathbf{y} , and \mathbf{Z} is the incidence matrix of random effects relating \mathbf{a} to \mathbf{y} . It was assumed that $E[\mathbf{y}] = \mathbf{X}\boldsymbol{\beta}$; $\text{Var}(\mathbf{a}) = \mathbf{H} \otimes \mathbf{S}_a$, $\text{Var}(\mathbf{e}) = \mathbf{I} \otimes \mathbf{S}_e$, where \mathbf{S}_a is the additive genetic covariance matrix; \mathbf{S}_e is the residual covariance matrix; \mathbf{H} is the matrix that combines the relationship matrices, based on the pedigree (\mathbf{A}), and the genomic information (\mathbf{G}); \mathbf{I} is the identify matrix; and \otimes denotes the direct product between the matrices.

In the ssGBLUP approach, the inverse of the relationship matrix (\mathbf{A}^{-1}) based on pedigree is combined with a genomic relationship matrix into a genomic-pedigree relationship \mathbf{H}^{-1} (Aguilar et al., 2010):

$$\mathbf{H}^{-1} = \mathbf{A}^{-1} + \begin{bmatrix} \mathbf{0} & \mathbf{0} \\ \mathbf{0} & \mathbf{G}^{-1} - \mathbf{A}_{22}^{-1} \end{bmatrix}$$

where, \mathbf{H}^{-1} is the inverse of the modified relationship matrix; \mathbf{A}_{22}^{-1} is the inverse of the pedigree relationship matrix for genotyped animals; and \mathbf{G}^{-1} is the inverse of the genomic relationship matrix (VanRaden, 2008), which is described as:

$$\mathbf{G} = \frac{\mathbf{Z}\mathbf{Z}'}{2 \sum_{i=1}^m p_i(1-p_i)}$$

where, $\mathbf{Z} = (\mathbf{M} - \mathbf{P})$, in which \mathbf{M} is the SNP incidence matrix, with m columns representing the number of markers and n lines representing the number of genotyped animals. Each element in \mathbf{M} was set to -1, 0 or 1, for genotypes aa, Aa, and AA,

respectively. \mathbf{P} is the matrix containing the allele frequencies expressed in $2p_i$, where p_i is the frequency of the second allele at locus i .

The multi-trait analysis was done by Bayesian inference. A total of 800,000 iterations were generated, with a burn-in of 10% (80,000 samples) and a sampling interval equal to 50. The posterior averages and standard deviations were estimated using the POSTGIBBSF90 software (Misztal et al., 2009), which summarizes the samples obtained in the Gibbs sampling programs. The convergence of data was verified by graphical analysis, through the Bayesian Output Analysis (BOA) package of software R (Smith, 2007).

3. RESULTS AND DISCUSSION

3.1. Genetic parameters for carcass and meat quality traits

The estimated heritabilities for the carcass traits and YW ranged from 0.28 to 0.34 (Table 2), indicating that they have enough genetic variability to obtain quick responses to selection. As for meat quality traits, estimates were of lower magnitude (0.13 to 0.18), showing greater environmental influence, and should respond slower to selection.

Studies that used part of the same database as in the present work (Tonussi et al., 2015; Fernandes Júnior et al., 2016a; Gordo et al., 2018), reported lower heritability estimate for LMA (0.10 to 0.28) and BF (0.08 to 0.21). Other studies carried out in Nellore cattle obtained heritability estimates closer to the obtained in this study (from 0.29 to 0.44) for LMA (Ceacero et al., 2016; Buzanskas et al., 2017; Kluska et al., 2018; Silva Neto et al., 2020), while for BF, the heritabilities showed a wide variation, from 0.17 to 0.59 (Yokoo et al., 2015; Ceacero et al., 2016; Silva Neto et al., 2020), for both traits obtained by ultrasound, indicating that selection events can promote rapid progress. Research with Nellore animals estimating genetic parameters for HCW are still scarce. The heritability estimates found in the literature for the breed range from 0.11 to 0.39 (Tonussi et al., 2015; Fernandes Júnior et al., 2016a; Gordo et al., 2018; Carvalho et al., 2019).

Table 2. Estimates of heritability coefficients (in bold on the diagonal), genetic correlations (above the diagonal) and their respective standard errors for yearling weight (YW), hot carcass weight (HCW), longissimus muscle area (LMA), backfat thickness (BF), marbling score (MARB), shear force tenderness (SF), and intramuscular fat content (IMF), obtained by multitrait analysis.

Trait	YW	HCW	LMA	BF	MARB	SF	IMF
YW	0.31±0.02	0.79±0.03	0.28±0.05	0.14±0.06	0.03±0.07	0.01±0.08	0.06±0.08
HCW		0.28±0.02	0.44±0.05	0.06±0.07	0.05±0.09	-0.22±0.09	0.17±0.11
LMA			0.34±0.02	-0.19±0.06	-0.03±0.07	-0.04±0.08	-0.11±0.09
BF				0.28±0.02	0.29±0.08	0.02±0.09	0.22±0.09
MARB					0.17±0.02	-0.06±0.09	0.90±0.07
SF						0.13±0.02	-0.20±0.11
IMF							0.18±0.03

As for genetic correlations, YW was shown to be highly correlated with HCW, suggesting that these traits are largely under the additive effects of the same genes. Furthermore, YW showed positive genetic correlations of moderate and low magnitude with LMA and BF, respectively (Table 2). These results indicate that selection for YW could lead, as a correlated response, to heavier carcasses and, in the long-term, in the degree of finish and yield of commercial cuts in this population.

Estimates of genetic correlations between carcass traits (Table 2) showed that HCW is moderate and positively associated with LMA, indicating that improvements in one trait should lead to genetic gains in the other. On the other hand, LMA and BF showed a negative and low correlation, suggesting that long-term selection for increasing LMA can produce animals with lower fat deposition. This result is superior to those found by Ceacero et al. (2016) and Kluska et al. (2018), who found low or close to null genetic associations between LMA and BF (0.09 ± 0.10 and 0.06 ± 0.06 , respectively) in the Nellore breed, indicating that selection for one of these traits will not imply in correlated response in the other. In contrast to our results, studies have found positive correlations of moderate magnitude in the same breed, ranging from 0.19 to 0.36 (Gordo et al., 2012; Caetano et al., 2013; Buzanskas et al., 2017). Genetic correlations of HCW with LMA and BF show a wide range from practically null to high estimates in cattle of different breeds (Do et al., 2016; Elzo et al., 2017; Savoia et al., 2019).

The estimate of genetic correlation between MARB and IMF was high and positive, which is expected from a biological point of view, since both traits assess the lipid content in meat, visually and chemically, respectively (Table 2). In this sense, the marbling score can be considered a good indicator of meat lipid content. IMF was negatively correlated with SF, indicating that in the long term, selection for increased tenderness can lead to higher intramuscular fat content in meat. Consistently, several studies using pure or composite Taurine breeds obtained estimates of genetic association between these traits, ranging from 0.56 to 1.00 (MacNeil et al., 2010; Wheeler et al., 2010; McAllister et al., 2011; Mateescu et al., 2014), while in the Nelore breed, Bonin et al. (2021) reported estimates of the genetic correlation between MARB and IMF measured in meat samples taken from the *Longissimus* muscle on the 5th and 12th ribs, of 0.74 and 0.78, respectively.

Most genetic correlations between carcass and meat traits were very low, practically null, indicating that these traits do not share the same genomic regions (Table 2). Both MARB and IMF showed positive and low-moderate genetic correlation estimates with BF. This result is superior to those found by Gordo et al. (2018), which obtained a positive correlation, but of low magnitude (0.14 ± 0.16), between MARB and BF, suggesting that in the long term, the production of carcasses with higher finishing can promote genetic progress for marbling. A negative but relatively low genetic association was estimated between HCW and SF, suggesting that selection for higher carcass weight should have as a correlated response, increased meat tenderness. These results corroborate the results found by Gordo et al. (2018), which estimated a genetic correlation of -0.27 ± 0.14 between HCW and SF in Nelore cattle. They are also in agreement with the findings by Reverter et al. (2003), who reported similar estimates between two groups of animals studied, of -0.20 (temperate animals) and -0.21 (tropically adapted animals).

3.2. Heritability estimates for female sexual precocity and their genetic correlations with carcass and meat quality traits

The low heritability estimate (Table 3) for AFC indicates a substantial influence of gene combinations and environmental effects on the expression of this trait. For SC

it was estimated a high heritability (Table 3), indicating that this trait must respond quickly to selection events.

Several studies conducted on the Nellore breed in recent years have reported heritability for AFC ranging from 0.08 to 0.24 (Boligon et al., 2015; Terakado et al., 2015; Buzanskas et al., 2017; Kluska et al., 2018; Lacerda et al., 2018; Schmidt et al., 2018; Brunes et al., 2020; Costa et al., 2020). According to Buzanskas et al. (2017), the increase in heritability estimates for AFC could be due to the increase in genetic variability that has been introduced through the selection of sexually precocious heifers and through greater control of environmental factors.

Heritability estimates for SC are generally of moderate to high magnitudes. When measured at yearling, heritability estimates found in the literature for the Nellore breed range from 0.33 to 0.52 (Boligon et al., 2015; Terakado et al., 2015; Buzanskas et al., 2017; Kluska et al., 2018; Lacerda; et al., 2018; Brunes et al., 2020). Based on the results of a meta-analysis study, which grouped several other studies with Nellore cattle, Oliveira et al. (2017) reported a heritability estimate of 0.56 for SC at yearling.

Table 3. Estimates of heritability coefficients (for AFC and SC), genetic correlations, and their respective standard errors between reproductive with carcass and meat quality traits, obtained by bi-trait analysis.

¹ Traits	AFC	SC
	<i>Heritability coefficients (h^2)</i>	
	0.06±0.005	0.45±0.006
	<i>Genetic correlations (r_G)</i>	
HCW	0.24±0.10	0.10±0.06
LMA	0.08±0.08	0.04±0.05
BF	-0.26±0.11	0.11±0.06
MARB	0.07±0.12	-0.08±0.07
SF	-0.05±0.17	0.09±0.11
IMF	0.18±0.16	0.03±0.10

¹AFC: age at first calving; SC: scrotal circumference; HCW: hot carcass weight; BF: backfat thickness; MARB: marbling score; SF: shear force tenderness; IMF: intramuscular fat content.

In general, carcass and meat quality traits were not genetically correlated with the indicative traits of female precocity. The estimate of genetic correlation between AFC and HCW was positive and, therefore, unfavorable, suggesting that precocious

heifers tend to generate progenies that have lighter carcasses, as well as bulls with merit to carcass weight would generate daughters that reach puberty later.

In contrast, the genetic correlation between AFC and BF was negative and of moderate magnitude, suggesting that additive genetic effects act antagonistically on these traits, however, this association was favorable, in view of that long-term selection to decrease AFC or increase BF must lead to a desirable correlated response in the other trait. Some studies with Nellore animals have also found negative and desirable genetic correlation estimates of moderate magnitude between BF and AFC (Caetano et al., 2013; Buzanskas et al., 2017; Kluska et al., 2018). Pires et al. (2016) reported an association of -0.69 ± 0.35 between the same traits in Canchim animals, indicating that greater fat deposition can result in benefits in sexual precocity. These findings are biologically expected since lipid production or fat deposition is directly associated with the metabolism of certain hormones (such as steroids and eicosanoids) that modulate reproductive events, in addition to having a direct effect on the transcription of encoding genes of proteins essential for reproduction (Mattos et al., 2000).

4. CONCLUSIONS

Carcass traits have enough genetic variability to respond quickly to selection, while low heritability estimates for meat quality traits indicate a slower response. In general, the correlations between carcass traits and those of meat quality were low to moderate, so, in the short or medium term, selection will imply small gains in correlated responses. Thus, to achieve significant genetic advances in carcass composition and meat quality, these traits must compose selection indices. In general, carcass and meat quality traits were not genetically correlated with the indicative traits of female precocity.

Despite the report of the existence of genetic correlations between age at first calving (AFC) with hot weight carcass (HWC) and backfat thickness (BF) in this study, the selection to obtain correlated responses in the other trait should not be efficient, since AFC showed practically null heritability, and HCW and BF are traits evaluated in the *post-mortem*, so the candidates for selection are slaughtered and cannot be subjected to reproduction.

5. REFERENCES

- Aguilar, I.; Misztal, I.; Johnson, D. L.; Legarra, A.; Tsuruta, S.; Lawlor, T. J. Hot topic: A unified approach to utilize phenotypic, full pedigree, and genomic information for genetic evaluation of Holstein final score. **Journal of Dairy Science**, v. 93, n. 2, p. 743-752, 2010.
- Arthaud, V. H.; Mandigo, R. W.; Koch, R. M.; Kotula, A. W. Carcass composition, quality and palatability attributes of bulls and steers fed different energy levels and killed at four ages. **Journal of Animal Science**, v. 44, n. 1, p. 53-64, 1977.
- Associação Brasileira Das Indústrias Exportadoras De Carne (ABIEC). **Beef Report: Perfil da Pecuária no Brasil**. 2019. Disponível em: <http://abiec.com.br/publicacoes/beef-report-2019/.aspx>. Acesso em: 07 de abr. 2020.
- Bligh, E. G.; Dyer, W. J. A rapid method of total lipid extraction and purification, **Canadian Journal. Biochemistry and Physiology**, v.37, p.911–917, 1959.
- Boligon, A. A.; Silveira, F. A.; Silveira, D. D.; Dionello, N. J. L.; Santana Junior, M. L.; Bignardi, A. B.; Souza, F. R. P. Reduced-rank models of growth and reproductive traits in Nelore cattle. **Theriogenology**, v. 83, n. 8, p. 1338-1343, 2015.
- Bonin, M. N.; Ferraz, J. B. S. et al. Visual body-scores selection and its influence on body size and ultrasound carcass traits in Nelore cattle. **Journal of animal science**, v. 93, n. 12, p. 5597-5606, 2015.
- Bonin, M. N.; Pedrosa, V. B. et al. Genetic parameters associated with meat quality of Nelore cattle at different anatomical points of longissimus: Brazilian standards. **Meat Science**, v. 171, p. 108281, 2021.
- Brunes, L. C.; Baldi, F.; e Costa, M. F. O.; Lobo, R. B.; Lopes, F. B.; Magnabosco, C. U. Genetic-quantitative analysis for reproductive traits in Nelore cattle selected for sexual precocity. **Animal Production Science**, v. 60, n. 7, p. 896-902, 2020.
- Buzanskas, M. E.; Pires, P. S.; Chud, T. C. S.; Bernardes, P. A.; Rola, L. D.; Savegnago, R. P.; Lôbo, R. B.; Munari, D. P. Parameter estimates for reproductive and carcass traits in Nelore beef cattle. **Theriogenology**, v. 92, p. 204-209, 2017.
- Caetano, S. L.; Savegnago, R. P.; Boligon, A. A.; Ramos, S. B.; Chud, T. C. S.; Lôbo, R. B.; Munari, D. P. Estimates of genetic parameters for carcass, growth and reproductive traits in Nelore cattle. **Livestock Science**, v. 155, n. 1, p. 1-7, 2013.

- Carvalho, M. E.; Baldi, F. S. et al. Genomic regions and genes associated with carcass quality in Nelore cattle. **Genetics and Molecular Research**, v. 18, n. 1, p. 1-15, 2019.
- Castro, L. M.; Magnabosco, C. U.; Sainz, R. D.; Faria, C. U.; Lopes, F. B. Quantitative genetic analysis for meat tenderness trait in Polled Nelore cattle. **Revista Ciência Agronômica**, v. 45, p. 393-402, 2014.
- Ceacero, T. M.; Mercadante, M. E. Z.; Cyrillo, J. N. S. G.; Canesin, R. C.; Bonilha, S. F. C.; Albuquerque, L. G. Phenotypic and genetic correlations of feed efficiency traits with growth and carcass traits in Nelore cattle selected for postweaning weight. **PLoS One**, v. 11, n. 8, p. e0161366, 2016.
- Costa, E. V.; Ventura, H. T.; Veroneze, R.; Silva, F. F.; Pereira, M. A.; Lopes, P. S. Estimated genetic associations among reproductive traits in Nelore cattle using Bayesian analysis. **Animal reproduction science**, v. 214, p. 106305, 2020.
- Cundiff, L. V.; Pond, W. G.; Bell, A. W. Beef cattle: Breeds and genetics. **Encyclopedia of Animal Science**. Ithaca: **Cornell University**, p. 74-76, 2004.
- Dias, L. T.; El Faro, L.; Albuquerque, L. G. Efeito da idade de exposição de novilhas à reprodução sobre estimativas de herdabilidade da idade ao primeiro parto em bovinos Nelore. **Arquivo Brasileiro de Medicina Veterinária e Zootecnia**, v. 56, p. 370-373, 2004.
- Do, C.; Park, B.; Kim, S.; Choi, T.; Yang, B.; Park, S.; Song, H. Genetic parameter estimates of carcass traits under national scale breeding scheme for beef cattle. **Asian-Australasian journal of animal sciences**, v. 29, n. 8, p. 1083, 2016.
- Elango, R.; Ball, R. O.; Pencharz, P. B. Amino acid requirements in humans: with a special emphasis on the metabolic availability of amino acids. **Amino acids**, v. 37, n. 1, p. 19, 2009.
- Eler, J. P.; Bignardi, A. B.; Ferraz, J. B. S.; Santana Junior, M. L. Genetic relationships among traits related to reproduction and growth of Nelore females. **Theriogenology**, v. 82, n. 5, p. 708-714, 2014.
- El-Hack, M. E. A.; Abdelnour, S. A.; Swelum, A. A.; Arif, M. The application of gene marker-assisted selection and proteomics for the best meat quality criteria and body measurements in Qinchuan cattle breed. **Molecular biology reports**, v. 45, n. 5, p. 1445-1456, 2018.

- Elzo, M. A.; Mateescu, R. G. et al. Genomic-polygenic and polygenic predictions for nine ultrasound and carcass traits in Angus-Brahman multibreed cattle using three sets of genotypes. **Livestock Science**, v. 202, p. 58-66, 2017.
- Feitosa, F. L. B.; Olivieri, B. F. et al. Genetic correlation estimates between beef fatty acid profile with meat and carcass traits in Nelore cattle finished in feedlot. **Journal of applied genetics**, v. 58, n. 1, p. 123-132, 2017.
- Fernandes Júnior, G. A. F.; Rosa, G. J. M. et al. Genomic prediction of breeding values for carcass traits in Nelore cattle. **Genetics Selection Evolution**, v. 48, n. 1, p. 7, 2016a.
- Gordo, D. G. M.; Baldi, F.; Lôbo, R. B.; Koury Filho, W.; Sainz, R. D.; Albuquerque, L. G. Genetic association between body composition measured by ultrasound and visual scores in Brazilian Nelore cattle. **Journal of Animal Science**, v. 90, n. 12, p. 4223-4229, 2012.
- Gordo, D. G. M.; Espigolan, R. et al. Genetic parameter estimates for carcass traits and visual scores including or not genomic information. **Journal of Animal Science**, v. 94, n. 5, p. 1821-1826, 2016.
- Gordo, D. G. M.; Espigolan, R.; Bresolin, T.; Fernandes Júnior, G. A.; Magalhães, A. F. B.; Braz, C. U.; Fernandes, W. B.; Baldi, F.; Albuquerque, L. G. Genetic analysis of carcass and meat quality traits in Nelore cattle. **Journal of animal science**, v. 96, n. 9, p. 3558-3564, 2018.
- Guarini, A. R.; Neves, H. H. R.; Schenkel, F. S.; Carneiro, R.; Oliveira, J. A.; Queiroz, S. A. Genetic relationship among reproductive traits in Nelore cattle. **animal**, v. 9, n. 5, p. 760-765, 2015.
- Kluska, S.; Olivieri, B. F. et al. Estimates of genetic parameters for growth, reproductive, and carcass traits in Nelore cattle using the single step genomic BLUP procedure. **Livestock science**, v. 216, p. 203-209, 2018.
- Lacerda, V. V.; Campos, G. S.; Roso, V. M.; Souza, F. R. P.; Brauner, C. C.; Boligon, A. A. Effect of mature size and body condition of Nelore females on the reproductive performance. **Theriogenology**, v. 118, p. 27-33, 2018.
- Leal-Gutiérrez, J. D.; Elzo, M. A.; Johnson, D. D.; Hamblen, H.; Mateescu, R. G. Genome wide association and gene enrichment analysis reveal membrane anchoring and structural proteins associated with meat quality in beef. **BMC**

- genomics**, v. 20, n. 1, p. 151, 2019.
- MacNeil, M. D.; Nkrumah, J. D.; Woodward, B. W.; Northcutt, S. L. Genetic evaluation of Angus cattle for carcass marbling using ultrasound and genomic indicators. **Journal of animal science**, v. 88, n. 2, p. 517-522, 2010.
- Magalhães, A. F. B.; Schenkel, F. S. et al. Genomic selection for meat quality traits in Nelore cattle. **Meat science**, v. 148, p. 32-37, 2019.
- Magalhães, A. F. B.; Teixeira, G. H. A. et al. Prediction of meat quality traits in Nelore cattle by near-infrared reflectance spectroscopy. **Journal of animal science**, v. 96, n. 10, p. 4229-4237, 2018.
- Magnabosco, C. U.; Lopes, F. B.; Fragoso, R. R.; Eifert, E. C.; Valente, B. D.; Rosa, G. J. M.; Sainz, R. D. Accuracy of genomic breeding values for meat tenderness in Polled Nelore cattle. **Journal of animal science**, v. 94, n. 7, p. 2752-2760, 2016.
- Mateescu, R. G.; Garrick, D. J.; Garmyn, A. J.; VanOverbeke, D. L.; Mafi, G. G.; Reecy, J. M. Genetic parameters for sensory traits in longissimus muscle and their associations with tenderness, marbling score, and intramuscular fat in Angus cattle. **Journal of animal science**, v. 93, n. 1, p. 21-27, 2014.
- Mattos, R.; Staples, C. R.; Thatcher, W. W. Effects of dietary fatty acids on reproduction in ruminants. **Reviews of reproduction**, v. 5, n. 1, p. 38-45, 2000.
- McAllister, C. M.; Speidel, S. E.; Crews Jr., D. H.; Enns, R. M. Genetic parameters for intramuscular fat percentage, marbling score, scrotal circumference, and heifer pregnancy in Red Angus cattle. **Journal of animal science**, v. 89, n. 7, p. 2068-2072, 2011.
- Mcphee, M. J.; Walmsley, B. J.; Dougherty, H. C.; McKiernan, W. A.; Oddy, V. H. Live animal predictions of carcass components and marble score in beef cattle: model development and evaluation. **Animal**, p. 1-10, 2020.
- Misztal, I.; Legarra, A.; Aguilar, I. Computing procedures for genetic evaluation including phenotypic, full pedigree, and genomic information. **Journal of Dairy Science**, v. 92, n. 9, p. 4648-4655, 2009.
- Misztal, I.; Tsuruta, S.; Strabel, T.; Auvray, B.; Druet, T.; Lee, D. H. Blupf90 and related programs (BGF90). In: **Proc. 7th World Congress on Genetics Applied to Livestock Production**, v.28, p.19-23, 2002.

- Mota, L. F. M.; Fernandes Jr, G. A.; Herrera, A. C.; Scalez, D. C. B.; Espigolan, R.; Magalhães, A. F. B.; Carvalheiro, R.; Baldi, F.; Albuquerque, L. G. Genomic reaction norm models exploiting genotype \times environment interaction on sexual precocity indicator traits in Nellore cattle. **Animal Genetics**, v. 51, n. 2, p. 210-223, 2020.
- Mwangi, F. W.; Charmley, E.; Gardiner, C. P.; Malau-Aduli, B. S.; Kinobe, R. T.; Malau-Aduli, A. E. Diet and Genetics Influence Beef Cattle Performance and Meat Quality Characteristics. **Foods**, v. 8, n. 12, p. 648, 2019.
- Neves, H. H. R.; Dos Reis, F. P.; Paterno, F. M.; Guarini, A. R.; Carvalheiro, R.; Silva, L. R.; Oliveira, J. A.; Queiroz, S. A. Herd-of-origin effect on the post-weaning performance of centrally tested Nellore beef cattle. **Tropical animal health and production**, v. 46, n. 7, p. 1235-1241, 2014.
- Oliveira, H. R.; Ventura, H. T.; Costa, E. V.; Pereira, M. A.; Veroneze, R.; Duarte, M. S.; Siqueira, O. H. G. B. D.; Fonseca e Silva, F. Meta-analysis of genetic-parameter estimates for reproduction, growth and carcass traits in Nellore cattle by using a random-effects model. **Animal Production Science**, v. 58, n. 9, p. 1575-1583, 2017.
- Pegolo, S.; Cecchinato, A.; Savoia, S.; Di Stasio, L.; Pauciullo, A.; Brugiapaglia, A.; Bittante, G.; Albera, A. Genome-wide association and pathway analysis of carcass and meat quality traits in Piemontese young bulls. **Animal**, v. 14, n. 2, p. 243-252, 2019.
- Pires, B. C.; Tholon, P. et al. Genetic analyses on bodyweight, reproductive, and carcass traits in composite beef cattle. **Animal Production Science**, v. 57, n. 3, p. 415-421, 2016.
- R Core Team. **R: a language and environment for statistical computing and graphics**. R Foundation for Statistical Computing: St. Louis, 2020.
- Regatieri, I. C.; Boligon, A. A. et al. Association between single nucleotide polymorphisms and sexual precocity in Nellore heifers. **Animal reproduction science**, v. 177, p. 88-96, 2017.
- Reverter, A.; Johnston, D. J. et al. Genetic and phenotypic characterisation of animal, carcass, and meat quality traits from temperate and tropically adapted beef breeds. 4. Correlations among animal, carcass, and meat quality traits. **Australian**

- Journal of Agricultural Research**, v. 54, n. 2, p. 149-158, 2003.
- Rosa, A. N.; Martins, E. N.; Menezes, G. R. O.; Silva, L. O. C. **Melhoramento genético aplicado em gado de corte: Programa Geneplus-Embrapa**. Brasília, DF: Embrapa; Campo Grande, MS: Embrapa Gado de Corte, 2013.
- Sargolzaei, M.; Chesnais, J. P.; Schenkel, F. S. A new approach for efficient genotype imputation using information from relatives. **BMC genomics**, v. 15, n. 1, p. 478, 2014.
- Savoia, S.; Albera, A.; Brugiapaglia, A.; Di Stasio, L.; Cecchinato, A.; Bittante, G. Heritability and genetic correlations of carcass and meat quality traits in Piemontese young bulls. **Meat science**, v. 156, p. 111-117, 2019.
- Schmidt, P. I., Campos, G. S.; Roso, V. M.; Souza, F. R. P.; Boligon, A. A. Genetic analysis of female reproductive efficiency, scrotal circumference and growth traits in Nelore cattle. **Theriogenology**, v. 128, p. 47-53, 2019.
- Schmidt, P. I.; Campos, G. S.; Lôbo, R. B.; Souza, F. R. P.; Brauner, C. C.; Boligon, A. A. Genetic analysis of age at first calving, accumulated productivity, stayability and mature weight of Nelore females. **Theriogenology**, v. 108, p. 81-87, 2018.
- Shiotsuki, L.; Silva, J. A. II; Albuquerque, L. G. Associação genética da prenhez aos 16 meses com o peso à desmama e o ganho de peso em animais da raça Nelore. **Revista Brasileira de Zootecnia**, v. 38, n. 7, p. 1211-1217, 2009.
- Silva, R. P.; Berton, M. P. et al. Genomic regions and enrichment analyses associated with carcass composition indicator traits in Nelore cattle. **Journal of animal breeding and genetics**, v. 136, n. 2, p. 118-133, 2019.
- Silva Neto, J. B.; Peripolli, E. et al. Genetic correlation estimates between age at puberty and growth, reproductive, and carcass traits in young Nelore bulls. **Livestock Science**, v. 241, p. 104266, 2020.
- Silveira, D. D.; De Vargas, L.; Pereira, R. J.; Campos, G. S.; Vaz, R. Z.; Lôbo, R. B.; Souza, F. R. P.; Boligon, A. A. Quantitative study of genetic gain for growth, carcass, and morphological traits of Nelore cattle. **Canadian Journal of Animal Science**, v. 99, n. 2, p. 296-306, 2018.
- Smith, B. J. boa: an R package for MCMC output convergence assessment and posterior inference. **Journal of statistical software**, v. 21, n. 11, p. 1-37, 2007.
- Terakado, A. P. N.; Boligon, A. A.; Baldi, F.; Silva, J. A. II V.; Albuquerque, L. G.

- Genetic associations between scrotal circumference and female reproductive traits in Nelore cattle. **Journal of Animal Science**, v. 93, n. 6, p. 2706-2713, 2015.
- Tonussi, R. L.; Espigolan, R. et al. Genetic association of growth traits with carcass and meat traits in Nelore cattle. **Genetics and Molecular Research**, v. 14, n. 4, p. 18713- 18719, 2015.
- United States Department Of Agriculture (USDA). U.S. **Standards for Grades of Feeder Cattle**. Washington: USDA, 2000. 4p.
- Vanraden, P. M. Efficient methods to compute genomic predictions. **Journal of dairy science**, v. 91, n. 11, p. 4414-4423, 2008.
- Vaz, F. N.; Restle, J.; Pádua, J. T.; Fonseca, C. A.; Pacheco, P. S. Características de carcaça e receita industrial com cortes primários da carcaça de machos nelore abatidos com diferentes pesos. **Ciência Animal Brasileira**, v. 14, n. 2, p. 199-207, 2013.
- Wheeler, T. L.; Cundiff, L. V.; Shackelford, S. D.; Koohmaraie, M. Characterization of biological types of cattle (Cycle VIII): Carcass, yield, and longissimus palatability traits. **Journal of animal science**, v. 88, n. 9, p. 3070-3083, 2010.
- Wheeler, T. L.; Koomaraie, M.; Shackelford, S. D. **Standardized warner-bratzler shear force procedures for meat tenderness measurement**. Clay Center: Roman L. Hruska U. S. MARC. USDA, 1995. 7p.
- Xia, J.; Qi, X. et al. Genome-wide association study identifies loci and candidate genes for meat quality traits in Simmental beef cattle. **Mammalian Genome**, v. 27, n. 5-6, p. 246-255, 2016.
- Yokoo, M. J.; Lôbo, R. B.; Magnabosco, C. U.; Rosa, G. J. M.; Forni, S.; Sainz, R. D.; Albuquerque, L. G. Genetic correlation of traits measured by ultrasound at yearling and 18 months of age in Nelore beef cattle. **Livestock Science**, v. 180, p. 34-40, 2015.

Chapter 3 – Genome-wide scans for carcass and meat quality traits in Nellore cattle

ABSTRACT – Beef plays a significant role in human nutrition and meat quality is defined by traits that guarantee consumers satisfaction. Carcass composition is of great importance for the beef industry, as its measurements are directly associated with the quantity and quality of the final product. However, although carcass and meat quality traits are important for the profitability of the production system, these have been little explored by breeding programs in Brazil. The present study aims to identify genomic regions responsible for the expression of economic important traits, in order to seek potential candidate genes acting in biological processes and metabolic pathways, associated with carcass (LMA: longissimus muscle area, BF: backfat thickness, and HCW: hot carcass weight) and meat quality traits (SF: shear-force tenderness, MARB: marbling score, and IMF: intramuscular fat content) in Nellore cattle. For this, 6,910 uncastrated males were feedlot finished and slaughtered at commercial slaughterhouses with an average age of 706.5 ± 79.6 days. The animals were genotyped using the Illumina Bovine HD Beadchip and the GeneSeek® Genomic Profilers HDi 75K and Low-Density 35K, and those genotyped with GGP panels were imputed to the HD panel using the FImpute v3 software, using the ARS-UCD1.2 reference map. The SNPs effects were estimated based on the weighted single-step GBLUP (WssGBLUP) approach, where two iterations were performed. The results of the GWAS analyzes were presented based on the proportion of additive variance explained by 1 Mb windows. The top 10 genomic regions explained 8.79, 12.06, and 9.01% of the additive genetic variance and harbored a total of 134, 158, and 93 positional candidate genes for LMA, BF, and HCW, respectively. For meat quality traits, the windows of greatest effect accounted for 14.72, 14.79, and 14.13% of the additive variance, and 137, 163, and 89 candidate genes were found for SF, MARB, and IMF, respectively. Among the candidate genes found, some stand out, such as *PPARGC1A*, *AQP3*, *AQP7*, *MYLK2*, *PLAGL2*, *PLAG1*, *XKR4*, *MYOD1*, *KCNJ11*, *WWOX*, *CARTPT*, *RAC1*, *PSAP*, *PLA2G16*, and *PLCB3*. These genes were previously associated with several traits, such as growth, carcass, quality of meat, feed intake and reproductive traits in Nellore and other cattle breeds. In general, the potential candidate genes found are involved in several signaling pathways such as: FoxO, which mediate the synthesis of growth factors and stress-regulated transcription factors that are involved in many physiological events; TGF- β , which mediates the fibrogenesis process by activating protein signaling to induce the expression of fibrogenic genes; mTOR, which is involved in the regulation of lipid synthesis through multiple effectors; flavor transduction pathway, which is involved in the biological processes of sensory perception of taste and acts in the regulation of food intake, thus defining the ingestive behavior; collagen chain trimerization, in which collagen, a protein abundantly expressed in connective tissue, influences the tenderness and texture of meat; lipid metabolism, which mediates the synthesis and degradation of lipids in cells; among other signaling pathways.

Keywords: beef cattle, carcass, genes, GWAS, meat quality, Nellore

1. INTRODUCTION

Due to the accelerated population growth, the demand for animal protein is expected to increase significantly in the coming decades, simultaneously with the decline or, at best, the constant availability of land dedicated to food production, as a result of climate change and alternative land uses. Given this scenario, the search for new technologies that allow a better understanding of the characteristics of economic interest for beef cattle farming is essential to achieve better rates of productivity, resource efficiency, and adaptation to changing environments (Simianer, 2016).

Beef plays a significant role in human nutrition. It is rich in bioactive nutrients and antioxidants beneficial to human health (Mann, 2018), in addition to presenting all essential amino acids (Williams, 2007; Mwangi et al., 2019) including high levels of lysine and methionine, compared to cereals and legumes, which have relatively low concentrations of these amino acids, respectively (Elango et al., 2009). Thus, the consumption of quality animal protein is essential for human growth, development, and health.

Meat quality is defined by traits that guarantee consumers satisfaction. The concept of "quality meat", most demanded by buyers, includes a series of sensory factors such as tenderness, juiciness, and flavor, which together contribute to a better meat palatability (Gordo et al., 2018). Meat tenderness is considered the most important sensory parameter, as it determines consumer satisfaction and purchase intention (Warner et al., 2021). The marbling score and intramuscular fat content are two different ways to assess the intramuscular fat content of meat. Intramuscular fat is directly linked to the quality of meat, contributing to the flavor, and preventing water loss from cooking (Mwangi et al., 2019).

Carcass composition is of great importance for the beef industry, as its measurements are directly associated with the quantity and quality of the final product. The longissimus muscle area (LMA) is an efficient indicator of muscle mass, carcass composition and edible portion (Gordo et al., 2018), and this trait is associated with the proportion of cuts that add commercial value for meat products (Caetano et al., 2013). The backfat thickness (BF) indicates the degree of carcass finishing and acts as a thermal insulator, protecting the carcass against the stiffness, darkening of muscles, and water loss, ensuring meat tenderness (Caetano et al., 2013; Baldassini et al.,

2017). The hot carcass weight (HCW) is directly related to the commercial value of the animal, since the amount paid to cattle breeders is, mainly, based on the carcass weight (Fernandes Júnior et al., 2016a; Gordo et al., 2018).

Considering that the Brazilian cattle herd is predominantly composed of animals with Zebu genetics (about 80%), the quality of meat produced in Brazil tends to be low. Zebu breeds produce leaner meat, with a lower marbling index and less tenderness, compared to European breeds, besides finishing late, partially due to the extensive production system adopted in Brazil (Cundiff et al., 2004; Albuquerque et al., 2006).

Livestock improvement through traditional methods, which combine phenotypic data and relatedness records for genetic evaluation of animals through statistical models, have been widely used for many years to achieve improvements in the capacity and functionality of production (Georges et al., 2019). However, although carcass composition and meat quality traits are important for the profitability of the production system, these have been little explored by breeding programs in Brazil. The difficulty in applying traditional selection on these characteristics is the main reason for this. Traits measurements can be expensive, both in terms of time and money, since meat quality traits, and sometimes those of the carcass, are measured in the *post-mortem*, which means that they cannot be measured in the potential candidates for breeding themselves, requiring the execution of progeny tests (Fernandes Júnior et al., 2016a; Fonseca et al., 2017; Leal-Gutiérrez; et al., 2019; Magalhães et al., 2019).

The use of genomic approaches becomes an alternative to partially overcome these obstacles that limit the improvement in the quality of *Bos indicus* beef. In this sense, Genome-wide Association Studies (GWAS) become a powerful tool to investigate the genetic architecture and identify genes that control the expression of economically important traits. GWAS have been used to discover quantitative trait loci (QTL) associated with phenotypes of interest. In this method, a complete genome scan is performed through statistical analysis, to identify genetic variants (mainly single nucleotide polymorphisms - SNP) in linkage disequilibrium with QTL of great effect on a certain trait, providing a better understanding of biological functions and genetic influence on phenotypic expression (Zhang et al., 2012; Yang et al., 2013; Magalhães et al., 2016; Magalhães et al., 2019; Pegolo et al., 2020).

Some GWAS already performed by our research group have identified candidate genes associated with the expression of carcass and meat traits (Lemos et al., 2016; Fernandes Júnior et al., 2016b; Magalhães et al., 2016; Oliveira Silva et al., 2017). However, those researches have been performed using the bovine genome map UMD3 or earlier versions in the GWAS analyzes. With the development of the new updated version of the reference map of the bovine genome (ARS-UCD1.2), which improves the location of the markers and contains additional SNP, allowing better detection of QTL and genomic predictions (Null et al., 2019), and the increase in the number of phenotyped and genotyped animals, the present study aims to identify genomic regions responsible for the expression of economic important traits using the reference map ARS-UCD1.2 and updated sets of phenotypes and genotypes, in order to seek potential candidate genes acting in biological processes and metabolic pathways, associated with carcass and meat quality traits in Nelore cattle.

2. MATERIAL AND METHODS

2.1. Phenotypic data

The database used in the present study is composed of information for carcass traits obtained in the *post-mortem*: longissimus muscle area (LMA), backfat thickness (BF), and hot carcass weight (HCW); and meat quality traits: shear force tenderness (SF), marbling score (MARB), and intramuscular fat content (IMF). Measurements were made on 6,910 Nelore males, born between 2008 and 2018, belonging to commercial herds that are part of four breeding programs (DeltaGen, Cia do Melhoramento, Paint – CRV Lagoa, and Nelore Qualitas) which integrate the Alliance Nelore database (www.gensys.com.br).

The animals were basically raised in grazing systems, with mineral supplementation during the dry season, and were confined in the finishing stage, fed a roughage-based diet, and slaughtered intact in commercial plants distributed in several Brazilian states, with a mean age of 706.5 ± 79.6 days.

HCW was obtained in kilograms by weighing the carcasses after the skinning and evisceration stages. To determine LMA (in square centimeters), the points quadrant method was used, and the BF (in millimeters) was measured with a caliper.

For SF, meat samples were prepared according to the standardized procedure proposed by Wheeler et al. (1995) and meat tenderness was determined using the Salter Warner-Bratzler Shear Force equipment. For IMF, the methodology described by Bligh and Dyer (1959) was adopted to determine the percentage of lipids in the meat samples. MARB was defined using a visual grading scale based on the USDA – Quality and Yield Grade (2000), attributing scores from 1 to 10 according to the marbling level. LMA, BF and meat measurements were obtained from samples of the *Longissimus thoracis* muscle collected between the 12th and 13th ribs of the left half carcass. It is important to note that the carcasses did not undergo to a maturation process, since this is the routine procedure in Brazil.

The contemporary groups (CG) for all traits included the variables: year and season of birth, farm (at birth, weaning, and yearling stages), and slaughter date. The birth season were: Spring (for animals born from August to January) and Autumn (from February to July).

For data consistency, observations with measurements of 3.5 standard deviations above or below the CG mean and CG with less than 5 animals were excluded from the analysis. The number of animals and descriptive statistics for each trait after the data consistency are shown in Table 4.

Table 4. Descriptive statistics of phenotypic information for hot carcass weight (HCW), longissimus muscle area (LMA), subcutaneous fat thickness (BF), marbling score (MARB), shear force tenderness (BF), and intramuscular fat content (IMF).

Trait	N	Mean	SD	*CV	Min	Max	NCG
HCW (kg)	6,611	290.24	34.02	11.72	166	424.60	108
LMA (cm ²)	6,190	70.56	9.63	13.64	40	112	103
BF (mm)	6,128	5.32	2.62	49.28	1	23	101
MARB	6,276	2.76	0.58	21.18	1.10	6	102
SF (kgf)	6,295	6.22	1.93	30.95	1.60	12.84	102
IMF (%)	3,812	0.78	0.37	48.20	0.12	3.61	75

*Percentage representation

N: number of observations; SD: standard deviation; CV: coefficient of variation; Min and Max: minimum and maximum values; NCG: number of contemporary groups.

2.2. Genotypic data

A total of 25,000 genotyped Nellore animals were used in this study. These animals were genotyped using the Illumina Bovine HD Beadchip (770K, Illumina Inc., San Diego, CA, USA), the GeneSeek® Genomic Profiler HDi 75K (GeneSeek In / c., Lincoln, NE) and the GeneSeek® Genomic Profile Low-Density 35K (GeneSeek In / c., Lincoln, NE), and those genotyped with GGP panels (75K and 35K) were imputed to the HD panel using the FImpute v3 software (Sargolzaei et al., 2014), using the ARS-UCD1.2 reference map.

The QCF90 software (Masuda et al., 2019) was used for the quality control of SNP markers and samples. Only SNP located in the autosomes and with a GeneCall score higher than 0.80 were considered in the analyzes. Furthermore, SNP located at the same genomic position, with MAF (Minor allele frequency) ≤ 0.05 , Call rate ≤ 0.90 , HWE (Hardy-Weinberg equilibrium) with p-value $\leq 10^{-5}$ and monomorphic SNP were removed. For samples, a Call rate threshold > 0.90 was set, and samples below this value were also excluded.

2.3. Genome-wide association analysis

The animal model used in GWAS analyzes included as random: additive and residual genetic effects; as fixed effects: CG (for all traits); date of analysis as classes (for BF, SF, and MARB) and; the linear effect of age at slaughter (for all traits) as covariate.

The matrix representation of the model is:

$$\mathbf{y} = \mathbf{X}\boldsymbol{\beta} + \mathbf{Z}\mathbf{a} + \mathbf{e}$$

where, \mathbf{y} is a vector of observations for each trait; $\boldsymbol{\beta}$ is the vector of fixed effects; \mathbf{a} is the vector of direct additive genetic effects, assumed as $\mathbf{a} \sim N(0, \mathbf{H}\sigma_a^2)$, where \mathbf{H} is the matrix that combines the kinship matrices, based on the pedigree (\mathbf{A}), and the genomic relationship matrix (\mathbf{G}) and σ_a^2 is the additive genetic variance; \mathbf{e} is the vector of residual effects associated with \mathbf{y} , assumed as $\mathbf{e} \sim N(0, \mathbf{I}\sigma_e^2)$, where \mathbf{I} is an identity matrix and σ_e^2 is the variance of residual effects; \mathbf{X} is the fixed effects incidence matrix relating $\boldsymbol{\beta}$ and \mathbf{y} ; and \mathbf{Z} is the incidence matrix of random effects relating \mathbf{a} and \mathbf{y} .

In the ssGBLUP procedure, the inverse of the numerator of the \mathbf{A}^{-1} kinship matrix is replaced by the combined matrix of the genomic-pedigree relation \mathbf{H}^{-1} (Aguilar et al., 2010):

$$\mathbf{H}^{-1} = \mathbf{A}^{-1} + \begin{bmatrix} \mathbf{0} & \mathbf{0} \\ \mathbf{0} & \mathbf{G}^{-1} - \mathbf{A}_{22}^{-1} \end{bmatrix}$$

where, \mathbf{H}^{-1} is the inverse of the modified kinship matrix; \mathbf{A}_{22}^{-1} is the inverse of the additive kinship matrix for genotyped animals; and \mathbf{G}^{-1} is the inverse of the genomic relationship matrix (VanRaden, 2008), which is described as:

$$\mathbf{G} = \frac{\mathbf{Z}\mathbf{Z}'}{2 \sum_{i=1}^m p_i(1-p_i)}$$

where, $\mathbf{Z} = (\mathbf{M} - \mathbf{P})$, in which \mathbf{M} is the SNP incidence matrix, with m columns representing the number of markers and n lines representing the number of genotyped animals. Each element in \mathbf{M} was set to -1, 0 or 1, for genotypes aa, Aa, and AA, respectively. \mathbf{P} is the matrix containing the allele frequencies expressed in $2p_i$, where p_i is the frequency of the second allele at locus i .

The effects of SNP were obtained iteratively based on the genomic values (GEBV) of the genotyped animals, using the POSTGSF90 software (Wang et al., 2012). The equation for computing the effect of SNP can be described as:

$$\hat{\mathbf{u}} = \lambda \mathbf{D}\mathbf{Z}'\mathbf{G}^{*-1}\hat{\mathbf{a}}_g = \mathbf{D}\mathbf{Z}'[\mathbf{Z}\mathbf{D}\mathbf{Z}']^{-1}\hat{\mathbf{a}}_g$$

where, $\hat{\mathbf{u}}$ is the effect vector of each SNP; \mathbf{D} is a diagonal matrix containing weights for the effect of SNP; \mathbf{Z}' is the transposed matrix that relates the genotypes of each locus; \mathbf{G}^{*-1} is the inverse matrix of weighted genomic relationships; $\hat{\mathbf{a}}_g$ is the vector with the predicted genetic values for genotyped animals, which is represented by a function of the effects of SNP ($\hat{\mathbf{a}}_g = \mathbf{Z}\mathbf{u}$); λ represents the proportion of genetic variation explained by the variation of SNP.

In the WssGBLUP procedure (Wang et al., 2012), the effect that each SNP contributes to the total genetic variance is calculate, using weights and iteratively, where the GEBV is computed only once and to estimate the effects of SNP two iterations are performed. In the first, \mathbf{D} it is an identity matrix ($\mathbf{D} = \mathbf{I}$) and for second iteration, \mathbf{D} was transformed into a diagonal matrix containing the weights for SNP effects computed in the first step. According to Wang et al. (2014), this procedure

allows to increase the weights of the SNP with greater effect and to reduce those with small effects.

The proportion of genetic variation explained by windows of 1 Mb, were calculated as presented by Wang et al. (2012):

$$\frac{\text{Var}(a_i)}{\sigma_a^2} \times 100\% = \frac{\text{Var}(\sum_{j=1} Z_j \hat{u}_j)}{\sigma_a^2} \times 100\%$$

where, a_i is the genetic value of the i^{th} region of 1 Mb; σ_a^2 is the total genetic variance; Z_j is the vector with the genotype of the j^{th} SNP for all animals; and \hat{u}_j is the estimated effect for the j^{th} SNP within the i -th region.

2.4. Functional analysis

Manhattan plots containing the genetic variance explained by 1 Mb windows were constructed to identify the chromosomal regions with the greatest effect on the expression of carcass and meat traits, using CMplot package for R. Candidate genes were identified in the SNP windows of greatest effect using the National Center for Biotechnology Information (NCBI) genome data visualization tool, considering the reference bovine genome map ARS-UCD1.2. A functional enrichment analysis was performed for each trait gene set using DAVID 6.8 Functional Annotation Tools (Huang et al., 2009a; 2009b) and GeneCodis Gene Annotations Co-occurrence Discovery (Carmona-Saez et al., 2007; Nogales-Cadenas et al., 2009; García-Moreno et al., 2021).

3. RESULTS AND DISCUSSION

3.1. GWAS for carcass traits

The top 10 genomic regions were located on chromosomes BTA 3, 4, 5, 9, 10, 11, 13, 14, 20, and 22 for Longissimus muscle area (Figure 1), on BTA 1, 2, 3, 13, 15, 17, 18, 20, 25, and 29 for backfat thickness (Figure 2), and on BTA 1, 2, 3, 5, 11, 12, 14, 17, and 23 for hot carcass weight (Figure 3). These top 10 regions accounted for 8.79, 12.06, and 9.01% of additive genetic variance and harbored a total of 134, 158, and 93 positional candidate genes for LMA, BF, and HCW, respectively (Tables 5, 6, and 7).

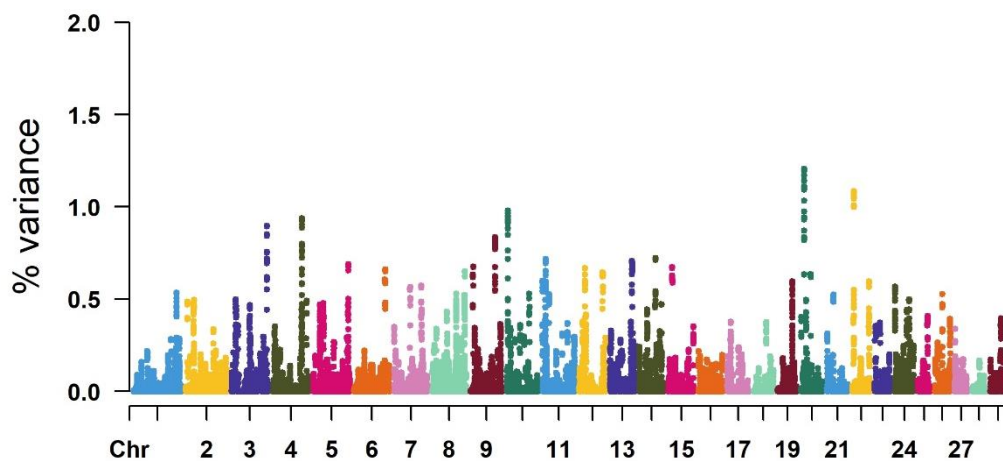


Figure 1. Manhattan plot presenting the proportion of direct additive genetic variance explained by windows of 1 Mb for LMA.

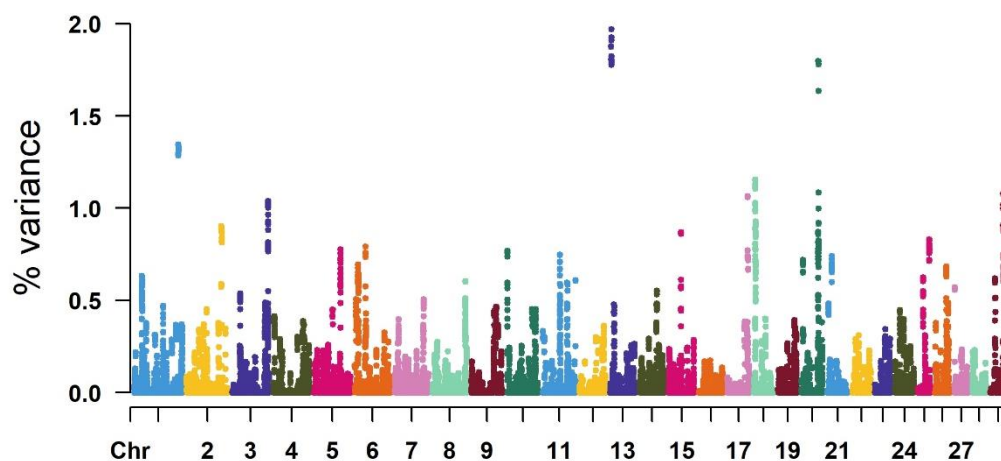


Figure 2. Manhattan plot presenting the proportion of direct additive genetic variance explained by windows of 1 Mb for BF.

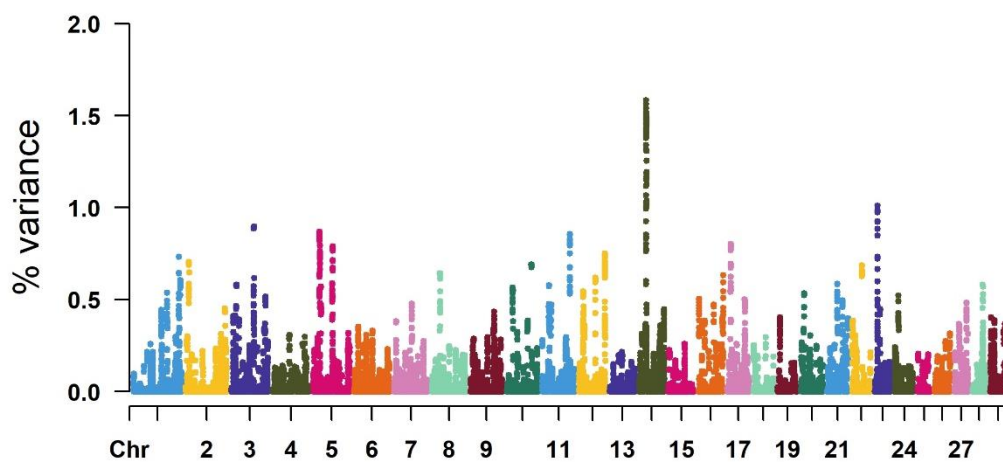


Figure 3. Manhattan plot presenting the proportion of direct additive genetic variance explained by windows of 1 Mb for HCW.

The functional enrichment analysis performed using DAVID software showed that 13 GO terms were significantly enriched in the biological process category for LMA (Table S1). Overall, the candidate genes are related to transcription from RNA polymerase II promoter (GO:0006366), lipid metabolic process (GO:00066290), cell-cell signaling (GO:0007267), protein stabilization (GO:0050821), protein phosphorylation (GO:0006468), oxidation-reduction process (GO:0055114), cell adhesion (GO:0007155), negative regulation of cell proliferation (GO:0008285), negative regulation of apoptotic process (GO:0043066), signal transduction (GO:0007165), regulation of transcription, DNA-templated (GO:0006355), transcription, DNA-templated (GO:0006351), and innate immune response (GO:0045087).

GeneCodis functional enrichment analysis (Table S1) clustered *TGFBR2* (transforming growth factor beta receptor 2), *STK4* (serine/threonine kinase 4), *CCNB1* (cyclin B1) and *ATG12* (autophagy related 12) genes, which acting on the FoxO signaling pathway (bta04068). FoxO (Forkhead box transcription factors) proteins are growth factor and stress-regulated transcription factors that are involved in many physiological events such as apoptosis, cell-cycle control, cellular differentiation, cell proliferation, glucose metabolism, and oxidative stress resistance (Gomes et al., 2008; Farhan et al., 2017). Studying Hanwoo cattle, Srikanth et al. (2020) used protein-protein interaction network to identify significant SNP that harbor genes that interact physically and found genes acting on the FoxO signaling pathway in association with carcass traits. Furthermore, polymorphisms in the gene encoding FoxO proteins were associated with growth traits in Qinchuan cattle (Sun et al., 2016).

The gene *CARTPT* (CART prepropeptide – BTA20, Table 5) is associated with satiety in response to leptin levels (Elias et al, 1998). Polymorphisms in leptin-promoting regions are associated with growth, body weight, feed intake, feeding behavior, and carcass traits in cattle (Nkrumah et al., 2005; Schenkel et al., 2005; Ferraz et al., 2009; Kulig and Kmíeé, 2009). Fernandes Júnior et al. (2016b) identified the *CARTPT* gene in association with the Longissimus muscle area in the Nellore breed, whose biological function is related to protein turnover, a process that is associated with growth and carcass traits obtained by ultrasound in Nellore cattle (Gomes et al., 2013).

SLC30A5 (solute carrier family 30 member 5) gene, located on BTA20 (Table 5), was reported by Karisa et al. (2013) in association with carcass traits in beef cattle. This gene encodes membrane-spanning molecules, many of which mediate the transport of zinc into beta cells to produce insulin (Karisa et al., 2013; Ackland and Michalczyk, 2016), which is related to ontogenesis of skeletal muscle (Gotoh et al., 2014).

ACTG2 (actin gamma 2, smooth muscle) on BTA11 (Table 5), provides instructions for the production of γ -actin proteins, which are components of the cytoskeleton, act on internal cell motility in different cell types (Papponen et al., 2009; Selga et al., 2011; Zhou et al., 2011), and forms multimers with myosin inside muscle cells to control cell contraction (James et al., 2021). In a study comparing Chinese Simmental steers and bulls, Zhou et al. (2011) found the *ACTG2* gene differentially expressed in the *Longissimus muscle* tissue of steers suggesting that the respective gene may play an important role in the regulation of steer meat quality.

The *TGFBR2* gene (BTA22, Table 5) is responsible for the expression of the transforming growth factor-beta receptor type 2 (TGF- β 2) protein and plays a critical role in growth regulation and development (Lawrence, 1996). This receptor has two extremities, one projects to the outside and the other remains inside the cell. A TGF- β (transforming growth factor-beta) protein binds to the extracellular domain of the TGF- β 2 receptor, forming a complex that transmits signals into the cell that trigger various responses, such as proliferation, differentiation, motility, apoptosis, and extracellular matrix synthesis (Lawrence, 1996; Levéen et al., 2002). The fibrogenesis process is mainly mediated by TGF- β signaling pathway, which activates SMAD proteins signaling (Gosselin et al., 2004; Decologne et al., 2007) to induce the expression of fibrogenic genes including collagen synthesis and enzymes catalyzing collagen cross-linking (Massague and Chen, 2000). Tizioto et al. (2013a) identified genes associated with meat tenderness from Nellore cattle acting in the TGF- β pathway. Also working with Nellore animals, Fernandes Júnior et al. (2016b) reported two genes for LMA that are associated with the cell cycle, process that involves genes of the TGF- β family.

Table 5. Chromosome (Chr), location, identification of genes and proportion of additive genetic variance (VarA) explained by windows with largest effects on LMA.

Chr	Location	Genes	VarA (%)
20	9800684_10800005	<i>CARTPT, MCCC2, LOC101907652, LOC101902413, BDP1, SERF1A, LOC100847365, SMN2, NAIP, GTF2H2, OCLN, MIR7858, MARVELD2, RAD17, AK6, TAF9, LOC101902475, CCDC125, TRNAE-CUC, CDK7, MRPS36, LOC101902030, CENPH, LOC101902547, CCNB1, SLC30A5</i>	1.20728
22	4765831_5764445	<i>MIR1814B, LOC100140865, TGFBR2, GADL1, LOC112443548, LOC112443493</i>	1.08537
10	4207216_5202403	<i>CCDC112, LOC787551, FEM1C, LOC107132809, LOC780975, TICAM2, LOC107132816, TMED7, LOC104973018, CDO1, ATG12, AP3S1, LVRN, LOC101903795, ARL14EPL, KIAA1191, SIMC1, LOC613765, THOC3</i>	0.98042
4	95388046_96386085	<i>LOC785077, MIR320B, PLXNA4</i>	0.93865
3	115689141_116684814	<i>ASB18, TRNAE-UUC, IQCA1, TRNAG-CCC, ACKR3, LOC104971869, LOC100335382, LOC112445895, COPS8, LOC101906731</i>	0.89811
9	79237934_80236183	<i>NMBR, GJE1, VTA1, ADGRG6, TRNAC-GCA, MIR2284AA-4, HIVEP2</i>	0.83692
14	52539717_53537941	<i>TRNAE-UUC, LOC112449580, TRNAC-ACA</i>	0.7236
11	10375999_11374851	<i>SLC4A5, MTHFD2, MOB1A, BOLA3, TET3, LOC112448751, DGUOK, ACTG2, LOC101909718, STAMBIP, C11H2orf78, DUSP11, LOC112448897, MIR2295, TPRKB, NAT8, ALMS1, LOC112448860, EGR4, FBXO41, CCT7, PRADC1, SMYD5, NOTO, LOC112448868, LOC101903026, LOC101903097, RAB11FIP5, MIR2294, SFXN5</i>	0.71747
13	72546080_73486255	<i>TOX2, JPH2, TRNAG-CCC, OSER1, GDAP1L1, FITM2, R3HDML, HNF4A, LOC112449432, TTPAL, SERINC3, PKIG, LOC112449399, LOC112449400, ADA, LOC101902669, LOC112449454, WISP2, KCNK15, RIMS4, YWHAB, PABPC1L, TOMM34, STK4, KCNS1, WFDC5</i>	0.70879
5	114142382_115139027	<i>MPPED1, LOC112446781, TRNAC-GCA, EFCAB6, SULT4A1, PNPLA5, LOC786474, PNPLA3, SAMM50, PARVB, TRNAC-GCA, PARVG, SHISAL1, RTL6</i>	0.69028

For BF, DAVID functional enrichment analysis (Table S2) revealed genes involved in apoptotic process (GO:0006915), cilium assembly (GO:0042384), angiogenesis (GO:0001525), intracellular signal transduction (GO:0035556), and regulation of transcription, DNA-templated (GO:0006355) processes. On the other hand, the GeneCodis results (Table S2) pointed to a genes' cluster including *LSS* (lanosterol synthase), *PLCB3* (phospholipase C beta 3), *PRLH* (prolactin releasing hormone), *PLA2G16* (phospholipase A2, group XVI), *NAA40* (N- α -acetyltransferase 40, NatD catalytic subunit), associated with the lipid metabolic process (GO:0006629)

The *NAA40* gene located on BTA29 (Table 6) produces N- α -acetyltransferase 40 histone, which is associated with the cellular acetyl-CoA levels, implying lipid synthesis and insulin signaling (Charidemou et al., 2022). Furthermore, in a meta-analysis, *NAA40* was identified as involved in the metabolism/transport of fatty acids or lipids in swine (Zhang et al., 2019). Also, on BTA29 (Table 6), *PLA2G16* encodes phospholipase A2 group XVI also known as adipocyte-specific phospholipase A2 (AdPLA) (Jaworski et al., 2009). AdPLA catalyzes the release of free fatty acids, mainly arachidonic acid, from membrane phospholipid stores, inducing eicosanoid biosynthesis (Funk et al., 2014). Arachidonic acid and eicosanoids have been implicated in several biological processes in adipose tissue, including regulation of differentiation (Forman et al., 1995; Reginato et al., 1998; Fajas et al., 2003), lipolysis (Kather and Simon, 1979; Fain et al., 2000) and glucose transport (Nugent et al., 2001). Jaworski et al. (2009) reported that AdPLA ablation prevents obesity in mice. Sun et al. (2012) identified polymorphisms in the *PLA2G16* gene that had significant effects on growth traits of Chinese cattle.

LGALS12 is another gene on BTA29 (Table 6) that encodes galectin-12, a member of the galectin family of β -galactosides binding proteins, which is an important regulator of adipose tissue development, acting on signal transduction that leads to hormonal stimulation for the induction of adipogenic factors essential for adipocyte differentiation (Yang et al., 2004). In mice, *LGALS12* was preferentially expressed by adipocytes and its ablation led to increased mitochondrial respiration of adipocytes, reduced adiposity, and improved insulin resistance (Yang et al., 2011). In production species, *LGALS12* was associated with intramuscular and subcutaneous fat development (Wu et al., 2019) and lean meat percentage (Ruan et al., 2021) in swine.

The *PRLH* located on BTA3 (Table 6) is a gene expressed in different tissues, including subcutaneous adipose tissue (ENSBTAG00000017615) and is associated with the regulation of prolactin expression and release in mammals (Gebreyesus et al., 2019). Prolactin is a highly versatile hormone whose functions are involved in reproductive processes, growth and development, osmoregulation, metabolism, immune regulation, brain function, and behavior (Carré and Binart, 2014). Furthermore, this hormone has been shown to induce lipogenesis in several tissues (Barber et al., 1991) and stimulate the expression of genes involved in lipid metabolism and milk protein synthesis (Shiu and Friesen, 1980; Akers et al., 1981; Lamberts and Macleod, 1990). In research conducted in hamsters, Cincotta and Meier (1987) observed a reduction in abdominal fat stores due to inhibition of prolactin secretion, concluding that the hormone plays an important role in the regulation of fat metabolism. In cattle, mutations in the *PRLH* gene were associated with heat tolerance in African *Bos indicus* (Kim et al., 2017) and Chinese breeds (Zeng et al., 2018).

The *WVOX* (WW domain containing oxidoreductase) gene, on BTA18 (Table 6), influences multiple pathways, including cholesterol homeostasis and fatty acid biosynthesis/triglyceride metabolism, processes that play a role in intramuscular fatty acid composition (Iatan et al., 2014; Grigoletto et al., 2020). This gene has been previously associated with loin eye area (Grigoletto et al., 2020), subcutaneous fat thickness (Fernandes Júnior et al., 2016b), and meat color (Lee et al., 2018) in different breeds of cattle, suggesting that *WVOX* may be an excellent candidate to improve the composition and quality of the final product.

The genes *PLCB3* (BTA29) and *RAC1* (ras-related C3 botulinum toxin substrate 1 – BTA25), possible candidates for BF (Table 6), were previously associated with lipid metabolism in membrane formation (Anitei et al., 2017). In cattle, it has been shown that *PLCB3* signaling is physiologically involved in ovulatory follicles and acts as a mediator of LH-induced differentiation responses of granulosa cells (Donadeu et al., 2011; Barros et al., 2013), and *RAC1* was associated with uterine capacity for pregnancy and fertility (Neupane et al., 2017). These findings indicate that both genes have pleiotropic properties and support the existence of a favorable genetic association (Caetano et al., 2013; Buzanskas et al., 2017; Kluska et al., 2018) between subcutaneous fat deposition and precocious/fertility traits of bovine females.

Table 6. Chromosome (Chr), location, identification of genes and proportion of additive genetic variance (VarA) explained by windows with largest effects on BF.

Chr	Location	Genes	VarA (%)
13	4307133_5305558	<i>LOC101901915</i>	1.9714
20	55672257_56658421	<i>LOC112442956, LOC112442957, LOC112442958, LOC112442959, LOC112442960, LOC112442961, LOC615245, LOC112442962, LOC107131579, LOC100849014, BASP1, LOC100849043, LOC112443053, MYO10, RETREG1</i>	1.79816
1	145109735_146106955	<i>LOC112448009, LOC101907800, COL18A1, LOC112448014, SLC19A1, LOC100849587, PCBP3, LOC107132220, LOC784761, COL6A1, COL6A2, FTCD, SPATC1L, LSS, MCM3AP, YBEY, C1H21orf58, PCNT</i>	1.34585
18	4968105_5965662	<i>VAT1L, LOC112442427, CLEC3A, WWOX</i>	1.15543
29	41737020_42719759	<i>LOC517475, HRASLS5, LGALS12, LOC613617, LOC536947, LOC618367, LOC614402, LOC100336631, PLA2G16, ATL3, RTN3, C29H11orf95, SPINDOC, LOC112444891, MARK2, MIR2406, RCOR2, NAA40, COX8A, OTUB1, MACROD1, FLRT1, STIP1, FERMT3, TRPT1, NUDT22, DNAJC4, VEGFB, FKBP2, PPP1R14B, PLCB3, BAD, GPR137, KCNK4, CATSPERZ, ESRRA, TRMT112, PRDX5, CCDC88B, RPS6KA4, TRNAE-UUC</i>	1.07803
17	65998516_66991682	<i>SEZ6L, ASPHD2, HPS4, SRRD, TFIP11, TPST2, CRYBB1, CRYBA4, LOC100847159, LOC614881, TRNAG-ACC, LOC112442108, LOC100849610</i>	1.06754
3	116841860_117838843	<i>COL6A3, LOC513039, LOC104970680, MLPH, RAB17, PRLH, LOC112446041, LRRFIP1, RBM44, RAMP1, MIR2902, UBE2F, LOC101904947, SCLY, ESPNL, KLHL30, ERF, ILKAP, LOC101905228, HES6, PER2, TRAF3IP1, ASB1, LOC107132358</i>	1.04075
2	113715036_114713312	<i>NYAP2, LOC104969981, LOC614695</i>	0.90257
15	39704690_40704354	<i>TEAD1, MIR2314, PARVA, TRNAG-UCC, MICAL2, TRNAV-CAC, LOC112441627, LOC112441626, DKK3</i>	0.87059
25	37292301_38290028	<i>TRRAP, TMEM130, TRNAG-CCC, NPTX2, LOC112444329, LOC101905575, LOC112444336, BAIAP2L1, LOC107131845, BRI3, TECPR1, BHLHA15, LMTK2, LOC104975913, LOC107131857, LOC112444303, LOC100850875, CCZ1, RSPH10B, PMS2, AIMP2, EIF2AK1, ANKRD61, LOC100848385, USP42, CYTH3, TRNAG-CCC, LOC100140431, LOC112444304, RAC1</i>	0.83187

Genome scan analysis showed that the region with the greatest effect on HCW is contained on chromosome 14, explaining 1.59% of the additive genetic variance (Table 7). This region harbors genes that have been associated with growth, carcass, feed intake, and reproduction traits (Lindholt-Perry et al., 2011; Saatchi et al., 2014), suggesting that the 22–26Mb region on BTA14 has a high influence on multiple traits of economic interest in livestock. Among all in this region, the genes *XKR4* (Kell blood group complex subunit-related family, member 4), *TMEM68* (transmembrane protein 68), *TGS1* (trimethylguanosine synthase 1), *LYN* (LYN proto-oncogene, Src family tyrosine kinase), *RPS20* (ribosomal protein S20), *MOS* (v-mos Moloney murine sarcoma viral oncogene homolog), *PLAG1* (pleomorphic adenoma gene 1 zinc finger), and *CHCHD7* (coiled-coil-helix-coiled-coil-helix domain containing 7) stand out.

XKR4 (Table 7) encodes a protein whose amino acid sequence plays important biological roles in cellular and lipid metabolism (Lindholt-Perry et al., 2011). Polymorphisms in or near to the *XKR4* gene have been identified and associated with birth weight, metabolic weight, growth traits, feed intake, and rump fat thickness in studies conducted in different bovine breeds (Bolormaa et al., 2011; Lindholt-Perry et al., 2011; Utsunomiya et al., 2013; Martínez et al., 2014; Terakado et al., 2018; An et al., 2019; Smith et al., 2019). Utsunomiya et al. (2013) reported that *XKR4* is a suggestive candidate gene for weight and carcass traits, that should be further explored in future studies in cattle.

TMEM68 is a gene expressed in the rumen, abomasum, intestine, and adipose tissue in cattle which may affect the biosynthetic processes of lipids (Srivastava et al., 2020). The *LYN* gene encodes a Src family kinase that is involved in cell proliferation, survival, differentiation, migration, adhesion, apoptosis, and cytokine release (Tatosyan and Mizenina, 2000; Taye et al., 2018). *RPS20* encodes a protein component of the 40S small ribosomal subunit, which is involved in protein synthesis. In mice, mutations in the *RPS20* gene cause pigmentary abnormalities with a pleiotropic effect on body size (McGowan et al., 2008). The gene *TGS1* produces an enzyme that methylates small nuclear and nucleolar RNAs (snRNAs and snoRNAs) and is involved in pre-mRNA splicing, transcription, and ribosome production (Blandino-Rosano et al., 2021). *MOS* transcribes a serine/threonine kinase that is expressed mainly in oocytes and regulates meiotic maturation (Sagata, 1997; Sahu et

al., 2018). Accumulation of MOS protein in the skeletal muscle of mice suggests that the gene plays an important role in the development of this tissue (Leibovitch et al., 1991). The *CHCHD7* gene transcribes essential factors for the assembly of mitochondrial cytochrome C oxidase (Cox) enzyme (Barros et al., 2004; Cavallaro, 2010; Banci et al., 2012; Oliveira et al., 2014). Cox acts as a terminal enzyme in the mitochondrial respiratory chain and is essential in the cellular energy production process (Tsukihara et al., 1996). Although the mechanisms of direct action on the expression of productive traits are unknown, all these genes were associated with several of these traits in cattle, such as growth, carcass, meat quality, feed intake, and reproductive traits (Pausch et al., 2011; Pryce et al., 2011; Lindholm-Perry et al., 2012; Utsunomiya et al., 2013; Cánovas et al., 2014; Ramayo-Caldas et al., 2014; Fernandes Júnior et al., 2016b; Magalhães et al., 2016; Oliveira Silva et al., 2017; Hay and Roberts, 2018; Campos et al., 2020).

PLAG1 gene was associated with body size, weight, carcass/meat quality, and reproduction in cattle (Fortes et al., 2013; Utsunomiya et al., 2013; Saatchi et al., 2014; Camargo et al., 2015; Fernandes Júnior et al., 2016b, Magalhães et al., 2016). Functional evidences indicate that *PLAG1* expresses a transcription factor that regulates IGF-2, insulin-like growth factor 2 (Van Dyck et al., 2007; Akhtar et al., 2012; Utsunomiya et al., 2017). IGF-2 is a cell growth and differentiation factor that plays an important role in muscle growth and myoblast proliferation and differentiation in mammals (Huang et al., 2014). Working with part of the database used in this study, Fernandes Júnior et al. (2016b) also identified and highlighted *PLAG1* as the most promising gene associated with carcass weight, as it has a pleiotropic effect on several traits of economic interest in livestock (Fortes et al., 2013).

Two members of the leucine-rich family of small proteoglycan genes (*LUM* – lumican and *DCN* – decorin) located in BTA5 (Table 7) were associated with HCW. Leucine-rich proteoglycans make up connective tissue and play an important role in regulating of collagen fibril formation and stabilization of collagen fibers (Iozzo, 1999). *LUM* gene is involved in the positive regulation of transforming growth factor β 1 production (GO:0032914). *DCN* is also involved in the regulation of the activity of transforming growth factor β 1 and participates in cell proliferation and differentiation (Yamaguchi et al., 1990; Nishimura et al., 2002).

Table 7. Chromosome (Chr), location, identification of genes and proportion of additive genetic variance (VarA) explained by windows with largest effects on HCW.

Chr	Location	Genes	VarA (%)
14	22487908_23486962	<i>XKR4, TRNAT-AGU, TMEM68, TGS1, LYN, RPS20, LOC112449628, LOC112449630, MOS, PLAG1, CHCHD7, SDR16C5, SDR16C6</i>	1.585
23	8267805_9265203	<i>HMGA1, SMIM29, NUDT3, LOC112443858, LOC112443903, LOC107131710, LOC100296311, RPS10, PACSIN1, SPDEF, C23H6orf106, LOC112443899, LOC112443896, SNRPC, UHRF1BP1, LOC112443807, TAF11, ANKS1A, TCP11, SCUBE3, LOC101907009, ZNF76</i>	1.01081
3	73392593_74391971	<i>NEGR1, TRNAW-CCA, ZRANB2, MIR186, PTGER3</i>	0.89777
5	20906335_21905700	<i>KERA, TRNAC-ACA, LUM, DCN, LOC112446653, LOC107132462, LOC112446654, SNORD107, LOC104972363</i>	0.87
11	89469532_90462309	<i>RNF144A, TRNAC-GCA, RSAD2, CMPK2</i>	0.85603
17	11330319_12328005	<i>TTC29, LOC112442098, LOC100336258, POU4F2, SLC10A7, LOC101906679, REELD1, LSM6, LOC112442132</i>	0.8047
5	62868893_63864715	<i>APAF1, LOC112446819, ANKS1B, LOC101907622, LOC101903783, LOC789481, FAM71C, LOC112441540</i>	0.78994
12	83608794_84605248	<i>ABHD13, TNFSF13B, MYO16, TRNAY-AUA, LOC112449089, LOC101905776, LOC101905821</i>	0.751
1	149114698_150106142	<i>HLCS, LOC112448075, RIPPLY3, LOC112448285, PIGP, TTC3, DSCR3, DYRK1A, KCNJ6</i>	0.73471
2	10704067_11695087	<i>FSIP2, LOC112443625, LOC100138706, LOC789157, LOC100138018, ZNF804A, LOC614531</i>	0.70506

3.2. GWAS for meat quality traits

The results of this study showed windows that stood out in terms of explained variance for all meat quality traits analyzed (Figures 4, 5, and 6). The 10 windows of greatest effect for shear-force tenderness, marbling, and intramuscular fat content explained 14.72, 14.79, and 14.13% of the additive genetic variance, respectively. These windows are located on chromosomes BTA 1, 5, 6, 7, 10, 11, 15, 23, and 26 for SF, on BTA 4, 7, 8, 10, 11, 12, 13, 15, and 20 for MARB, and on BTA 8, 9, 11, 12, 13, 19, 22, and 28 for IMF, totaling 137, 163 and 89 candidate genes, respectively (Tables 8, 9 and 10).

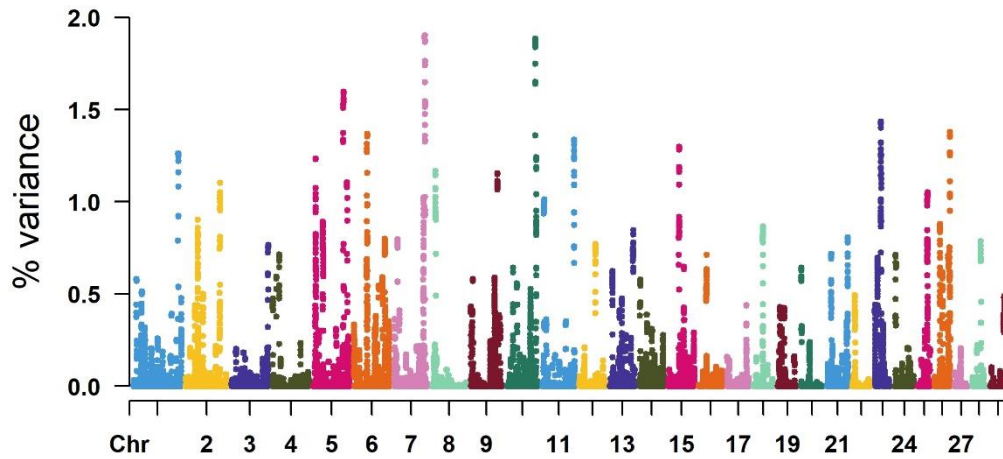


Figure 4. Manhattan plot presenting the proportion of direct additive genetic variance explained by windows of 1 Mb for SF.

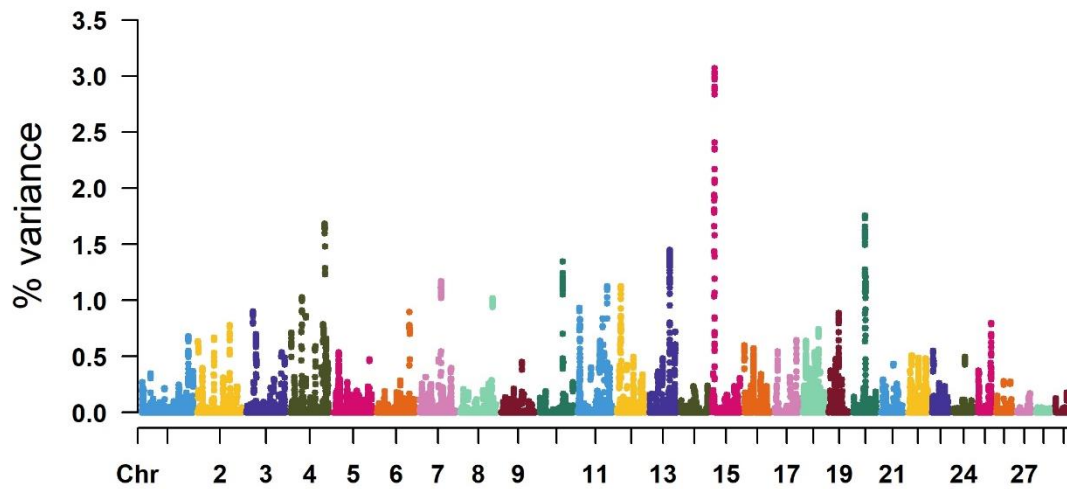


Figure 5. Manhattan plot presenting the proportion of direct additive genetic variance explained by windows of 1 Mb for MARB.

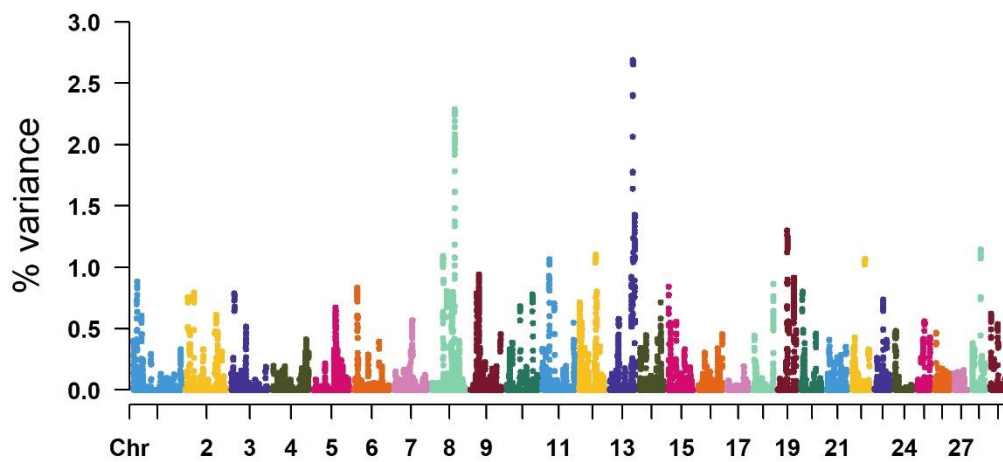


Figure 6. Manhattan plot presenting the proportion of direct additive genetic variance explained by windows of 1 Mb for IMF.

The DAVID software enrichment analysis (Table S4) for meat shear force (SF) revealed a cluster of genes of BTA5 (*T2R12*, *T2R10C*, *T2R65A*, *BOTA-T2R10B*, *TAS2R7*, *TAS2R10*, *TAS2R42*, *TAS2R46*, *LOC100140395*, *LOC782957*, *LOC528422*) that participate in the functional pathway of flavor transduction (bta04742) and are involved in the biological processes of sensory taste perception (GO:0050909) and detection of chemical stimulus involved in sensory perception of bitter taste (GO:0001580). The type two taste receptor family (TAS2R) and bitter taste receptor family (T2R) are G protein-coupled receptors responsible for distinguishing bitter-tasting compounds. Studies have shown that the activation of G protein-coupled receptors is involved in the maintenance of skeletal muscle and may supposedly mediate myofibrillar maturation and growth (Guttridge, 2011). Furthermore, it is probably that *TAS2R* and *T2R* genes act in the regulation of food intake, being determining factors in food choice, thus defining the ingestive behavior (Wu et al., 2002; Henslee et al., 2020). Given the importance of feed and nutrition in aspects of meat quality (Wood et al., 1999; Maltin et al., 2003), these groups of genes may have a strong influence on meat tenderness in Nellore cattle.

The *MEP1A* (meprin A subunit alpha) gene located on BTA23 (Table 8), is associated with several biological pathways, including the collagen chain trimerization pathway (Jang et al., 2018). Collagen is a protein abundantly expressed in connective tissue and influences tenderness and texture of meat. These desirable properties seem to be associated with *post-mortem* collagen degradation and the action of collagenases, which imply the alteration of the connective tissue structure, guaranteeing the desired softness and texture. (Weston et al., 2002). From GWAS analysis, Jang et al. (2018) identified *MEP1A* as a candidate gene contributing to tenderness in Berkshire pigs.

Functional evidence suggests that the *GLRX3* (glutaredoxin 3) gene on BTA26 (Table 8), plays a role in protecting mammalian cells against oxidative stress (Lillig et al., 2008). Oxidative stress can influence the reduction of collagen synthesis by intramuscular fibroblasts in some muscles, which can lead to decreased collagen degradation and, therefore, increased meat toughness (Archile-Contreras and Purslow, 2011). Thus, *GLRX3* can have a great influence on meat quality, ensuring its tenderness.

The gene encoding peroxisome proliferator-activated receptor- γ coactivator-1 α (*PPARGC1A*) was located within a region on BTA6 (Table 8). *PPARGC1A* is a coactivator of oxidative phosphorylation genes that control glucose and lipid transport and oxidation, skeletal muscle fiber formation, and mitochondrial biogenesis (Puigserver et al., 1998; Soria et al., 2009). Furthermore, *PPARGC1A* mediates the expression of genes involved in adipogenesis, leading to an increase in intramuscular fat content, which suggests a potential influence on tenderness (Rosen et al., 2002; Li et al., 2012). The *PPARGC1A* gene has been associated with several production traits, such as growth, carcass, meat quality, and reproductive traits in different breeds of cattle (Soria et al., 2009; Komisarek and Walendowska, 2012; Sevane et al., 2013; Shin and Chung, 2013; Ramayo-Caldas et al., 2014).

The *MYOD1* (myogenic differentiation 1) bovine gene mapped on chromosome 15 (Table 8), is a member of the *MYOD* gene family. The *MYOD* family consists of four structurally and functionally related genes that regulate skeletal myogenesis (Te Pas et al., 1999). *MYOD* genes regulate myoblast differentiation by inducing cell cycle arrest, a prerequisite for myogenic initiation (Braun et al., 1994), and are involved in the regulation of skeletal muscle growth, development, and repair, from the embryonic stage to its postnatal maturation and function (Te Pas et al., 1999; Dedieu et al., 2002). Skeletal muscle development is an important physiological process in meat-producing animals, and thus, because of their roles in muscle growth and development, these genes are considered potential candidates for meat production traits (Rexroad et al., 2001; Bhuiyan et al., 2009; Du et al., 2013; Tizioto et al., 2013a).

Also, on BTA15 (Table 8), *KCNJ11* (potassium voltage-gated channel subfamily J member 11) encodes a membrane protein that controls the flow of K^+ into the cell (Tizioto et al., 2013b). Supposedly high levels of K^+ ions are related to meat tenderness (Mateescu et al., 2013) as well, the addition of K-lactate to freshly slaughtered beef muscle leads to more tender meat (Walsh et al., 2010). In addition, this gene plays a role in glycogen storage, a mechanism involved in the *post-mortem* conversion of muscle to meat (Alekseev et al., 2010; Tricario et al., 2016).

Although they are not located in the window explaining the greatest proportion of additive genetic variance in this study, *MYOD1* and *KCNJ11* can be considered promising candidate genes for SF, since they are located in BTA15, within/near a

region that harbors a QTL which influences meat tenderness (Rexroad et al., 2001), including in the Nellore breed (Tizioto et al., 2013a; 2013b).

Table 8. Chromosome (Chr), location, identification of genes and proportion of additive genetic variance (VarA) explained by windows with largest effects on SF.

Chr	Location	Genes	VarA (%)
7	99989561_100987050	<i>ST8SIA4</i> , <i>LOC112447567</i> , <i>LOC112447498</i> , <i>LOC112447568</i>	1.90475
10	92728846_93718657	<i>SEL1L</i> , <i>TRNAK-UUU</i> , <i>TRNAK-CUU</i> , <i>LOC785767</i>	1.8849
5	98191406_99099643	<i>ETV6</i> , <i>LOC112446828</i> , <i>LOC112446741</i> , <i>LOC616478</i> , <i>LOC112446742</i> , <i>LOC100140395</i> , <i>TAS2R42</i> , <i>SMIM10L1</i> , <i>T2R45P</i> , <i>TAS2R46</i> , <i>LOC782957</i> , <i>LOC101903336</i> , <i>T2R43P</i> , <i>T2R65A</i> , <i>LOC100141277</i> , <i>T2R12</i> , <i>BOTA-</i> <i>T2R10B</i> , <i>LOC100138383</i> , <i>TAS2R10</i> , <i>T2R10C</i> , <i>TAS2R9</i> , <i>TAS2R8</i> , <i>TAS2R7</i> , <i>LOC104972542</i> , <i>YBX3</i> , <i>STYK1</i> , <i>MAGOHB</i> , <i>KLRA1</i> , <i>LOC101902742</i> , <i>LOC101902704</i> , <i>LOC513869</i>	1.59902
23	20043222_21035197	<i>MEP1A</i> , <i>ADGRF5</i> , <i>LOC112443908</i> , <i>ADGRF1</i> , <i>LOC100296156</i> , <i>TNFRSF21</i> , <i>CD2AP</i> , <i>ADGRF2</i> , <i>ADGRF4</i> , <i>OPN5</i> , <i>LOC107131722</i>	1.43652
26	49416849_50414892	<i>GLRX3</i> , <i>LOC112444515</i> , <i>LOC112444512</i> , <i>TRNAC-ACA</i> , <i>TCERG1L</i> , <i>SYCE1</i> , <i>CYP2E1</i> , <i>LOC528422</i> , <i>LOC112444506</i>	1.3799
6	42520487_43518582	<i>LOC112447151</i> , <i>LOC104972733</i> , <i>LOC112447204</i> , <i>PPARGC1A</i>	1.36901
11	103686161_104681538	<i>LHX3</i> , <i>QSOX2</i> , <i>LOC787891</i> , <i>GPSM1</i> , <i>LOC101902280</i> , <i>DNLZ</i> , <i>CARD9</i> , <i>SNAPC4</i> , <i>ENTR1</i> , <i>PMPCA</i> , <i>INPP5E</i> , <i>SEC16A</i> , <i>NOTCH1</i> , <i>LOC112448856</i> , <i>EGFL7</i> , <i>MIR126</i> , <i>AGPAT2</i> , <i>LOC101902839</i> , <i>LOC101902895</i> , <i>FAM69B</i> , <i>LOC107132967</i> , <i>LOC112448923</i> , <i>LOC112448928</i> , <i>LOC789606</i> , <i>LOC100848307</i> , <i>LOC112448857</i> , <i>ABO</i> , <i>LOC112448956</i> , <i>SURF6</i> , <i>MED22</i> , <i>RPL7A</i> , <i>LOC112448907</i> , <i>LOC112448908</i> , <i>LOC112448904</i> , <i>LOC112448903</i> , <i>LOC112448905</i> , <i>LOC100139115</i> , <i>SURF2</i> , <i>SURF4</i> , <i>STKLD1</i> , <i>LOC107132968</i> , <i>REXO4</i> , <i>ADAMTS13</i> , <i>CACFD1</i> , <i>SLC2A6</i> , <i>LOC112448858</i> , <i>TRNAC-GCA</i> , <i>MYMK</i> , <i>ADAMTSL2</i> , <i>FAM163B</i> , <i>DBH</i> , <i>SARDH</i> , <i>VAV2</i>	1.33734
15	34666995_35656053	<i>SERGEF</i> , <i>TRNAC-ACA</i> , <i>KCNC1</i> , <i>MYOD1</i> , <i>OTOG</i> , <i>USH1C</i> , <i>ABCC8</i> , <i>KCNJ11</i> , <i>NCR3LG1</i> , <i>NUCB2</i> , <i>LOC112441567</i> , <i>PIK3C2A</i> , <i>LOC101904314</i> , <i>RPS13</i> , <i>PLEKHA7</i> , <i>LOC112441697</i>	1.30066
1	146784680_147763482	<i>RUNX1</i> , <i>LOC112448042</i> , <i>MIR2285A</i> , <i>LOC112448047</i>	1.26233
10	95715171_96714876	<i>MIR2293</i>	1.24236

For MARB, GeneCodis functional analysis (Table S5) revealed genes that act in the mTOR (bta04150), TGF- β (bta04350), lipid metabolism (bta00561, bta00564), thermogenesis (bta04714), and actin cytoskeleton regulation (bta04810) signaling pathways, in addition to regulating biological processes involved in the skeletal muscle cell/satellite cell differentiation (GO:0014816, GO:0035914) and regulation of muscle filament sliding (GO:0032971). This suggests a relationship between muscle and lipid metabolism in intramuscular fat deposition. According to Silva et al. (2020), the variation in the content of MARB may be due to the processes of absorption, synthesis, and degradation of intramyocellular and extramyocellular lipids, which involves the metabolic pathways in myofibers.

Based on enrichment analysis, it was found that *TXN* (thioredoxin) and *TXNDC8* (thioredoxin domain containing 8), both located on BTA8 (Table 9), participate in the glycerol ether metabolic process (GO:0006662). Glycerol ethers are ether lipid precursors, which are important structural components of cell membranes (Dean and Lodhi, 2018) and have been identified as potential endogenous ligands of the peroxisome proliferator-activated receptor-gamma (PPAR γ), a key receptor in adipose tissue development and lipid metabolism (Davies et al., 2001; Zhang et al., 2004; Tsukahara et al., 2006; Ahmadian et al., 2013). Also, one study investigated the interaction between *TXNIP* (thioredoxin-interacting protein) and *TXN* in adipocyte development, and the authors found that *TXNIP* binds to *TRX* inhibiting its function, affecting the adipogenesis process (Chutkow and Lee, 2011). Correspondingly, another study demonstrated that *TXNIP* deficiency led to increased adipogenesis in preadipocytes and fibroblasts of embryonic mice, while *TXNIP* overexpression resulted in impaired adipocyte differentiation (Rojanathammanee et al., 2014). These results elucidate the important role of thioredoxin in adipogenesis, suggesting a strong influence on marbling fat.

MYLK2 (BTA13 – Table 9), a gene that participates in myosin light chain binding (GO:0032027), is predominantly expressed in skeletal muscle fibers and is essential for muscle contraction, composing the main myofibrillar proteins in muscle cells (Janin et al., 2018). This gene is a regulatory target of Ca²⁺/calmodulin and is responsible for myosin light chain phosphorylation, playing an important role in insulin-stimulated glucose transport in adipocytes (Choi et al., 2006). In this sense, knowing the

importance of glucose in the synthesis of fatty acids, glycerol, and ATP in adipocytes, *MYLK2* can influence the deposition of intramuscular fat. In a transcriptome study, Silva et al. (2020) found differentially expressed alternative splicing transcripts belonging to the *MYLK2* gene in Nellore animals pooled for high intramuscular fat.

Functional analysis revealed that *RICTOR* (BTA20 – Table 9) is involved in the mTOR signaling pathway (bta04150). The mammalian (mechanistic) target of rapamycin (mTOR) is a serine/threonine protein kinase, which consists of two complexes called mTORC1 and mTORC2, which *RICTOR* is a component. mTOR signaling is involved in the regulation of lipid synthesis through multiple effectors, such as sterol regulatory element-binding proteins (SREBP) and PPAR γ (Lamming and Sabatini, 2013). SREBP are transcription factors that modulate proteins involved in fatty acid synthesis (Mihaylova and Shaw, 2011) and its interaction with mTOR is critical for the activation of lipogenic genes in response to nutrient intake (Caron et al., 2015). PPAR γ , as mentioned earlier, plays an important role in lipid metabolism, as it promotes the uptake of free fatty acids and accumulation of triacylglycerol in adipose tissue (Ahmadian et al., 2013), and mTOR is a critical mediator of the lipogenic actions of PPAR γ activation (Blanchard et al., 2012). There is evidence that mTOR ablation resulted in insulin resistance and inhibited the development of adipose tissue in mice (Shan et al., 2016), elucidating the important role of the mTOR signaling pathway in adipogenesis.

The *PLAGL2* (pleomorphic adenoma gene-like 2), located on chromosome 13 (Table 9), is a homolog of the *PLAG1* gene, which plays a role in regulating important aspects of dietary lipid absorption (Van Dyck et al., 2007). In a recent GWAS study the *PLAGL2* gene was associated to subcutaneous and rump fat thickness in Montana Tropical composite beef cattle (Grigoletto et al., 2020), reinforcing the gene role in lipid metabolism. Although there is no concrete functional evidence of how *PLAGL2* acts in the signaling pathways of lipid metabolism, it is necessary that the gene be further investigated in order to associate it, not only with the marbling index, but with other productive traits in Nellore cattle, since *PLAGL2* is a homolog of *PLAG1*, a promising gene with a pleiotropic effect on several traits of economic interest in livestock

Table 9. Chromosome (Chr), location, identification of genes and proportion of additive genetic variance (VarA) explained by windows with largest effects on MARB.

Chr	Location	Genes	VarA (%)
15	6703457_7694135	LOC112441715, CEP126, ANGPTL5, LOC787373, TRPC6, LOC787452	3.07144
20	35294968_36279695	FYB1, RICTOR, OSMR, LOC104975274, LOC101906686, LOC101906739, LIFR, EGFLAM, LOC104975277	1.7577
4	105450260_106449584	MGAM, LOC100296901, LOC112446429, LOC101902292, PRSS58, LOC780846, LOC780933, PRSS1, LOC112446443, LOC101902375, LOC615948, LOC101907820, LOC789121, LOC100297263, LOC104972311, LOC101903084, LOC101904744, LOC112441528, LOC112446430, LOC100299076, LOC101902875, LOC112446437, LOC617189, LOC112446444, LOC104972445, LOC112446433, LOC617183, LOC112446434, LOC112446445, LOC104972274, LOC112446431, LOC783945, LOC112446438, LOC783647, LOC100300510, LOC112446448, LOC107132437, LOC112446449, LOC101904319, LOC100851681, LOC509513, LOC101904045, LOC101909872, LOC112446440, LOC112446447, LOC101903590, LOC101910001, LOC101904148, LOC112446441, LOC101903755, LOC112446446, LOC101903933, LOC101903865, LOC101904075, LOC112446439, LOC101902874, LOC112446435, LOC104968514, LOC100336982, LOC100336993, LOC101902921, LOC101902797, LOC112446436, LOC107132438, LOC112446442, LOC101902515, LOC101902455, LOC112446432, LOC786254, PRSS2, LOC505349, EPHB6, TRPV6, TRPV5, LLCFC1, KEL, LOC107132449, LOC107132445, LOC107132446, LOC107132447, OR6V1, LOC107132448	1.68442
13	61076541_62074803	REM1, HM13, LOC101906008, ID1, COX4I2, BCL2L1, LOC107133075, TPX2, MYLK2, FOXS1, LOC618409, DUSP15, TTLL9, PDRG1, XKR7, CCM2L, HCK, TM9SF4, PLAGL2, POFUT1, KIF3B, ASXL1, NOL4L, LOC112449324, LOC104973860	1.45244
10	69813228_70811343	CCDC198, SLC35F4, ARMH4, LOC101905452, LOC101906445, ACTR10, TRNAK-CUU, PSMA3, ARID4A, TOMM20L, TIMM9, KIAA0586	1.34905
7	64637123_65634855	GRIA1, LOC100140426, LOC104969225, FAM114A2, LOC112447577, MFAP3, SMIM15, GALNT10	1.17019
12	11635245_12628866	LOC107132986, VWA8, DGKH, AKAP11, LOC112449151	1.127
11	89658792_90657611	RNF144A, TRNAC-GCA, RSAD2, CMPK2, LOC107132955	1.12498
4	35671229_36666662	LOC112446326, SEMA3A, LOC112446369	1.02808
8	99166550_100157127	LOC112447758, PALM2, LOC107132734, LOC112447963, AKAP2, C8H9orf152, TXN, TXNDC8, SVEP1	1.02085

The main pathways enriched by GeneCodis for IMF (Table S6) were glycosaminoglycan biosynthesis (bta00532, bta00533, bta00534), glycosphingolipid biosynthesis (bta00601), vasopressin-regulated water reabsorption (bta04962), ubiquitin mediated proteolysis (bta04120), sphingolipid metabolism (bta00600), mTOR signaling pathway (bta04150), regulation of lipolysis in adipocytes (bta04923), thermogenesis (bta04714), and metabolic pathways (bta01100).

Nuclear receptor 3 coactivator (*NCOA3*) is located within the region (BTA13) explaining the greatest proportion of the additive variance of intramuscular fat content (Table 10) in this study. This gene plays an important role in lipid metabolism, as well as adipogenesis and obesity, by regulating the expression of the peroxisome proliferator-activated receptor γ (PPAR γ), a factor master of adipocyte differentiation and metabolism (Louet et al., 2006; Lefterova et al., 2014). Studies with swine provide evidence that *NCOA3* may be associated with intramuscular fat deposition or metabolism (Han et al., 2017; Wang et al., 2020c).

AQP3 and *AQP7*, both located on chromosome 8 (Table 10), encode aquaglyceroporins (AQP), a subgroup of proteins belonging to the aquaporin family. AQP are integral membrane proteins that drive the transport of water, glycerol, and other small solutes in adipocytes, in response to osmotic gradients (Hara-Chikuma and Verkman, 2006). The production of glycerol and its flow in adipocytes modulate lipid and glycemic homeostasis and, eventually, control the accumulation of body fat (Hibuse et al., 2005; Prudente et al., 2007). Aquaglyceroporin genes have been associated with obesity in humans and mice (Hara-Chikuma et al., 2005; Miranda et al., 2010), intramuscular adipogenesis in swine (Wang et al., 2020a), and subcutaneous fat deposition in cattle (Fernandes Júnior et al., 2016b). According to Fernandes Júnior et al. (2016b), lipid metabolism occurs in a similar way among mammals, and given the reports of association with similar traits in other species, *AQP3* and *AQP7* are plausible candidate genes.

The *DDIT4* (DNA damage-inducible transcript 4) gene, located in BTA28 (Table 10), regulates cell growth, proliferation, and survival by inhibiting mTOR1 (mechanistic target of rapamycin complex 1) activity in response to hypoxia and/or nutrient restriction (Sofer et al., 2005; DeYoung et al., 2008). mTORC1 is involved in increasing the biosynthesis and storage of lipids in response to insulin (Porstmann et al., 2008),

and considering its role as an inhibitor of mTORC1, *DDIT4* can be involved in lipogenesis and/or adipogenesis processes. In a study evaluating the fatty acid profile in intramuscular fat of the Longissimus thoracis muscle, Lemos et al. (2018) reported the same region that harbors *DDIT4* (BTA28), in association with lauric acid from Nellore cattle intramuscular fat.

The prosaposin (*PSAP*), located on chromosome 10 (Table 10), is a gene widely expressed in different tissues. This gene is an important factor in lipid metabolism since *PSAP* expression patterns suggest that the gene is associated with fat development due to its high expression in the early stage of adipocyte differentiation (Wang et al., 2020b). Polymorphisms in this gene were related to morphological, growth, carcass, and meat quality traits in different bovine breeds (Guo et al., 2016; Wang et al., 2020b; Zhao et al., 2021).

TRDN (triadin), located on BTA9 (Table 10), regulates the release of Ca^{2+} in the sarcoplasmic reticulum to promote muscle contraction (Arce-Recinos et al., 2021), however, its biological role in lipid deposition is not elucidated. Investigating gene expression patterns associated with fat deposition in bovine Longissimus muscle, Sasaki et al. (2005) observed higher levels in the expression of *TRDN* in the low marbling steers group than in the high marbling steers group. The researchers suggested that the decrease in *TRDN* expression might promote the proliferation, differentiation, or maturation of cells of the adipocyte lineage, weakening the structural integrity of the sarcomere and resulting in deposition of intramuscular fat (Sasaki et al., 2005). In a study conducted in pigs, *TRDN* was associated with intramuscular fat deposition (Serão et al., 2010), which suggests that the gene might be a candidate for improving the intramuscular fat content of Nellore beef.

Table 10. Chromosome (Chr), location, identification of genes and proportion of additive genetic variance (VarA) explained by windows with largest effects on IMF.

Chr	Location	Genes	VarA (%)
13	75697375_76695701	<i>EYA2, LOC112449339, ZMYND8, LOC101905203, LOC112449409, LOC104973934, LOC112449425, LOC112449385, NCOA3, SULF2, LOC112449340, LOC112449386, LOC100847661, LOC112449341, TRNAK-UUU, TRNAG-GCC, LOC100295371</i>	2.69118
8	74248099_75247877	<i>STMN4, TRIM35, LOC112447822, PTK2B, CHRNA2, EPHX2, LOC781381, GULO, LOC107132711, HTD2, LOC781261, APTX, DNAJA1, SMU1, B4GALT1, SPINK4, BAG1, CHMP5, NFX1, AQP7, AQP3, NOL6, UBE2R2</i>	2.29019
13	81732628_82730117	<i>DOK5, TRNAL-UAA, LOC101903665, LOC112449388, LOC112449389</i>	1.42923
19	31528976_32528184	<i>HS3ST3A1, LOC112442639, COX10, HS3ST3B1</i>	1.30097
28	27356520_28353587	<i>UNC5B, SLC29A3, LOC107131944, CDH23, C28H10orf105, VSIR, PSAP, CHST3, LOC104969714, SPOCK2, ASCC1, LOC112444781, LOC783294, ANAPC16, LOC112444748, DDIT4, LOC112444749, LOC112444774</i>	1.14615
12	53954994_54953149	<i>LOC112449133, LOC112449162, LOC112449159, RBM26, NDFIP2, LOC617043, LOC104973609</i>	1.10554
8	36503847_37501041	<i>PTPRD, DMAC1</i>	1.09309
22	41598889_42597887	<i>FHIT, LOC112443500, C22H3orf67</i>	1.0693
11	23094939_24091589	<i>LOC615674</i>	1.06621
9	27149972_28146296	<i>NKAIN2, MIR2478, TRDN, LOC112448023, LOC112448021, LOC112448022, LOC112448154, LOC101904186, LOC100848869</i>	0.94167

4. CONCLUSIONS

The genome-wide association study (GWAS) indicated regions of great effect on different chromosomes harboring candidate genes with biological functions that can be directly or indirectly associated with the expression of carcass and meat quality traits in the Nellore breed. Some of these genomic regions harbor genes that have been previously associated with growth, carcass, meat quality, feed intake, and reproductive traits in Nellore and other cattle breeds, such as *PPARGC1A*, *AQP3/AQP7*, *MYLK2*, *PLAGL2*, *PLAG1*, *XKR4*, *MYOD1*, *KCNJ11*, *WVVOX*, *CARTPT*, *RAC1*, *PSAP*, *PLA2G16*, and *PLCB3*. In general, the potential candidate genes found are involved in several signaling pathways such as: FoxO, which mediate the synthesis of growth factors and stress-regulated transcription factors; TGF- β , which mediates the

fibrogenesis process; mTOR, which is involved in the regulation of lipid synthesis; flavor transduction pathway, which is involved in the biological processes of sensory perception of taste and acts in the regulation of food intake; collagen chain trimerization, which influences tenderness and texture of meat; lipid metabolism, which mediates the synthesis and degradation of lipids in cells; among other signaling pathways. The combination of the results obtained from the GWAS and functional enrichment analysis allow us to better understand important biological processes, providing references for the understanding, in genetic-molecular terms, of these characteristics.

5. REFERENCES

- Ackland, M. L.; Michalczyk, A. A. Zinc and infant nutrition. **Archives of biochemistry and biophysics**, v. 611, p. 51-57, 2016.
- Aguilar, I.; Misztal, I.; Johnson, D. L.; Legarra, A.; Tsuruta, S.; Lawlor, T. J. Hot topic: A unified approach to utilize phenotypic, full pedigree, and genomic information for genetic evaluation of Holstein final score. **Journal of Dairy Science**, v. 93, n. 2, p. 743-752, 2010.
- Ahmadian, M.; Suh, J. M.; Hah, N.; Liddle, C.; Atkins, A. R.; Downes, M.; Evans, R. M. PPAR γ signaling and metabolism: the good, the bad and the future. **Nature medicine**, v. 19, n. 5, p. 557-566, 2013.
- Akersr, M. R., Bauman, D. E.; Capuco, A. V.; Goodman, G. T.; Tucker, A. H. Prolactin regulation of milk secretion and biochemical differentiation of mammary epithelial cells in periparturient cows. **Endocrinology**, v. 109, n. 1, p. 23-30, 1981.
- Akhtar, M.; Holmgren, C.; Göndör, A.; Vesterlund, M.; Kanduri, C.; Larsson, C.; Ekström, T. J. Cell type and context-specific function of PLAG1 for IGF2 P3 promoter activity. **International journal of oncology**, v. 41, n. 6, p. 1959-1966, 2012.
- Albuquerque, L. G. Mercadante, M. E. Z.; Eler, J. P. Recents studies on the genetic basis for the selection of *Bos indicus* for beef production. In: **Proceedings of the 8th World Congress on Genetics Applied to Livestock Production, Belo Horizonte, Minas Gerais, Brazil, 13-18 August, 2006**. Instituto Prociência, 2006.

p. 03-22.

- Alekseev, A. E.; Reyes, S. et al. Sarcolemmal ATP-sensitive K⁺ channels control energy expenditure determining body weight. **Cell metabolism**, v. 11, n. 1, p. 58-69, 2010.
- An, B.; Xia, J. et al. Genome-wide association study reveals candidate genes associated with body measurement traits in Chinese Wagyu beef cattle. **Animal genetics**, v. 50, n. 4, p. 386-390, 2019.
- Anitei, M.; Stange, C. et al. Spatiotemporal control of lipid conversion, actin-based mechanical forces, and curvature sensors during clathrin/AP-1-coated vesicle biogenesis. **Cell reports**, v. 20, n. 9, p. 2087-2099, 2017.
- Arce-Recinos, C.; Chay-Canul, A. J.; Alarcón-Zúñiga, B.; Ramos-Juárez, J. A.; Vargas-Villamil, L. M.; Aranda-Ibáñez, E. M.; Sánchez-Villegas, N. D. C.; Costa, R. L. D. Feed efficiency indexes in hair sheep: meat quality and associated genes. Review. **Revista mexicana de ciencias pecuarias**, v. 12, n. 2, p. 523-552, 2021.
- Archile-Contreras, A. C.; Purslow, P. P. Oxidative stress may affect meat quality by interfering with collagen turnover by muscle fibroblasts. **Food Research International**, v. 44, n. 2, p. 582-588, 2011.
- Arthaud, V. H.; Mandigo, R. W.; Koch, R. M.; Kotula, A. W. Carcass composition, quality and palatability attributes of bulls and steers fed different energy levels and killed at four ages. **Journal of Animal Science**, v. 44, n. 1, p. 53-64, 1977.
- Baldassini, W. A.; Chardulo, L. A. L. et al. Meat quality traits of Nellore bulls according to different degrees of backfat thickness: a multivariate approach. **Animal Production Science**, v. 57, n. 2, p. 363-370, 2017.
- Banci, L.; Bertini, I.; Ciofi-Baffoni, S.; Jaiswal, D.; Neri, S.; Peruzzini, R.; Winkelmann, J. Structural characterization of CHCHD5 and CHCHD7: two atypical human twin CX9C proteins. **Journal of structural biology**, v. 180, n. 1, p. 190-200, 2012.
- Barber, M. C.; Finley, E.; Vernon, R. G. Mechanisms whereby prolactin modulates lipogenesis in sheep mammary gland. **Hormone and metabolic research**, v. 23, n. 03, p. 143-145, 1991.
- Barros, C. M.; Satrapa, R. A.; Castilho, A. C. S.; Fontes, P. K.; Razza, E. M.; Ereno, R. L.; Nogueira, F. G. Effect of superstimulatory treatments on the expression of genes related to ovulatory capacity, oocyte competence and embryo development

- in cattle. **Reproduction, Fertility and Development**, v. 25, n. 1, p. 17-25, 2012.
- Bhuiyan, M. S. A.; Kim, N. K.; Cho, Y. M.; Yoon, D.; Kim, K. S.; Jeon, J. T.; Lee, J. H. Identification of SNPs in MYOD gene family and their associations with carcass traits in cattle. **Livestock Science**, v. 126, n. 1-3, p. 292-297, 2009.
- Blanchard, P. G.; Festuccia, W. T. Major involvement of mTOR in the PPAR γ -induced stimulation of adipose tissue lipid uptake and fat accretion [S]. **Journal of lipid research**, v. 53, n. 6, p. 1117-1125, 2012.
- Blandino-Rosano, M.; Romaguera-Llacer, P.; Lin, A.; Reddy, J. K.; Bernal-Mizrachi, E. TGS1: a novel regulator of β -cell mass and function. **bioRxiv**, 2021.
- Bligh, E. G.; Dyer, W. J. A rapid method of total lipid extraction and purification, **Canadian Journal. Biochemistry and Physiology**, v.37, p.911–917, 1959.
- Bolormaa, S.; Porto Neto, L. R.; Zhang, Y. D.; Bunch, R. J.; Harrison, B. E.; Goddard, M. E.; Barendse, W. A genome-wide association study of meat and carcass traits in Australian cattle. **Journal of animal science**, v. 89, n. 8, p. 2297-2309, 2011.
- Braun, T.; Bober, E.; Rudnicki, M. A.; Jaenisch, R.; Arnold, H. H. MyoD expression marks the onset of skeletal myogenesis in Myf-5 mutant mice. **Development**, v. 120, n. 11, p. 3083-3092, 1994.
- Buzanskas, M. E.; Pires, P. S.; Chud, T. C. S.; Bernardes, P. A.; Rola, L. D.; Savegnago, R. P.; Lôbo, R. B.; Munari, D. P. Parameter estimates for reproductive and carcass traits in Nelore beef cattle. **Theriogenology**, v. 92, p. 204-209, 2017.
- Caetano, S. L.; Savegnago, R. P.; Boligon, A. A.; Ramos, S. B.; Chud, T. C. S.; Lôbo, R. B.; Munari, D. P. Estimates of genetic parameters for carcass, growth and reproductive traits in Nellore cattle. **Livestock Science**, v. 155, n. 1, p. 1-7, 2013.
- Camargo, G. M. F.; Porto-Neto, L. R.; Kelly, M. J.; Bunch, R. J.; McWilliam, S. M.; Tonhati, H.; Lehnert, S. A.; Fortes, M. R. S.; Moore, S. S. Non-synonymous mutations mapped to chromosome X associated with andrological and growth traits in beef cattle. **BMC genomics**, v. 16, n. 1, p. 1-10, 2015.
- Campos, G. S.; Sollero, B. P. et al. Tag-SNP selection using Bayesian genomewide association study for growth traits in Hereford and Braford cattle. **Journal of Animal Breeding and Genetics**, v. 137, n. 5, p. 449-467, 2020.
- Cánovas, A.; Reverter, A. et al. Multi-tissue omics analyses reveal molecular regulatory networks for puberty in composite beef cattle. **PLoS one**, v. 9, n. 7, p.

- e102551, 2014.
- Carmona-Saez, P.; Chagoyen, M.; Tirado, F.; Carazo, J. M.; Pascual-Montano, A. GENECODIS: a web-based tool for finding significant concurrent annotations in gene lists. **Genome biology**, v. 8, n. 1, p. 1-8, 2007.
- Caron, A.; Richard, D.; Laplante, M. The roles of mTOR complexes in lipid metabolism. **Annual review of nutrition**, v. 35, p. 321-348, 2015.
- Carré, N.; Binart, N. Prolactin and adipose tissue. **Biochimie**, v. 97, p. 16-21, 2014.
- Cavallaro, G. Genome-wide analysis of eukaryotic twin CX 9 C proteins. **Molecular BioSystems**, v. 6, n. 12, p. 2459-2470, 2010.
- Charidemou, E.; Tsiarli, M. A.; Theophanous, A.; Yilmaz, V.; Pitsouli, C.; Strati, K.; Griffin, J. L.; Kirmizis, A. Histone acetyltransferase NAA40 modulates acetyl-CoA levels and lipid synthesis. **BMC biology**, v. 20, n. 1, p. 1-18, 2022.
- Choi, Y. O.; Ryu, H. J.; Kim, H. R.; Song, Y. S.; Kim, C.; Lee, W.; Choe, H.; Leem, C. H.; Jang, Y. J. Implication of phosphorylation of the myosin II regulatory light chain in insulin-stimulated GLUT4 translocation in 3T3-F442A adipocytes. **Experimental & molecular medicine**, v. 38, n. 2, p. 180-189, 2006.
- Chutkow, W. A.; Lee, R. T. Thioredoxin Regulates Adipogenesis through Thioredoxin-interacting Protein (Txnip) Protein Stability* \diamond . **Journal of Biological Chemistry**, v. 286, n. 33, p. 29139-29145, 2011.
- Cincotta, A. H.; Meier, A. H. Reduction of body fat stores by inhibition of prolactin secretion. **Experientia**, v. 43, n. 4, p. 416-417, 1987.
- Cundiff, L. V.; Pond, W. G.; Bell, A. W. Beef cattle: Breeds and genetics. **Encyclopedia of Animal Science**. Ithaca: **Cornell University**, p. 74-76, 2004.
- Davies, S. S.; Pontsler, A. V. et al. Oxidized alkyl phospholipids are specific, high affinity peroxisome proliferator-activated receptor γ ligands and agonists. **Journal of Biological Chemistry**, v. 276, n. 19, p. 16015-16023, 2001.
- Dean, J. M.; Lodhi, I. J. Structural and functional roles of ether lipids. **Protein & cell**, v. 9, n. 2, p. 196-206, 2018.
- Decolonne, N.; Kolb, M.; Margetts, P. J.; Menetrier, F.; Artur, Y.; Garrido, C.; Gauldie, J.; Camus, P.; Bonniaud, P. TGF- β 1 induces progressive pleural scarring and subpleural fibrosis. **The Journal of Immunology**, v. 179, n. 9, p. 6043-6051, 2007.

- Dedieu, S.; Mazeret, G.; Cottin, P.; Brustis, J. J. Involvement of myogenic regulator factors during fusion in the cell line C2C12. **International Journal of Developmental Biology**, v. 46, n. 2, p. 235-241, 2002.
- DeYoung, M. P.; Horak, P.; Sofer, A.; Sgroi, D.; Ellisen, L. W. Hypoxia regulates TSC1/2–mTOR signaling and tumor suppression through REDD1-mediated 14–3–3 shuttling. **Genes & development**, v. 22, n. 2, p. 239-251, 2008.
- Donadeu, F. X.; Esteves, C. L.; Doyle, L. K.; Walker, C. A.; Schauer, S. N.; Diaz, C. A. Phospholipase C β 3 mediates LH-induced granulosa cell differentiation. **Endocrinology**, v. 152, n. 7, p. 2857-2869, 2011.
- Du, X. H.; Gan, Q. F.; Yuan, Z. R.; Gao, X.; Zhang, L. P.; Gao, H. J.; Li, J. Y.; Xu, S. Z. Polymorphism of MyoD1 and Myf6 genes and associations with carcass and meat quality traits in beef cattle. **Genet. Mol. Res**, v. 12, p. 6708-6717, 2013.
- Elias, C. F.; Lee, C.; Jelly, J.; Aschkenasi, C.; Ahima, R. S.; Couceyro, P. R.; Kuhar, M. J.; Saper, C. B.; Elmquist, J. K. Leptin activates hypothalamic CART neurons projecting to the spinal cord. **Neuron**, v. 21, n. 6, p. 1375-1385, 1998.
- Fain, J. N.; Leffler, C. W.; Bahouth, S. W. Eicosanoids as endogenous regulators of leptin release and lipolysis by mouse adipose tissue in primary culture. **Journal of lipid research**, v. 41, n. 10, p. 1689-1694, 2000.
- Fajas, L.; Miard, S.; Briggs, M.R.; Auwerx, J. Selective cyclo-oxygenase-2 inhibitors impair adipocyte differentiation through inhibition of the clonal expansion phase. **Journal of lipid research**, v. 44, n. 9, p. 1652-1659, 2003.
- Farhan, M.; Wang, H.; Gaur, U.; Little, P. J.; Xu, J.; Zheng, W. FOXO signaling pathways as therapeutic targets in cancer. **International journal of biological sciences**, v. 13, n. 7, p. 815, 2017.
- Fernandes Júnior, G. A. F.; Rosa, G. J. M. et al. Genomic prediction of breeding values for carcass traits in Nelore cattle. **Genetics Selection Evolution**, v. 48, n. 1, p. 7, 2016a.
- Fernandes Júnior, G. A.; Costa, R. B. et al. Genome scan for postmortem carcass traits in Nelore cattle. **Journal of animal science**, v. 94, n. 10, p. 4087-4095, 2016b.
- Ferraz, J. B. S.; Pinto, L. F. B.; Meirelles, F. V.; Eler, J. P.; Rezende, F. M.; Oliveira, E. C. M.; Almeida, H. B.; Woodward, B.; Nkrumah, D. Association of single

- nucleotide polymorphisms with carcass traits in Nellore cattle. **Genet. Mol. Res**, v. 8, n. 4, p. 1360-1366, 2009.
- Fonseca, L. F. S.; Gimenez, D. F. J.; Santos Silva, D. B.; Barthelson, R.; Baldi, F.; Ferro, J. A.; Albuquerque, L. G. Differences in global gene expression in muscle tissue of Nellore cattle with divergent meat tenderness. **BMC genomics**, v. 18, n. 1, p. 945, 2017.
- Forman, B. M.; Tontonoz, P.; Chen, J.; Brun, R. P.; Spiegelman, B. M.; Evans, R. M. 15-deoxy- Δ 12, 14-prostaglandin J2 is a ligand for the adipocyte determination factor PPAR γ . **Cell**, v. 83, n. 5, p. 803-812, 1995.
- Fortes, M. R. S.; Kemper, K. et al. Evidence for pleiotropism and recent selection in the PLAG1 region in Australian B eef cattle. **Animal genetics**, v. 44, n. 6, p. 636-647, 2013.
- Funk, C. D.; Song, W. -C.; Fitzgerald, G. A. Prostaglandins and other lipid mediators in reproductive medicine. In: **Yen & Jaffe's Reproductive Endocrinology**. WB Saunders, 2014. p. 108-123. e4.
- García-Moreno, A.; López-Domínguez, R.; Ramirez-Mena, A.; Pascual-Montano, A.; Aparicio-Puerta, E.; Hackenberg, M.; Carmona-Saez, P. GeneCodis 4: Expanding the modular enrichment analysis to regulatory elements. **bioRxiv**, 2021.
- Gebreyesus, G.; Buitenhuis, A. J.; Poulsen, N. A.; Visker, M. H. P. W.; Zhang, Q.; van Valenberg, H. J. F.; Sun, D.; Bovenhuis, H. Multi-population GWAS and enrichment analyses reveal novel genomic regions and promising candidate genes underlying bovine milk fatty acid composition. **BMC genomics**, v. 20, n. 1, p. 1-16, 2019.
- Georges, M.; Charlier, C.; Hayes, B. Harnessing genomic information for livestock improvement. **Nature Reviews Genetics**, v. 20, n. 3, p. 135-156, 2019.
- Gomes, A. R.; Brosens, J. J.; Lam, E. W. -F. Resist or die: FOXO transcription factors determine the cellular response to chemotherapy. **Cell Cycle**, v. 7, n. 20, p. 3133-3136, 2008.
- Gomes, R. C.; Silva, S. L. et al. Protein synthesis and degradation gene SNPs related to feed intake, feed efficiency, growth, and ultrasound carcass traits in Nellore cattle. **Embrapa Gado de Corte-Artigo em periódico indexado (ALICE)**, 2013.
- Gordo, D. G. M.; Espigolan, R.; Bresolin, T.; Fernandes Júnior, G. A.; Magalhães, A.

- F. B.; Braz, C. U.; Fernandes, W. B.; Baldi, F.; Albuquerque, L. G. Genetic analysis of carcass and meat quality traits in Nelore cattle. **Journal of animal science**, v. 96, n. 9, p. 3558-3564, 2018.
- Gosselin, L. E.; Williams, J. E.; Deering, M.; Brazeau, D; Koury, S; Martinez, D. A. Localization and early time course of TGF- β 1 mRNA expression in dystrophic muscle. **Muscle & Nerve: Official Journal of the American Association of Electrodiagnostic Medicine**, v. 30, n. 5, p. 645-653, 2004.
- Gotoh, T.; Takahashi, H.; Nishimura, T.; Kuchida, K.; Mannen, H. Meat produced by Japanese Black cattle and Wagyu. **Animal Frontiers**, v. 4, n. 4, p. 46-54, 2014.
- Grigoletto, L.; Ferraz, J. B. S.; Oliveira, H. R.; Eler, J. P.; Bussiman, F. O.; Silva, B. C. A.; Baldi, F.; Brito, L. F. Genetic architecture of carcass and meat quality traits in Montana tropical® composite beef cattle. **Frontiers in genetics**, v. 11, p. 123, 2020.
- Guo, P.; Zhao, Z.; Yan, S.; Li, J.; Xiao, H.; Yang, D.; Zhao, Y.; Jiang, P.; Yang, R. PSAP gene variants and haplotypes reveal significant effects on carcass and meat quality traits in Chinese Simmental-cross cattle. **Archives Animal Breeding**, v. 59, n. 4, p. 461-468, 2016.
- Guttridge, D. C. Making Muscles Grow by G Protein–Coupled Receptor Signaling. **Science Signaling**, v. 4, n. 201, p. pe45-pe45, 2011.
- Han, H.; Gu, S.; Chu, W.; Sun, W.; Wei, W.; Dang, X.; Tian, Y.; Liu, K.; Chen, J. miR-17-5p regulates differential expression of NCOA3 in pig intramuscular and subcutaneous adipose tissue. **Lipids**, v. 52, n. 11, p. 939-949, 2017.
- Hara-Chikuma, M.; Sohara, E.; Rai, T.; Ikawa, M.; Okabe, M.; Sasaki, S.; Uchida, S.; Verkman, A. S. Progressive adipocyte hypertrophy in aquaporin-7-deficient mice: adipocyte glycerol permeability as a novel regulator of fat accumulation. **Journal of Biological Chemistry**, v. 280, n. 16, p. 15493-15496, 2005.
- Hara-Chikuma, M.; Verkman, A. S. Physiological roles of glycerol-transporting aquaporins: the aquaglyceroporins. **Cellular and Molecular Life Sciences CMLS**, v. 63, n. 12, p. 1386-1392, 2006.
- Hay; E. H.; Roberts, A. Genome-wide association study for carcass traits in a composite beef cattle breed. **Livestock Science**, v. 213, p. 35-43, 2018.
- Henslee, D.; Murdoch, B.; Yelich, J.; Taylor, J. B.; Ellison, M. Comparative genomics

- of the sheep Tas2r repertoire to cattle, goat, human, dog, and mice. **Animal Gene**, v. 17, p. 200107, 2020.
- Hibuse, T.; Maeda, N. Aquaporin 7 deficiency is associated with development of obesity through activation of adipose glycerol kinase. **Proceedings of the National Academy of Sciences**, v. 102, n. 31, p. 10993-10998, 2005.
- Huang, D. W.; Sherman, B. T.; Lempicki, R. A. Bioinformatics enrichment tools: paths toward the comprehensive functional analysis of large gene lists. **Nucleic acids research**, v. 37, n. 1, p. 1-13, 2009a.
- Huang, D. W.; Sherman, B. T.; Lempicki, R. A. Systematic and integrative analysis of large gene lists using DAVID bioinformatics resources. **Nature protocols**, v. 4, n. 1, p. 44-57, 2009b.
- Huang, Y. Z.; Zhan, Z. Y. et al. SNP and haplotype analysis reveal IGF2 variants associated with growth traits in Chinese Qinchuan cattle. *Molecular biology reports*, v. 41, n. 2, p. 591-598, 2014.
- Iatani, I.; Choi, H. Y. et al. The WWOX gene modulates high-density lipoprotein and lipid metabolism. **Circulation: Cardiovascular Genetics**, v. 7, n. 4, p. 491-504, 2014.
- Iozzo, R. V. The biology of the small leucine-rich proteoglycans: functional network of interactive proteins. **Journal of Biological Chemistry**, v. 274, n. 27, p. 18843-18846, 1999.
- James, K. N.; Lau, M. et al. Expanding the genotypic spectrum of ACTG2-related visceral myopathy. **Molecular Case Studies**, v. 7, n. 3, p. a006085, 2021.
- Jang, D.; Yoon, J.; Taye, M.; Lee, W.; Kwon, T.; Shim, S.; Kim, H. Multivariate genome-wide association studies on tenderness of Berkshire and Duroc pig breeds. **Genes & genomics**, v. 40, n. 7, p. 701-705, 2018.
- Janin, A.; Bessière, F.; Chauveau, S.; Chevalier, P.; Millat, G. First identification of homozygous truncating CSRP3 variants in two unrelated cases with hypertrophic cardiomyopathy. **Gene**, v. 676, p. 110-116, 2018.
- Jaworski, K.; Ahmadian, M. et al. AdPLA ablation increases lipolysis and prevents obesity induced by high-fat feeding or leptin deficiency. **Nature medicine**, v. 15, n. 2, p. 159-168, 2009.
- Karisa, B. K.; Thomson, J.; Wang, Z.; Bruce, H. L.; Plastow, C. S.; Moore, S. S.

- Candidate genes and biological pathways associated with carcass quality traits in beef cattle. **Canadian Journal of Animal Science**, v. 93, n. 3, p. 295-306, 2013.
- Kather, H.; Simon, B. Biphasic effects of prostaglandin E2 on the human fat cell adenylate cyclase. **The Journal of Clinical Investigation**, v. 64, n. 2, p. 609-612, 1979.
- Kim, J.; Hanotte, O. et al. The genome landscape of indigenous African cattle. **Genome biology**, v. 18, n. 1, p. 1-14, 2017.
- Kluska, S.; Olivieri, B. F. et al. Estimates of genetic parameters for growth, reproductive, and carcass traits in Nelore cattle using the single step genomic BLUP procedure. **Livestock science**, v. 216, p. 203-209, 2018.
- Komisarek, J.; Walendowska, A. Analysis of the PPARGC1A gene as a potential marker for productive and reproductive traits in cattle. **Folia Biologica (Kraków)**, v. 60, n. 3-4, p. 171-174, 2012.
- Kulig, H.; Kmieć, M. Association between leptin gene polymorphisms and growth traits in Limousin cattle. **Russian journal of genetics**, v. 45, n. 6, p. 738-741, 2009.
- Lamberts, S. W. L.; Macleod, R. M. Regulation of prolactin secretion at the level of the lactotroph. **Physiological Reviews**, v. 70, n. 2, p. 279-318, 1990.
- Lamming, D. W.; Sabatini, D. M. A central role for mTOR in lipid homeostasis. **Cell metabolism**, v. 18, n. 4, p. 465-469, 2013.
- Lawrence, D. A. Transforming growth factor-beta: a general review. **European cytokine network**, v. 7, n. 3, p. 363-374, 1996.
- Leal-Gutiérrez, J. D.; Elzo, M. A.; Johnson, D. D.; Hamblen, H.; Mateescu, R. G. Genome wide association and gene enrichment analysis reveal membrane anchoring and structural proteins associated with meat quality in beef. **BMC genomics**, v. 20, n. 1, p. 151, 2019.
- Lee, S.; Min-Wook, H.; So-Young, C.; Kim, J. WPSII-5 Genome-wide association analysis to identify QTL for carcass traits in Korean native cattle. **Journal of Animal Science**, v. 96, n. Suppl 3, p. 516, 2018.
- Lefterova, M. I.; Haakonsson, A. K.; Lazar, M. A.; Mandrup, S. PPAR γ and the global map of adipogenesis and beyond. **Trends in Endocrinology & Metabolism**, v. 25, n. 6, p. 293-302, 2014.
- Leibovitch, S. A.; Guillier, M.; Lenormand, J. L.; Leibovitch, M. P. Accumulation of the

- c-mos protein is correlated with post-natal development of skeletal muscle. **Oncogene**, v. 6, n. 9, p. 1617-1622, 1991.
- Lemos, M. V. A.; Chiaia, H. L. J. et al. Genome-wide association between single nucleotide polymorphisms with beef fatty acid profile in Nellore cattle using the single step procedure. **BMC genomics**, v. 17, n. 1, p. 213, 2016.
- Lemos, M. V. A.; Peripolli, E. Association study between copy number variation and beef fatty acid profile of Nellore cattle. **Journal of applied genetics**, v. 59, n. 2, p. 203-223, 2018.
- Levéen, P.; Larsson, J.; Ehinger, M.; Cilio, C. M.; Sundler, M.; Sjöstrand, L. J.; Holmdahl, R.; Karlsson, S. Induced disruption of the transforming growth factor beta type II receptor gene in mice causes a lethal inflammatory disorder that is transplantable. **Blood, The Journal of the American Society of Hematology**, v. 100, n. 2, p. 560-568, 2002.
- Li, W. Z.; Zhao, S. M.; Huang, Y.; Yang, M. H.; Pan, H. B.; Zhang, X.; Ge, C. R.; Gao, S. Z. Expression of lipogenic genes during porcine intramuscular preadipocyte differentiation. **Research in veterinary science**, v. 93, n. 3, p. 1190-1194, 2012.
- Lillig, C. H.; Berndt, C.; Holmgren, A. Glutaredoxin systems. **Biochimica et Biophysica Acta (BBA)-General Subjects**, v. 1780, n. 11, p. 1304-1317, 2008.
- Lindholm-Perry, A. K. Kuehn, L. A.; Smith, T. P. L.; Ferrell, C. L.; Jenkins, T. G.; Freetly, H. C.; Snelling, W. M. A region on BTA14 that includes the positional candidate genes LYPLA1, XKR4 and TMEM68 is associated with feed intake and growth phenotypes in cattle 1. **Animal genetics**, v. 43, n. 2, p. 216-219, 2011.
- Louet, J. F.; Coste, A.; Amazit, L.; Tannour-Louet, M.; Wu, R. C.; Tsai, S. Y.; Tsai, M. -J.; Auwerx, J.; O'Malley, B. W. Oncogenic steroid receptor coactivator-3 is a key regulator of the white adipogenic program. **Proceedings of the National Academy of Sciences**, v. 103, n. 47, p. 17868-17873, 2006.
- Magalhães, A. F. B.; Camargo, G. M. F. et al. Genome-wide association study of meat quality traits in Nellore cattle. **PloS one**, v. 11, n. 6, p. e0157845, 2016.
- Magalhães, A. F. B.; Schenkel, F. S. et al. Genomic selection for meat quality traits in Nelore cattle. **Meat science**, v. 148, p. 32-37, 2019.
- Maltin, C.; Balcerzak, D.; Tilley, R.; Delday, M. Determinants of meat quality: tenderness. **Proceedings of the Nutrition Society**, v. 62, n. 2, p. 337-347, 2003.

- Mann, N. J. A brief history of meat in the human diet and current health implications. **Meat science**, v. 144, p. 169-179, 2018.
- Martínez, R.; Gómez, Y.; Rocha, J. F. M. Genome-wide association study on growth traits in Colombian creole breeds and crossbreeds with Zebu cattle. **Genet Mol Res**, v. 13, n. 3, p. 6420-6432, 2014.
- Massagué, J.; Chen, Y. -G. Controlling TGF- β signaling. **Genes & development**, v. 14, n. 6, p. 627-644, 2000.
- Masuda, Y.; Legarra, A.; Aguilar, I.; Misztal, I. 331 Efficient quality control methods for genomic and pedigree data used in routine genomic evaluation. **Journal of Animal Science**, v. 97, n. Supplement_3, p. 50-51, 2019.
- Mateescu, R. G.; Garmyn, A. J. Genetic parameters for concentrations of minerals in longissimus muscle and their associations with palatability traits in Angus cattle. **Journal of Animal Science**, v. 91, n. 3, p. 1067-1075, 2013.
- McGowan, K. A.; Li, J. Z. et al. Ribosomal mutations cause p53-mediated dark skin and pleiotropic effects. **Nature genetics**, v. 40, n. 8, p. 963-970, 2008.
- Mihaylova, M. M.; Shaw, R. J. The AMPK signalling pathway coordinates cell growth, autophagy and metabolism. **Nature cell biology**, v. 13, n. 9, p. 1016-1023, 2011.
- Miranda, M.; Escote, X.; Ceperuelo-Mallafre, V.; Alcaide, M. J.; Simon, I.; Vilarrasa, N.; Wabitsch, M.; Vendrell, J. Paired subcutaneous and visceral adipose tissue aquaporin-7 expression in human obesity and type 2 diabetes: differences and similarities between depots. **The journal of clinical endocrinology & metabolism**, v. 95, n. 7, p. 3470-3479, 2010.
- Misztal, I.; Legarra, A.; Aguilar, I. Computing procedures for genetic evaluation including phenotypic, full pedigree, and genomic information. **Journal of Dairy Science**, v. 92, n. 9, p. 4648-4655, 2009.
- Mwangi, F. W.; Charmley, E.; Gardiner, C. P.; Malau-Aduli, B. S.; Kinobe, R. T.; Malau-Aduli, A. E. O. Diet and Genetics Influence Beef Cattle Performance and Meat Quality Characteristics. **Foods**, v. 8, n. 12, p. 648, 2019.
- Neupane, M.; Geary, T. W.; Kiser, J. N.; Burns, G. W.; Hansen, P.J.; Spencer, T. E.; Neiberghs, H. L. Loci and pathways associated with uterine capacity for pregnancy and fertility in beef cattle. **PLoS One**, v. 12, n. 12, p. e0188997, 2017.
- Nishimura, T.; Futami, E.; Taneichi, A.; Mori, T.; Hattori, A. Decorin expression during

- development of bovine skeletal muscle and its role in morphogenesis of the intramuscular connective tissue. **Cells Tissues Organs**, v. 171, n. 2-3, p. 199-214, 2002.
- Nkrumah, J. D.; Li, C.; Yu, J.; Hansen, C.; Keisler, D. H.; Moore, S. S. Polymorphisms in the bovine leptin promoter associated with serum leptin concentration, growth, feed intake, feeding behavior, and measures of carcass merit. **Journal of Animal Science**, v. 83, n. 1, p. 20-28, 2005.
- Nogales-Cadenas, R.; Carmona-Saez, P.; Vazquez, M.; Vicente, C.; Yang, X.; Tirado, F.; Carazo, J. M.; Pascual-Montano, A. GeneCodis: interpreting gene lists through enrichment analysis and integration of diverse biological information. **Nucleic acids research**, v. 37, n. suppl_2, p. W317-W322, 2009.
- Nugent, C.; Prins, J. B.; Whitehead, J. P.; Wentworth, J. M.; Chatterjee, V. K. K. Arachidonic acid stimulates glucose uptake in 3T3-L1 adipocytes by increasing GLUT1 and GLUT4 levels at the plasma membrane: Evidence for involvement of lipoxygenase metabolites and peroxisome proliferator-activated receptor γ . **Journal of Biological Chemistry**, v. 276, n. 12, p. 9149-9157, 2001.
- Null, D.; VanRaden, P. M.; Rosen, B.; O'Connell, J.; Bickhart, D. Using the ARS-UCD1.2 reference genome in US evaluations. **Interbull Bulletin**, n. 55, p. 30-34, 2019.
- Oliveira Silva, R. M.; Stafuzza, N. B. et al. Genome-wide association study for carcass traits in an experimental Nelore cattle population. **PloS one**, v. 12, n. 1, 2017.
- Oliveira, A. S. F.; Campos, S. R.; Baptista, A. M.; Soares, C. M. Coupling between protonation and conformation in cytochrome c oxidase: Insights from constant-pH MD simulations. **Biochimica et Biophysica Acta (BBA)-Bioenergetics**, v. 1857, n. 6, p. 759-771, 2016.
- Papponen, H.; Kaisto, T.; Leinonen, S.; Kaakinen, M.; Metsikko, K. Evidence for γ -actin as a Z disc component in skeletal myofibers. **Experimental Cell Research**, v. 315, n. 2, p. 218-225, 2009.
- Pausch, H.; Flisikowski, K.; Jung, S.; Emmerling, R.; Edel, C.; Götz, K. U.; Fries, R. Genome-wide association study identifies two major loci affecting calving ease and growth-related traits in cattle. **Genetics**, v. 187, n. 1, p. 289-297, 2011.
- Pegolo, S.; Cecchinato, A.; Savoia, S.; Di Stasio, L.; Pauciullo, A.; Brugiapaglia, A.; Bittante, G.; Albera, A. Genome-wide association and pathway analysis of carcass

- and meat quality traits in Piemontese young bulls. **Animal**, v. 14, n. 2, p. 243-252, 2019.
- Porstmann, T.; Santos, C. R.; Griffiths, B.; Cully, M.; Wu, M.; Leever, S.; Griffiths, J. R.; Chung, Y. L.; Schulze, A. SREBP activity is regulated by mTORC1 and contributes to Akt-dependent cell growth. **Cell metabolism**, v. 8, n. 3, p. 224-236, 2008.
- Prudente, S.; Flex, E. A functional variant of the adipocyte glycerol channel aquaporin 7 gene is associated with obesity and related metabolic abnormalities. **Diabetes**, v. 56, n. 5, p. 1468-1474, 2007.
- Pryce, J. E.; Hayes, B. J.; Bolormaa, S.; Goddard, M. E. Polymorphic regions affecting human height also control stature in cattle. **Genetics**, v. 187, n. 3, p. 981-984, 2011.
- Puigserver, P.; Wu, Z.; Park, C. W.; Graves, R.; Wright, M.; Spiegelman, B. M. A cold-inducible coactivator of nuclear receptors linked to adaptive thermogenesis. **Cell**, v. 92, n. 6, p. 829-839, 1998.
- Ramayo-Caldas, Y.; Fortes, M. R. S. et al. A marker-derived gene network reveals the regulatory role of PPARGC1A, HNF4G, and FOXP3 in intramuscular fat deposition of beef cattle. **Journal of Animal Science**, v. 92, n. 7, p. 2832-2845, 2014.
- Reginato, M. J.; Krakow, S. L.; Bailey, S. T.; Lazar, M. A. Prostaglandins promote and block adipogenesis through opposing effects on peroxisome proliferator-activated receptor γ . **Journal of Biological Chemistry**, v. 273, n. 4, p. 1855-1858, 1998.
- Rexroad III, C. E.; Bennett, G. L.; Stone, R. T.; Keele, J. W.; Fahrenkrug, S. C.; Freking, B. A.; Kappes, S. M.; Smith, T. P. Comparative mapping of BTA15 and HSA11 including a region containing a QTL for meat tenderness. **Mammalian Genome**, v. 12, n. 7, p. 561-565, 2001.
- Rojanathammanee, L.; Rakoczy, S.; Kopchick, J.; Brown-Borg, H. M. Effects of insulin-like growth factor 1 on glutathione S-transferases and thioredoxin in growth hormone receptor knockout mice. **Age**, v. 36, n. 4, p. 1-13, 2014.
- Rosen, E. D.; Hsu, C. H.; Wang, X.; Sakai, S.; Freeman, M. W.; Gonzalez, F. J.; Spiegelman, B. M. C/EBP α induces adipogenesis through PPAR γ : a unified pathway. **Genes & development**, v. 16, n. 1, p. 22-26, 2002.

- Ruan, D.; Zhuang, Z. et al. Weighted single-step GWAS identified candidate genes associated with growth traits in a Duroc pig population. **Genes**, v. 12, n. 1, p. 117, 2021.
- Saatchi, M.; Schnabel, R. D.; Taylor, J. F.; Garrick, D. J. Large-effect pleiotropic or closely linked QTL segregate within and across ten US cattle breeds. **BMC genomics**, v. 15, n. 1, p. 1-17, 2014.
- Sagata, N. What does Mos do in oocytes and somatic cells?. **BioEssays**, v. 19, n. 1, p. 13-21, 1997.
- Sahu, K.; Gupta, A. et al. Role of granulosa cell mitogen-activated protein kinase 3/1 in gonadotropin-mediated meiotic resumption from diplotene arrest of mammalian oocytes. **Growth Factors**, v. 36, n. 1-2, p. 41-47, 2018.
- Sargolzaei, M.; Chesnais, J. P.; Schenkel, F. S. A new approach for efficient genotype imputation using information from relatives. **BMC genomics**, v. 15, n. 1, p. 478, 2014.
- Sasaki, Y.; Nagai, K. Exploration of genes showing intramuscular fat deposition-associated expression changes in musculus longissimus muscle. **Animal Genetics**, v. 37, n. 1, p. 40-46, 2006.
- Schenkel, F. S.; Miller, S. P. et al. Association of single nucleotide polymorphisms in the leptin gene with carcass and meat quality traits of beef cattle. **Journal of animal science**, v. 83, n. 9, p. 2009-2020, 2005.
- Seabury, C. M.; Oldeschulte, D. L. et al. Genome-wide association study for feed efficiency and growth traits in US beef cattle. **BMC genomics**, v. 18, n. 1, p. 1-25, 2017.
- Selga, E.; Pérez-Cano, F. J.; Franch, À.; Ramírez-Santana, C.; Rivero, M.; Ciudad, C. J.; Castellote, C.; Noé, V. Gene expression profiles in rat mesenteric lymph nodes upon supplementation with Conjugated Linoleic Acid during gestation and suckling. **BMC genomics**, v. 12, n. 1, p. 1-13, 2011.
- Serão, N. V. L.; Veroneze, R.; Ribeiro, A. M. F.; Verardo, L. L.; Braccini Neto, J.; Gasparino, E.; Campos, C. F.; Lopes, P. S.; Guimarães, S. E. F. Candidate gene expression and intramuscular fat content in pigs. **Journal of Animal Breeding and Genetics**, v. 128, n. 1, p. 28-34, 2011.
- Sevane, N.; Armstrong, E.; Cortés, O.; Wiener, P.; Wong, R. P.; Dunner, S.; Gemqual

- Consortium. Association of bovine meat quality traits with genes included in the PPARG and PPARGC1A networks. **Meat Science**, v. 94, n. 3, p. 328-335, 2013.
- Shan, T.; Zhang, P.; Jiang, Q.; Xiong, Y.; Wang, Y.; Kuang, S. Adipocyte-specific deletion of mTOR inhibits adipose tissue development and causes insulin resistance in mice. **Diabetologia**, v. 59, n. 9, p. 1995-2004, 2016.
- Shin, S.; Chung, E. Novel SNPs in the bovine ADIPOQ and PPARGC1A genes are associated with carcass traits in Hanwoo (Korean cattle). **Molecular biology reports**, v. 40, n. 7, p. 4651-4660, 2013.
- Shiu, R. P. C.; Friesen, H. G. Mechanism of action of prolactin in the control of mammary gland function. **Annual Review of Physiology**, v. 42, n. 1, p. 83-96, 1980.
- Silva, D. B. S., Fonseca, L. F. S. et al. Spliced genes in muscle from Nelore Cattle and their association with carcass and meat quality. **Scientific reports**, v. 10, n. 1, p. 1-13, 2020.
- Simianer, H. Genomic and other revolutions—why some technologies are quickly adopted and others are not. **Animal Frontiers**, v. 6, n. 1, p. 53-58, 2016.
- Smith, J. L.; Wilson, M. L.; Nilson, S. M.; Rowan, T. N.; Oldeschulte, D. L.; Schnabel, R. D.; Decker, J. E.; Seabury, C. M. Genome-wide association and genotype by environment interactions for growth traits in US Gelbvieh cattle. **BMC genomics**, v. 20, n. 1, p. 1-13, 2019.
- Sofer, A.; Lei, K.; Johannessen, C. M.; Ellisen, L. W. Regulation of mTOR and cell growth in response to energy stress by REDD1. **Molecular and cellular biology**, v. 25, n. 14, p. 5834-5845, 2005.
- Soria, L. A.; Corva, P. M. Association of a novel polymorphism in the bovine PPARGC1A gene with growth, slaughter and meat quality traits in Brangus steers. **Molecular and cellular probes**, v. 23, n. 6, p. 304-308, 2009.
- Srikanth, K.; Lee, S. -H. et al. A gene-set enrichment and protein–protein interaction network-based GWAS with regulatory SNPs identifies candidate genes and pathways associated with carcass traits in hanwoo cattle. **Genes**, v. 11, n. 3, p. 316, 2020.
- Srivastava, S.; Srikanth, K.; Won, S.; Son, J. -H.; Park, J. -E.; Park, W.; Chai, H. -H.; Lim, D. Haplotype-based genome-wide association study and identification of

- candidate genes associated with carcass traits in Hanwoo cattle. **Genes**, v. 11, n. 5, p. 551, 2020.
- Stafuzza, N. B.; Oliveira Silva, R. M.; Oliveira Fragomeni, B.; Masuda, Y.; Huang, Y.; Gray, K.; Lourenco, D. A. L. A genome-wide single nucleotide polymorphism and copy number variation analysis for number of piglets born alive. **BMC genomics**, v. 20, n. 1, p. 1-11, 2019.
- Sun, J.; Zhu, J.; Xue, J.; Zhang, C.; Lan, X.; Lei, C.; Chen, H. Haplotype combinations of AdPLA gene polymorphisms associate with growth traits in Chinese cattle. **Molecular biology reports**, v. 39, n. 6, p. 7069-7076, 2012.
- Sun, Y.; Xue, J.; Guo, W.; Li, M.; Huang, Y.; Lan, X.; Lei, C.; Zhang, C.; Chen, H. Haplotypes of bovine FoxO1 gene sequence variants and association with growth traits in Qinchuan cattle. **Journal of genetics**, v. 93, n. 2, p. 8-14, 2016.
- Tatosyan, A. G.; Mizenina, O. A. Kinases of the Src family: structure and functions. **BIOCHEMISTRY C/C OF BIOKHMIIA**, v. 65, n. 1, p. 49-58, 2000.
- Taye, M.; Yoon, J.; Dessie, T.; Cho, S.; Oh, S. J.; Lee, H. -K.; Kim, H. Deciphering signature of selection affecting beef quality traits in Angus cattle. **Genes & genomics**, v. 40, n. 1, p. 63-75, 2018.
- Te Pas, M. F. W.; Soumillion, A.; Harders, F. L.; Verburg, F. J.; Van den Bosch, T. J.; Galesloot, P.; Meuwissen, T. H. E. Influences of myogenin genotypes on birth weight, growth rate, carcass weight, backfat thickness, and lean weight of pigs. **Journal of Animal Science**, v. 77, n. 9, p. 2352-2356, 1999.
- Terakado, A. P. N.; Costa, R. B. et al. Genome-wide association study for growth traits in Nelore cattle. **Animal**, v. 12, n. 7, p. 1358-1362, 2018.
- Tizioto, P. C.; Decker, J. E. et al. Genome scan for meat quality traits in Nelore beef cattle. **Physiological genomics**, v. 45, n. 21, p. 1012-1020, 2013a.
- Tizioto, P. C.; Gasparin, G. et al. Identification of KCNJ11 as a functional candidate gene for bovine meat tenderness. **Physiological Genomics**, v. 45, n. 24, p. 1215-1221, 2013b.
- Tricarico, D.; Selvaggi, M. et al. ATP sensitive potassium channels in the skeletal muscle function: involvement of the KCNJ11 (Kir6. 2) gene in the determination of mechanical warner bratzer shear force. **Frontiers in physiology**, v. 7, p. 167, 2016.

- Tsukahara, T.; Tsukahara, R. et al. Different residues mediate recognition of 1-O-oleyllysophosphatidic acid and rosiglitazone in the ligand binding domain of peroxisome proliferator-activated receptor γ . **Journal of Biological Chemistry**, v. 281, n. 6, p. 3398-3407, 2006.
- Tsukihara, T.; Aoyama, H.; Yamashita, E.; Tomizaki, T.; Yamaguchi, H.; Shinzawa-Itoh, K.; Nakashima, R.; Yaono, R.; Yoshikawa, S. The whole structure of the 13-subunit oxidized cytochrome c oxidase at 2.8 Å. **Science**, v. 272, n. 5265, p. 1136-1144, 1996.
- United States Department Of Agriculture (USDA). U.S. **Standards for Grades of Feeder Cattle**. Washington: USDA, 2000. 4p.
- Utsunomiya, Y. T.; Carmo, A. S. et al. Genome-wide association study for birth weight in Nellore cattle points to previously described orthologous genes affecting human and bovine height. **BMC genetics**, v. 14, n. 1, p. 1-12, 2013.
- Van Dyck, F.; Braem, C. V. et al. Loss of the Plagl2 transcription factor affects lacteal uptake of chylomicrons. **Cell metabolism**, v. 6, n. 5, p. 406-413, 2007.
- Vanraden, P. M. Efficient methods to compute genomic predictions. **Journal of dairy science**, v. 91, n. 11, p. 4414-4423, 2008.
- Walsh, H.; Martins, S.; O'Neill, E. E.; Kerry, J. P.; Kenny, T.; Ward, P. The effect of sodium lactate, potassium lactate, carrageenan, whey protein concentrate, yeast extract and fungal proteinases on the cook yield and tenderness of bovine chuck muscles. **Meat science**, v. 85, n. 2, p. 230-234, 2010.
- Wang, H.; Misztal, I. et al. Genome-wide association mapping including phenotypes from relatives without genotypes in a single-step (ssGWAS) for 6-week body weight in broiler chickens. **Frontiers in genetics**, v. 5, p. 134, 2014.
- Wang, H.; Misztal, I.; Aguilar, I.; Legarra, A.; Muir, W. M. Genome-wide association mapping including phenotypes from relatives without genotypes. **Genetics Research**, v.94, n.2, p.73-83, 2012.
- Wang, L.; Li, J.; Hou, X.; Yan, H.; Zhang, L.; Liu, X.; Gao, H.; Zhao, F.; Wang, L. Genome-Wide Identification of RNA Editing Sites Affecting Intramuscular Fat in Pigs. **Animals**, v. 10, n. 9, p. 1616, 2020c.
- Wang, S.; Zhao, H. Exploring of InDel in bovine PSAP gene and their association with growth traits in different development stages. **Animal Biotechnology**, p. 1-12,

2020b.

- Wang, X.; Yang, J.; Yao, Y.; Shi, X. E.; Yang, G.; Li, X. AQP3 Facilitates Proliferation and Adipogenic Differentiation of Porcine Intramuscular Adipocytes. **Genes**, v. 11, n. 4, p. 453, 2020a.
- Warner, R.; Wheeler, T. L. et al. Meat tenderness: advances in biology, biochemistry, molecular mechanisms and new technologies. **Meat Science**, p. 108657, 2021.
- Weston, A. R.; Rogers, R. W.; Althen, T. G. The role of collagen in meat tenderness. **The Professional Animal Scientist**, v. 18, n. 2, p. 107-111, 2002.
- Wheeler, T. L.; Koomaraie, M.; Shackelford, S. D. **Standardized warner-bratzler shear force procedures for meat tenderness measurement**. Clay Center: Roman L. Hruska U. S. MARC. USDA, 1995. 7p.
- Williams, P. Nutritional composition of red meat. **Nutrition & Dietetics**, v. 64, p. S113-S119, 2007.
- Wood, J. D.; Enser, M.; Fisher, A.; Nute, G. R.; Richardson, R. I.; Sheard, P. R. Manipulating meat quality and composition. **Proceedings of the nutrition society**, v. 58, n. 2, p. 363-370, 1999.
- Wu, S. V.; Rozengurt, N.; Yang, M.; Young, S. H.; Sinnott-Smith, J.; Rozengurt, E. Expression of bitter taste receptors of the T2R family in the gastrointestinal tract and enteroendocrine STC-1 cells. **Proceedings of the National Academy of Sciences**, v. 99, n. 4, p. 2392-2397, 2002.
- Wu, W.; Zhang, D.; Yin, Y.; Ji, M.; Xu, K.; Huang, X.; Peng, Y.; Zhang, J. Comprehensive transcriptomic view of the role of the LGALS12 gene in porcine subcutaneous and intramuscular adipocytes. **BMC genomics**, v. 20, n. 1, p. 1-13, 2019.
- Yamaguchi, Y.; Mann, D. M.; Ruoslahti, E. Negative regulation of transforming growth factor- β by the proteoglycan decorin. **Nature**, v. 346, n. 6281, p. 281-284, 1990.
- Yang, J.; Lee, S. H.; Goddard, M. E.; Visscher, P. M. Genome-wide complex trait analysis (GCTA): methods, data analyses, and interpretations. In: **Genome-wide association studies and genomic prediction**. Humana Press, Totowa, NJ, 2013. p. 215-236.
- Yang, R. -Y.; Hsu, D. K.; Yu, L.; Chen, H. -Y.; Liu, F. -T. Galectin-12 is required for adipogenic signaling and adipocyte differentiation. **Journal of Biological**

- Chemistry**, v. 279, n. 28, p. 29761-29766, 2004.
- Yang, R. -Y.; Yu, L.; Graham, J. L.; Hsu, D. K.; Lloyd, K. C. K.; Havel, P. J.; Liu, F. -T. Ablation of a galectin preferentially expressed in adipocytes increases lipolysis, reduces adiposity, and improves insulin sensitivity in mice. **Proceedings of the National Academy of Sciences**, v. 108, n. 46, p. 18696-18701, 2011.
- Zeng, L.; Chen, N.; Ning, Q.; Yao, Y.; Chen, H.; Dang, R.; Zhang, H.; Lei, C. PRLH and SOD 1 gene variations associated with heat tolerance in Chinese cattle. **Animal genetics**, v. 49, n. 5, p. 447-451, 2018.
- Zhang, C.; Baker, D. L. et al. Lysophosphatidic acid induces neointima formation through PPAR γ activation. **The Journal of experimental medicine**, v. 199, n. 6, p. 763-774, 2004.
- Zhang, H.; Wang, Z.; Wang, S.; Li, H. Progress of genome wide association study in domestic animals. **Journal of animal science and biotechnology**, v. 3, n. 1, p. 26, 2012.
- Zhang, J.; Zhang, Y. et al. Landscape of Loci and Candidate Genes for Muscle Fatty Acid Composition in Pigs Revealed by Multiple Population Association Analysis. **Frontiers in genetics**, p. 1067, 2019.
- Zhao, H.; Wu, M.; Yi, X.; Tang, X.; Chen, P.; Wang, S.; Sun, X. Functional analysis of haplotypes in bovine PSAP gene and their relationship with beef cattle production traits. **Animals**, v. 11, n. 1, p. 49, 2021.
- Zhou, Z. -K., Gao, X.; Li, J. -Y.; Chen, J. -B.; Xu, S. -Z. Effect of castration on carcass quality and differential gene expression of longissimus muscle between steer and bull. **Molecular Biology Reports**, v. 38, n. 8, p. 5307-5312, 2011.

6. SUPPLEMENTARY INFORMATION

Table S1. Results of functional enrichment analyzes performed in DAVID and GeneCodis for LMA.

Description	Annotation_ID	Pvalue	Genes
DAVID			
Basal transcription factors	bta03022	0.016738078	<i>CDK7, TAF9, GTF2H2</i>
Transcription from RNA polymerase II promoter	GO:0006366	0.020995988	<i>CDK7, TAF9, GTF2H2, HIVEP2</i>
FoxO signaling pathway	bta04068	0.022747109	<i>CCNB1, STK4, ATG12, TGFB2</i>
Lipid metabolic process	GO:0006629	0.025126808	<i>HNF4A, ALMS1, PNPLA5</i>
Cell-cell signaling	GO:0007267	0.038412782	<i>LVRN, CARTPT, WISP2</i>
Protein stabilization	GO:0050821	0.078791872	<i>TAF9, STK4, CCT7</i>
Endocytosis	bta04144	0.101560155	<i>VTA1, STAMBP, RAB11FIP5, TGFB2</i>
Cell cycle	bta04110	0.113700722	<i>CDK7, CCNB1, YWHAB</i>
Protein phosphorylation	GO:0006468	0.129054957	<i>DGUOK, GTF2H2, STK4</i>
Hippo signaling pathway	bta04390	0.154468523	<i>MOB1A, YWHAB, TGFB2</i>
RNA transport	bta03013	0.167548022	<i>SMN2, THOC3, PABPC1L</i>
Oxidation-reduction process	GO:0055114	0.174331953	<i>KIAA1191, MRPS36, MTHFD2, CDO1</i>
Cell adhesion	GO:0007155	0.186378144	<i>PARVG, PARVB, WISP2</i>
Purine metabolism	bta00230	0.195947052	<i>DGUOK, AK6, ADA</i>
Metabolic pathways	bta01100	0.202860526	<i>MCCC2, DGUOK, LOC786474, MTHFD2, PNPLA3, GADL1, AK6, CDO1, ADA</i>
Negative regulation of cell proliferation	GO:0008285	0.260106203	<i>HNF4A, STK4, COPS8</i>
Innate immune response	GO:0045087	0.277044467	<i>TICAM2, SERINC3, ATG12</i>
Negative regulation of apoptotic process	GO:0043066	0.309163283	<i>TAF9, ALMS1, NAIP</i>
Signal transduction	GO:0007165	0.549412418	<i>LVRN, HIVEP2, WISP2</i>
Regulation of transcription, DNA-templated	GO:0006355	0.765818005	<i>EGR4, GTF2H2, HIVEP2</i>
Transcription, DNA-templated	GO:0006351	0.767445213	<i>EGR4, HNF4A, GTF2H2</i>
GeneCodis			
Basal transcription factors	bta03022	0.037671679	<i>CDK7, GTF2H2, TAF9</i>

Taurine and hypotaurine metabolism	bta00430	0.037671679	<i>GADL1, CDO1</i>
FoxO signaling pathway	bta04068	0.083006507	<i>TGFBR2, STK4, CCNB1, ATG12</i>
L-cysteine catabolic process	GO:0019448	0.101601765	<i>CDO1</i>
regulation of triglyceride biosynthetic process	GO:0010866	0.101601765	<i>FITM2</i>
hypoxanthine salvage	GO:0043103	0.101601765	<i>ADA</i>
bicellular tight junction assembly	GO:0070830	0.101601765	<i>MARVELD2, OCLN</i>
purine deoxyribonucleoside metabolic process	GO:0046122	0.101601765	<i>DGUOK</i>
protein stabilization	GO:0050821	0.101601765	<i>CDK7, CCT7, STK4, TAF9</i>
taurine biosynthetic process	GO:0042412	0.101601765	<i>CDO1</i>
fatty-acyl-CoA catabolic process	GO:0036115	0.101601765	<i>FITM2</i>
actin cytoskeleton reorganization	GO:0031532	0.101601765	<i>PARVG, PARVB</i>
ornithine metabolic process	GO:0006591	0.101601765	<i>HNF4A</i>
dAMP salvage	GO:0106383	0.101601765	<i>DGUOK</i>
regulation of cell differentiation involved in embryonic placenta development	GO:0060800	0.101601765	<i>STK4</i>
response to interleukin-12	GO:0070671	0.101601765	<i>TICAM2</i>
cell-cell junction organization	GO:0045216	0.101601765	<i>MARVELD2, OCLN</i>
positive regulation of substrate-dependent cell migration, cell attachment to substrate	GO:1904237	0.101601765	<i>STK4</i>
sequestering of triglyceride	GO:0030730	0.101601765	<i>FITM2</i>
detection of virus	GO:0009597	0.101601765	<i>SERINC3</i>
negative regulation of adenosine receptor signaling pathway	GO:0060169	0.101601765	<i>ADA</i>
polynucleotide 5' dephosphorylation	GO:0098507	0.101601765	<i>DUSP11</i>
adenosine catabolic process	GO:0006154	0.101601765	<i>ADA</i>
regulation of transferase activity	GO:0051338	0.101601765	<i>PKIG</i>
positive regulation of interleukin-18-mediated signaling pathway	GO:2000494	0.101601765	<i>TICAM2</i>
oculomotor nerve development	GO:0021557	0.101601765	<i>ACKR3</i>
dGTP metabolic process	GO:0046070	0.101601765	<i>DGUOK</i>
positive regulation of epinephrine secretion	GO:0032812	0.101601765	<i>CARTPT</i>
bombesin receptor signaling pathway	GO:0031989	0.101601765	<i>NMBR</i>
nucleotide metabolic process	GO:0009117	0.101601765	<i>DGUOK, ADA</i>
inosine biosynthetic process	GO:0046103	0.101601765	<i>ADA</i>
positive regulation of blood-brain barrier permeability	GO:1905605	0.101601765	<i>OCLN</i>
organic substance biosynthetic process	GO:1901576	0.101601765	<i>DGUOK</i>
positive regulation of transmission of nerve impulse	GO:0051971	0.101601765	<i>CARTPT</i>
vascular associated smooth muscle contraction	GO:0014829	0.102419661	<i>ACTG2</i>
tight junction organization	GO:0120193	0.102419661	<i>OCLN</i>

phosphorylation	GO:0016310	0.102419661	<i>MOB1A, CDK7, DGUOK, TGFB2, AK6, STK4</i>
C-terminal protein lipidation	GO:0006501	0.102419661	<i>ATG12</i>
protein insertion into mitochondrial outer membrane	GO:0045040	0.102419661	<i>SAMM50</i>
primitive hemopoiesis	GO:0060215	0.102419661	<i>STK4</i>
lipid homeostasis	GO:0055088	0.102419661	<i>HNF4A, FITM2</i>
cell differentiation involved in embryonic placenta development	GO:0060706	0.102419661	<i>STK4</i>
cellular triglyceride homeostasis	GO:0035356	0.102419661	<i>FITM2</i>
COP9 signalosome assembly	GO:0010387	0.102419661	<i>COPS8</i>
purine ribonucleoside monophosphate biosynthetic process	GO:0009168	0.102419661	<i>ADA</i>
endocardium development	GO:0003157	0.102419661	<i>STK4</i>
cytoplasmic sequestering of protein	GO:0051220	0.102419661	<i>YWHAB</i>
tRNA threonylcarbamoyladenosine modification	GO:0002949	0.102419661	<i>TPRKB</i>
TRAM-dependent toll-like receptor 4 signaling pathway	GO:0035669	0.102419661	<i>TICAM2</i>
negative regulation of organ growth	GO:0046621	0.109898828	<i>STK4</i>
viral mRNA export from host cell nucleus	GO:0046784	0.109898828	<i>THOC3</i>
negative regulation of bone resorption	GO:0045779	0.109898828	<i>CARTPT</i>
DNA-templated transcription, termination	GO:0006353	0.109898828	<i>SMN2</i>
mesenchyme migration	GO:0090131	0.109898828	<i>ACTG2</i>
cobalt ion transport	GO:0006824	0.109898828	<i>SLC30A5</i>
regulation of bone remodeling	GO:0046850	0.109898828	<i>CARTPT</i>
mitochondrial respiratory chain complex assembly	GO:0033108	0.109898828	<i>SAMM50</i>
positive regulation of response to cytokine stimulus	GO:0060760	0.109898828	<i>TAF9</i>
regulation of gastrulation	GO:0010470	0.109898828	<i>HNF4A</i>
mitotic DNA replication checkpoint signaling	GO:0033314	0.109898828	<i>RAD17</i>
negative regulation of cAMP-dependent protein kinase activity	GO:2000480	0.113166507	<i>PKIG</i>
telomere maintenance via recombination	GO:0000722	0.113166507	<i>TPRKB</i>
positive regulation of chemokine (C-C motif) ligand 5 production	GO:0071651	0.113166507	<i>TICAM2</i>
negative regulation of phosphatidylinositol 3-kinase signaling	GO:0014067	0.113166507	<i>STAMBP</i>
positive regulation of extrinsic apoptotic signaling pathway via death domain receptors	GO:1902043	0.113166507	<i>STK4</i>
detection of bacterium	GO:0016045	0.113166507	<i>NAIP</i>
regulation of glucose transmembrane transport	GO:0010827	0.113166507	<i>OCLN</i>
autophagy of nucleus	GO:0044804	0.113166507	<i>ATG12</i>
phosphatidylserine metabolic process	GO:0006658	0.113166507	<i>SERINC3</i>
positive regulation of toll-like receptor 4 signaling pathway	GO:0034145	0.113166507	<i>TICAM2</i>
viral budding	GO:0046755	0.113166507	<i>VTA1</i>

positive regulation of endoplasmic reticulum stress-induced intrinsic apoptotic signaling pathway	GO:1902237	0.113166507	<i>SERINC3</i>
central nervous system development	GO:0007417	0.114003852	<i>STK4, NOTO</i>
Golgi organization	GO:0007030	0.114003852	<i>TICAM2, TMED7</i>
adult feeding behavior	GO:0008343	0.118279992	<i>CARTPT</i>
lipid droplet formation	GO:0140042	0.118279992	<i>FITM2</i>
Golgi to vacuole transport	GO:0006896	0.118279992	<i>AP3S1</i>
negative regulation of protein dephosphorylation	GO:0035308	0.118279992	<i>YWHAB</i>
ubiquitin-dependent protein catabolic process via the C-end degron rule pathway	GO:0140627	0.118279992	<i>FEM1C</i>
positive regulation of establishment of protein localization to telomere	GO:1904851	0.118279992	<i>CCT7</i>
negative regulation of protein import into nucleus	GO:0042308	0.118279992	<i>PKIG</i>
negative regulation of G protein-coupled receptor signaling pathway	GO:0045744	0.118279992	<i>YWHAB</i>
transcription by RNA polymerase II	GO:0006366	0.12189842	<i>CDK7, GTF2H2</i>
hepatocyte apoptotic process	GO:0097284	0.124955995	<i>STK4</i>
positive regulation of blood pressure	GO:0045777	0.124955995	<i>CARTPT</i>
sulfation	GO:0051923	0.124955995	<i>SULT4A1</i>
response to zinc ion	GO:0010043	0.124955995	<i>SLC30A5</i>
negative regulation of appetite	GO:0032099	0.124955995	<i>CARTPT</i>
positive regulation of sequestering of triglyceride	GO:0010890	0.124955995	<i>FITM2</i>
neural tube formation	GO:0001841	0.124955995	<i>STK4</i>
hippo signaling	GO:0035329	0.132378379	<i>STK4</i>
mitotic intra-S DNA damage checkpoint signaling	GO:0031573	0.132378379	<i>RAD17</i>
hepatocyte differentiation	GO:0070365	0.132378379	<i>HNF4A</i>
sulfur compound metabolic process	GO:0006790	0.132378379	<i>SULT4A1</i>
box C/D snoRNP assembly	GO:0000492	0.132378379	<i>TAF9</i>
pyroptosis	GO:0070269	0.132378379	<i>NAIP</i>
negative regulation of intrinsic apoptotic signaling pathway in response to DNA damage	GO:1902230	0.132378379	<i>ACKR3</i>
phosphorylation of RNA polymerase II C-terminal domain	GO:0070816	0.132378379	<i>CDK7</i>
RNA metabolic process	GO:0016070	0.132378379	<i>DUSP11</i>
2-oxoglutarate metabolic process	GO:0006103	0.132378379	<i>MRPS36</i>
type B pancreatic cell development	GO:0003323	0.132378379	<i>HNF4A</i>
protein deneddylation	GO:0000338	0.132378379	<i>COPS8</i>
cristae formation	GO:0042407	0.132378379	<i>SAMM50</i>
cell adhesion	GO:0007155	0.132378379	<i>WISP2, PARVG, ADA, PARVB</i>
tetrahydrofolate interconversion	GO:0035999	0.132378379	<i>MTHFD2</i>
negative regulation of DNA replication	GO:0008156	0.132378379	<i>RAD17</i>

cellular biosynthetic process	GO:0044249	0.132378379	<i>DGUOK</i>
signal transduction involved in regulation of gene expression	GO:0023019	0.132378379	<i>HNF4A</i>
RNA polymerase II preinitiation complex assembly	GO:0051123	0.138750714	<i>TAF9</i>
protein targeting	GO:0006605	0.138750714	<i>YWHAB</i>
sex differentiation	GO:0007548	0.138750714	<i>HNF4A</i>
phospholipid homeostasis	GO:0055091	0.138750714	<i>HNF4A</i>
peptide catabolic process	GO:0043171	0.138750714	<i>LVRN</i>
nucleoside monophosphate phosphorylation	GO:0046940	0.138750714	<i>AK6</i>
establishment of endothelial barrier	GO:0061028	0.140787812	<i>MARVELD2</i>
multivesicular body sorting pathway	GO:0071985	0.140787812	<i>VTA1</i>
late endosome to vacuole transport via multivesicular body sorting pathway	GO:0032511	0.140787812	<i>VTA1</i>
protein phosphorylation	GO:0006468	0.140787812	<i>CDK7, DGUOK, TGFB2, STK4, TAF9</i>
monoubiquitinated histone deubiquitination	GO:0035521	0.140787812	<i>TAF9</i>
kinetochore assembly	GO:0051382	0.140787812	<i>CENPH</i>
protein targeting to mitochondrion	GO:0006626	0.140787812	<i>TOMM34</i>
regulation of phosphorylation	GO:0042325	0.140787812	<i>RAD17</i>
transmembrane receptor protein serine/threonine kinase signaling pathway	GO:0007178	0.140787812	<i>TGFB2</i>
endoplasmic reticulum to Golgi vesicle-mediated transport	GO:0006888	0.14822097	<i>TICAM2, TMED7</i>
lipid droplet organization	GO:0034389	0.14822097	<i>FITM2</i>
negative regulation of Ras protein signal transduction	GO:0046580	0.14822097	<i>STAMBP</i>
histone lysine methylation	GO:0034968	0.14822097	<i>SMYD5</i>
cellular glucose homeostasis	GO:0001678	0.1539222	<i>CARTPT</i>
negative regulation of cell population proliferation	GO:0008285	0.1539222	<i>HNF4A, STK4, ACKR3</i>
regulation of MAPK cascade	GO:0043408	0.1539222	<i>STK4</i>
response to interleukin-1	GO:0070555	0.1539222	<i>TAF9</i>
mitotic cell cycle phase transition	GO:0044772	0.1539222	<i>CCNB1</i>
zinc ion transmembrane transport	GO:0071577	0.15913637	<i>SLC30A5</i>
monoubiquitinated histone H2A deubiquitination	GO:0035522	0.15913637	<i>TAF9</i>
carboxylic acid metabolic process	GO:0019752	0.15913637	<i>GADL1</i>
anterograde synaptic vesicle transport	GO:0048490	0.15913637	<i>AP3S1</i>
positive regulation of glucose import	GO:0046326	0.15913637	<i>OCLN</i>
protein tetramerization	GO:0051262	0.16159131	<i>STK4</i>
regulation of G1/S transition of mitotic cell cycle	GO:2000045	0.16159131	<i>CDK7</i>
branching involved in blood vessel morphogenesis	GO:0001569	0.16159131	<i>STK4</i>
negative regulation of proteasomal ubiquitin-dependent protein catabolic process	GO:0032435	0.16159131	<i>TAF9</i>

triglyceride homeostasis	GO:0070328	0.16159131	<i>HNF4A</i>
intracellular protein transport	GO:0006886	0.16159131	<i>TICAM2, AP3S1, TMED7</i>
DNA damage checkpoint signaling	GO:0000077	0.16159131	<i>RAD17</i>
anterograde axonal transport	GO:0008089	0.168307726	<i>AP3S1</i>
positive regulation of catalytic activity	GO:0043085	0.168307726	<i>YWHAB</i>
positive regulation of transcription initiation from RNA polymerase II promoter	GO:0060261	0.168307726	<i>TAF9</i>
positive regulation of telomere maintenance via telomerase	GO:0032212	0.173514405	<i>CCT7</i>
mRNA transcription by RNA polymerase II	GO:0042789	0.173514405	<i>TAF9</i>
regulation of cell morphogenesis	GO:0022604	0.173514405	<i>FITM2</i>
spliceosomal snRNP assembly	GO:0000387	0.173514405	<i>SMN2</i>
T cell activation	GO:0042110	0.178393929	<i>ADA</i>
cellular zinc ion homeostasis	GO:0006882	0.178393929	<i>SLC30A5</i>
nucleobase-containing compound metabolic process	GO:0006139	0.178393929	<i>DGUOK</i>
transcription initiation from RNA polymerase II promoter	GO:0006367	0.178393929	<i>CDK7</i>
lipid storage	GO:0019915	0.181492269	<i>FITM2</i>
response to glucose	GO:0009749	0.181492269	<i>HNF4A</i>
zinc ion transport	GO:0006829	0.181492269	<i>SLC30A5</i>
protein K63-linked deubiquitination	GO:0070536	0.181492269	<i>STAMBP</i>
regulation of cytokine production	GO:0001817	0.181492269	<i>TICAM2</i>
defense response to virus	GO:0051607	0.181492269	<i>TICAM2, SERINC3</i>
binding of sperm to zona pellucida	GO:0007339	0.183416087	<i>CCT7</i>
immune system process	GO:0002376	0.183416087	<i>TICAM2, SERINC3, ATG12</i>
toxin transport	GO:1901998	0.183416087	<i>CCT7</i>
DNA-templated transcription, initiation	GO:0006352	0.183416087	<i>TAF9</i>
regulation of insulin secretion	GO:0050796	0.183416087	<i>HNF4A</i>
autophagy of mitochondrion	GO:0000422	0.183416087	<i>ATG12</i>
innate immune response	GO:0045087	0.186327478	<i>TICAM2, SERINC3, ATG12</i>
cellular response to hydrogen peroxide	GO:0070301	0.189006699	<i>OSER1</i>
signal transduction	GO:0007165	0.201912251	<i>WISP2, TICAM2, STK4, LVRN, YWHAB, NMBR, ACKR3</i>
regulation of cyclin-dependent protein serine/threonine kinase activity	GO:0000079	0.203422852	<i>CCNB1</i>
keratinocyte differentiation	GO:0030216	0.205568001	<i>STK4</i>
histone H3 acetylation	GO:0043966	0.205568001	<i>TAF9</i>
mitotic cytokinesis	GO:0000281	0.205568001	<i>STAMBP</i>
chaperone-mediated protein folding	GO:0061077	0.205568001	<i>CCT7</i>
regulation of lipid metabolic process	GO:0019216	0.205568001	<i>HNF4A</i>

mitotic spindle organization	GO:0007052	0.207548993	<i>CENPH</i>
one-carbon metabolic process	GO:0006730	0.207548993	<i>MTHFD2</i>
mRNA export from nucleus	GO:0006406	0.207548993	<i>THOC3</i>
mitotic metaphase plate congression	GO:0007080	0.207548993	<i>CCNB1</i>
nucleotide-excision repair	GO:0006289	0.207548993	<i>GTF2H2</i>
phospholipid biosynthetic process	GO:0008654	0.211693103	<i>FITM2</i>
positive regulation of protein kinase activity	GO:0045860	0.211693103	<i>CARTPT</i>
receptor internalization	GO:0031623	0.211693103	<i>ACKR3</i>
positive regulation of fat cell differentiation	GO:0045600	0.214494591	<i>STK4</i>
regulation of blood pressure	GO:0008217	0.214494591	<i>LVRN</i>
intracellular receptor signaling pathway	GO:0030522	0.214494591	<i>HNF4A</i>
tricarboxylic acid cycle	GO:0006099	0.214494591	<i>MRPS36</i>
xenobiotic metabolic process	GO:0006805	0.22063928	<i>HNF4A</i>
amino acid transport	GO:0006865	0.226677615	<i>SFXN5</i>
vasculogenesis	GO:0001570	0.230162972	<i>ACKR3</i>
negative regulation of cysteine-type endopeptidase activity involved in apoptotic process	GO:0043154	0.230162972	<i>NAIP</i>
phagocytosis	GO:0006909	0.230162972	<i>TICAM2</i>
anatomical structure development	GO:0048856	0.235946072	<i>HNF4A</i>
sphingolipid metabolic process	GO:0006665	0.241630004	<i>SERINC3</i>
regulation of growth	GO:0040008	0.244680968	<i>TGFBR2</i>
regulation of circadian rhythm	GO:0042752	0.244680968	<i>HNF4A</i>
glutathione metabolic process	GO:0006749	0.244680968	<i>GDAP1L1</i>
negative regulation of cell death	GO:0060548	0.248859007	<i>WISP2</i>
negative regulation of protein phosphorylation	GO:0001933	0.248859007	<i>OCN</i>
negative regulation of protein kinase activity	GO:0006469	0.256856128	<i>PKIG</i>
cell morphogenesis	GO:0000902	0.256856128	<i>STK4</i>
positive regulation of interleukin-6 production	GO:0032755	0.256856128	<i>TICAM2</i>
cellular response to starvation	GO:0009267	0.256856128	<i>CARTPT</i>
positive regulation of protein binding	GO:0032092	0.258139435	<i>STK4</i>
apoptotic process	GO:0006915	0.258139435	<i>NAIP, TGFBR2, STK4</i>
biological_process	GO:0008150	0.258139435	<i>KIAA1191</i>
calcium-mediated signaling	GO:0019722	0.258139435	<i>ACKR3</i>
RNA splicing	GO:0008380	0.260585845	<i>THOC3, SMN2</i>
positive regulation of interferon-gamma production	GO:0032729	0.260585845	<i>TICAM2</i>
autophagosome assembly	GO:0000045	0.260585845	<i>ATG12</i>
circadian regulation of gene expression	GO:0032922	0.26418065	<i>CARTPT</i>

positive regulation of peptidyl-serine phosphorylation	GO:0033138	0.26418065	<i>STK4</i>
SMAD protein signal transduction	GO:0060395	0.268942491	<i>HNF4A</i>
Purine metabolism	bta00230	0.271755058	<i>DGUOK, AK6, ADA</i>
Nucleotide excision repair	bta03420	0.271755058	<i>CDK7, GTF2H2</i>
Cell cycle	bta04110	0.271755058	<i>CDK7, CCNB1, YWHAB</i>
cation transport	GO:0006812	0.272341235	<i>SLC30A5</i>
regulation of transcription by RNA polymerase II	GO:0006357	0.272341235	<i>HNF4A, HIVEP2, GTF2H2, NOTO, EGR4, TAF9</i>
cellular protein localization	GO:0034613	0.276931904	<i>YWHAB</i>
cholesterol homeostasis	GO:0042632	0.281447154	<i>HNF4A</i>
Endocytosis	bta04144	0.286539883	<i>TGFBR2, STAMBP, VTA1, RAB11FIP5</i>
chromosome segregation	GO:0007059	0.294552536	<i>CENPH</i>
chemokine-mediated signaling pathway	GO:0070098	0.294552536	<i>ACKR3</i>
blood coagulation	GO:0007596	0.294552536	<i>HNF4A</i>
mRNA transport	GO:0051028	0.298778143	<i>THOC3</i>
cell chemotaxis	GO:0060326	0.302934234	<i>ACKR3</i>
protein import into nucleus	GO:0006606	0.307021924	<i>STK4</i>
Hippo signaling pathway	bta04390	0.310979836	<i>MOB1A, TGFBR2, YWHAB</i>
Hepatitis B	bta05161	0.310979836	<i>TGFBR2, TICAM2, YWHAB</i>
inflammatory response	GO:0006954	0.314894641	<i>NAIP, TICAM2</i>
protein deubiquitination	GO:0016579	0.320315394	<i>STAMBP</i>
transcription, DNA-templated	GO:0006351	0.324150899	<i>GTF2H2</i>
cellular response to lipopolysaccharide	GO:0071222	0.331632379	<i>TICAM2</i>
negative regulation of catalytic activity	GO:0043086	0.331632379	<i>YWHAB</i>
sensory perception of sound	GO:0007605	0.335280344	<i>MARVELD2</i>
peptidyl-tyrosine dephosphorylation	GO:0035335	0.338624032	<i>DUSP11</i>
mRNA processing	GO:0006397	0.338624032	<i>THOC3, SMN2</i>
negative regulation of canonical Wnt signaling pathway	GO:0090090	0.340906891	<i>STK4</i>
protein autophosphorylation	GO:0046777	0.344367457	<i>STK4</i>
negative regulation of cell growth	GO:0030308	0.347770591	<i>HNF4A</i>
positive regulation of cytosolic calcium ion concentration	GO:0007204	0.351117185	<i>ACKR3</i>
cytoskeleton organization	GO:0007010	0.354408114	<i>FITM2</i>
glucose homeostasis	GO:0042593	0.367052916	<i>HNF4A</i>
intracellular signal transduction	GO:0035556	0.368330628	<i>STK4, ASB18</i>
neuropeptide signaling pathway	GO:0007218	0.368580789	<i>CARTPT</i>

positive regulation of gene expression	GO:0010628	0.375043969	<i>OCLN, ACTG2</i>
DNA repair	GO:0006281	0.385646765	<i>RAD17, GTF2H2</i>
defense response to bacterium	GO:0042742	0.39035617	<i>NAIP</i>
protein transport	GO:0015031	0.39035617	<i>AP3S1, TMED7, VTA1</i>
chemotaxis	GO:0006935	0.39035617	<i>ACKR3</i>
negative regulation of apoptotic process	GO:0043066	0.39035617	<i>NAIP, TAF9</i>
peptidyl-serine phosphorylation	GO:0018105	0.409989046	<i>STK4</i>
neuron differentiation	GO:0030182	0.412473728	<i>NOTO</i>
positive regulation of MAPK cascade	GO:0043410	0.425400838	<i>CARTPT</i>
positive regulation of ERK1 and ERK2 cascade	GO:0070374	0.425400838	<i>ACKR3</i>
chemical synaptic transmission	GO:0007268	0.427679031	<i>CARTPT</i>
protein folding	GO:0006457	0.429916536	<i>CCT7</i>
G protein-coupled receptor signaling pathway	GO:0007186	0.430725314	<i>CARTPT, NMBR, ACKR3</i>
proteasome-mediated ubiquitin-dependent protein catabolic process	GO:0043161	0.441965549	<i>FEM1C</i>
positive regulation of protein phosphorylation	GO:0001934	0.447788747	<i>STK4</i>
cellular response to DNA damage stimulus	GO:0006974	0.455380849	<i>RAD17, GTF2H2</i>
autophagy	GO:0006914	0.455380849	<i>ATG12</i>
protein dephosphorylation	GO:0006470	0.468071874	<i>DUSP11</i>
ion transmembrane transport	GO:0034220	0.481933724	<i>SFXN5</i>
angiogenesis	GO:0001525	0.481933724	<i>ACKR3</i>
cell cycle	GO:0007049	0.486522006	<i>RAD17, CCNB1</i>
metabolic process	GO:0008152	0.486522006	<i>MTHFD2</i>
negative regulation of gene expression	GO:0010629	0.486522006	<i>OCLN</i>
dephosphorylation	GO:0016311	0.497873988	<i>DUSP11</i>
nervous system development	GO:0007399	0.560406339	<i>SMN2</i>
positive regulation of apoptotic process	GO:0043065	0.572464717	<i>STK4</i>
protein ubiquitination	GO:0016567	0.579558935	<i>ASB18, FEM1C</i>
RNA degradation	bta03018	0.588372575	<i>PABPC1L</i>
NOD-like receptor signaling pathway	bta04621	0.588372575	<i>NAIP, ATG12</i>
Pancreatic cancer	bta05212	0.588372575	<i>TGFBR2</i>
Hepatitis C	bta05160	0.588372575	<i>YWHAB, OCLN</i>
One carbon pool by folate	bta00670	0.588372575	<i>MTHFD2</i>
PD-L1 expression and PD-1 checkpoint pathway in cancer	bta05235	0.588372575	<i>TICAM2</i>
Cytokine-cytokine receptor interaction	bta04060	0.588372575	<i>TGFBR2, ACKR3</i>
Cysteine and methionine metabolism	bta00270	0.588372575	<i>CDO1</i>
Cellular senescence	bta04218	0.588372575	<i>TGFBR2, CCNB1</i>

Autophagy - other	bta04136	0.588372575	ATG12
NF-kappa B signaling pathway	bta04064	0.588372575	TICAM2
Ribosome biogenesis in eukaryotes	bta03008	0.588372575	AK6
TGF-beta signaling pathway	bta04350	0.588372575	TGFBR2
Legionellosis	bta05134	0.588372575	NAIP
Bile secretion	bta04976	0.588372575	SLC4A5
Chagas disease	bta05142	0.588372575	TGFBR2
Primary immunodeficiency	bta05340	0.588372575	ADA
AGE-RAGE signaling pathway in diabetic complications	bta04933	0.588372575	TGFBR2
Nucleocytoplasmic transport	bta03013	0.588372575	THOC3
Toll-like receptor signaling pathway	bta04620	0.588372575	TICAM2
Oocyte meiosis	bta04114	0.588372575	CCNB1, YWHAB
RIG-I-like receptor signaling pathway	bta04622	0.588372575	ATG12
Viral protein interaction with cytokine and cytokine receptor	bta04061	0.588372575	ACKR3
Valine, leucine and isoleucine degradation	bta00280	0.588372575	MCCC2
Non-small cell lung cancer	bta05223	0.588372575	STK4
Biosynthesis of cofactors	bta01240	0.588372575	AK6, MTHFD2
Adherens junction	bta04520	0.588372575	TGFBR2
Pertussis	bta05133	0.588372575	TICAM2
Progesterone-mediated oocyte maturation	bta04914	0.588372575	CCNB1
Chronic myeloid leukemia	bta05220	0.588372575	TGFBR2
Pantothenate and CoA biosynthesis	bta00770	0.588372575	GADL1
Focal adhesion	bta04510	0.588372575	PARVG, PARVB
beta-Alanine metabolism	bta00410	0.588372575	GADL1
Tight junction	bta04530	0.588372575	MARVELD2, OCLN
mRNA surveillance pathway	bta03015	0.588372575	PABPC1L
Hippo signaling pathway - multiple species	bta04392	0.588372575	MOB1A
p53 signaling pathway	bta04115	0.588372575	CCNB1
Viral carcinogenesis	bta05203	0.588372575	GTF2H2, YWHAB
Maturity onset diabetes of the young	bta04950	0.588372575	HNF4A
Colorectal cancer	bta05210	0.588372575	TGFBR2
ubiquitin-dependent protein catabolic process	GO:0006511	0.597753546	FEM1C
Th17 cell differentiation	bta04659	0.599122635	TGFBR2
positive regulation of transcription by RNA polymerase II	GO:0045944	0.599922408	HNF4A, CDK7, TAF9
MAPK signaling pathway	bta04010	0.603939375	TGFBR2, STK4
Leukocyte transendothelial migration	bta04670	0.605532599	OCLN

Osteoclast differentiation	bta04380	0.606198029	<i>TGFBR2</i>
Relaxin signaling pathway	bta04926	0.606529764	<i>TGFBR2</i>
Spliceosome	bta03040	0.606529764	<i>THOC3</i>
Vascular smooth muscle contraction	bta04270	0.606529764	<i>ACTG2</i>
AMPK signaling pathway	bta04152	0.606529764	<i>HNF4A</i>
Lysosome	bta04142	0.606529764	<i>AP3S1</i>
Necroptosis	bta04217	0.606529764	<i>TICAM2</i>
Cell adhesion molecules	bta04514	0.609262667	<i>OCLN</i>
Autophagy - animal	bta04140	0.611664944	<i>ATG12</i>
lipid metabolic process	GO:0006629	0.614212037	<i>HNF4A, FITM2</i>
Gastric cancer	bta05226	0.619649857	<i>TGFBR2</i>
transmembrane transport	GO:0055085	0.625000349	<i>SLC30A5, SFXN5</i>
cell differentiation	GO:0030154	0.625840841	<i>HNF4A, TGFBR2</i>
immune response	GO:0006955	0.625840841	<i>ACKR3</i>
ion transport	GO:0006811	0.635388401	<i>SLC30A5, SFXN5</i>
Hepatocellular carcinoma	bta05225	0.652623873	<i>TGFBR2</i>
Transcriptional misregulation in cancer	bta05202	0.652623873	<i>TGFBR2</i>
Metabolic pathways	bta01100	0.652623873	<i>GADL1, DGUOK, AK6, ADA, CDO1, MCCC2, MTHFD2</i>
Axon guidance	bta04360	0.661399784	<i>PLXNA4</i>
cell division	GO:0051301	0.66302716	<i>CCNB1</i>
vesicle-mediated transport	GO:0016192	0.664724654	<i>AP3S1</i>
Human immunodeficiency virus 1 infection	bta05170	0.673097509	<i>CCNB1</i>
Lipid and atherosclerosis	bta05417	0.673097509	<i>TICAM2</i>
Diabetic cardiomyopathy	bta05415	0.677927285	<i>TGFBR2</i>
Human T-cell leukemia virus 1 infection	bta05166	0.695568428	<i>TGFBR2</i>
Ras signaling pathway	bta04014	0.709195777	<i>STK4</i>
Salmonella infection	bta05132	0.722636036	<i>NAIP</i>
Pathways in cancer	bta05200	0.736481479	<i>TGFBR2, STK4</i>
negative regulation of transcription, DNA-templated	GO:0045892	0.782939697	<i>HNF4A</i>
Neuroactive ligand-receptor interaction	bta04080	0.818449657	<i>NMBR</i>
PI3K-Akt signaling pathway	bta04151	0.818449657	<i>YWHAB</i>
positive regulation of transcription, DNA-templated	GO:0045893	0.857803934	<i>HNF4A</i>
proteolysis	GO:0006508	0.883869301	<i>LVRN</i>
negative regulation of transcription by RNA polymerase II	GO:0000122	0.89631138	<i>PKIG</i>
regulation of transcription, DNA-templated	GO:0006355	0.982180148	<i>HNF4A</i>

Table S2. Results of functional enrichment analyzes performed in DAVID and GeneCodis for BF.

Description	Annotation_ID	Pvalue	Genes
DAVID			
Focal adhesion	bta04510	1.14E-04	<i>BAD, COL6A2, COL6A1, VEGFB, COL6A3, PARVA, RAC1</i>
Protein digestion and absorption	bta04974	0.003940223	<i>COL18A1, COL6A2, COL6A1, COL6A3</i>
PI3K-Akt signaling pathway	bta04151	0.009512771	<i>BAD, COL6A2, COL6A1, VEGFB, COL6A3, RAC1</i>
substrate adhesion-dependent cell spreading	GO:0034446	0.013816757	<i>PARVA, RAC1, FERMT3</i>
ECM-receptor interaction	bta04512	0.043584916	<i>COL6A2, COL6A1, COL6A3</i>
Ras signaling pathway	bta04014	0.060046135	<i>PLA2G16, BAD, VEGFB, RAC1</i>
apoptotic process	GO:0006915	0.076411654	<i>AIMP2, RTN3, PRDX5, BAD</i>
cilium assembly	GO:0042384	0.077521251	<i>TRAF3IP1, RAB17, PCNT</i>
angiogenesis	GO:0001525	0.137554651	<i>COL18A1, VEGFB, RAMP1</i>
Alzheimer's disease	bta05010	0.14860069	<i>COX8A, PLCB3, BAD</i>
intracellular signal transduction	GO:0035556	0.149671841	<i>RPS6KA4, PLCB3, MARK2, ASB1</i>
Pathways in cancer	bta05200	0.194785531	<i>PLCB3, BAD, VEGFB, RAC1</i>
Rap1 signaling pathway	bta04015	0.198024458	<i>PLCB3, VEGFB, RAC1</i>
Metabolic pathways	bta01100	0.52592914	<i>COX8A, PLA2G16, PLCB3, SCLY, LSS, FTCD</i>
regulation of transcription, DNA-templated	GO:0006355	0.794854335	<i>HES6, TFIP11, LRRFIP1</i>
GeneCodis			
Focal adhesion	bta04510	0.002045911	<i>PARVA, RAC1, BAD, COL6A2, COL6A3, VEGFB, COL6A1</i>
cytoskeleton-dependent intracellular transport	GO:0030705	0.061967637	<i>CCDC88B, MYO10</i>
Protein digestion and absorption	bta04974	0.07201279	<i>COL18A1, COL6A2, COL6A3, COL6A1</i>
peptidyl-tyrosine sulfation	GO:0006478	0.096219715	<i>TPST2</i>
sulfur oxidation	GO:0019417	0.096219715	<i>MICAL2</i>
positive regulation of transcription via serum response element binding	GO:0010735	0.096219715	<i>MICAL2</i>
regulation of cysteine-type endopeptidase activity involved in apoptotic process	GO:0043281	0.096219715	<i>BAD</i>
peptidyl-glutamate ADP-deribosylation	GO:0140291	0.096219715	<i>MACROD1</i>
positive regulation of aminoacyl-tRNA ligase activity	GO:1903632	0.096219715	<i>AIMP2</i>

cellular response to nicotine	GO:0071316	0.096219715	<i>BAD</i>
positive regulation of intrinsic apoptotic signaling pathway in response to osmotic stress	GO:1902220	0.096219715	<i>BAD</i>
regulation of cell-cell adhesion mediated by integrin	GO:0033632	0.096219715	<i>FERMT3</i>
triterpenoid biosynthetic process	GO:0016104	0.096219715	<i>LSS</i>
positive regulation of glucokinase activity	GO:0033133	0.096219715	<i>BAD</i>
glucose catabolic process	GO:0006007	0.096219715	<i>BAD</i>
nucleosome organization	GO:0034728	0.096219715	<i>MCM3AP</i>
purine nucleoside metabolic process	GO:0042278	0.096219715	<i>MACROD1</i>
rRNA (guanine-N7)-methylation	GO:0070476	0.096219715	<i>TRMT112</i>
cellular response to lipid	GO:0071396	0.096219715	<i>BAD</i>
peptidyl-glutamine methylation	GO:0018364	0.096219715	<i>TRMT112</i>
ADP metabolic process	GO:0046031	0.096219715	<i>BAD</i>
positive regulation of type B pancreatic cell development	GO:2000078	0.096219715	<i>BAD</i>
type II pneumocyte differentiation	GO:0060510	0.096219715	<i>AIMP2</i>
spliceosomal complex disassembly	GO:0000390	0.096219715	<i>TFIP11</i>
histone H3-S10 phosphorylation	GO:0043987	0.096219715	<i>RPS6KA4</i>
methotrexate transport	GO:0051958	0.096219715	<i>SLC19A1</i>
histone acetylation	GO:0016573	0.096219715	<i>TRRAP, MCM3AP</i>
positive regulation of mitochondrial membrane potential	GO:0010918	0.101831318	<i>BAD</i>
protein de-ADP-ribosylation	GO:0051725	0.101831318	<i>MACROD1</i>
regulation of bone remodeling	GO:0046850	0.101831318	<i>GPR137</i>
N-acylphosphatidylethanolamine metabolic process	GO:0070292	0.101831318	<i>HRASLS5</i>
folic acid transport	GO:0015884	0.101831318	<i>SLC19A1</i>
folate import across plasma membrane	GO:1904447	0.101831318	<i>SLC19A1</i>
positive regulation of protein phosphorylation	GO:0001934	0.101831318	<i>SPATC1L, RAC1, VEGFB</i>
negative regulation of bone resorption	GO:0045779	0.101831318	<i>GPR137</i>
negative regulation of myotube differentiation	GO:0010832	0.101831318	<i>BHLHA15</i>
apoptotic process	GO:0006915	0.101831318	<i>AIMP2, BAD, WWOX, RTN3, PRDX5</i>
regulation of neutrophil migration	GO:1902622	0.101831318	<i>RAC1</i>
glomerular visceral epithelial cell differentiation	GO:0072112	0.101831318	<i>BASP1</i>
positive regulation of histone phosphorylation	GO:0033129	0.101831318	<i>RPS6KA4</i>
negative regulation of transcription by RNA polymerase III	GO:0016480	0.101831318	<i>PRDX5</i>
pore complex assembly	GO:0046931	0.101831318	<i>BAD</i>
positive regulation of cAMP-dependent protein kinase activity	GO:2000481	0.101831318	<i>SPATC1L</i>
negative regulation of histone H2A K63-linked ubiquitination	GO:1901315	0.101831318	<i>OTUB1</i>

histone H3-S28 phosphorylation	GO:0043988	0.101831318	<i>RPS6KA4</i>
positive regulation of endoplasmic reticulum tubular network organization	GO:1903373	0.101831318	<i>ATL3</i>
type B pancreatic cell proliferation	GO:0044342	0.101831318	<i>BAD</i>
regulation of bone resorption	GO:0045124	0.101831318	<i>GPR137</i>
intracellular distribution of mitochondria	GO:0048312	0.101831318	<i>BHLHA15</i>
macromolecule metabolic process	GO:0043170	0.114751885	<i>TFIP11</i>
negative regulation of double-strand break repair	GO:2000780	0.114751885	<i>OTUB1</i>
integrin activation	GO:0033622	0.114751885	<i>FERMT3</i>
Golgi organization	GO:0007030	0.114751885	<i>ATL3, BHLHA15</i>
establishment or maintenance of epithelial cell apical/basal polarity	GO:0045197	0.114751885	<i>MARK2</i>
vascular endothelial growth factor receptor signaling pathway	GO:0048010	0.125298077	<i>VEGFB</i>
histone phosphorylation	GO:0016572	0.125298077	<i>RPS6KA4</i>
protein deubiquitination	GO:0016579	0.125298077	<i>OTUB1, USP42</i>
positive regulation of mast cell chemotaxis	GO:0060754	0.125298077	<i>VEGFB</i>
positive regulation of protein kinase A signaling	GO:0010739	0.125298077	<i>SPATC1L</i>
PI3K-Akt signaling pathway	bta04151	0.128542585	<i>RAC1, BAD, COL6A2, COL6A3, VEGFB, COL6A1</i>
somatic hypermutation of immunoglobulin genes	GO:0016446	0.129855943	<i>MCM3AP</i>
activation of cysteine-type endopeptidase activity	GO:0097202	0.129855943	<i>BAD</i>
regulation of ossification	GO:0030278	0.129855943	<i>GPR137</i>
N-terminal protein amino acid acetylation	GO:0006474	0.129855943	<i>NAA40</i>
Rac protein signal transduction	GO:0016601	0.129855943	<i>RAC1</i>
vitamin transport	GO:0051180	0.129855943	<i>SLC19A1</i>
male genitalia development	GO:0030539	0.129855943	<i>ASB1</i>
leukocyte cell-cell adhesion	GO:0007159	0.133429562	<i>FERMT3</i>
positive regulation of histone acetylation	GO:0035066	0.133429562	<i>RPS6KA4</i>
regulation of RNA metabolic process	GO:0051252	0.133429562	<i>PCBP3</i>
regulation of mitochondrial membrane permeability	GO:0046902	0.133429562	<i>BAD</i>
vascular endothelial growth factor signaling pathway	GO:0038084	0.133429562	<i>VEGFB</i>
positive regulation of rRNA processing	GO:2000234	0.133429562	<i>TRMT112</i>
protein neddylation	GO:0045116	0.133429562	<i>UBE2F</i>
establishment of cell polarity	GO:0030010	0.138054248	<i>MARK2</i>
actin filament depolymerization	GO:0030042	0.138054248	<i>MICAL2</i>
glucose homeostasis	GO:0042593	0.138054248	<i>BAD, BHLHA15</i>
mitochondrial calcium ion transmembrane transport	GO:0006851	0.138054248	<i>BHLHA15</i>
regulation of filopodium assembly	GO:0051489	0.138054248	<i>MYO10</i>

positive regulation of B cell differentiation	GO:0045579	0.138054248	<i>BAD</i>
positive regulation of TORC1 signaling	GO:1904263	0.140248163	<i>GPR137</i>
tRNA splicing, via endonucleolytic cleavage and ligation	GO:0006388	0.140248163	<i>TRPT1</i>
induction of positive chemotaxis	GO:0050930	0.140248163	<i>VEGFB</i>
engulfment of apoptotic cell	GO:0043652	0.140248163	<i>RAC1</i>
reticulophagy	GO:0061709	0.140248163	<i>RETREG1</i>
interleukin-1-mediated signaling pathway	GO:0070498	0.140248163	<i>RPS6KA4</i>
regulation of axonogenesis	GO:0050770	0.140248163	<i>MARK2</i>
release of cytochrome c from mitochondria	GO:0001836	0.145230735	<i>BAD</i>
regulation of protein kinase activity	GO:0045859	0.145230735	<i>TRPT1</i>
actin polymerization or depolymerization	GO:0008154	0.145230735	<i>SPATC1L</i>
coronary vasculature development	GO:0060976	0.145230735	<i>VEGFB</i>
positive regulation of T cell differentiation	GO:0045582	0.145230735	<i>BAD</i>
negative regulation of osteoclast differentiation	GO:0045671	0.148045016	<i>GPR137</i>
rRNA methylation	GO:0031167	0.148045016	<i>TRMT112</i>
cell projection assembly	GO:0030031	0.148045016	<i>RAC1</i>
positive regulation of proteolysis	GO:0045862	0.148045016	<i>BAD</i>
histone lysine methylation	GO:0034968	0.148045016	<i>TRMT112</i>
regulation of cell shape	GO:0008360	0.148045016	<i>RAC1, MYO10</i>
intrinsic apoptotic signaling pathway	GO:0097193	0.148991172	<i>BAD</i>
steroid hormone mediated signaling pathway	GO:0043401	0.148991172	<i>ESRRA</i>
positive regulation of insulin secretion involved in cellular response to glucose stimulus	GO:0035774	0.148991172	<i>BAD</i>
positive regulation of release of cytochrome c from mitochondria	GO:0090200	0.148991172	<i>BAD</i>
poly(A)+ mRNA export from nucleus	GO:0016973	0.148991172	<i>MCM3AP</i>
regulation of macromolecule metabolic process	GO:0060255	0.148991172	<i>TRRAP</i>
peptidyl-serine phosphorylation	GO:0018105	0.148991172	<i>MARK2, RPS6KA4</i>
platelet aggregation	GO:0070527	0.149761785	<i>FERMT3</i>
motor neuron axon guidance	GO:0008045	0.149761785	<i>RAC1</i>
negative regulation of signaling receptor activity	GO:2000272	0.149761785	<i>DKK3</i>
histone H2A acetylation	GO:0043968	0.149761785	<i>NAA40</i>
cortical cytoskeleton organization	GO:0030865	0.149761785	<i>RAC1</i>
extrinsic apoptotic signaling pathway via death domain receptors	GO:0008625	0.149761785	<i>BAD</i>
semaphorin-plexin signaling pathway	GO:0071526	0.149761785	<i>RAC1</i>
primary metabolic process	GO:0044238	0.151696623	<i>TFIP11</i>
vesicle-mediated transport	GO:0016192	0.151696623	<i>HPS4, RTN3, CCZ1</i>

biomineral tissue development	GO:0031214	0.151696623	<i>TFIP11</i>
positive regulation of insulin secretion	GO:0032024	0.151696623	<i>BAD</i>
mitochondrial electron transport, cytochrome c to oxygen	GO:0006123	0.151696623	<i>COX8A</i>
regulation of microtubule cytoskeleton organization	GO:0070507	0.151696623	<i>MARK2</i>
cellular response to reactive oxygen species	GO:0034614	0.157291193	<i>PRDX5</i>
extrinsic apoptotic signaling pathway in absence of ligand	GO:0097192	0.157291193	<i>BAD</i>
hydrogen peroxide catabolic process	GO:0042744	0.157291193	<i>PRDX5</i>
cardiac muscle contraction	GO:0060048	0.158627512	<i>VEGFB</i>
ATP metabolic process	GO:0046034	0.158627512	<i>BAD</i>
protein K48-linked deubiquitination	GO:0071108	0.158627512	<i>OTUB1</i>
sensory perception of pain	GO:0019233	0.158627512	<i>RETREG1</i>
regulation of G protein-coupled receptor signaling pathway	GO:0008277	0.158627512	<i>RAMP1</i>
substrate adhesion-dependent cell spreading	GO:0034446	0.158627512	<i>FERMT3</i>
autophagy	GO:0006914	0.159642667	<i>RETREG1, GPR137</i>
intracellular signal transduction	GO:0035556	0.159642667	<i>ASB1, MARK2, RPS6KA4</i>
negative regulation of protein-containing complex assembly	GO:0031333	0.162292917	<i>TFIP11</i>
cell redox homeostasis	GO:0045454	0.162292917	<i>PRDX5</i>
sprouting angiogenesis	GO:0002040	0.166957527	<i>VEGFB</i>
intrinsic apoptotic signaling pathway in response to DNA damage	GO:0008630	0.166957527	<i>BAD</i>
cell motility	GO:0048870	0.166957527	<i>RAC1</i>
ECM-receptor interaction	bta04512	0.167342876	<i>COL6A2, COL6A3, COL6A1</i>
endoplasmic reticulum organization	GO:0007029	0.170101249	<i>ATL3</i>
positive regulation of cysteine-type endopeptidase activity involved in apoptotic process	GO:0043280	0.170101249	<i>BAD</i>
heart development	GO:0007507	0.170101249	<i>VEGFB, MICAL2</i>
oxidative phosphorylation	GO:0006119	0.170101249	<i>COX8A</i>
cholesterol biosynthetic process	GO:0006695	0.171787288	<i>LSS</i>
cellular response to mechanical stimulus	GO:0071260	0.171787288	<i>BAD</i>
cell maturation	GO:0048469	0.171787288	<i>BHLHA15</i>
protein O-linked glycosylation	GO:0006493	0.171787288	<i>VEGFB</i>
extrinsic apoptotic signaling pathway	GO:0097191	0.171787288	<i>BAD</i>
nitrogen compound metabolic process	GO:0006807	0.174521668	<i>TFIP11</i>
heart looping	GO:0001947	0.174521668	<i>MICAL2</i>
lens development in camera-type eye	GO:0002088	0.174521668	<i>CRYBB1</i>
establishment or maintenance of cell polarity	GO:0007163	0.174521668	<i>RAC1</i>
histone H4 acetylation	GO:0043967	0.180733772	<i>NAA40</i>

histone H3 acetylation	GO:0043966	0.184297833	<i>MCM3AP</i>
chaperone-mediated protein folding	GO:0061077	0.184297833	<i>FKBP2</i>
histone deacetylation	GO:0016575	0.184297833	<i>RCOR2</i>
mRNA export from nucleus	GO:0006406	0.188934639	<i>MCM3AP</i>
positive regulation of neuron projection development	GO:0010976	0.188934639	<i>MARK2</i>
actin cytoskeleton reorganization	GO:0031532	0.193412994	<i>PARVA</i>
tRNA methylation	GO:0030488	0.193412994	<i>TRMT112</i>
intracellular receptor signaling pathway	GO:0030522	0.193960798	<i>ESRRA</i>
endoplasmic reticulum unfolded protein response	GO:0030968	0.193960798	<i>BHLHA15</i>
cellular response to glucose starvation	GO:0042149	0.193960798	<i>BHLHA15</i>
negative regulation of Wnt signaling pathway	GO:0030178	0.193960798	<i>DKK3</i>
positive chemotaxis	GO:0050918	0.193960798	<i>VEGFB</i>
apoptotic signaling pathway	GO:0097190	0.199363509	<i>BAD</i>
positive regulation of epithelial cell proliferation	GO:0050679	0.204663966	<i>BAD</i>
negative regulation of protein binding	GO:0032091	0.207273343	<i>TFIP11</i>
positive regulation of cell division	GO:0051781	0.207273343	<i>VEGFB</i>
negative regulation of cysteine-type endopeptidase activity involved in apoptotic process	GO:0043154	0.207273343	<i>PRDX5</i>
negative regulation of transcription, DNA-templated	GO:0045892	0.214147267	<i>BASP1, SPINDOC, RCOR2</i>
steroid biosynthetic process	GO:0006694	0.214671922	<i>LSS</i>
cellular response to hypoxia	GO:0071456	0.214671922	<i>BAD</i>
positive regulation of endothelial cell proliferation	GO:0001938	0.214671922	<i>VEGFB</i>
protein-containing complex assembly	GO:0065003	0.218191312	<i>AIMP2</i>
protein peptidyl-prolyl isomerization	GO:0000413	0.218191312	<i>FKBP2</i>
regulation of actin cytoskeleton organization	GO:0032956	0.228884172	<i>RAC1</i>
spermatogenesis	GO:0007283	0.23181653	<i>SPATC1L, USP42</i>
calcium-mediated signaling	GO:0019722	0.23792787	<i>BHLHA15</i>
regulation of autophagy	GO:0010506	0.239540011	<i>GPR137</i>
activation of cysteine-type endopeptidase activity involved in apoptotic process	GO:0006919	0.239540011	<i>BAD</i>
cell-matrix adhesion	GO:0007160	0.239540011	<i>FERMT3</i>
positive regulation of protein ubiquitination	GO:0031398	0.243823299	<i>AIMP2</i>
Human papillomavirus infection	bta05165	0.256767772	<i>HES6, BAD, COL6A2, COL6A3, COL6A1</i>
cell-cell signaling	GO:0007267	0.257658778	<i>BHLHA15</i>
cellular response to oxidative stress	GO:0034599	0.257658778	<i>PRDX5</i>
translational initiation	GO:0006413	0.267066668	<i>EIF2AK1</i>

regulation of cell migration	GO:0030334	0.270929888	RAC1
response to hypoxia	GO:0001666	0.279992486	VEGFB
ossification	GO:0001503	0.287258554	CLEC3A
small GTPase mediated signal transduction	GO:0007264	0.287258554	RAC1
integrin-mediated signaling pathway	GO:0007229	0.290791827	FERMT3
neuron migration	GO:0001764	0.292669622	RAC1
cellular oxidant detoxification	GO:0098869	0.292669622	PRDX5
response to oxidative stress	GO:0006979	0.296064567	PRDX5
intracellular protein transport	GO:0006886	0.297979067	RAMP1, MLPH
Ras signaling pathway	bta04014	0.313838722	RAC1, BAD, VEGFB, PLA2G16
phosphorylation	GO:0016310	0.319526381	EIF2AK1, TRRAP, RPS6KA4
negative regulation of canonical Wnt signaling pathway	GO:0090090	0.320171375	DKK3
microtubule cytoskeleton organization	GO:0000226	0.327839586	MARK2
cytoskeleton organization	GO:0007010	0.335330588	MICAL2
positive regulation of angiogenesis	GO:0045766	0.346117286	VEGFB
regulation of transcription, DNA-templated	GO:0006355	0.346117286	HES6, LRRFIP1, TRRAP, ESRRB, RPS6KA4
negative regulation of neuron apoptotic process	GO:0043524	0.346208239	RETREG1
cytokine-mediated signaling pathway	GO:0019221	0.346208239	BAD
cell population proliferation	GO:0008283	0.348800749	BAD
protein homooligomerization	GO:0051260	0.355635826	ATL3
protein phosphorylation	GO:0006468	0.361892967	EIF2AK1, MARK2, RPS6KA4
nucleic acid phosphodiester bond hydrolysis	GO:0090305	0.364674078	YBEY
actin filament organization	GO:0007015	0.383332794	RAC1
neuron differentiation	GO:0030182	0.3894293	BHLHA15
VEGF signaling pathway	bta04370	0.392542747	RAC1, BAD
Prion disease	bta05020	0.392542747	RAC1, BAD, COX8A, STIP1
rRNA processing	GO:0006364	0.395382334	YBEY
Renal cell carcinoma	bta05211	0.410860535	RAC1, BAD
Acute myeloid leukemia	bta05221	0.410860535	BAD, PER2
cell adhesion	GO:0007155	0.412735773	PARVA, FERMT3
visual perception	GO:0007601	0.423550193	CRYBB1
cellular response to DNA damage stimulus	GO:0006974	0.423550193	OTUB1, MACROD1
Pancreatic cancer	bta05212	0.446427686	RAC1, BAD
positive regulation of cell migration	GO:0030335	0.44669259	FERMT3
protein dephosphorylation	GO:0006470	0.448042357	ILKAP
Wnt signaling pathway	GO:0016055	0.452815188	WWOX

Neurotrophin signaling pathway	bta04722	0.475406878	<i>RAC1, BAD</i>
Hippo signaling pathway - multiple species	bta04392	0.475406878	<i>TEAD1</i>
Selenocompound metabolism	bta00450	0.475406878	<i>SCLY</i>
Colorectal cancer	bta05210	0.475406878	<i>RAC1, BAD</i>
Circadian rhythm	bta04710	0.475406878	<i>PER2</i>
Measles	bta05162	0.475406878	<i>EIF2AK1, BAD</i>
alpha-Linolenic acid metabolism	bta00592	0.475406878	<i>PLA2G16</i>
Histidine metabolism	bta00340	0.475406878	<i>FTCD</i>
Fc gamma R-mediated phagocytosis	bta04666	0.475406878	<i>RAC1, MYO10</i>
Linoleic acid metabolism	bta00591	0.475406878	<i>PLA2G16</i>
Antifolate resistance	bta01523	0.475406878	<i>SLC19A1</i>
Maturity onset diabetes of the young	bta04950	0.475406878	<i>BHLHA15</i>
Mismatch repair	bta03430	0.475406878	<i>PMS2</i>
AGE-RAGE signaling pathway in diabetic complications	bta04933	0.475406878	<i>RAC1, VEGFB</i>
Vitamin digestion and absorption	bta04977	0.475406878	<i>SLC19A1</i>
One carbon pool by folate	bta00670	0.475406878	<i>FTCD</i>
Steroid biosynthesis	bta00100	0.475406878	<i>LSS</i>
Chemical carcinogenesis - reactive oxygen species	bta05208	0.475406878	<i>RAC1, BAD, COX8A</i>
regulation of apoptotic process	GO:0042981	0.477510027	<i>BAD</i>
Hepatitis C	bta05160	0.489744275	<i>EIF2AK1, BAD</i>
MAPK signaling pathway	bta04010	0.489744275	<i>RAC1, VEGFB, RPS6KA4</i>
Non-alcoholic fatty liver disease	bta04932	0.516083131	<i>RAC1, COX8A</i>
positive regulation of apoptotic process	GO:0043065	0.560416042	<i>BAD</i>
Adherens junction	bta04520	0.567860897	<i>RAC1</i>
Endocrine resistance	bta01522	0.567860897	<i>BAD</i>
Non-small cell lung cancer	bta05223	0.567860897	<i>BAD</i>
Peroxisome	bta04146	0.567860897	<i>PRDX5</i>
Diabetic cardiomyopathy	bta05415	0.567860897	<i>RAC1, COX8A</i>
Amyotrophic lateral sclerosis	bta05014	0.567860897	<i>RAC1, BAD, COX8A</i>
Melanoma	bta05218	0.567860897	<i>BAD</i>
Human immunodeficiency virus 1 infection	bta05170	0.567860897	<i>RAC1, BAD</i>
ErbB signaling pathway	bta04012	0.567860897	<i>BAD</i>
Choline metabolism in cancer	bta05231	0.567860897	<i>RAC1</i>
Fc epsilon RI signaling pathway	bta04664	0.567860897	<i>RAC1</i>
EGFR tyrosine kinase inhibitor resistance	bta01521	0.567860897	<i>BAD</i>
Bacterial invasion of epithelial cells	bta05100	0.567860897	<i>RAC1</i>

cAMP signaling pathway	bta04024	0.567860897	<i>RAC1, BAD</i>
Arachidonic acid metabolism	bta00590	0.567860897	<i>PLA2G16</i>
Pathways of neurodegeneration - multiple diseases	bta05022	0.567860897	<i>RAC1, BAD, COX8A</i>
Salmonella infection	bta05132	0.567860897	<i>RAC1, CYTH3</i>
Circadian entrainment	bta04713	0.567860897	<i>PER2</i>
Regulation of lipolysis in adipocytes	bta04923	0.567860897	<i>PLA2G16</i>
Glycerophospholipid metabolism	bta00564	0.567860897	<i>PLA2G16</i>
Viral myocarditis	bta05416	0.567860897	<i>RAC1</i>
Natural killer cell mediated cytotoxicity	bta04650	0.567860897	<i>RAC1</i>
Chronic myeloid leukemia	bta05220	0.567860897	<i>BAD</i>
Fanconi anemia pathway	bta03460	0.567860897	<i>PMS2</i>
Platinum drug resistance	bta01524	0.567860897	<i>BAD</i>
Viral carcinogenesis	bta05203	0.567860897	<i>RAC1, BAD</i>
Pancreatic secretion	bta04972	0.567860897	<i>RAC1</i>
Rap1 signaling pathway	bta04015	0.567860897	<i>RAC1, VEGFB</i>
Chemokine signaling pathway	bta04062	0.567860897	<i>RAC1, BAD</i>
Cardiac muscle contraction	bta04260	0.567860897	<i>COX8A</i>
Lipid and atherosclerosis	bta05417	0.567860897	<i>RAC1, BAD</i>
B cell receptor signaling pathway	bta04662	0.567860897	<i>RAC1</i>
Endometrial cancer	bta05213	0.567860897	<i>BAD</i>
Alzheimer disease	bta05010	0.567860897	<i>BAD, COX8A, RTN3</i>
Herpes simplex virus 1 infection	bta05168	0.567860897	<i>EIF2AK1, BAD</i>
Ether lipid metabolism	bta00565	0.567860897	<i>PLA2G16</i>
Prostate cancer	bta05215	0.567860897	<i>BAD</i>
Toll-like receptor signaling pathway	bta04620	0.567860897	<i>RAC1</i>
RNA splicing	GO:0008380	0.577070045	<i>TFIP11</i>
ubiquitin-dependent protein catabolic process	GO:0006511	0.58501562	<i>USP42</i>
lipid metabolic process	GO:0006629	0.589646009	<i>LSS, NAA40</i>
Osteoclast differentiation	bta04380	0.599096211	<i>RAC1</i>
Toxoplasmosis	bta05145	0.599096211	<i>BAD</i>
TNF signaling pathway	bta04668	0.599096211	<i>RPS6KA4</i>
Sphingolipid signaling pathway	bta04071	0.599096211	<i>RAC1</i>
Pathways in cancer	bta05200	0.599096211	<i>RAC1, BAD, VEGFB</i>
Leukocyte transendothelial migration	bta04670	0.599096211	<i>RAC1</i>
Thyroid hormone signaling pathway	bta04919	0.599429783	<i>BAD</i>
Platelet activation	bta04611	0.599429783	<i>FERMT3</i>

regulation of gene expression	GO:0010468	0.602397582	<i>PCBP3</i>
cell differentiation	GO:0030154	0.602397582	<i>AIMP2, USP42</i>
Autophagy - animal	bta04140	0.605355826	<i>BAD</i>
Vascular smooth muscle contraction	bta04270	0.605355826	<i>RAMP1</i>
Oxidative phosphorylation	bta00190	0.605355826	<i>COX8A</i>
Yersinia infection	bta05135	0.605355826	<i>RAC1</i>
Insulin signaling pathway	bta04910	0.605355826	<i>BAD</i>
Relaxin signaling pathway	bta04926	0.605355826	<i>VEGFB</i>
Ubiquitin mediated proteolysis	bta04120	0.605355826	<i>UBE2F</i>
Phospholipase D signaling pathway	bta04072	0.605355826	<i>CYTH3</i>
Phagosome	bta04145	0.605355826	<i>RAC1</i>
Fluid shear stress and atherosclerosis	bta05418	0.605355826	<i>RAC1</i>
Neutrophil extracellular trap formation	bta04613	0.605355826	<i>RAC1</i>
Apoptosis	bta04210	0.605355826	<i>BAD</i>
proteolysis	GO:0006508	0.607698127	<i>YBEY, OTUB1</i>
Wnt signaling pathway	bta04310	0.608612079	<i>RAC1</i>
Tuberculosis	bta05152	0.608612079	<i>BAD</i>
Hippo signaling pathway	bta04390	0.608612079	<i>TEAD1</i>
Protein processing in endoplasmic reticulum	bta04141	0.608612079	<i>EIF2AK1</i>
Hepatitis B	bta05161	0.608612079	<i>BAD</i>
Hepatocellular carcinoma	bta05225	0.608612079	<i>BAD</i>
Tight junction	bta04530	0.608612079	<i>RAC1</i>
cGMP-PKG signaling pathway	bta04022	0.608612079	<i>BAD</i>
Transcriptional misregulation in cancer	bta05202	0.61235416	<i>PER2</i>
Axon guidance	bta04360	0.61911165	<i>RAC1</i>
Kaposi sarcoma-associated herpesvirus infection	bta05167	0.61911165	<i>RAC1</i>
negative regulation of cell population proliferation	GO:0008285	0.622778883	<i>AIMP2</i>
Epstein-Barr virus infection	bta05169	0.635506945	<i>RAC1</i>
Chemical carcinogenesis - receptor activation	bta05207	0.635822018	<i>BAD</i>
Human cytomegalovirus infection	bta05163	0.652309167	<i>RAC1</i>
Proteoglycans in cancer	bta05205	0.652309167	<i>RAC1</i>
mRNA processing	GO:0006397	0.653038303	<i>TFIP11</i>
Regulation of actin cytoskeleton	bta04810	0.655390051	<i>RAC1</i>
Human T-cell leukemia virus 1 infection	bta05166	0.655390051	<i>TRRAP</i>
Thermogenesis	bta04714	0.676289262	<i>COX8A</i>
Calcium signaling pathway	bta04020	0.680285024	<i>VEGFB</i>

Endocytosis	bta04144	0.680690908	<i>CYTH3</i>
DNA repair	GO:0006281	0.699494006	<i>TRRAP</i>
negative regulation of apoptotic process	GO:0043066	0.703599908	<i>PRDX5</i>
Parkinson disease	bta05012	0.708473994	<i>COX8A</i>
translation	GO:0006412	0.72127071	<i>AIMP2</i>
regulation of catalytic activity	GO:0050790	0.727915429	<i>CCZ1</i>
regulation of transcription by RNA polymerase II	GO:0006357	0.74589163	<i>BHLHA15, RCOR2, ESRRA</i>
Huntington disease	bta05016	0.749268524	<i>COX8A</i>
positive regulation of transcription by RNA polymerase II	GO:0045944	0.783797953	<i>BHLHA15, RPS6KA4</i>
Neuroactive ligand-receptor interaction	bta04080	0.789820246	<i>PRLH</i>
Metabolic pathways	bta01100	0.793508718	<i>FTCD, SCLY, LSS, COX8A, PLA2G16</i>
protein ubiquitination	GO:0016567	0.834590056	<i>ASB1</i>
negative regulation of transcription by RNA polymerase II	GO:0000122	0.882956789	<i>PCBP3</i>
G protein-coupled receptor signaling pathway	GO:0007186	0.884475197	<i>BHLHA15</i>
signal transduction	GO:0007165	0.908758322	<i>PRLH, MYO10</i>

Table S3. Results of functional enrichment analyzes performed in DAVID and GeneCodis for HCW.

Description	Annotation_ID	Pvalue	Genes
DAVID			
Metabolic pathways	bta01100	0.841983307	<i>HLCS, PIGP, CMPK2</i>
GeneCodis			
diphosphoinositol polyphosphate catabolic process	GO:0071544	0.030789778	<i>NUDT3</i>
intestine smooth muscle contraction	GO:0014827	0.030789778	<i>PTGER3</i>
cornea development in camera-type eye	GO:0061303	0.030789778	<i>KERA</i>
negative regulation of gastric acid secretion	GO:0060455	0.030789778	<i>PTGER3</i>
dUDP biosynthetic process	GO:0006227	0.030789778	<i>CMPK2</i>
negative regulation of amacrine cell differentiation	GO:1902870	0.030789778	<i>POU4F2</i>
positive regulation of germinal center formation	GO:0002636	0.030789778	<i>TNFSF13B</i>
RNA decapping	GO:0110154	0.030789778	<i>NUDT3</i>
positive regulation of transforming growth factor beta1 production	GO:0032914	0.030789778	<i>LUM</i>
positive regulation of cell fate commitment	GO:0010455	0.030789778	<i>SPDEF</i>
regulation of retinal ganglion cell axon guidance	GO:0090259	0.030789778	<i>POU4F2</i>

dorsal root ganglion development	GO:1990791	0.036480587	<i>POU4F2</i>
negative regulation of cell fate commitment	GO:0010454	0.036480587	<i>SPDEF</i>
positive regulation of toll-like receptor 7 signaling pathway	GO:0034157	0.036480587	<i>RSAD2</i>
CD4-positive, alpha-beta T cell differentiation	GO:0043367	0.036480587	<i>RSAD2</i>
prostate gland growth	GO:0060736	0.036480587	<i>PLAG1</i>
lung goblet cell differentiation	GO:0060480	0.036480587	<i>SPDEF</i>
peptide cross-linking via chondroitin 4-sulfate glycosaminoglycan	GO:0019800	0.036480587	<i>DCN</i>
dTTP biosynthetic process	GO:0006235	0.036480587	<i>CMPK2</i>
organ growth	GO:0035265	0.036480587	<i>PLAG1</i>
negative regulation of collagen fibril organization	GO:1904027	0.036480587	<i>DCN</i>
positive regulation of dendrite development	GO:1900006	0.036480587	<i>PACSIN1</i>
positive regulation of T-helper 2 cell cytokine production	GO:2000553	0.036480587	<i>RSAD2</i>
positive regulation of glial cell proliferation	GO:0060252	0.036480587	<i>PLAG1</i>
positive regulation of immune response	GO:0050778	0.036480587	<i>RSAD2</i>
diadenosine hexaphosphate catabolic process	GO:1901909	0.036480587	<i>NUDT3</i>
dTDP biosynthetic process	GO:0006233	0.036480587	<i>CMPK2</i>
adenosine 5'-(hexahydrogen pentaphosphate) catabolic process	GO:1901911	0.036480587	<i>NUDT3</i>
B cell costimulation	GO:0031296	0.036480587	<i>TNFSF13B</i>
diphosphoinositol polyphosphate metabolic process	GO:0071543	0.036480587	<i>NUDT3</i>
negative regulation of vascular endothelial growth factor signaling pathway	GO:1900747	0.036480587	<i>DCN</i>
mRNA 5'-splice site recognition	GO:0000395	0.036480587	<i>SNRPC</i>
CD4-positive, alpha-beta T cell activation	GO:0035710	0.036480587	<i>RSAD2</i>
negative regulation of adipose tissue development	GO:1904178	0.036480587	<i>POU4F2</i>
positive regulation of transcription by RNA polymerase II	GO:0045944	0.036480587	<i>DCN, SPDEF, POU4F2, LUM, PLAG1</i>
positive regulation of toll-like receptor 9 signaling pathway	GO:0034165	0.036480587	<i>RSAD2</i>
diadenosine pentaphosphate catabolic process	GO:1901907	0.036480587	<i>NUDT3</i>
positive regulation of mitochondrial depolarization	GO:0051901	0.044346406	<i>DCN</i>
gland morphogenesis	GO:0022612	0.051787783	<i>PLAG1</i>
positive regulation of osteoclast differentiation	GO:0045672	0.05740156	<i>POU4F2</i>
B cell homeostasis	GO:0001782	0.05740156	<i>TNFSF13B</i>
retinal ganglion cell axon guidance	GO:0031290	0.058399709	<i>POU4F2</i>
protein depalmitoylation	GO:0002084	0.058399709	<i>ABHD13</i>
plasma membrane tubulation	GO:0097320	0.058399709	<i>PACSIN1</i>
intracellular estrogen receptor signaling pathway	GO:0030520	0.058399709	<i>POU4F2</i>
nucleoside triphosphate biosynthetic process	GO:0009142	0.058399709	<i>CMPK2</i>
intestinal epithelial cell development	GO:0060576	0.06288528	<i>SPDEF</i>

regulation of endocytosis	GO:0030100	0.06288528	<i>PACSIN1</i>
positive regulation of axon extension	GO:0045773	0.063203516	<i>POU4F2</i>
positive regulation by host of viral transcription	GO:0043923	0.063203516	<i>TAF11</i>
nucleoside monophosphate phosphorylation	GO:0046940	0.063203516	<i>CMPK2</i>
negative regulation of protein secretion	GO:0050709	0.063203516	<i>RSAD2</i>
RNA polymerase II preinitiation complex assembly	GO:0051123	0.063203516	<i>TAF11</i>
T cell costimulation	GO:0031295	0.068153098	<i>TNFSF13B</i>
cilium organization	GO:0044782	0.071606039	<i>TTC29</i>
protein localization to membrane	GO:0072657	0.071606039	<i>PACSIN1</i>
positive regulation of glucose import	GO:0046326	0.072919645	<i>POU4F2</i>
axon extension	GO:0048675	0.072919645	<i>POU4F2</i>
positive regulation of mitochondrial fission	GO:0090141	0.072919645	<i>DCN</i>
positive regulation of macroautophagy	GO:0016239	0.072919645	<i>DCN</i>
mRNA splicing, via spliceosome	GO:0000398	0.072919645	<i>LSM6, SNRPC</i>
negative regulation of endothelial cell migration	GO:0010596	0.072919645	<i>DCN</i>
synaptic vesicle endocytosis	GO:0048488	0.072919645	<i>PACSIN1</i>
nucleoside diphosphate phosphorylation	GO:0006165	0.072919645	<i>CMPK2</i>
positive regulation of transcription initiation from RNA polymerase II promoter	GO:0060261	0.080614528	<i>TAF11</i>
negative regulation of viral genome replication	GO:0045071	0.080614528	<i>RSAD2</i>
cilium movement	GO:0003341	0.080660111	<i>TTC29</i>
mRNA transcription by RNA polymerase II	GO:0042789	0.080660111	<i>TAF11</i>
cellular response to cytokine stimulus	GO:0071345	0.080660111	<i>POU4F2</i>
spliceosomal snRNP assembly	GO:0000387	0.080660111	<i>SNRPC</i>
transcription initiation from RNA polymerase II promoter	GO:0006367	0.084099409	<i>TAF11</i>
regulation of immune response	GO:0050776	0.087432104	<i>TNFSF13B</i>
retina development in camera-type eye	GO:0060041	0.089437432	<i>POU4F2</i>
positive regulation of B cell proliferation	GO:0030890	0.089437432	<i>TNFSF13B</i>
neuromuscular process controlling balance	GO:0050885	0.090140719	<i>POU4F2</i>
GPI anchor biosynthetic process	GO:0006506	0.090140719	<i>PIGP</i>
negative regulation of cell differentiation	GO:0045596	0.090140719	<i>POU4F2</i>
ubiquitin-dependent protein catabolic process	GO:0006511	0.091082646	<i>TTC3, RNF144A</i>
positive regulation of cell differentiation	GO:0045597	0.095992334	<i>POU4F2</i>
neuron projection morphogenesis	GO:0048812	0.097573972	<i>PACSIN1</i>
tumor necrosis factor-mediated signaling pathway	GO:0033209	0.097573972	<i>TNFSF13B</i>
B cell differentiation	GO:0030183	0.099069921	<i>TNFSF13B</i>
phospholipase C-activating G protein-coupled receptor signaling pathway	GO:0007200	0.099069921	<i>PTGER3</i>

positive regulation of T cell proliferation	GO:0042102	0.101682516	<i>TNFSF13B</i>
neuron development	GO:0048666	0.10422444	<i>PACSIN1</i>
protein K48-linked ubiquitination	GO:0070936	0.116348033	<i>TTC3</i>
collagen fibril organization	GO:0030199	0.116348033	<i>LUM</i>
positive regulation of autophagy	GO:0010508	0.117260032	<i>DCN</i>
multicellular organism growth	GO:0035264	0.117260032	<i>PLAG1</i>
positive regulation of phosphatidylinositol 3-kinase signaling	GO:0014068	0.119435953	<i>DCN</i>
response to virus	GO:0009615	0.124979299	<i>RSAD2</i>
cellular response to insulin stimulus	GO:0032869	0.126998992	<i>POU4F2</i>
regulation of transcription, DNA-templated	GO:0006355	0.130885107	<i>SPDEF, POU4F2, HMGA1, PLAG1</i>
axonogenesis	GO:0007409	0.130885107	<i>POU4F2</i>
positive regulation of proteasomal ubiquitin-dependent protein catabolic process	GO:0032436	0.132754795	<i>RNF144A</i>
negative regulation of angiogenesis	GO:0016525	0.134577631	<i>DCN</i>
MAPK cascade	GO:0000165	0.164490813	<i>POU4F2</i>
transcription, DNA-templated	GO:0006351	0.171958862	<i>PLAG1</i>
cellular response to lipopolysaccharide	GO:0071222	0.175660649	<i>CMPK2</i>
sensory perception of sound	GO:0007605	0.175660649	<i>POU4F2</i>
RNA processing	GO:0006396	0.175660649	<i>ZRANB2</i>
peptidyl-tyrosine phosphorylation	GO:0018108	0.182597323	<i>LYN</i>
positive regulation of cytosolic calcium ion concentration	GO:0007204	0.186505909	<i>PTGER3</i>
cytoskeleton organization	GO:0007010	0.187515566	<i>PACSIN1</i>
axon guidance	GO:0007411	0.191261776	<i>POU4F2</i>
adenylate cyclase-activating G protein-coupled receptor signaling pathway	GO:0007189	0.200336399	<i>PTGER3</i>
actin filament organization	GO:0007015	0.222327464	<i>PACSIN1</i>
neuron differentiation	GO:0030182	0.225451762	<i>POU4F2</i>
protein polyubiquitination	GO:0000209	0.236111255	<i>RNF144A</i>
protein ubiquitination	GO:0016567	0.238457242	<i>TTC3, RNF144A</i>
visual perception	GO:0007601	0.246652733	<i>LUM</i>
defense response to virus	GO:0051607	0.258898098	<i>RSAD2</i>
heart development	GO:0007507	0.268378744	<i>POU4F2</i>
negative regulation of gene expression	GO:0010629	0.275255906	<i>PLAG1</i>
protein phosphorylation	GO:0006468	0.282671977	<i>TAF11, LYN</i>
negative regulation of transcription by RNA polymerase II	GO:0000122	0.294459392	<i>SPDEF, POU4F2</i>
endocytosis	GO:0006897	0.30114504	<i>PACSIN1</i>
positive regulation of apoptotic process	GO:0043065	0.332124359	<i>SPDEF</i>
RNA splicing	GO:0008380	0.343469696	<i>LSM6</i>

immune response	GO:0006955	0.379341101	<i>TNFSF13B</i>
inflammatory response	GO:0006954	0.38920512	<i>PTGER3</i>
intracellular protein transport	GO:0006886	0.402263788	<i>DSCR3</i>
mRNA processing	GO:0006397	0.406041012	<i>LSM6</i>
Legionellosis	bta05134	0.429274416	<i>APAF1</i>
Hepatitis C	bta05160	0.429274416	<i>RSAD2, APAF1</i>
Lipid and atherosclerosis	bta05417	0.429274416	<i>LYN, APAF1</i>
Biosynthesis of cofactors	bta01240	0.429274416	<i>SDR16C5, CMPK2</i>
TGF-beta signaling pathway	bta04350	0.429274416	<i>DCN</i>
Intestinal immune network for IgA production	bta04672	0.429274416	<i>TNFSF13B</i>
Apoptosis - multiple species	bta04215	0.429274416	<i>APAF1</i>
Biotin metabolism	bta00780	0.429274416	<i>HLCS</i>
GABAergic synapse	bta04727	0.429274416	<i>KCNJ6</i>
Ribosome	bta03010	0.429274416	<i>RPS20, RPS10</i>
Long-term depression	bta04730	0.429274416	<i>LYN</i>
Progesterone-mediated oocyte maturation	bta04914	0.429274416	<i>MOS</i>
Circadian entrainment	bta04713	0.429274416	<i>KCNJ6</i>
Fc gamma R-mediated phagocytosis	bta04666	0.429274416	<i>LYN</i>
Small cell lung cancer	bta05222	0.429274416	<i>APAF1</i>
p53 signaling pathway	bta04115	0.429274416	<i>APAF1</i>
GnRH secretion	bta04929	0.429274416	<i>KCNJ6</i>
Rheumatoid arthritis	bta05323	0.429274416	<i>TNFSF13B</i>
Basal transcription factors	bta03022	0.429274416	<i>TAF11</i>
NF-kappa B signaling pathway	bta04064	0.429274416	<i>LYN, TNFSF13B</i>
RNA degradation	bta03018	0.429274416	<i>LSM6</i>
Glycosylphosphatidylinositol (GPI)-anchor biosynthesis	bta00563	0.429274416	<i>PIGP</i>
Spliceosome	bta03040	0.429274416	<i>LSM6, SNRPC</i>
Influenza A	bta05164	0.429274416	<i>RSAD2, APAF1</i>
Epstein-Barr virus infection	bta05169	0.429274416	<i>LYN, APAF1</i>
Pyrimidine metabolism	bta00240	0.429274416	<i>CMPK2</i>
Regulation of lipolysis in adipocytes	bta04923	0.429274416	<i>PTGER3</i>
B cell receptor signaling pathway	bta04662	0.429274416	<i>LYN</i>
Retinol metabolism	bta00830	0.429274416	<i>SDR16C5</i>
Fc epsilon RI signaling pathway	bta04664	0.429274416	<i>LYN</i>
Coronavirus disease - COVID-19	bta05171	0.429274416	<i>RPS20, RPS10</i>
Morphine addiction	bta05032	0.429274416	<i>KCNJ6</i>

Proteoglycans in cancer	bta05205	0.429274416	<i>DCN, LUM</i>
Platinum drug resistance	bta01524	0.429274416	<i>APAF1</i>
immune system process	GO:0002376	0.433008067	<i>RSAD2</i>
innate immune response	GO:0045087	0.433008067	<i>RSAD2</i>
positive regulation of gene expression	GO:0010628	0.433008067	<i>PLAG1</i>
translation	GO:0006412	0.45941834	<i>RPS20</i>
Serotonergic synapse	bta04726	0.463845565	<i>KCNJ6</i>
Estrogen signaling pathway	bta04915	0.46701763	<i>KCNJ6</i>
Cholinergic synapse	bta04725	0.46701763	<i>KCNJ6</i>
Dopaminergic synapse	bta04728	0.46701763	<i>KCNJ6</i>
Platelet activation	bta04611	0.46701763	<i>LYN</i>
Oocyte meiosis	bta04114	0.46701763	<i>MOS</i>
Apoptosis	bta04210	0.46701763	<i>APAF1</i>
Measles	bta05162	0.46701763	<i>APAF1</i>
Cell adhesion molecules	bta04514	0.470669454	<i>NEGR1</i>
Oxytocin signaling pathway	bta04921	0.476946092	<i>KCNJ6</i>
Retrograde endocannabinoid signaling	bta04723	0.476946092	<i>KCNJ6</i>
Hepatitis B	bta05161	0.477025152	<i>APAF1</i>
Tuberculosis	bta05152	0.494446392	<i>APAF1</i>
Kaposi sarcoma-associated herpesvirus infection	bta05167	0.498931452	<i>LYN</i>
Chemokine signaling pathway	bta04062	0.498931452	<i>LYN</i>
Viral carcinogenesis	bta05203	0.498931452	<i>LYN</i>
Pathways in cancer	bta05200	0.515716363	<i>PTGER3, APAF1</i>
Human cytomegalovirus infection	bta05163	0.537665334	<i>PTGER3</i>
cAMP signaling pathway	bta04024	0.540419248	<i>PTGER3</i>
Regulation of actin cytoskeleton	bta04810	0.540419248	<i>MOS</i>
Calcium signaling pathway	bta04020	0.560932	<i>PTGER3</i>
regulation of transcription by RNA polymerase II	GO:0006357	0.564988524	<i>SPDEF, POU4F2</i>
Parkinson disease	bta05012	0.579615808	<i>APAF1</i>
Cytokine-cytokine receptor interaction	bta04060	0.579615808	<i>TNFSF13B</i>
Prion disease	bta05020	0.579615808	<i>APAF1</i>
Herpes simplex virus 1 infection	bta05168	0.58167393	<i>APAF1</i>
phosphorylation	GO:0016310	0.60068181	<i>LYN</i>
Huntington disease	bta05016	0.604209293	<i>APAF1</i>
Metabolic pathways	bta01100	0.605962621	<i>SDR16C5, PIGP, CMPK2, HLCS</i>
cell differentiation	GO:0030154	0.613300673	<i>SPDEF</i>

transmembrane transport	GO:0055085	0.613300673	<i>SLC10A7</i>
Neuroactive ligand-receptor interaction	bta04080	0.636928604	<i>PTGER3</i>
Amyotrophic lateral sclerosis	bta05014	0.637091457	<i>APAF1</i>
G protein-coupled receptor signaling pathway	GO:0007186	0.644913285	<i>PTGER3</i>
Alzheimer disease	bta05010	0.657065871	<i>APAF1</i>
Pathways of neurodegeneration - multiple diseases	bta05022	0.724601354	<i>APAF1</i>
signal transduction	GO:0007165	0.857006549	<i>PTGER3</i>

Table S4. Results of functional enrichment analyzes performed in DAVID and GeneCodis for SF.

Description	Annotation_ID	Pvalue	Genes
DAVID			
Taste transduction	bta04742	3.89E-12	<i>TAS2R7, T2R12, BOTA-T2R10B, TAS2R42, LOC100140395, TAS2R10, TAS2R46, LOC782957, T2R10C</i>
detection of chemical stimulus involved in sensory perception of bitter taste	GO:0001580	1.18E-06	<i>T2R12, BOTA-T2R10B, TAS2R10, LOC782957, T2R10C</i>
sensory perception of taste	GO:0050909	0.001522184	<i>T2R65A, TAS2R42, TAS2R46</i>
cell surface receptor signaling pathway	GO:0007166	0.021852938	<i>ADGRF2, ADGRF1, ADGRF4, ADGRF5</i>
transcription, DNA-templated	GO:0006351	0.420848987	<i>MED22, MYOD1, PPARGC1A, ETV6</i>
cell differentiation	GO:0030154	0.059457963	<i>SNAPC4, STYK1, USH1C, ETV6</i>
regulation of transcription from RNA polymerase II promoter	GO:0006357	0.069879696	<i>MED22, SNAPC4, ETV6, RUNX1</i>
regulation of cell proliferation	GO:0042127	0.111204588	<i>STYK1, DBH, TNFRSF21</i>
oxidation-reduction process	GO:0055114	0.350875791	<i>GLRX3, CYP2E1, DBH</i>
Metabolic pathways	bta01100	0.490273587	<i>INPP5E, SARDH, CYP2E1, DBH, PIK3C2A, AGPAT2, ABO</i>
positive regulation of transcription from RNA polymerase II promoter	GO:0045944	0.66808279	<i>LHX3, MYOD1, PPARGC1A</i>
GeneCodis			
sensory perception of taste	GO:0050909	4.31E-10	<i>TAS2R10, TAS2R42, T2R65A, TAS2R46, T2R10C, T2R12, BOTA-T2R10B</i>

detection of chemical stimulus involved in sensory perception of bitter taste	GO:0001580	1.49E-09	<i>TAS2R10, T2R65A, TAS2R46, T2R10C, T2R12, BOTA-T2R10B</i>
Taste transduction	bta04742	3.87E-09	<i>TAS2R10, TAS2R7, TAS2R42, TAS2R8, T2R65A, TAS2R46, T2R10C, T2R12, BOTA-T2R10B</i>
G protein-coupled receptor signaling pathway	GO:0007186	4.99E-05	<i>TAS2R10, ADGRF1, TAS2R42, T2R65A, TAS2R46, ADGRF2, T2R10C, ADGRF5, T2R12, BOTA-T2R10B, ADGRF4</i>
response to stimulus	GO:0050896	8.84E-05	<i>TAS2R10, TAS2R42, T2R65A, TAS2R46, T2R10C, T2R12, BOTA-T2R10B</i>
cell surface receptor signaling pathway	GO:0007166	0.010108139	<i>ADGRF1, ADGRF2, ADGRF5, ADGRF4</i>
skeletal muscle tissue regeneration	GO:0043403	0.023398156	<i>MYMK, MYOD1</i>
myoblast fusion	GO:0007520	0.023398156	<i>MYMK, MYOD1</i>
positive regulation of developmental process	GO:0051094	0.053985898	<i>RUNX1</i>
negative regulation of myoblast proliferation	GO:2000818	0.053985898	<i>MYOD1</i>
positive regulation of skeletal muscle hypertrophy	GO:1904206	0.053985898	<i>MYMK</i>
myoblast fate determination	GO:0007518	0.053985898	<i>MYOD1</i>
plasma membrane fusion	GO:0045026	0.053985898	<i>MYMK</i>
positive regulation of snRNA transcription by RNA polymerase II	GO:1905382	0.053985898	<i>MYOD1</i>
synaptonemal complex organization	GO:0070193	0.053985898	<i>SYCE1</i>
negative regulation of interleukin-5 production	GO:0032714	0.053985898	<i>TNFRSF21</i>
negative regulation of interleukin-13 production	GO:0032696	0.053985898	<i>TNFRSF21</i>
oligodendrocyte apoptotic process	GO:0097252	0.057460876	<i>TNFRSF21</i>
protein processing involved in protein targeting to mitochondrion	GO:0006627	0.057460876	<i>PMPCA</i>
ventral spinal cord interneuron specification	GO:0021521	0.057460876	<i>LHX3</i>
medial motor column neuron differentiation	GO:0021526	0.057460876	<i>LHX3</i>
brush border assembly	GO:1904970	0.057460876	<i>USH1C</i>
positive regulation of ATP biosynthetic process	GO:2001171	0.057460876	<i>PPARGC1A</i>
positive regulation of organelle organization	GO:0010638	0.057460876	<i>SURF4</i>
cellular response to oxygen levels	GO:0071453	0.057460876	<i>MYOD1</i>
positive regulation of phospholipid biosynthetic process	GO:0071073	0.057460876	<i>ADGRF5</i>
skeletal muscle fiber adaptation	GO:0043503	0.057460876	<i>MYOD1</i>
vitellogenesis	GO:0007296	0.057460876	<i>ETV6</i>

mesenchymal cell apoptotic process	GO:0097152	0.057460876	<i>ETV6</i>
protein localization to microvillus	GO:1904106	0.057460876	<i>USH1C</i>
octopamine biosynthetic process	GO:0006589	0.057460876	<i>DBH</i>
positive regulation of muscle cell differentiation	GO:0051149	0.05864026	<i>MYOD1</i>
dopamine catabolic process	GO:0042420	0.05864026	<i>DBH</i>
positive regulation of mitochondrion organization	GO:0010822	0.05864026	<i>PPARGC1A</i>
myotube differentiation involved in skeletal muscle regeneration	GO:0014908	0.05864026	<i>MYOD1</i>
positive regulation of skeletal muscle tissue regeneration	GO:0043415	0.05864026	<i>MYOD1</i>
regulation of lipid transport	GO:0032368	0.05864026	<i>SURF4</i>
regulation of oligodendrocyte differentiation	GO:0048713	0.05864026	<i>TNFRSF21</i>
negative regulation of protein localization to cilium	GO:1903565	0.05864026	<i>INPP5E</i>
myeloid leukocyte differentiation	GO:0002573	0.05864026	<i>RUNX1</i>
positive regulation of granulocyte differentiation	GO:0030854	0.05864026	<i>RUNX1</i>
epoxygenase P450 pathway	GO:0019373	0.05864026	<i>CYP2E1</i>
myotube cell development	GO:0014904	0.05864026	<i>MYOD1</i>
response to ATP	GO:0033198	0.05864026	<i>KCNJ11</i>
myoblast fusion involved in skeletal muscle regeneration	GO:0014905	0.05864026	<i>MYMK</i>
signal transduction	GO:0007165	0.060817511	<i>TAS2R10, TNFRSF21, TAS2R42, T2R65A, TAS2R46, T2R10C, T2R12, BOTA-T2R10B</i>
positive regulation of protein localization to cilium	GO:1903566	0.063570842	<i>ENTR1</i>
B cell apoptotic process	GO:0001783	0.063570842	<i>TNFRSF21</i>
protein exit from endoplasmic reticulum	GO:0032527	0.063570842	<i>SEC16A</i>
spinal cord motor neuron cell fate specification	GO:0021520	0.063570842	<i>LHX3</i>
energy reserve metabolic process	GO:0006112	0.063570842	<i>ADGRF5</i>
negative regulation of interleukin-10 production	GO:0032693	0.063570842	<i>TNFRSF21</i>
negative regulation of chromatin binding	GO:0035562	0.063570842	<i>MYOD1</i>
catecholamine biosynthetic process	GO:0042423	0.063570842	<i>DBH</i>
norepinephrine biosynthetic process	GO:0042421	0.063570842	<i>DBH</i>
Golgi organization	GO:0007030	0.064517671	<i>SEC16A, SURF4</i>
response to muscle activity	GO:0014850	0.071363399	<i>PPARGC1A</i>
regulation of microvillus length	GO:0032532	0.071363399	<i>USH1C</i>
negative regulation of myelination	GO:0031642	0.071363399	<i>TNFRSF21</i>
negative regulation of B cell proliferation	GO:0030889	0.071363399	<i>TNFRSF21</i>
protein localization to endoplasmic reticulum exit site	GO:0070973	0.071363399	<i>SEC16A</i>
cellular response to tumor necrosis factor	GO:0071356	0.072930206	<i>TNFRSF21, MYOD1</i>

myotube differentiation	GO:0014902	0.07768367	<i>MYOD1</i>
negative regulation of macrophage activation	GO:0043031	0.07768367	<i>ADGRF5</i>
myoblast differentiation	GO:0045445	0.07768367	<i>MYOD1</i>
COPII vesicle coating	GO:0048208	0.07768367	<i>SEC16A</i>
positive regulation of binding	GO:0051099	0.07768367	<i>MYOD1</i>
negative regulation of appetite	GO:0032099	0.085268513	<i>NUCB2</i>
striated muscle cell differentiation	GO:0051146	0.085268513	<i>MYOD1</i>
negative regulation of cardiac muscle hypertrophy	GO:0010614	0.085268513	<i>GLRX3</i>
pharyngeal arch artery morphogenesis	GO:0061626	0.085268513	<i>ADGRF5</i>
spinal cord association neuron differentiation	GO:0021527	0.089563687	<i>LHX3</i>
synaptonemal complex assembly	GO:0007130	0.089563687	<i>SYCE1</i>
inositol phosphate dephosphorylation	GO:0046855	0.089563687	<i>INPP5E</i>
positive regulation of skeletal muscle fiber development	GO:0048743	0.089563687	<i>MYOD1</i>
glomerular filtration	GO:0003094	0.089563687	<i>ADGRF5</i>
positive regulation of CREB transcription factor activity	GO:0032793	0.089563687	<i>ADGRF1</i>
regulation of ion transmembrane transport	GO:0034765	0.094105538	<i>KCNJ11, KCNC1</i>
cellular response to glucocorticoid stimulus	GO:0071385	0.095192157	<i>MYOD1</i>
organic acid metabolic process	GO:0006082	0.095192157	<i>CYP2E1</i>
regulation of the force of heart contraction	GO:0002026	0.095192157	<i>GLRX3</i>
surfactant homeostasis	GO:0043129	0.095192157	<i>ADGRF5</i>
positive regulation of cilium assembly	GO:0045724	0.095192157	<i>ENTR1</i>
negative regulation of insulin secretion	GO:0046676	0.095192157	<i>KCNJ11</i>
cellular response to estradiol stimulus	GO:0071392	0.095192157	<i>MYOD1</i>
positive regulation of myoblast fusion	GO:1901741	0.095192157	<i>MYOD1</i>
lipoprotein transport	GO:0042953	0.095192157	<i>SURF4</i>
negative regulation of protein secretion	GO:0050709	0.095192157	<i>SERGEF</i>
pituitary gland development	GO:0021983	0.095192157	<i>LHX3</i>
hematopoietic stem cell proliferation	GO:0071425	0.095192157	<i>ETV6</i>
neuron differentiation	GO:0030182	0.102865124	<i>RUNX1, LHX3</i>
potassium ion transmembrane transport	GO:0071805	0.1076918	<i>KCNJ11, KCNC1</i>
maturation of LSU-rRNA	GO:0000470	0.1076918	<i>RPL7A</i>
ribosomal small subunit biogenesis	GO:0042274	0.1076918	<i>SURF6</i>
negative regulation of T cell proliferation	GO:0042130	0.1076918	<i>TNFRSF21</i>
positive regulation of transcription, DNA-templated	GO:0045893	0.112555715	<i>RUNX1, LHX3, PPARGC1A, MYOD1</i>
positive regulation of myoblast differentiation	GO:0045663	0.112816031	<i>MYOD1</i>
erythrocyte development	GO:0048821	0.112816031	<i>ADGRF5</i>

potassium ion transport	GO:0006813	0.114507342	<i>KCNJ11, KCNC1</i>
motor neuron axon guidance	GO:0008045	0.117597424	<i>LHX3</i>
synapse assembly	GO:0007416	0.117597424	<i>ADGRF1</i>
skeletal muscle fiber development	GO:0048741	0.120892367	<i>MYOD1</i>
protein import into mitochondrial matrix	GO:0030150	0.120892367	<i>DNLZ</i>
phosphatidylinositol dephosphorylation	GO:0046856	0.120892367	<i>INPP5E</i>
negative regulation of neuron death	GO:1901215	0.120892367	<i>PPARGC1A</i>
positive regulation of interleukin-2 production	GO:0032743	0.122773957	<i>RUNX1</i>
respiratory electron transport chain	GO:0022904	0.122773957	<i>PPARGC1A</i>
phosphatidylinositol metabolic process	GO:0046488	0.122773957	<i>INPP5E</i>
intracellular transport	GO:0046907	0.122773957	<i>SEC16A</i>
humoral immune response	GO:0006959	0.122773957	<i>TNFRSF21</i>
cell differentiation	GO:0030154	0.127058933	<i>LHX3, ETV6, USH1C, MYOD1</i>
sialylation	GO:0097503	0.127823626	<i>ST8SIA4</i>
ribosomal large subunit biogenesis	GO:0042273	0.13342941	<i>SURF6</i>
regulation of transcription, DNA-templated	GO:0006355	0.13342941	<i>RUNX1, LHX3, ETV6, PPARGC1A, MYOD1, DNLZ</i>
positive regulation of transcription by RNA polymerase II	GO:0045944	0.13342941	<i>RUNX1, LHX3, ETV6, PPARGC1A, MYOD1</i>
energy homeostasis	GO:0097009	0.134958308	<i>PPARGC1A</i>
skeletal muscle tissue development	GO:0007519	0.134958308	<i>MYOD1</i>
regulation of cell differentiation	GO:0045595	0.134958308	<i>RUNX1</i>
endoplasmic reticulum organization	GO:0007029	0.135949095	<i>SEC16A</i>
regulation of insulin secretion	GO:0050796	0.135949095	<i>KCNJ11</i>
dorsal/ventral pattern formation	GO:0009953	0.135949095	<i>LHX3</i>
placenta development	GO:0001890	0.135949095	<i>LHX3</i>
skeletal muscle cell differentiation	GO:0035914	0.135949095	<i>MYOD1</i>
potassium ion import across plasma membrane	GO:1990573	0.140145338	<i>KCNJ11</i>
nuclear-transcribed mRNA catabolic process, nonsense-mediated decay	GO:0000184	0.140145338	<i>MAGOHB</i>
carbohydrate transport	GO:0008643	0.144181218	<i>SLC2A6</i>
neuron apoptotic process	GO:0051402	0.144181218	<i>TNFRSF21</i>
regulation of cytokinesis	GO:0032465	0.146916578	<i>ENTR1</i>
histone H4 acetylation	GO:0043967	0.146916578	<i>MYOD1</i>
inner ear development	GO:0048839	0.146916578	<i>LHX3</i>
regulation of lipid metabolic process	GO:0019216	0.150643142	<i>ADGRF5</i>
histone H3 acetylation	GO:0043966	0.150643142	<i>MYOD1</i>

muscle organ development	GO:0007517	0.154232233	<i>MYOD1</i>
memory	GO:0007613	0.154232233	<i>ADGRF1</i>
phospholipid biosynthetic process	GO:0008654	0.157690066	<i>AGPAT2</i>
neurogenesis	GO:0022008	0.157690066	<i>ETV6</i>
myelination	GO:0042552	0.166632622	<i>TNFRSF21</i>
xenobiotic metabolic process	GO:0006805	0.166632622	<i>CYP2E1</i>
chondrocyte differentiation	GO:0002062	0.17097055	<i>RUNX1</i>
hemopoiesis	GO:0030097	0.17522227	<i>RUNX1</i>
anatomical structure development	GO:0048856	0.178117462	<i>MYOD1</i>
regulation of RNA splicing	GO:0043484	0.178117462	<i>MYOD1</i>
glucose metabolic process	GO:0006006	0.179652428	<i>KCNJ11</i>
fat cell differentiation	GO:0045444	0.179652428	<i>ADGRF5</i>
T cell receptor signaling pathway	GO:0050852	0.179652428	<i>TNFRSF21</i>
regulation of circadian rhythm	GO:0042752	0.182342958	<i>PPARGC1A</i>
lipid homeostasis	GO:0055088	0.182342958	<i>SURF4</i>
nervous system process	GO:0050877	0.184938801	<i>KCNJ11</i>
regulation of alternative mRNA splicing, via spliceosome	GO:0000381	0.184938801	<i>MYOD1</i>
response to xenobiotic stimulus	GO:0009410	0.18870185	<i>KCNJ11</i>
cellular response to starvation	GO:0009267	0.192393231	<i>MYOD1</i>
meiotic cell cycle	GO:0051321	0.196014459	<i>SYCE1</i>
circadian regulation of gene expression	GO:0032922	0.20438818	<i>PPARGC1A</i>
cellular response to oxidative stress	GO:0034599	0.217297339	<i>PPARGC1A</i>
mRNA transport	GO:0051028	0.239068531	<i>MAGOHB</i>
cell division	GO:0051301	0.241681719	<i>SYCE1, ENTR1</i>
regulation of transcription by RNA polymerase II	GO:0006357	0.243305414	<i>RUNX1, LHX3, ETV6, MYOD1, MED22</i>
ossification	GO:0001503	0.243305414	<i>RUNX1</i>
vesicle-mediated transport	GO:0016192	0.243305414	<i>SEC16A, CACFD1</i>
transcription, DNA-templated	GO:0006351	0.257859412	<i>MYOD1</i>
regulation of membrane potential	GO:0042391	0.259341523	<i>KCNJ11</i>
mitochondrion organization	GO:0007005	0.259341523	<i>PPARGC1A</i>
positive regulation of DNA-binding transcription factor activity	GO:0051091	0.259341523	<i>PPARGC1A</i>
protein transport	GO:0015031	0.259341523	<i>SEC16A, ENTR1, SURF4</i>
rhythmic process	GO:0048511	0.259341523	<i>PPARGC1A</i>
neuron projection development	GO:0031175	0.259341523	<i>ADGRF1</i>
sensory perception of sound	GO:0007605	0.259341523	<i>USH1C</i>

ribosome biogenesis	GO:0042254	0.28187716	<i>RPL7A</i>
protein localization to plasma membrane	GO:0072659	0.288043354	<i>SEC16A</i>
glucose homeostasis	GO:0042593	0.290212425	<i>ADGRF5</i>
negative regulation of neuron apoptotic process	GO:0043524	0.290629692	<i>PPARGC1A</i>
adaptive immune response	GO:0002250	0.290629692	<i>TNFRSF21</i>
adenylate cyclase-activating G protein-coupled receptor signaling pathway	GO:0007189	0.296469557	<i>ADGRF1</i>
protein homooligomerization	GO:0051260	0.298474547	<i>KCNC1</i>
regulation of catalytic activity	GO:0050790	0.303329817	<i>GPSM1, SERGEF</i>
cell projection organization	GO:0030030	0.305996551	<i>ENTR1</i>
protein folding	GO:0006457	0.349760084	<i>DNLZ</i>
cell cycle	GO:0007049	0.368894237	<i>SYCE1, ENTR1</i>
autophagy	GO:0006914	0.37551901	<i>SEC16A</i>
protein stabilization	GO:0050821	0.386175333	<i>DNLZ</i>
fatty acid metabolic process	GO:0006631	0.393398302	<i>CYP2E1</i>
regulation of apoptotic process	GO:0042981	0.412495293	<i>CARD9</i>
protein glycosylation	GO:0006486	0.424947734	<i>ST8SIA4</i>
mRNA splicing, via spliceosome	GO:0000398	0.428392102	<i>MAGOHB</i>
endocytosis	GO:0006897	0.440184452	<i>SURF4</i>
lipid metabolic process	GO:0006629	0.478214029	<i>CYP2E1, AGPAT2</i>
carbohydrate metabolic process	GO:0005975	0.478214029	<i>ABO</i>
transmembrane transport	GO:0055085	0.488117094	<i>SLC2A6, KCNC1</i>
RNA splicing	GO:0008380	0.490640618	<i>MAGOHB</i>
ion transport	GO:0006811	0.49965567	<i>KCNJ11, KCNC1</i>
regulation of gene expression	GO:0010468	0.518693678	<i>MYOD1</i>
mRNA processing	GO:0006397	0.572211044	<i>MAGOHB</i>
negative regulation of apoptotic process	GO:0043066	0.624525543	<i>LHX3</i>
translation	GO:0006412	0.642073478	<i>RPS13</i>
Alcoholic liver disease	bta04936	0.697097309	<i>CYP2E1, PPARGC1A</i>
Arachidonic acid metabolism	bta00590	0.697097309	<i>CYP2E1</i>
Th1 and Th2 cell differentiation	bta04658	0.697097309	<i>NOTCH1</i>
Drug metabolism - other enzymes	bta00983	0.697097309	<i>CYP2E1</i>
Notch signaling pathway	bta04330	0.697097309	<i>NOTCH1</i>
Longevity regulating pathway	bta04211	0.697097309	<i>PPARGC1A</i>
Fc gamma R-mediated phagocytosis	bta04666	0.697097309	<i>VAV2</i>
T cell receptor signaling pathway	bta04660	0.697097309	<i>VAV2</i>
Cocaine addiction	bta05030	0.697097309	<i>GPSM1</i>

Chronic myeloid leukemia	bta05220	0.697097309	<i>RUNX1</i>
Type II diabetes mellitus	bta04930	0.697097309	<i>KCNJ11, ABCC8</i>
GnRH secretion	bta04929	0.697097309	<i>KCNJ11</i>
Bacterial invasion of epithelial cells	bta05100	0.697097309	<i>CD2AP</i>
Th17 cell differentiation	bta04659	0.697097309	<i>RUNX1</i>
Glycerolipid metabolism	bta00561	0.697097309	<i>AGPAT2</i>
Drug metabolism - cytochrome P450	bta00982	0.697097309	<i>CYP2E1</i>
Tight junction	bta04530	0.697097309	<i>RUNX1, YBX3</i>
B cell receptor signaling pathway	bta04662	0.697097309	<i>VAV2</i>
Protein digestion and absorption	bta04974	0.697097309	<i>MEP1A</i>
mRNA surveillance pathway	bta03015	0.697097309	<i>MAGOHB</i>
ABC transporters	bta02010	0.697097309	<i>ABCC8</i>
C-type lectin receptor signaling pathway	bta04625	0.697097309	<i>CARD9</i>
Ribosome	bta03010	0.697097309	<i>RPL7A, RPS13</i>
Adipocytokine signaling pathway	bta04920	0.697097309	<i>PPARGC1A</i>
Phosphatidylinositol signaling system	bta04070	0.697097309	<i>INPP5E, PIK3C2A</i>
Endocrine resistance	bta01522	0.697097309	<i>NOTCH1</i>
Glycerophospholipid metabolism	bta00564	0.697097309	<i>AGPAT2</i>
Fc epsilon RI signaling pathway	bta04664	0.697097309	<i>VAV2</i>
Leukocyte transendothelial migration	bta04670	0.697097309	<i>VAV2</i>
Glycine, serine and threonine metabolism	bta00260	0.697097309	<i>SARDH</i>
Transcriptional misregulation in cancer	bta05202	0.697097309	<i>RUNX1, ETV6</i>
Tyrosine metabolism	bta00350	0.697097309	<i>DBH</i>
MicroRNAs in cancer	bta05206	0.697097309	<i>NOTCH1, MIR126</i>
Metabolism of xenobiotics by cytochrome P450	bta00980	0.697097309	<i>CYP2E1</i>
Natural killer cell mediated cytotoxicity	bta04650	0.697097309	<i>VAV2</i>
Fat digestion and absorption	bta04975	0.697097309	<i>AGPAT2</i>
Glucagon signaling pathway	bta04922	0.697097309	<i>PPARGC1A</i>
Inositol phosphate metabolism	bta00562	0.697097309	<i>INPP5E, PIK3C2A</i>
Nucleocytoplasmic transport	bta03013	0.697097309	<i>MAGOHB</i>
Coronavirus disease - COVID-19	bta05171	0.697097309	<i>RPL7A, RPS13</i>
Acute myeloid leukemia	bta05221	0.697097309	<i>RUNX1</i>
Glycosphingolipid biosynthesis - lacto and neolacto series	bta00601	0.697097309	<i>ABO</i>
Steroid hormone biosynthesis	bta00140	0.697097309	<i>CYP2E1</i>
Insulin resistance	bta04931	0.697097309	<i>PPARGC1A</i>
Linoleic acid metabolism	bta00591	0.697097309	<i>CYP2E1</i>

Insulin secretion	bta04911	0.697097309	<i>KCNJ11, ABCC8</i>
Chemical carcinogenesis - DNA adducts	bta05204	0.697097309	<i>CYP2E1</i>
apoptotic process	GO:0006915	0.698868571	<i>TNFRSF21</i>
Thyroid hormone signaling pathway	bta04919	0.70040114	<i>NOTCH1</i>
AMPK signaling pathway	bta04152	0.70040114	<i>PPARGC1A</i>
Yersinia infection	bta05135	0.71088575	<i>VAV2</i>
Spliceosome	bta03040	0.71088575	<i>MAGOHB</i>
Apelin signaling pathway	bta04371	0.71088575	<i>PPARGC1A</i>
Insulin signaling pathway	bta04910	0.71088575	<i>PPARGC1A</i>
Phospholipase D signaling pathway	bta04072	0.712795388	<i>AGPAT2</i>
Spinocerebellar ataxia	bta05017	0.712795388	<i>MYOD1</i>
NOD-like receptor signaling pathway	bta04621	0.712795388	<i>CARD9</i>
Breast cancer	bta05224	0.712795388	<i>NOTCH1</i>
Non-alcoholic fatty liver disease	bta04932	0.712795388	<i>CYP2E1</i>
Tuberculosis	bta05152	0.72456931	<i>CARD9</i>
Protein processing in endoplasmic reticulum	bta04141	0.72456931	<i>SEL1L</i>
Chemokine signaling pathway	bta04062	0.741058727	<i>VAV2</i>
Metabolic pathways	bta01100	0.741058727	<i>DBH, INPP5E, ABO, CYP2E1, PIK3C2A, AGPAT2, SARDH</i>
Focal adhesion	bta04510	0.74291576	<i>VAV2</i>
cAMP signaling pathway	bta04024	0.74291576	<i>VAV2</i>
Proteoglycans in cancer	bta05205	0.74291576	<i>VAV2</i>
Chemical carcinogenesis - reactive oxygen species	bta05208	0.74291576	<i>CYP2E1</i>
Regulation of actin cytoskeleton	bta04810	0.74291576	<i>VAV2</i>
Rap1 signaling pathway	bta04015	0.74291576	<i>VAV2</i>
Lipid and atherosclerosis	bta05417	0.74291576	<i>VAV2</i>
Thermogenesis	bta04714	0.752700297	<i>PPARGC1A</i>
Salmonella infection	bta05132	0.762804875	<i>PIK3C2A</i>
Cytokine-cytokine receptor interaction	bta04060	0.768358662	<i>TNFRSF21</i>
Prion disease	bta05020	0.768358662	<i>NOTCH1</i>
Pathways in cancer	bta05200	0.768358662	<i>NOTCH1, RUNX1</i>
Herpes simplex virus 1 infection	bta05168	0.769185481	<i>CARD9</i>
Huntington disease	bta05016	0.787902101	<i>PPARGC1A</i>
Human papillomavirus infection	bta05165	0.798839114	<i>NOTCH1</i>
proteolysis	GO:0006508	0.807775542	<i>PMPCA</i>
negative regulation of transcription by RNA polymerase II	GO:0000122	0.823303867	<i>ETV6</i>

Table S5. Results of functional enrichment analyzes performed in DAVID and GeneCodis for MARB.

Description	Annotation_ID	Pvalue	Genes
DAVID			
digestion	GO:0007586	0.003942035	<i>PRSS1, PRSS2, LOC780933</i>
Influenza A	bta05164	0.023102138	<i>PRSS1, RSAD2, PRSS2, LOC780933</i>
proteolysis	GO:0006508	0.025310057	<i>PRSS1, PRSS58, PRSS2, LOC780933</i>
Protein digestion and absorption	bta04974	0.035866771	<i>PRSS1, PRSS2, LOC780933</i>
Pancreatic secretion	bta04972	0.045708679	<i>PRSS1, PRSS2, LOC780933</i>
Neuroactive ligand-receptor interaction	bta04080	0.084599515	<i>GRIA1, PRSS1, PRSS2, LOC780933</i>
NF-kappa B signaling pathway	bta04064	0.041495948	<i>LOC100300510, LOC509513, BCL2L1</i>
Transcriptional misregulation in cancer	bta05202	0.123956503	<i>LOC100300510, LOC509513, BCL2L1</i>
Ras signaling pathway	bta04014	0.204712072	<i>LOC100300510, LOC509513, BCL2L1</i>
HTLV-I infection	bta05166	0.247233905	<i>LOC100300510, LOC509513, BCL2L1</i>
protein folding	GO:0006457	0.057178177	<i>TXN, TXNDC8, PDRG1</i>
Jak-STAT signaling pathway	bta04630	0.100808338	<i>LIFR, OSMR, BCL2L1</i>
Calcium signaling pathway	bta04020	0.145804691	<i>MYLK2, LOC100300510, LOC509513</i>
spermatogenesis	GO:0007283	0.147900668	<i>ARID4A, TXNDC8, BCL2L1</i>
Rap1 signaling pathway	bta04015	0.177379463	<i>LOC100300510, LOC509513, ID1</i>
positive regulation of cell proliferation	GO:0008284	0.238028083	<i>LIFR, OSMR, BCL2L1</i>
transcription, DNA-templated	GO:0006351	0.373307643	<i>ASXL1, ID1, PLAGL2, TXN</i>
negative regulation of transcription from RNA polymerase II promoter	GO:0000122	0.451505904	<i>ASXL1, ID1, TXN</i>
Metabolic pathways	bta01100	0.459052115	<i>MGAM, COX4I2, LOC100296901, CMPK2, GALNT10, DGKH</i>
GeneCodis			
glycerol ether metabolic process	GO:0006662	0.003875352	<i>TXN, TXNDC8</i>
negative regulation of high voltage-gated calcium channel activity	GO:1901842	0.053038887	<i>REM1</i>
phosphatidylserine exposure on apoptotic cell surface	GO:0070782	0.053038887	<i>XKR7</i>

striated muscle contraction	GO:0006941	0.053038887	<i>MYLK2</i>
positive regulation of immune response	GO:0050778	0.053038887	<i>RSAD2</i>
positive regulation of peptidyl-cysteine S-nitrosylation	GO:2000170	0.053038887	<i>TXN</i>
negative regulation of hydrogen peroxide-induced cell death	GO:1903206	0.053038887	<i>TXN</i>
CD4-positive, alpha-beta T cell activation	GO:0035710	0.053038887	<i>RSAD2</i>
histone H3-K9 trimethylation	GO:0036124	0.053038887	<i>ARID4A</i>
anterograde dendritic transport of neurotransmitter receptor complex	GO:0098971	0.053038887	<i>KIF3B</i>
dUDP biosynthetic process	GO:0006227	0.053038887	<i>CMPK2</i>
response to nitric oxide	GO:0071731	0.053038887	<i>TXN</i>
positive regulation of toll-like receptor 7 signaling pathway	GO:0034157	0.053038887	<i>RSAD2</i>
positive regulation of T-helper 2 cell cytokine production	GO:2000553	0.053038887	<i>RSAD2</i>
regulation of muscle filament sliding	GO:0032971	0.053038887	<i>MYLK2</i>
microtubule-based movement	GO:0007018	0.053038887	<i>ACTR10, KIF3B</i>
regulation of endopeptidase activity	GO:0052548	0.053038887	<i>PSMA3</i>
positive regulation of ion transmembrane transporter activity	GO:0032414	0.053038887	<i>TRPC6</i>
mitotic spindle assembly	GO:0090307	0.053038887	<i>KIF3B, TPX2</i>
dTDP biosynthetic process	GO:0006233	0.053038887	<i>CMPK2</i>
CD4-positive, alpha-beta T cell differentiation	GO:0043367	0.053038887	<i>RSAD2</i>
skeletal muscle satellite cell differentiation	GO:0014816	0.053038887	<i>MYLK2</i>
positive regulation of toll-like receptor 9 signaling pathway	GO:0034165	0.053038887	<i>RSAD2</i>
dTTP biosynthetic process	GO:0006235	0.053038887	<i>CMPK2</i>
oncostatin-M-mediated signaling pathway	GO:0038165	0.053038887	<i>LIFR</i>
establishment of Sertoli cell barrier	GO:0097368	0.053038887	<i>ARID4A</i>
retrograde axonal transport of mitochondrion	GO:0098958	0.053038887	<i>ACTR10</i>
negative regulation of protein export from nucleus	GO:0046826	0.053038887	<i>TXN</i>
fucose metabolic process	GO:0006004	0.053038887	<i>POFUT1</i>
protein O-linked fucosylation	GO:0036066	0.053038887	<i>POFUT1</i>
opsin transport	GO:0036372	0.053038887	<i>KIF3B</i>
leukemia inhibitory factor signaling pathway	GO:0048861	0.053038887	<i>LIFR</i>
regulation of gene expression by genomic imprinting	GO:0006349	0.054316376	<i>ARID4A</i>
apoptotic process involved in development	GO:1902742	0.054316376	<i>XKR7</i>
ciliary neurotrophic factor-mediated signaling pathway	GO:0070120	0.054316376	<i>LIFR</i>
manganese ion transport	GO:0006828	0.054316376	<i>TRPC6</i>
histone H4-K20 trimethylation	GO:0034773	0.054316376	<i>ARID4A</i>
vacuolar proton-transporting V-type ATPase complex assembly	GO:0070072	0.054316376	<i>TM9SF4</i>
positive regulation of protein localization to cell surface	GO:2000010	0.054316376	<i>TM9SF4</i>

cardiac muscle tissue morphogenesis	GO:0055008	0.06190619	<i>MYLK2</i>
regulation of mitotic spindle organization	GO:0060236	0.06190619	<i>TPX2</i>
positive regulation of protein exit from endoplasmic reticulum	GO:0070863	0.068760313	<i>TM9SF4</i>
histone H3-K4 trimethylation	GO:0080182	0.068760313	<i>ARID4A</i>
nucleoside triphosphate biosynthetic process	GO:0009142	0.068856357	<i>CMPK2</i>
positive regulation of calcium ion transport	GO:0051928	0.068856357	<i>TRPC6</i>
TOR signaling	GO:0031929	0.068856357	<i>RICTOR</i>
response to radiation	GO:0009314	0.068856357	<i>TXN</i>
protein polyglutamylation	GO:0018095	0.068856357	<i>TLL9</i>
ionotropic glutamate receptor signaling pathway	GO:0035235	0.068856357	<i>GRIA1</i>
positive regulation of DNA binding	GO:0043388	0.07786477	<i>TXN</i>
nucleoside monophosphate phosphorylation	GO:0046940	0.07786477	<i>CMPK2</i>
engulfment of apoptotic cell	GO:0043652	0.07786477	<i>XKR7</i>
negative regulation of protein secretion	GO:0050709	0.07786477	<i>RSAD2</i>
neuromuscular synaptic transmission	GO:0007274	0.07786477	<i>MYLK2</i>
protein localization to membrane	GO:0072657	0.088252486	<i>TM9SF4</i>
regulation of Notch signaling pathway	GO:0008593	0.088252486	<i>POFUT1</i>
digestion	GO:0007586	0.088252486	<i>PRSS2</i>
erythrocyte development	GO:0048821	0.093816506	<i>ARID4A</i>
nucleoside diphosphate phosphorylation	GO:0006165	0.097517893	<i>CMPK2</i>
regulation of intracellular pH	GO:0051453	0.097517893	<i>TM9SF4</i>
mitochondrial electron transport, cytochrome c to oxygen	GO:0006123	0.102615478	<i>COX4I2</i>
extrinsic apoptotic signaling pathway in absence of ligand	GO:0097192	0.105821788	<i>BCL2L1</i>
negative regulation of viral genome replication	GO:0045071	0.105821788	<i>RSAD2</i>
collagen catabolic process	GO:0030574	0.110511918	<i>PRSS2</i>
regulation of cytosolic calcium ion concentration	GO:0051480	0.114218006	<i>TRPC6</i>
cell redox homeostasis	GO:0045454	0.114218006	<i>TXN</i>
negative regulation of intrinsic apoptotic signaling pathway	GO:2001243	0.114218006	<i>BCL2L1</i>
intrinsic apoptotic signaling pathway in response to DNA damage	GO:0008630	0.114218006	<i>BCL2L1</i>
response to cytokine	GO:0034097	0.114218006	<i>LIFR</i>
skeletal muscle cell differentiation	GO:0035914	0.116666749	<i>MYLK2</i>
oxidative phosphorylation	GO:0006119	0.116666749	<i>COX4I2</i>
protein O-linked glycosylation	GO:0006493	0.11896455	<i>POFUT1</i>
intraciliary transport	GO:0042073	0.11896455	<i>KIF3B</i>
proteasomal protein catabolic process	GO:0010498	0.12477501	<i>PSMA3</i>
activation of protein kinase activity	GO:0032147	0.12477501	<i>TPX2</i>

somitogenesis	GO:0001756	0.12477501	<i>POFUT1</i>
spermatogenesis	GO:0007283	0.126670817	<i>ARID4A, TXNDC8</i>
peptidyl-threonine phosphorylation	GO:0018107	0.126670817	<i>MYLK2</i>
ubiquitin-dependent protein catabolic process	GO:0006511	0.132787703	<i>RNF144A, PSMA3</i>
cellular protein modification process	GO:0006464	0.151105996	<i>TLL9</i>
phagocytosis	GO:0006909	0.151105996	<i>TM9SF4</i>
T cell receptor signaling pathway	GO:0050852	0.158737347	<i>FYB1</i>
single fertilization	GO:0007338	0.16148346	<i>TRPC6</i>
proteolysis	GO:0006508	0.164801472	<i>PRSS2, PRSS58, HM13</i>
response to virus	GO:0009615	0.164801472	<i>RSAD2</i>
flagellated sperm motility	GO:0030317	0.164801472	<i>TLL9</i>
negative regulation of DNA-binding transcription factor activity	GO:0043433	0.171701637	<i>ID1</i>
positive regulation of proteasomal ubiquitin-dependent protein catabolic process	GO:0032436	0.172511015	<i>RNF144A</i>
proteolysis involved in cellular protein catabolic process	GO:0051603	0.172511015	<i>PSMA3</i>
circadian regulation of gene expression	GO:0032922	0.172511015	<i>ID1</i>
positive regulation of peptidyl-serine phosphorylation	GO:0033138	0.172511015	<i>TXN</i>
response to hypoxia	GO:0001666	0.203199227	<i>TM9SF4</i>
integrin-mediated signaling pathway	GO:0007229	0.21289274	<i>FYB1</i>
cellular response to lipopolysaccharide	GO:0071222	0.229976876	<i>CMPK2</i>
peptidyl-tyrosine phosphorylation	GO:0018108	0.237659605	<i>HCK</i>
Notch signaling pathway	GO:0007219	0.237659605	<i>POFUT1</i>
protein autophosphorylation	GO:0046777	0.237659605	<i>MYLK2</i>
microtubule cytoskeleton organization	GO:0000226	0.238867711	<i>TLL9</i>
positive regulation of cytosolic calcium ion concentration	GO:0007204	0.240040427	<i>TRPC6</i>
protein localization to plasma membrane	GO:0072659	0.248224094	<i>FYB1</i>
cytokine-mediated signaling pathway	GO:0019221	0.250221917	<i>LIFR</i>
calcium ion transmembrane transport	GO:0070588	0.250221917	<i>TRPC6</i>
negative regulation of transcription, DNA-templated	GO:0045892	0.252185057	<i>ARID4A, ID1</i>
calcium ion transport	GO:0006816	0.255432408	<i>TRPC6</i>
apoptotic process	GO:0006915	0.25773842	<i>BCL2L1, TPX2</i>
regulation of cell shape	GO:0008360	0.270010709	<i>PALM2</i>
protein polyubiquitination	GO:0000209	0.295657705	<i>RNF144A</i>
protein folding	GO:0006457	0.295973941	<i>PDRG1</i>
defense response to virus	GO:0051607	0.325936848	<i>RSAD2</i>
cilium assembly	GO:0060271	0.333911318	<i>KIF3B</i>
heart development	GO:0007507	0.333911318	<i>POFUT1</i>

angiogenesis	GO:0001525	0.333911318	<i>POFUT1</i>
ion transmembrane transport	GO:0034220	0.333911318	<i>GRIA1</i>
phosphorylation	GO:0016310	0.34028947	<i>HCK, MYLK2</i>
regulation of apoptotic process	GO:0042981	0.341548751	<i>BCL2L1</i>
protein glycosylation	GO:0006486	0.351729793	<i>POFUT1</i>
Other types of O-glycan biosynthesis	bta00514	0.35376786	<i>POFUT1, GALNT10</i>
Amyotrophic lateral sclerosis	bta05014	0.35376786	<i>BCL2L1, COX4I2, ACTR10, GRIA1, PSMA3</i>
Parkinson disease	bta05012	0.35376786	<i>BCL2L1, TXN, COX4I2, PSMA3</i>
Pathways of neurodegeneration - multiple diseases	bta05022	0.35376786	<i>BCL2L1, COX4I2, ACTR10, GRIA1, PSMA3</i>
Axon guidance	bta04360	0.35376786	<i>SEMA3A, EPHB6, TRPC6</i>
Huntington disease	bta05016	0.35376786	<i>COX4I2, ACTR10, GRIA1, PSMA3</i>
JAK-STAT signaling pathway	bta04630	0.35376786	<i>LIFR, BCL2L1, OSMR</i>
ion transport	GO:0006811	0.369673365	<i>TRPC6, GRIA1</i>
protein phosphorylation	GO:0006468	0.375945663	<i>HCK, MYLK2</i>
negative regulation of transcription by RNA polymerase II	GO:0000122	0.386790838	<i>TXN, ID1</i>
nervous system development	GO:0007399	0.386790838	<i>POFUT1</i>
immune response	GO:0006955	0.452921912	<i>FYB1</i>
vesicle-mediated transport	GO:0016192	0.488373743	<i>KIF3B</i>
cell division	GO:0051301	0.488373743	<i>TPX2</i>
positive regulation of cell population proliferation	GO:0008284	0.511848874	<i>LIFR</i>
immune system process	GO:0002376	0.511848874	<i>RSAD2</i>
positive regulation of gene expression	GO:0010628	0.511848874	<i>MYLK2</i>
innate immune response	GO:0045087	0.511848874	<i>RSAD2</i>
Starch and sucrose metabolism	bta00500	0.551262074	<i>MGAM</i>
Apoptosis	bta04210	0.551262074	<i>BCL2L1</i>
PI3K-Akt signaling pathway	bta04151	0.551262074	<i>BCL2L1, OSMR</i>
Small cell lung cancer	bta05222	0.551262074	<i>BCL2L1</i>
Oxidative phosphorylation	bta00190	0.551262074	<i>COX4I2</i>
Circadian entrainment	bta04713	0.551262074	<i>GRIA1</i>
Galactose metabolism	bta00052	0.551262074	<i>MGAM</i>
Fluid shear stress and atherosclerosis	bta05418	0.551262074	<i>TXN</i>
Influenza A	bta05164	0.551262074	<i>PRSS2, RSAD2</i>
Proteasome	bta03050	0.551262074	<i>PSMA3</i>
mTOR signaling pathway	bta04150	0.551262074	<i>RICTOR</i>

Non-alcoholic fatty liver disease	bta04932	0.551262074	<i>COX4I2</i>
Mucin type O-glycan biosynthesis	bta00512	0.551262074	<i>GALNT10</i>
Cytokine-cytokine receptor interaction	bta04060	0.551262074	<i>LIFR, OSMR</i>
Gastric acid secretion	bta04971	0.551262074	<i>MYLK2</i>
Measles	bta05162	0.551262074	<i>BCL2L1</i>
Dopaminergic synapse	bta04728	0.551262074	<i>GRIA1</i>
Endocrine and other factor-regulated calcium reabsorption	bta04961	0.551262074	<i>TRPV5</i>
Glycerolipid metabolism	bta00561	0.551262074	<i>DGKH</i>
Toxoplasmosis	bta05145	0.551262074	<i>BCL2L1</i>
Pancreatic cancer	bta05212	0.551262074	<i>BCL2L1</i>
Apelin signaling pathway	bta04371	0.551262074	<i>MYLK2</i>
Vascular smooth muscle contraction	bta04270	0.551262074	<i>MYLK2</i>
Protein digestion and absorption	bta04974	0.551262074	<i>PRSS2</i>
Pyrimidine metabolism	bta00240	0.551262074	<i>CMPK2</i>
Retrograde endocannabinoid signaling	bta04723	0.551262074	<i>GRIA1</i>
Phospholipase D signaling pathway	bta04072	0.551262074	<i>DGKH</i>
Mineral absorption	bta04978	0.551262074	<i>TRPV6</i>
Parathyroid hormone synthesis, secretion and action	bta04928	0.551262074	<i>TRPV5</i>
Autophagy - animal	bta04140	0.551262074	<i>BCL2L1</i>
Spinocerebellar ataxia	bta05017	0.551262074	<i>GRIA1, PSMA3</i>
cGMP-PKG signaling pathway	bta04022	0.551262074	<i>TRPC6, MYLK2</i>
Platelet activation	bta04611	0.551262074	<i>MYLK2</i>
Neuroactive ligand-receptor interaction	bta04080	0.551262074	<i>PRSS2, GRIA1</i>
NF-kappa B signaling pathway	bta04064	0.551262074	<i>BCL2L1</i>
Biosynthesis of cofactors	bta01240	0.551262074	<i>CMPK2</i>
Salmonella infection	bta05132	0.551262074	<i>TXN, ACTR10</i>
Choline metabolism in cancer	bta05231	0.551262074	<i>DGKH</i>
Long-term depression	bta04730	0.551262074	<i>GRIA1</i>
Nicotine addiction	bta05033	0.551262074	<i>GRIA1</i>
Carbohydrate digestion and absorption	bta04973	0.551262074	<i>MGAM</i>
Glycerophospholipid metabolism	bta00564	0.551262074	<i>DGKH</i>
Cardiac muscle contraction	bta04260	0.551262074	<i>COX4I2</i>
Long-term potentiation	bta04720	0.551262074	<i>GRIA1</i>
p53 signaling pathway	bta04115	0.551262074	<i>BCL2L1</i>
Apoptosis - multiple species	bta04215	0.551262074	<i>BCL2L1</i>
Glutamatergic synapse	bta04724	0.551262074	<i>GRIA1</i>

EGFR tyrosine kinase inhibitor resistance	bta01521	0.551262074	<i>BCL2L1</i>
Mitophagy - animal	bta04137	0.551262074	<i>BCL2L1</i>
Phosphatidylinositol signaling system	bta04070	0.551262074	<i>DGKH</i>
Pancreatic secretion	bta04972	0.551262074	<i>PRSS2</i>
TGF-beta signaling pathway	bta04350	0.551262074	<i>ID1</i>
Prion disease	bta05020	0.551262074	<i>COX4I2, PSMA3</i>
Amphetamine addiction	bta05031	0.551262074	<i>GRIA1</i>
Chronic myeloid leukemia	bta05220	0.551262074	<i>BCL2L1</i>
NOD-like receptor signaling pathway	bta04621	0.551262074	<i>BCL2L1, TXN</i>
Oxytocin signaling pathway	bta04921	0.551262074	<i>MYLK2</i>
Salivary secretion	bta04970	0.551262074	<i>TRPV6</i>
Platinum drug resistance	bta01524	0.551262074	<i>BCL2L1</i>
Yersinia infection	bta05135	0.551262074	<i>FYB1</i>
Hippo signaling pathway	bta04390	0.551262074	<i>ID1</i>
Rap1 signaling pathway	bta04015	0.551262074	<i>ID1, FYB1</i>
Signaling pathways regulating pluripotency of stem cells	bta04550	0.551262074	<i>LIFR, ID1</i>
Alzheimer disease	bta05010	0.551262074	<i>COX4I2, PSMA3</i>
Hepatitis C	bta05160	0.551262074	<i>RSAD2</i>
Fc gamma R-mediated phagocytosis	bta04666	0.551262074	<i>HCK</i>
Hepatocellular carcinoma	bta05225	0.569920807	<i>BCL2L1</i>
cell adhesion	GO:0007155	0.569951669	<i>TM9SF4</i>
Transcriptional misregulation in cancer	bta05202	0.577331416	<i>BCL2L1</i>
Kaposi sarcoma-associated herpesvirus infection	bta05167	0.578990814	<i>HCK</i>
Chemokine signaling pathway	bta04062	0.578990814	<i>HCK</i>
Focal adhesion	bta04510	0.597590749	<i>MYLK2</i>
Human immunodeficiency virus 1 infection	bta05170	0.597590749	<i>BCL2L1</i>
Diabetic cardiomyopathy	bta05415	0.597590749	<i>COX4I2</i>
Lipid and atherosclerosis	bta05417	0.597590749	<i>BCL2L1</i>
cAMP signaling pathway	bta04024	0.603650503	<i>GRIA1</i>
Human T-cell leukemia virus 1 infection	bta05166	0.603650503	<i>BCL2L1</i>
Regulation of actin cytoskeleton	bta04810	0.603650503	<i>MYLK2</i>
Chemical carcinogenesis - reactive oxygen species	bta05208	0.603650503	<i>COX4I2</i>
Olfactory transduction	bta04740	0.603895701	<i>OR6V1</i>
Ras signaling pathway	bta04014	0.603895701	<i>BCL2L1</i>
Thermogenesis	bta04714	0.603895701	<i>COX4I2</i>
Calcium signaling pathway	bta04020	0.60542382	<i>MYLK2</i>

cell cycle	GO:0007049	0.606224672	TPX2
Herpes simplex virus 1 infection	bta05168	0.649979281	BCL2L1
Metabolic pathways	bta01100	0.649979281	DGKH, GALNT10, COX4I2, CMPK2, MGAM
protein ubiquitination	GO:0016567	0.671565753	RNF144A
cell differentiation	GO:0030154	0.701022054	ID1
transmembrane transport	GO:0055085	0.701022054	TRPC6
protein transport	GO:0015031	0.702069592	TIMM9
positive regulation of transcription by RNA polymerase II	GO:0045944	0.825516611	ARID4A
Pathways in cancer	bta05200	0.858718711	BCL2L1
regulation of transcription, DNA-templated	GO:0006355	0.897895103	FOXS1
regulation of transcription by RNA polymerase II	GO:0006357	0.898716116	ARID4A

Table S6. Results of functional enrichment analyzes performed in DAVID and GeneCodis for IMF.

Description	Annotation_ID	Pvalue	Genes
DAVID			
Metabolic pathways	bta01100	0.691685662	GULO, B4GALT1, EPHX2, COX10
GeneCodis			
urea transmembrane transport	GO:0071918	0.006477835	AQP7, AQP3
glycerol transport	GO:0015793	0.006477835	AQP7, AQP3
renal water absorption	GO:0070295	0.007183028	AQP7, AQP3
water transport	GO:0006833	0.014992992	AQP7, AQP3
negative regulation of extrinsic apoptotic signaling pathway in absence of ligand	GO:2001240	0.033076573	EYA2, UNC5B
cellular response to oxygen-glucose deprivation	GO:0090650	0.034583741	AQP3
negative regulation of intracellular signal transduction	GO:1902532	0.034583741	DDIT4
diadenosine triphosphate catabolic process	GO:0015964	0.034583741	FHIT
signal complex assembly	GO:0007172	0.034583741	PTK2B
protein-containing complex disassembly	GO:0032984	0.034583741	DDIT4
protein galactosylation	GO:0042125	0.034583741	B4GALT1
development of secondary sexual characteristics	GO:0045136	0.034583741	B4GALT1
regulation of neurotrophin TRK receptor signaling pathway	GO:0051386	0.034583741	DOK5
heme O biosynthetic process	GO:0048034	0.034583741	COX10

esophagus smooth muscle contraction	GO:0014846	0.034583741	<i>SULF2</i>
regulation of multicellular organismal process	GO:0051239	0.034583741	<i>PTK2B</i>
vacuolar transport	GO:0007034	0.034583741	<i>CHMP5, NDFIP2</i>
heparan sulfate proteoglycan metabolic process	GO:0030201	0.034583741	<i>SULF2</i>
regulation of leukocyte chemotaxis	GO:0002688	0.034583741	<i>PTK2B</i>
negative regulation of establishment of protein localization to mitochondrion	GO:1903748	0.034583741	<i>DNAJA1</i>
tRNA export from nucleus	GO:0006409	0.043161925	<i>NOL6</i>
negative regulation of MHC class II biosynthetic process	GO:0045347	0.043161925	<i>NFX1</i>
negative regulation of nitrosative stress-induced intrinsic apoptotic signaling pathway	GO:1905259	0.043161925	<i>DNAJA1</i>
anterior/posterior axon guidance	GO:0033564	0.043161925	<i>UNC5B</i>
regulation of acrosome reaction	GO:0060046	0.043161925	<i>B4GALT1</i>
lactose biosynthetic process	GO:0005989	0.043161925	<i>B4GALT1</i>
negative regulation of protein transport	GO:0051224	0.043161925	<i>NDFIP2</i>
regulation of hepatocyte proliferation	GO:2000345	0.043161925	<i>SULF2</i>
negative regulation of transporter activity	GO:0032410	0.043161925	<i>NDFIP2</i>
heme A biosynthetic process	GO:0006784	0.043161925	<i>COX10</i>
histone dephosphorylation	GO:0016576	0.043161925	<i>EYA2</i>
striated muscle tissue development	GO:0014706	0.043161925	<i>EYA2</i>
epithelial cell differentiation involved in prostate gland development	GO:0060742	0.049250641	<i>PSAP</i>
regulation of protein transport	GO:0051223	0.049250641	<i>DNAJA1</i>
oligosaccharide biosynthetic process	GO:0009312	0.049250641	<i>B4GALT1</i>
nucleoside transport	GO:0015858	0.049250641	<i>SLC29A3</i>
L-ascorbic acid biosynthetic process	GO:0019853	0.049250641	<i>GULO</i>
cytochrome complex assembly	GO:0017004	0.049250641	<i>COX10</i>
positive regulation of apoptotic process	GO:0043065	0.049250641	<i>DNAJA1, TRIM35, B4GALT1</i>
glial cell-derived neurotrophic factor receptor signaling pathway	GO:0035860	0.049250641	<i>SULF2</i>
positive regulation of immune system process	GO:0002684	0.049250641	<i>AQP3</i>
urea transport	GO:0015840	0.049250641	<i>AQP3</i>
netrin-activated signaling pathway	GO:0038007	0.053994458	<i>UNC5B</i>
penetration of zona pellucida	GO:0007341	0.053994458	<i>B4GALT1</i>
protein sulfation	GO:0006477	0.053994458	<i>HS3ST3B1</i>
protein localization to mitochondrion	GO:0070585	0.053994458	<i>DNAJA1</i>
purine nucleotide metabolic process	GO:0006163	0.053994458	<i>FHIT</i>
positive regulation of epithelial cell proliferation involved in wound healing	GO:0060054	0.053994458	<i>B4GALT1</i>
respiratory chain complex IV assembly	GO:0008535	0.053994458	<i>COX10</i>
regulation of receptor recycling	GO:0001919	0.053994458	<i>CHMP5</i>

prostate gland growth	GO:0060736	0.053994458	<i>PSAP</i>
viral budding	GO:0046755	0.05825016	<i>CHMP5</i>
glycoprotein biosynthetic process	GO:0009101	0.05825016	<i>B4GALT1</i>
epithelial cell development	GO:0002064	0.05825016	<i>B4GALT1</i>
angiogenesis involved in wound healing	GO:0060055	0.05825016	<i>B4GALT1</i>
liver regeneration	GO:0097421	0.05825016	<i>SULF2</i>
glomerular basement membrane development	GO:0032836	0.05825016	<i>SULF2</i>
neurotrophin TRK receptor signaling pathway	GO:0048011	0.05825016	<i>DDIT4</i>
acute inflammatory response	GO:0002526	0.05825016	<i>B4GALT1</i>
nucleoside transmembrane transport	GO:1901642	0.062388783	<i>SLC29A3</i>
cellular respiration	GO:0045333	0.062388783	<i>COX10</i>
innervation	GO:0060384	0.062388783	<i>SULF2</i>
negative regulation of JUN kinase activity	GO:0043508	0.062388783	<i>DNAJA1</i>
cellular response to muramyl dipeptide	GO:0071225	0.062388783	<i>CHMP5</i>
single strand break repair	GO:0000012	0.062388783	<i>APTX</i>
regulation of cellular component organization	GO:0051128	0.062388783	<i>PTK2B</i>
regulation of actin cytoskeleton reorganization	GO:2000249	0.064816548	<i>PTK2B</i>
vesicle budding from membrane	GO:0006900	0.064816548	<i>CHMP5</i>
mitochondrial outer membrane permeabilization	GO:0097345	0.064816548	<i>EYA2</i>
suppression of viral release by host	GO:0044790	0.064816548	<i>TRIM35</i>
response to nicotine	GO:0035094	0.064816548	<i>CHRNA2</i>
negative regulation of peptidyl-threonine phosphorylation	GO:0010801	0.064816548	<i>DDIT4</i>
negative regulation of glycolytic process	GO:0045820	0.064816548	<i>DDIT4</i>
galactose metabolic process	GO:0006012	0.064816548	<i>B4GALT1</i>
regulation of sodium ion transport	GO:0002028	0.068413258	<i>NKAIN2</i>
glycosylation	GO:0070085	0.068413258	<i>B4GALT1</i>
viral budding via host ESCRT complex	GO:0039702	0.068413258	<i>CHMP5</i>
viral budding from plasma membrane	GO:0046761	0.068413258	<i>CHMP5</i>
chondrocyte development	GO:0002063	0.068413258	<i>SULF2</i>
glomerular filtration	GO:0003094	0.068413258	<i>SULF2</i>
neuron differentiation	GO:0030182	0.070628567	<i>DOK5, DDIT4</i>
regulation of centrosome duplication	GO:0010824	0.071483423	<i>CHMP5</i>
mitochondrial fission	GO:0000266	0.071483423	<i>COX10</i>
androgen receptor signaling pathway	GO:0030521	0.071483423	<i>DNAJA1</i>
sulfur compound metabolic process	GO:0006790	0.071483423	<i>CHST3</i>
positive regulation of neuron death	GO:1901216	0.071483423	<i>DDIT4</i>

regulation of TOR signaling	GO:0032006	0.073333034	<i>DDIT4</i>
midbody abscission	GO:0061952	0.073333034	<i>CHMP5</i>
negative regulation of fibroblast growth factor receptor signaling pathway	GO:0040037	0.073333034	<i>SULF2</i>
nuclear membrane reassembly	GO:0031468	0.073333034	<i>CHMP5</i>
leukocyte migration	GO:0050900	0.073333034	<i>B4GALT1</i>
intrinsic apoptotic signaling pathway by p53 class mediator	GO:0072332	0.073333034	<i>FHIT</i>
cellular response to dexamethasone stimulus	GO:0071549	0.073333034	<i>DDIT4</i>
late endosome to vacuole transport via multivesicular body sorting pathway	GO:0032511	0.07643123	<i>CHMP5</i>
multivesicular body sorting pathway	GO:0071985	0.07643123	<i>CHMP5</i>
chondroitin sulfate biosynthetic process	GO:0030206	0.07643123	<i>CHST3</i>
negative regulation of mitotic cell cycle	GO:0045930	0.07643123	<i>TRIM35</i>
synaptic transmission, cholinergic	GO:0007271	0.07643123	<i>CHRNA2</i>
lysosomal transport	GO:0007041	0.079208211	<i>PSAP</i>
late endosome to lysosome transport	GO:1902774	0.079208211	<i>CHMP5</i>
nucleus organization	GO:0006997	0.079208211	<i>CHMP5</i>
aerobic respiration	GO:0009060	0.079208211	<i>COX10</i>
regulation of microtubule polymerization or depolymerization	GO:0031110	0.079208211	<i>STMN4</i>
plasma membrane repair	GO:0001778	0.084851292	<i>CHMP5</i>
regulation of biological quality	GO:0065008	0.087050758	<i>PTK2B</i>
positive regulation of Wnt signaling pathway	GO:0030177	0.087050758	<i>SULF2</i>
odontogenesis	GO:0042476	0.087050758	<i>AQP3</i>
N-acetylglucosamine metabolic process	GO:0006044	0.087050758	<i>CHST3</i>
negative regulation of peptidyl-serine phosphorylation	GO:0033137	0.087050758	<i>DDIT4</i>
negative regulation of proteasomal ubiquitin-dependent protein catabolic process	GO:0032435	0.089039008	<i>FHIT</i>
positive regulation of vascular endothelial growth factor production	GO:0010575	0.089039008	<i>SULF2</i>
regulation of mitotic spindle assembly	GO:1901673	0.089039008	<i>CHMP5</i>
response to retinoic acid	GO:0032526	0.089039008	<i>AQP3</i>
negative regulation of TOR signaling	GO:0032007	0.089039008	<i>DDIT4</i>
heme biosynthetic process	GO:0006783	0.091612573	<i>COX10</i>
extrinsic apoptotic signaling pathway in absence of ligand	GO:0097192	0.091612573	<i>EYA2</i>
ubiquitin-dependent protein catabolic process via the multivesicular body sorting pathway	GO:0043162	0.091612573	<i>CHMP5</i>
intrinsic apoptotic signaling pathway in response to DNA damage by p53 class mediator	GO:0042771	0.091612573	<i>DDIT4</i>
response to heat	GO:0009408	0.094000402	<i>DNAJA1</i>
regulation of bone mineralization	GO:0030500	0.094000402	<i>PTK2B</i>

regulation of angiogenesis	GO:0045765	0.094000402	<i>PTK2B</i>
endosome to lysosome transport	GO:0008333	0.094000402	<i>CHMP5</i>
embryonic skeletal system development	GO:0048706	0.098567069	<i>SULF2</i>
regulation of immune response	GO:0050776	0.103043477	<i>VSIR</i>
binding of sperm to zona pellucida	GO:0007339	0.10657921	<i>B4GALT1</i>
chaperone cofactor-dependent protein refolding	GO:0051085	0.10657921	<i>BAG1</i>
lysosome organization	GO:0007040	0.110854516	<i>CHMP5</i>
adenylate cyclase-inhibiting G protein-coupled receptor signaling pathway	GO:0007193	0.111560807	<i>PSAP</i>
metal ion transport	GO:0030001	0.111560807	<i>NDFIP2</i>
autophagosome maturation	GO:0097352	0.111560807	<i>CHMP5</i>
positive regulation of DNA repair	GO:0045739	0.111560807	<i>EYA2</i>
reactive oxygen species metabolic process	GO:0072593	0.111560807	<i>DDIT4</i>
carbohydrate metabolic process	GO:0005975	0.114445103	<i>CHST3, B4GALT1</i>
regulation of lipid metabolic process	GO:0019216	0.116897354	<i>PSAP</i>
regulation of postsynaptic membrane potential	GO:0060078	0.116897354	<i>CHRNA2</i>
regulation of cell adhesion	GO:0030155	0.116897354	<i>PTK2B</i>
response to wounding	GO:0009611	0.116897354	<i>SULF2</i>
mitotic metaphase plate congression	GO:0007080	0.120698245	<i>CHMP5</i>
excitatory postsynaptic potential	GO:0060079	0.131691856	<i>CHRNA2</i>
protein N-linked glycosylation	GO:0006487	0.131691856	<i>B4GALT1</i>
wound healing	GO:0042060	0.131691856	<i>B4GALT1</i>
bone development	GO:0060348	0.143096316	<i>SULF2</i>
anatomical structure development	GO:0048856	0.143096316	<i>EYA2</i>
sphingolipid metabolic process	GO:0006665	0.145449757	<i>PSAP</i>
cellular response to hypoxia	GO:0071456	0.145449757	<i>AQP3</i>
cartilage development	GO:0051216	0.14772574	<i>SULF2</i>
positive regulation of phosphatidylinositol 3-kinase signaling	GO:0014068	0.14772574	<i>UNC5B</i>
nervous system process	GO:0050877	0.147941629	<i>CHRNA2</i>
negative regulation of signal transduction	GO:0009968	0.147941629	<i>DDIT4</i>
regulation of alternative mRNA splicing, via spliceosome	GO:0000381	0.147941629	<i>SMU1</i>
negative regulation of cell death	GO:0060548	0.147941629	<i>CHMP5</i>
flagellated sperm motility	GO:0030317	0.150070115	<i>DNAJA1</i>
double-strand break repair	GO:0006302	0.150070115	<i>APTX</i>
protein autoubiquitination	GO:0051865	0.153118924	<i>NFX1</i>
negative regulation of protein ubiquitination	GO:0031397	0.156115822	<i>DNAJA1</i>
positive regulation of protein ubiquitination	GO:0031398	0.162996192	<i>NDFIP2</i>

Glycosaminoglycan biosynthesis - heparan sulfate / heparin	bta00534	0.17735066	<i>HS3ST3A1, HS3ST3B1</i>
negative regulation of peptidase activity	GO:0010466	0.1813207	<i>SPINK4</i>
regulation of cell migration	GO:0030334	0.183984874	<i>PTK2B</i>
response to hypoxia	GO:0001666	0.190367601	<i>DDIT4</i>
DNA repair	GO:0006281	0.193741161	<i>EYA2, APTX</i>
negative regulation of cell migration	GO:0030336	0.199084394	<i>ZMYND8</i>
neuron migration	GO:0001764	0.200267229	<i>DDIT4</i>
transmembrane receptor protein tyrosine kinase signaling pathway	GO:0007169	0.200267229	<i>DOK5</i>
mitochondrion organization	GO:0007005	0.209788566	<i>COX10</i>
cellular response to lipopolysaccharide	GO:0071222	0.212053841	<i>CHMP5</i>
regulation of membrane potential	GO:0042391	0.212997627	<i>CHRNA2</i>
kidney development	GO:0001822	0.212997627	<i>SULF2</i>
positive regulation of canonical Wnt signaling pathway	GO:0090263	0.213908228	<i>SULF2</i>
peptidyl-tyrosine dephosphorylation	GO:0035335	0.213908228	<i>EYA2</i>
peptidyl-tyrosine phosphorylation	GO:0018108	0.219439921	<i>PTK2B</i>
axon guidance	GO:0007411	0.234846984	<i>UNC5B</i>
negative regulation of neuron apoptotic process	GO:0043524	0.238658336	<i>UNC5B</i>
cellular response to DNA damage stimulus	GO:0006974	0.238658336	<i>EYA2, APTX</i>
extracellular matrix organization	GO:0030198	0.243734701	<i>B4GALT1</i>
apoptotic process	GO:0006915	0.253594127	<i>FHIT, DDIT4</i>
nucleic acid phosphodiester bond hydrolysis	GO:0090305	0.253594127	<i>APTX</i>
brain development	GO:0007420	0.261476069	<i>DDIT4</i>
regulation of cell population proliferation	GO:0042127	0.276715644	<i>PTK2B</i>
rRNA processing	GO:0006364	0.276715644	<i>NOL6</i>
chemical synaptic transmission	GO:0007268	0.280958912	<i>CHRNA2</i>
negative regulation of endopeptidase activity	GO:0010951	0.280958912	<i>SPINK4</i>
positive regulation of MAPK cascade	GO:0043410	0.280958912	<i>DOK5</i>
protein folding	GO:0006457	0.282323991	<i>DNAJA1</i>
autophagy	GO:0006914	0.306344196	<i>CHMP5</i>
defense response to virus	GO:0051607	0.310238654	<i>DDIT4</i>
protein dephosphorylation	GO:0006470	0.312376912	<i>EYA2</i>
protein stabilization	GO:0050821	0.312376912	<i>BAG1</i>
protein ubiquitination	GO:0016567	0.318089398	<i>ANAPC16, TRIM35</i>
ion transmembrane transport	GO:0034220	0.322418992	<i>CHRNA2</i>
negative regulation of gene expression	GO:0010629	0.325974351	<i>NDFIP2</i>
protein glycosylation	GO:0006486	0.343783319	<i>B4GALT1</i>

lipid metabolic process	GO:0006629	0.343783319	<i>PSAP, B4GALT1</i>
mRNA splicing, via spliceosome	GO:0000398	0.34627423	<i>SMU1</i>
transmembrane transport	GO:0055085	0.350866756	<i>AQP7, AQP3</i>
chromatin organization	GO:0006325	0.369434746	<i>EYA2</i>
response to stimulus	GO:0050896	0.386302434	<i>PTK2B</i>
spermatogenesis	GO:0007283	0.402530086	<i>DNAJA1</i>
RNA splicing	GO:0008380	0.402726969	<i>SMU1</i>
regulation of transcription, DNA-templated	GO:0006355	0.407917717	<i>ZMYND8, ASCC1, NFX1</i>
ubiquitin-dependent protein catabolic process	GO:0006511	0.407917717	<i>NDFIP2</i>
negative regulation of cell population proliferation	GO:0008285	0.44941638	<i>B4GALT1</i>
signal transduction	GO:0007165	0.453087797	<i>PTK2B, UNC5B, CHRNA2</i>
mRNA processing	GO:0006397	0.472031536	<i>SMU1</i>
cell division	GO:0051301	0.472031536	<i>ANAPC16</i>
positive regulation of cell population proliferation	GO:0008284	0.506397405	<i>PTK2B</i>
innate immune response	GO:0045087	0.507461366	<i>TRIM35</i>
negative regulation of apoptotic process	GO:0043066	0.51710263	<i>DNAJA1</i>
cell adhesion	GO:0007155	0.563239168	<i>B4GALT1</i>
Natural killer cell mediated cytotoxicity	bta04650	0.579344128	<i>PTK2B</i>
Small cell lung cancer	bta05222	0.579344128	<i>FHIT</i>
Mannose type O-glycan biosynthesis	bta00515	0.579344128	<i>B4GALT1</i>
GnRH signaling pathway	bta04912	0.579344128	<i>PTK2B</i>
Estrogen signaling pathway	bta04915	0.579344128	<i>NCOA3</i>
Cell adhesion molecules	bta04514	0.579344128	<i>VSIR</i>
Sphingolipid metabolism	bta00600	0.579344128	<i>PSAP</i>
Glycosaminoglycan biosynthesis - keratan sulfate	bta00533	0.579344128	<i>B4GALT1</i>
Leukocyte transendothelial migration	bta04670	0.579344128	<i>PTK2B</i>
Alcoholism	bta05034	0.579344128	<i>SLC29A3</i>
Glycosaminoglycan biosynthesis - chondroitin sulfate / dermatan sulfate	bta00532	0.579344128	<i>CHST3</i>
Other types of O-glycan biosynthesis	bta00514	0.579344128	<i>B4GALT1</i>
Hepatitis B	bta05161	0.579344128	<i>PTK2B</i>
N-Glycan biosynthesis	bta00510	0.579344128	<i>B4GALT1</i>
Autophagy - animal	bta04140	0.579344128	<i>DDIT4</i>
Regulation of lipolysis in adipocytes	bta04923	0.579344128	<i>AQP7</i>
Yersinia infection	bta05135	0.579344128	<i>PTK2B</i>
Purine metabolism	bta00230	0.579344128	<i>FHIT</i>
Oocyte meiosis	bta04114	0.579344128	<i>ANAPC16</i>

Non-small cell lung cancer	bta05223	0.579344128	<i>FHIT</i>
Endocrine resistance	bta01522	0.579344128	<i>NCOA3</i>
Thyroid hormone signaling pathway	bta04919	0.579344128	<i>NCOA3</i>
Necroptosis	bta04217	0.579344128	<i>CHMP5</i>
Lysosome	bta04142	0.579344128	<i>PSAP</i>
Arachidonic acid metabolism	bta00590	0.579344128	<i>EPHX2</i>
Glycosphingolipid biosynthesis - lacto and neolacto series	bta00601	0.579344128	<i>B4GALT1</i>
mTOR signaling pathway	bta04150	0.579344128	<i>DDIT4</i>
Protein processing in endoplasmic reticulum	bta04141	0.579344128	<i>DNAJA1, BAG1</i>
Breast cancer	bta05224	0.579344128	<i>NCOA3</i>
Porphyrin metabolism	bta00860	0.579344128	<i>COX10</i>
Various types of N-glycan biosynthesis	bta00513	0.579344128	<i>B4GALT1</i>
Biosynthesis of cofactors	bta01240	0.579344128	<i>COX10, GULO</i>
Cell cycle	bta04110	0.579344128	<i>ANAPC16</i>
Galactose metabolism	bta00052	0.579344128	<i>B4GALT1</i>
Progesterone-mediated oocyte maturation	bta04914	0.579344128	<i>ANAPC16</i>
Oxidative phosphorylation	bta00190	0.579344128	<i>COX10</i>
Vasopressin-regulated water reabsorption	bta04962	0.579344128	<i>AQP3</i>
Ascorbate and aldarate metabolism	bta00053	0.579344128	<i>GULO</i>
Ubiquitin mediated proteolysis	bta04120	0.579344128	<i>ANAPC16, UBE2R2</i>
Ribosome biogenesis in eukaryotes	bta03008	0.579344128	<i>NOL6</i>
PPAR signaling pathway	bta03320	0.579344128	<i>AQP7</i>
Phospholipase D signaling pathway	bta04072	0.579344128	<i>PTK2B</i>
Peroxisome	bta04146	0.579344128	<i>EPHX2</i>
negative regulation of transcription, DNA-templated	GO:0045892	0.581578422	<i>ZMYND8</i>
cell cycle	GO:0007049	0.597420653	<i>ANAPC16</i>
Chemokine signaling pathway	bta04062	0.617272855	<i>PTK2B</i>
Axon guidance	bta04360	0.617272855	<i>UNC5B</i>
Chemical carcinogenesis - receptor activation	bta05207	0.622245427	<i>EPHX2</i>
Human immunodeficiency virus 1 infection	bta05170	0.622245427	<i>PTK2B</i>
Human T-cell leukemia virus 1 infection	bta05166	0.627287233	<i>ANAPC16</i>
MicroRNAs in cancer	bta05206	0.627287233	<i>DDIT4</i>
Human cytomegalovirus infection	bta05163	0.627287233	<i>PTK2B</i>
Chemical carcinogenesis - reactive oxygen species	bta05208	0.627287233	<i>EPHX2</i>
Endocytosis	bta04144	0.630242739	<i>CHMP5</i>
Calcium signaling pathway	bta04020	0.630242739	<i>PTK2B</i>

Thermogenesis	bta04714	0.630242739	<i>COX10</i>
Metabolic pathways	bta01100	0.649276528	<i>B4GALT1, FHIT, COX10, EPHX2, GULO</i>
cell differentiation	GO:0030154	0.701447177	<i>EYA2</i>
ion transport	GO:0006811	0.706385049	<i>CHRNA2</i>
protein phosphorylation	GO:0006468	0.710077291	<i>PTK2B</i>
Human papillomavirus infection	bta05165	0.717645749	<i>NFX1</i>
negative regulation of transcription by RNA polymerase II	GO:0000122	0.719299637	<i>NFX1</i>
PI3K-Akt signaling pathway	bta04151	0.726677737	<i>DDIT4</i>
Neuroactive ligand-receptor interaction	bta04080	0.726677737	<i>CHRNA2</i>
Pathways in cancer	bta05200	0.847695378	<i>NCOA3</i>